Abstract

Appelboom, Timothy William. Effects of In-Stream Processes on the Fate of Nitrogen and Phosphorous in Drainage Canals of Forested Watersheds. (Under the direction of Dr. G.M. Chescheir and Dr. R.W. Skaggs.)

As time progressed and populations increased, human activities related to the production of resources such as food, timber, clothing, and energy have focused on enhancing biological systems to increase yields. This has resulted in the altering of the natural cycles of nitrogen and phosphorous throughout the world. The objectives of this study were to; 1. conduct a literature review of forest stream hydrologic and nutrient inputs, outputs, and transformations and their associated contributions to the overall budgets, 2. quantify these inputs, outputs, and transformations for a drainage network section in the lower coastal plain of North Carolina, and 3. develop a mathematical relationship to describe nitrate removal from forest drainage systems that can be used in modeling.

Upstream inflow, rainfall/throughfall, and subsurface flow along with litterfall and lateral movement were measured as inputs, outflow at the outlet and denitrification were measures as outputs to the drainage section. Denitrification was estimated using seven methods; in stream tanks, undisturbed cores, background N^{15} and O^{18} concentrations, N^{15} enrichment, diffusion calculations, mass balance, and modeling.

During this study, 6.7 kg of nitrate was removed through demitrification during the first years flow period (85 days) and 19.8 kg dur4ing the second years flow period (82 days) from the 1900 meter log and 3 meter wide drainage canal section studied.

The mathematical relationship to describe the nitrate removal rate is based on a depth and concentration independent term which takes temperature into account. This relationship is based on a term called a mass transfer coefficient (ρ). This relationship resulted in a mass transfer coefficient (ρ) of 0.064 m/day at 25^{o}C.

Dedication

This work is dedicated to my wife, Theresa and my son Connor

Biography

Timothy W. Appelboom was born May 31, 1960 in Grand Rapids, Michigan. He moved to central Florida where he lived until graduating from high school. He attended the University of Florida from August 1978 to August 1983 where he received a BS degree in Forest Resources and Conservation in the department of Forestry. He returned to central Florida where he worked as a technician at the Citrus Research and Education Canter in entomology and nematology. During this period he traveled extensively visiting five continents (South America, North America, Africa, Europe, and Asia). Between 1993 and 1995 he took five background engineering courses before starting graduate school. In 1995, he began graduate school in the Department of Biological and Agricultural Engineering at North Carolina State University where he studied sediment production and transport from forest roads. He married Theresa (Zito) Appelboom on May 1999. He finished his masters degree in 2000. He then continued on to work on a doctoral degree in Agricultural Engineering in the Department of Biological and Agricultural Engineering at North Carolina State University where he studied in-stream processes which effect the conversions and removal of nitrogen and phosphorous species from forested watershed drainage systems.. His son Connor was born in December 2003. He finished his doctorate in Biological and Agricultural Engineering in 2004.

Acknowledgments

This research could not have been completed without the assistance and support of many people. I wish to thank Dr. G.M. Chescheir and Dr. R.W. Skaggs for serving as co-chairs of my committee, and Dr. Gilliam, Dr. Amatya, and Dr. Malcom for serving on as committee members. I am very grateful to my committee members for their support, encouragement, guidance, and confidence throughout this study.

I am also thankful to the department of Biological and Agricultural Engineering of North Carolina State University for its many forms of support. Field research for this study was conducted on lands owned and managed by the Weyerhaeuser Company. I wish to thank this organization for their cooperation and contributions during the course of this study, especially Joe Hughs, Joe Bergman, Jamie Nettles, Cliff Tyson.

I wish to thank Wilson Huntley and Jay Frick for their assistance in completing this project. I wish to thank Eugene Boyce for his tireless assistance in the installation, maintenance, and data collection during this study.

Lastly, and most importantly, I wish to thank my wife Theresa for fully supporting my decision to continue on with my studies. Without her support and love I would not have been able to complete this degree.

Table of Content

Chapter 3

Chapter 4

Chapter 5

List of Tables

List of Figures

General Introduction

As time has progressed and populations have increased, human activities related to the production of resources such as food, timber, clothing, and energy have focused on enhancing biological systems to increase yields. Manipulations of these systems have included fertilization, irrigation, and fossil fuel use, resulting in increased density production. Many of these activities have had an adverse effect on the environment, as they have influenced the equilibrium of natural cycles (such as carbon, sulfur, nitrogen, and phosphorous) on every continent (Erisman et al., 1998; EEA, 1995). Effects on the carbon cycle have resulted in increased CO_2 release, causing concern about global climate change (Erisman et al., 1998). Effects on the sulfur cycle have resulted in increased sulfur emissions, raising concerns of toxicity to humans and acidification of the environment (Erisman et al., 1998). More recently, nitrogen and phosphorous have been recognized for their importance to agricultural and forest production as well as for their roles as limiting nutrients in the eutrophication of lakes, streams, estuaries, and near coastal oceans (Erisman et al., 1998; Binkley et al., 1999). Nitrogen's roles in health threats such as methemoglobinemia (blue Baby syndrome) (Binkley et al., 1999), diuresis (USEPA, 2002), and hemorrhaging of the spleen (USEPA, 2002) have also come under sharper scrutiny.

Increased nitrogen and phosphorous transport to coastal and aquatic environments (Gulf of Mexico (Rabalais et al., 2002), North Sea (North Sea Task Force, 1993), Baltic Sea (EEA, 1995), Black Sea (Mee, 1992), Chesapeake Bay (Officer et al., 1984)) have been linked to increases in riverine nutrient loads. These increases in nutrients carried by streams and rivers have many sources, including agriculture, forestry, municipalities, and atmospheric deposition (Poor et al., 2001). The increase in riverine nutrient loads has

encouraged greater attention to the importance of these flowing waters in the removal of excess nitrogen and phosphorous along their lengths (Christensen et al., 1990).

The quality of waters flowing from forested watersheds is typically higher than water under any other land use (USEPA, 1995), with an average nitrate nitrogen concentration ca. 0.23 mg-N/L and phosphorous concentration of ca. 0.02 mg/L (Omernik, 1977). These levels are much lower than those found in agricultural drainage waters in the United States, which have average concentrations of total nitrogen and phosphorous nine times greater than those of forested drainage waters (Omernik, 1977). Concerns regarding water quality from managed forested watersheds arise from the increase in forest fertilization (Binkley et al. 1999), increased mineralization/nitrification and leaching from forest soils during drying and wetting sequences (Lamersdorf, 1998), increases in atmospheric nitrogen deposition (Seely, 1998), and routing of agricultural waters through forested areas.

Developed countries have implemented, or are in the process of implementing, management practices that reduce nutrient losses to surface waters from agricultural fields, managed and unmanaged forests, and municipalities. There is also the potential of nutrient removal from the rivers and streams themselves. Studies have shown the potential for nutrient removal from running waters through actions termed in-stream processes (e.g., Hill, 1988; Meyer et al., 1981; Triska et al., 1984; Duff and Triska, 1990; Wyer and Kay, 1989). An in-stream process is the transformation of an element by physical, chemical, or biological process, resulting in a change in the physical or chemical state of the element, or a change in the particle size in which it is associated (Meyer et al., 1981; Cummins, 1974; Boling et al., 1981). Researchers have found that nitrate concentrations within a stream can be reduced by the in-stream processes of denitrification (Chatarpaul et al., 1979; Swank and Caskey, 1982;

Hill and Sanmagadas, 1985; Campbell et al., 2000; Jensen et al., 1994; Seitzinger, 1988) and macrophyte uptake (Cooper and Cooke, 1984).

Birgand (2000) conducted an extensive review and discussion of nitrogen and phosphorous inputs to, and fates in, rivers and streams from watersheds with agricultural land use in a number of developed countries around the world.

The impacts of in-stream processes on the amount of nitrogen and phosphorous delivered to sensitive receiving waters from a watershed has implications with regard to the management of that watershed. If limited resources are available to reduce nitrogen loads from fields and some nitrogen removal occurs in the streams, then practices implemented to reduce nitrogen losses at the field scale would be most efficient in those fields that are least affected by in-stream losses of nitrogen. A good understanding of the processes and rates of nitrogen removal in streams is therefore needed to make the assessment required to manage nitrogen losses at the watershed scale effectively.

Objectives

The objectives of this study are to: 1) identify and determine the contribution of each nutrient input and output on the overall nutrient budget of a forest stream, 2) identify the in-stream processes responsible for nutrient removal from the stream and determine the amount of nutrients that can be removed from the stream through these processes, and 3) develop a mathematical relationship to describe this removal rate.

A literature review of forest stream hydrologic and nutrient inputs, outputs, and transformations and their associated contributions to the overall nutrient budget was conducted (Chapter 1). The hydrologic and nutrient input and output amounts (Chapter 2) and denitrification rates (Chapter 3) were determined to generate a water balance and

nutrient budget for a typical drainage network section in the lower coastal plain of North Carolina. A mathematical relationship to describe nitrate removal from surface waters was developed (Chapter 4).

References

Binkley, D., H. Burnham, and H.L. Allen. 1999. Water quality impacts of forest fertilization with nitrogen and phosphorous. For. Ecol. and Manage. 121: 191-213.

Birgand, F. Quantification and Modeling of In-Stream Processes in Agricultural Canals of the Lower Coastal Plain. Dissertation, 469pp, North Carolina State University, Raleigh, 2000.

Boling, R.H., E.D. Goodman, J.A. van Sickle, J.O. Zimmer, K.W. Cummins, R.C. Busch, and S.G. Fisher. 1981. Metabolism of a desert stream. Freshwater Biol. 11: 301-307.

Campbell, J.L., J.W. Hornbeck, W.H. McDowell, D.C. Busco, J.B. Shanley, and G.E. Likens. 2000. Dissolved organic nitrogen budgets for upland, forested ecosystems in New England. Biogeochem. 49: 123-142.

Chatarpaul, L., J.B. Robinson, and N.K. Kaushik. 1979. Role of tubificid worms on nitrogen transformations in stream sediment. J. Fish. Res. Board Can. 36: 673-678.

Christensen, P.B., L.P. Neilsen, J. Sørensen, and N.P. Revsbech. 1990. Denitrification in nitrate-rich streams: Diurnal and seasonal variation related to benthic oxygen metabolism. Limnol. Oceanogr. 35(3): 640-651.

Cooper, A.B., and J.G. Cooke. 1984. Nitrate loss and transformation in two vegetated headwater streams. N. Z. J. March Freshwater Res. 18: 441-450.

Cummins, K.W. 1974. Structure and function of stream ecosystems. BioScience 24: 631 641.

Duff, J.H. and F.J. Triska. 1990. Denitrification in sediments from the hyporheic zone adjacent to a small forested stream. Can. J. Fish. Aquat. Sci. 47: 1140-1147.

EEA. 1995. Europe's Environment, the Dobris Assessment. European Environment Agency, Copenhagen.

Erisman, J.W., T. Brydges, K. Bull, E. Cowling, P. Grennfelt, L. Nordberg, K. Satake, T. Schneider, S. Smeulders, K. Hoek, J.R. Wisniewski, and J. Wisnniewski. 1998. Nitrogen the Confer-N-s. First International Nitrogen Conference. March 23-27, 1998. Noordwijkerhout, Netherlands.

Hill, A.R. 1988. Factors influencing nitrate depletion in a rural stream. Hydrobiologia 160: 111-122.

Hill, A.R., and K. Sanmugadas. 1985. Denitrification rates in relation to stream sediment characteristics. Wat. Res. 19: 1579-1586.

Jensen. K., N.P. Sloth, N. Risgaard-Petersen, S. Rysgaard, and N.P. Revsbech. 1994. Estimation of nitrification and denitrification from microprofiles of oxygen and nitrate in model sediment systems. Appl. Environ. Microbiol. 60(6): 2094-2100.

Lamersdorf, N.P., K. Blanck, M. Bredemeier, and Y.-J. Xu. 1998. Drought experiments within the solling roof project. Chemosphere 36(4-5): 1161-1166.

Mee, L.D. 1992. The Black Sea in crisis: a need for concerted international action. Ambio. 21: 278-286.

Meyer, J.L., G.E. Likens, and J. Sloane. 1981. Phosphorous, nitrogen and organic carbon flux in a headwater stream. Arch. Hydrobiol. 91(1): 28-44.

North Sea Quality Status Report. North Sea Task Force. 1993. International Council for the Exploration of the Sea. Olsen and Olsen, Fredensborg, Denmark. 132 pp.

Officer, C.B., R.B. Biggs, J.L. Taft, L.E. Cronin, M.A. Tyler, W.R. Boynton. 1984. Chesapeake Bay anoxia. Science 223(4631): 22-27.

Omernik, J.M. 1977. Nonpoint Source-Stream Nutrient Level Relationships: A Nationwide Study. US EPA Report EPA-600/3-77-1056. Corvallis, OR.

Poor, N., R. Pribble, and H. Greening. 2001. Direct wet and dry deposition of ammonia, nitric acid, ammonium and nitrate to the Tampa Bay Estuary, FL, USA. Atmospheric Environment 35: 3947-3955.

Rabalais, N.N, R.E. Turner, and D. Scavia. 2002. Beyond science policy: Gulf of Mexico Hypoxia and the Mississippi River. BioScience 52(2): 129-142.

Seely, B., K. Lajtha, and G.D. Salvucci. 1998. Transformation and retention of nitrogen in a coastal forest ecosystem. Biogeochem. 42: 325-343.

Seitzinger, S.P. 1988. Denitrification in freshwater and coastal marine ecosystems: ecological and geochemical significance. Limnol. Oceanogr. 33(4): 702-704.

Swank, W.T., and W.H. Caskey. 1982. Nitrate depletion in a second-order mountain stream. J. Environ. Qual. 11: 581-584.

Triska, F.J., J.R. Sedell, K.Cromack Jr., S.V. Gregory, and F.M. McCorison. 1984. Nitrogen budget for a small coniferous forest stream. Ecol. Monog. 54(1): 119-140.

USEPA. 1995. National Water Quality Inventory, 1994. Report to Congress. EPA841-R-95005. Office of Water, USEPA, Washington, DC.

USEPA. 2002. Fact Sheet: Nitrates and Nitrites. United States Environmental Protection Agency, Washington, DC.

Wyer, M., and D. Kay. 1989. Experimental assessment of rates of nitrate removal by river bed sediments. J. Inst. Wat. Environ. Manag. 3(3): 273-279.

Chapter 1

Literature Review and Values of Inputs, Outputs, and In-Stream Processes Involved in Nitrogen and Phosphorous Conversion and Removal from Flowing Waters in Forested Watersheds

1.1 Stream Inputs

Nitrogen and phosphorous inputs to surface waters are categorized as point source and diffuse (non-point) source (Owens et al., 1972). Point sources are sewage effluents, industrial wastes, and other sources that have a distinct point of origin such as an outlet pipe. Point sources were not present within the study area and thus will not be discussed further. The diffuse sources can be divided into three categories at the stream level: hydrological sources, allochthonous sources, and autochthonous sources (Triska et al., 1984).

1.1.1 Hydrologic Sources

Hydrologic sources can be subdivided into precipitation (Seely et al., 1998), throughfall (Miller et al., 1998), groundwater (Triska et al., 1984), and surface runoff (Figure 1.1) (Cooke and Cooper, 1988). In studies conducted in Watershed 10 on the H. J. Andrews Experimental Forest, Oregon, Triska et al. (1984) found that hydrologic inputs accounted for 74% of all nitrogen inputs for the stream. Meyer et al. (1981) found that 89% of all nitrogen inputs (31% from throughfall and groundwater and 58% from lateral channels) and 72% of all phosphorous inputs (13% from throughfall and groundwater and 59% from lateral channels) entered Bear Brook, New Hampshire, via hydrologic inputs. The Meyer et al. (1981) study included inputs of nitrogen and phosphorous from lateral channels as hydrologic inputs. These will not be considered in this report, as there were no lateral inputs

to the canal study reach presented here. Percentage inputs from these sources are presented from Meyer et al. (1981) to account for all the inputs.

1.1.1.1 Precipitation and Throughfall

Precipitation is rainfall that falls uninterrupted to the ground (Figure 1.1). Precipitation gathers dissolved and particulate nitrogen and phosphorous compounds from the atmosphere. Nitrogen comes in the form of nitrate from electrical fixation in the atmosphere, industrial emissions, and the soil surface; ammonia released from industrial sites and the soil surface; and organic forms from fine residues swept into the atmosphere from the earth's surface (Tisdale et al.,1993). Percentages of nitrogen species for rainfall ranged from 42% organic, 39% nitrate, and 18% ammonium (Seely et al., 1988) to 18% organic, 53% nitrate, and 28% ammonium (Campbell et al., 2000). Of the few studies that measured precipitation inputs of phosphorous, neither phosphate nor organic phosphorous were present, though Johnston (1991) reported an average annual deposition rate of 0.04g total phosphorous per square meter across the United States. Nitrogen and phosphorus concentrations in precipitation from different locations are given in Table 1.1.

Throughfall is precipitation that has been intercepted by the forest canopy and has passed through it (Figure 1.1). A portion of the precipitation (16% to 36% on a yearly basis, based on literature review data reporting both precipitation and throughfall rates) is lost to the canopy, reducing the precipitation amount that reaches the ground. Amatya et al. (1996) found that canopy interception for a mid-rotation aged loblolly pine plantation in Carteret County, North Carolina, ranged from 5% to 25% on a per storm basis during the period from February 2, 1988, to January 19, 1993.

The nitrogen species found in throughfall are a combination of those gathered from the atmosphere in precipitation and the accumulation of primarily nitrate and organic nitrogen from dry deposition on the leaf surface (Hamburg and Lin, 1998), Leaching of the leaves themselves also increased nitrogen in throughfall (De Schrijver et al., 2000). Triska et al. (1984) observed that 70% to 95% of precipitation reaching the stream became nutrient-enriched by dripping through the canopy. Though all species of nitrogen are present in precipitation and throughfall, organic nitrogen makes up the bulk of them (Wollum and Davey, 1975). Seely et al. (1998) found the percentages of nitrogen species for throughfall to be 49% organic, 42% nitrate, and 9% ammonium. All measurable phosphorous in throughfall originated in the forest canopy and was found to contain equal amounts (50% each) of phosphate and organic phosphorous (McDonald and Healey, 2000; Robertson et al., 2000). Nitrogen and phosphorus concentrations in throughfall from different locations are given in Table 1.2.

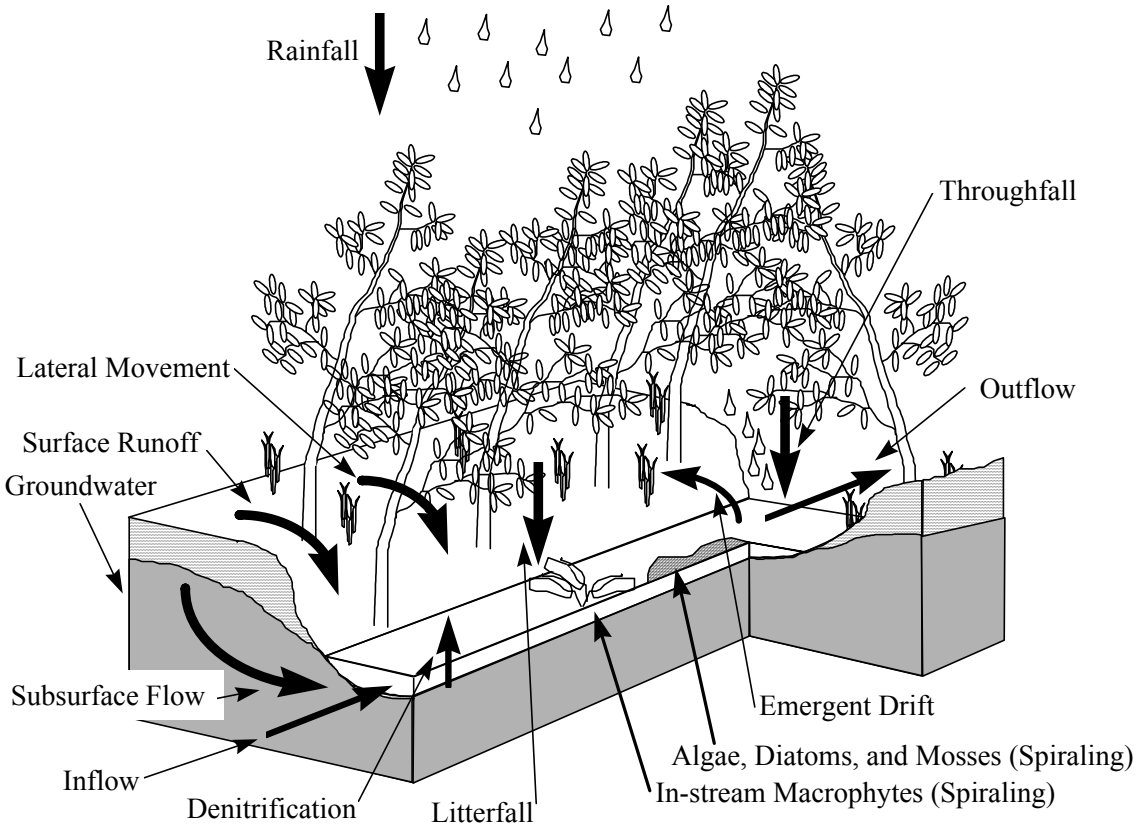

Figure 1.1. Nutrient inputs and outputs in a stream ecosystem.

The concentrations of nitrogen compounds in precipitation and throughfall have a significant spatial and temporal variation due to proximity to, and prevailing winds from, anthropogenic sources such as industrial emissions and areas of intensified animal production (Callesen et al., 1999). The proximity of these anthropogenic sources is important in that they emit nitrogen and phosphorous compounds in gaseous and particulate forms as byproducts of their operations. The prevailing winds carry these emissions either to or away from the site, depending on direction. Variations in forest type (variety makeup, density, age) (Seely et al., 1998), herbivore activity (Webb et al., 1995), and random hydrologic events (Hyer et al., 1995) all will cause differences in the concentrations of the different nitrogen

and phosphorous species in throughfall. Van Miegroet et al. (1994) found that younger vegetation had less nutrient leaching from the canopy than older vegetation. Herbivore activity reduced the amount of leachable substrate available, thus reducing the nutrient additions to throughfall. Random hydrologic events varied in nutrient content of throughfall due to time periods between events. Longer periods allowed for more accumulation of dry deposition of nitrogen and phosphorous compounds in the canopy.

Triska et al. (1984) found that throughfall/precipitation consisted of 2% of the total direct nitrogen inputs to the study stream. Meyer et al. (1981) found throughfall/precipitation consisted of 3% of the total nitrogen inputs and 4% of the total phosphorous inputs to the study stream.

Table 1.1. Volume-weighted mean solution concentrations for nutrients in precipitation from different locations.

Location	Period	Rainfall mm/yr	NH4-N mg/L	NO3-N mg/L	DON-N mg/L	Total N Mg/L	PO4-P mg/L	Total P mg/L	Source
Waquoit Bay, Massachusetts	June 1993 - May 1995	829	0.09	0.19	0.21	0.49	0.00	-	Seely et al., 1988
New Hampshire	1994-1997	1535	0.17	0.32	0.11	0.60	-	-	Campbell et al., 2000
Lewiston, North Carolina	2000	1009	0.23	1.01	-	-	-	-	NADP, 2000[1]
Bradford, Florida	2000	948	0.12	0.84	-	-	-	-	NADP, 2000[1]
Greenville, Maine	2000	1094	0.11	0.70	-	-	-	-	NADP, 2000[1]
Yosemite, California	2000	1347	0.11	0.31	-	-	-	-	NADP, 2000[1]
Mount Rainier, Washington	2000	1072	0.02	0.25	-	-	-	-	NADP, 2000[1]
Sinks Canyon, Wyoming	2000	401	0.13	0.57	-	-	-	-	NADP, 2000[1]
Ashland, Missouri	2000	1081	0.35	1.33	-	-	-	-	NADP, 2000[1]
Sonora, Texas	2000	566	0.22	0.64	-	-	-	-	NADP, 2000[1]
Purdue University, Indiana	2000	873	0.40	1.46	-	-	-	-	NADP, 2000[1]
Flanders, Belgium	Sept. 1998 - Aug. 1999	980	1.29	0.45	-	-	-	-	De Schrijver et al., 2000
Gisburn, England	Nov. 1987 - Mar. 1991	1578	0.9	3.1	-	-	-	-	Robertson et al., 2000
Wekeromsche Zand, Netherlands	Mar. 1989 - Dec. 1992	750	2.01	1.25	-	-	-	-	Berg and Verhoef, 1998
Manaus, Brazil	April 1996 - Mar 1997	2672	-	-	-	0.20	-	0.00	Schroth et al.,2001
Plymouth, North Carolina	Jan. 2001 - June 2002	1026	0.35	0.22	0.86	1.43	0.03	0.08	This study

[1] National Atmospheric Deposition Program, 2000 Annual and Seasonal Data Summary (web address http://nadp.sws.uiuc.edu/).

Table 1.2. Volume-weighted mean solution concentrations for nutrients in throughfall from different locations.

Location	Period	Through-fall mm/yr (% inter-ception)[1]	Stand Type	NH_4-N mg/L	NO_3-N mg/L	DON-N mg/L	Total N mg/L	PO_4-P mg/L	Total P mg/L	Source
Waquoit Bay, Massachusetts	June 1993 - May 1995	687 (17)	Mixed Oaks	0.13	0.42	0.44	0.99	0.01	-	Seely et al., 1988
Watershed 10, Oregon	1972-1974	2360	Douglas Fir	-	-	-	0.13	-	-	Triska et al., 1984
Flanders, Belgium	Sept. 1998 - Aug. 1999	814 (17)	Silver Birch	2.65	0.77	-	-	-	-	De Schrijver et al., 2000
Flanders, Belgium	Sept. 1998 - Aug. 1999	638 (35)	Corsican Pine	12.74	2.38	-	-	-	-	De Schrijver et al., 2000
Gisburn, England	Nov. 1987 - Mar. 1991	1015 (36)	Scots Pine	3.6	6.2	-	-	0.00	0.00	Robertson et al., 2000
Wekeromsche Zand, Netherlands	Jan. 1990 - Dec. 1992	484 (35)	Scots Pine	8.65	2.10	-	-	-	-	Berg and Verhoef, 1998
Bear Brook, Hubbard Brook Experimental Forest, New Hampshire	Sept. 1968 - Aug. 1969	636	Mixed Hardwood	-	-	-	2.68	-	0.11	Meyer et al., 1981
Manaus, Brazil	April 1996 - Mar 1997	2218 (17)	*Eschweilera*	-	-	-	0.71	-	0.01	Schroth et al.,2001
Manaus, Brazil	April 1996 - Mar 1997	2351 (12)	*Oenocarpus*	-	-	-	0.60	-	0.01	Schroth et al.,2001
Blue Mountains, Jamaica	Sept 1992 - Sept. 1994	1270	Mixed Forest	0.04	0.02	0.03	0.09	0.03	0.03	McDonald et al., 2000
Plymouth, North Carolina	Jan. 2001 - June 2002	744 (27)	Mixed Forest	0.37	0.40	1.71	2.48	0.16	0.23	This study

[1]Percent interception in the percent of rainfall intercepted and held in the canopy.

1.1.1.2 Groundwater

Nitrogen inputs via groundwater in forested watersheds (Figure 1.1) occur in the forms of dissolved ammonium, nitrate, and organic forms, with the bulk in organic forms (Tisdale et al., 1993). Phosphorous forms are in organic and inorganic phosphate (PO_4). The sources of nitrogen and phosphorous in subsurface flow in forests are precipitation/throughfall, litterfall, dry deposition, fertilizers, biological fixation, and animal waste that enter the soil and soil solution (Tisdale et al., 1993). Nitrogen species are transformed within the soil to other forms of nitrogen via mineralization (organic-N transformed to ammonium), immobilization (ammonium and nitrate transformed to organic forms), nitrification (ammonium transformed to nitrate), and denitrification (nitrate to gaseous nitrogen forms) (Wollum and Davey, 1975; Tisdale et al., 1993). Phosphorous is converted between the organic and inorganic forms via mineralization (organic-P transformed to phosphate) and immobilization (phosphate transformed to organic-P) (Tisdale et al., 1993). The amounts and types of nitrogen species and phosphorous forms within the subsurface flow are influenced by inputs to and transformations within the soil, organism populations, pH, soil aeration, plant uptake, temperature, and the available carbon (Callesen et al., 1999; Tisdale et al., 1993; Wollum and Davey, 1975).

Percentages of nitrogen species for groundwater ranged from 95% organic, 5% nitrate, and 0% ammonium (Triska et al., 1984) to 47% organic, 11% nitrate, and 41% ammonium (Campbell et al., 2000). Triska et al. (1984) found that groundwater contributed 72% of the total direct nitrogen inputs to the study stream, while Meyer et al. (1981) reported a 28% nitrogen contribution from groundwater. Few studies looked at groundwater phosphorous content. Meyer et al. (1981) and Robertson et al. (2000) found no measurable

phosphorous in the groundwater, though Meyer et al. (1981) reported that 9% of the total phosphorous inputs to the stream were from groundwater. Nitrogen and phosphorus concentrations in groundwater from different locations are given in Table 1.3.

1.1.1.3 Surface Runoff

Nitrogen supplied to a stream (Figure 1.1) through surface runoff is primarily composed of dissolved organic, with smaller concentrations of nitrate and ammonium (Cooke and Cooper, 1988). Phosphorous supplied through surface runoff is primarily in the form of phosphate (McDonald and Healey, 2000). Runoff losses from forested watersheds are heavily influenced by soil properties: slope, soil type, surface roughness (bedding, litter layer composition, etc.), infiltration rates, antecedent moisture conditions, and drainage intensity, as well as stand characteristics (species, planting density, understory vegetation, etc.). Surface runoff from forested sites generally is low due to higher water storage capacity, better subsurface drainage, and looser soils (McDonald and Healey, 2000), as well as increased use of management practices that reduce surface runoff, non-point nutrient sources, and reduce erosion (McClurkin and Duffy, 1975). Locations of potential surface runoff in forests include skid trails and loading areas (Croke et al., 2000).

Percentages of nitrogen species in runoff ranged from 72% organic-N, 3% nitrate, and 25% ammonium with phosphorous reported only as total phosphorous (Sauer et al., 2000) to 33% organic, 11% nitrate, and 56% ammonium, with phosphorous forms present almost exclusively as phosphate (McDonald and Healey et al., 2000). Both Triska et al. (1984) and Meyer et al. (1981) reported no surface runoff to their study stream. Nitrogen and phosphorus concentrations in surface runoff from different locations are given in Table 1.4

Table 1.3. Average concentrations of nutrients in groundwater from different locations.

Location	Period	Drainage (mm)	Stand Type	NH_4-N mg/L	NO_3-N mg/L	DON-N mg/L	Total N mg/L	PO_4-P mg/L	Total P mg/L	Source
Waquoit Bay, Massachusetts	June 1993 - May 1995	404	Mixed Oaks	0.03	0.01	0.13	0.17	0.00	-	Seely et al., 1988[1]
Flanders, Belgium	Sept. 1998 - Aug. 1999	383	Silver Birch	0.37	6.63	-	-	-	-	De Schrijver et al., 2000
Flanders, Belgium	Sept. 1998 - Aug. 1999	363	Corsican Pine	0.91	15.54	-	-	-	-	De Schrijver et al., 2000
Gisburn, England	Nov. 1987 - Mar. 1991	-	Scots Pine	0.00	1.3	-	-	0.00	0.00	Robertson et al., 2000
Watershed 10, Oregon	1972 - 1974	-	Douglas Fir	0.00	0.38 kg to stream	8.49 kg to stream	8.87 kg to stream	-	-	Triska et al. 1984
Lye Brook Wilderness, Vermont	June 1994 - October 1995	28	Mixed Forest	0.34	0.29	0.50	1.13	-	-	Campbell et al., 2000
Coastal Plain, South Carolina	---	-	Loblolly Pine	0.06	0.20	-	-	-	-	Wells et al.,1985
Tennessee	---	-	Yellow Poplar	-	0.4	-	-	-	-	Johnson and Todd, 1988
Oak Ridge, Tennessee	---	-	Sycamore	-	0.1	-	-	-	-	van Miegroet et al., 1994
Central Sweden	---	-	Norway Spruce	0.23	0.11	-	-	-	-	Nohrstedt, 1992
Klosterhede, Denmark	---	-	Norway Spruce	0.01	0.1	-	-	-	-	Gunderson and Rasmussen, 1995
Hubbard Brook Experimental Forest, New Hampshire	Sept. 1968 - Aug. 1969	-	Mixed Hardwood	0.02	0.25	0.04	0.31	-	0.00	Meyer et al., 1981
Plymouth North Carolina	Jan. 2001 - June 2002	-	Mixed Forest	0.28	1.48	1.35	3.11	0.01	0.01	This Study

Table 1.4. Average volume weighted concentrations of nutrients in surface runoff from different locations.

Location	Period	Runoff mm/yr	Stand Type	NH_4-N mg/L	NO_3-N mg/L	DON-N mg/L	Total N mg/L	PO_4-P mg/L	Total P mg/L	Source
Washington County, Arkansas	single event (25-yr rainstorm)	-	Mixed Hardwood	0.18 kg/ha	0.02 kg/ha	0.52 kg/ha	0.72 kg/ha	-	0.47	Sauer et al., 2000
Blue Mountains, Jamaica	Sept. 1992 - Sept. 1994	2.90	Mixed Forest	2.59	0.59	1.95	5.13	1.03	1.03	McDonald and Healey, 2000

1.1.2 Allochthonous sources

Allochthonous sources are the particulate organic inputs from the adjacent terrestrial environment (litterfall and lateral movement) as a source of fixed carbon and nutrients for in situ biological processes (Figure 1.1) (Triska et al., 1984; Cooke and Cooper, 1988). Triska et al. (1984) found that allochthonous inputs accounted for 9% of all nitrogen inputs for the stream, while Meyer et al. (1981) found that 11% of all nitrogen inputs and 28% of all phosphorous inputs to the stream were from litterfall. All nitrogen and phosphorous from allochthonous sources were reported as organic in all three studies.

Litterfall is composed of materials such as leaves, twigs, branches, cones, flowers, fruit, and insect frass that fall from the forest canopy. Concentrations of elements in litter are influenced by their concentrations within the soil. When concentrations in the soil are low, the concentrations in the litter are often very low due to translocation of the nutrients within the tree prior to leaf abscission (Berg and Verhoef, 1998). Triska et al. (1984) found litterfall had its lowest concentration of nitrogen content during the summer and fall, when natural abscission is occurring. Most litterfall in deciduous forests occurs during the fall months (primarily November, and intermittently during other periods with leaves present) and from the onset of moisture stress (June to November) for coniferous forests (Triska et al., 1984). McDonald and Healey (2000) found litterfall to be slightly higher from January to July, the driest period of the year, in the Blue Mountains of Jamaica. Gosz et al (1972) found that a majority (50%) of the litterfall occurred in the months of September and October. Organic nitrogen content of litterfall ranged from 5.4 mg/g to 13.6 mg/g. Nitrogen and phosphorus concentrations in litterfall from different locations are given in Table 1.5.

Triska et al. (1984) and McDowell and Fisher (1976) reported laterally transported material. Triska found that most lateral inputs occurred from December to May, with only 34% entering during November (compared to 68% from litterfall during November). Triska also found that total lateral inputs composed 12% of the total nitrogen inputs to his study stream. Phosphorus content and transport in lateral inputs was not reported in any study. Nitrogen and phosphorus concentrations in laterally transported material from different locations can be found in Table 1.6.

Peterson and Cummings (1974) divided leaf processing into three phases: 1) leaching, 2) initial microbial processing, and 3) animal-microbial conversion. McDowell and Fisher (1976) found that litter that entered a stream rapidly lost soluble constituents via abiotic leaching in the first one to three days (20%-30% by weight for deciduous species and 3%-13% for evergreen species), with a much reduced loss rate thereafter. Wetzel and Manny (1972) reported that the total dissolved nitrogen was leached within the first 12 hours of their study. The increase in total dissolved organic nitrogen from the leachate decreased to normal levels within 24 to 69 days and was matched by an equivalent increase in nitrates within the stream. Leachates are mainly reducing sugars, polyphenols, and amino acids (Suberkropp et al., 1976). The leached amino acids can then be mineralized into inorganic ammonium and phosphate. Leachates are an important source of dissolved organic matter and are rapidly removed from the water column to the sediments (Wetzel and Manny, 1972). Wetzel and Manny (1972) found that litter inputs to their study stream caused a drop in nitrate concentration in the water column after the first 24 hours. They determined that this was due to the sudden increase in heterotrophs (the second phase of leaf processing). Heterotrophs have a low carbon-to-nitrogen ratio, so they incorporate dissolved nitrogen from the water

column into their tissue to increase their growth. This same response was observed in many other studies (e.g. Suberkropp et al., 1976; McDowell and Fisher, 1976; Boling et al., 1975; Berg and Verhoef, 1998). Factors affecting leaching and decomposition of litterfall include flow rates, microbial populations present, physical and chemical regimes, and season (Wetzel and Manny, 1972).

Table 1.5. Average amount of nutrients in litterfall from different locations.

Location	Period	Stand Type	Litterfall Mass kg/ha/yr	Total N mg/g	Total P mg/g	Source
Blue Mountains, Jamaica	September 1992 - September 1994	Mixed Forest	9318	8.33	0.91	McDonald and Healey, 2000
Black Forest, Germany	1995	Norway Spruce	-	17.1	-	Lorenz et al., 2000
Black Sturgeon Forest, Ontario, Canada	1995	Black Spruce	-	10.1	-	Lorenz et al., 2000
Wekeromsche Zand, Netherlands	Jan. 1990 - December 1992	Scots Pine	3650	9.0	-	Berg and Verhoef, 1998
Laurel Creek, Ontario, Canada	1997	Mixed Hardwood	3238	7.52	-	Oelbermann and Gordon, 2000
South Carolina	Oct. 1982 - April 1984	Mixed Hardwood (Stream)	5947	-	-	Muzika et al., 1987
South Carolina	Oct. 1982 - April 1984	Mixed Hardwood (riverine)	5517	-	-	Muzika et al., 1987
Hubbard Brook Experimental Forest, New Hampshire	September 1968 - Aug. 1969	Mixed Hardwood	-	49.0 kg/yr to stream	3.3 kg/yr to stream	Meyer et al., 1981
Hubbard Brook Experimental Forest, New Hampshire	Oct. 1968 - Oct. 1969	Mixed Hardwood	5702	9.5	0.7	Gosz et al., 1972
Watershed 10, Oregon	1972 - 1974	Douglas Fir	1931	5.4	-	Triska et al., 1984
Plymouth, North Carolina	Jan. 2001 - June 2002	Mixed Forest	4891	12.1	0.7	This study

Table 1.6. Average amount of nutrients in lateral litter movement from different locations.

Location	Period	Stand Type	Litterfall Mass kg/ha/yr	Total N mg/g	Total P mg/g	Source
Sunderland, Massachusetts	September 5, 1974 - Nov. 21 1977	Mixed Forest	710	-	-	McDowell and Fisher, 1976
Watershed 10, Oregon	1972 - 1974	Douglas Fir (lateral movement)	2900	6.0	-	Triska et al., 1984

Not all litter is decomposed. The undecomposed portion of litter is termed refractory material (Wetzel and Manny, 1972). Jewel (1971) reported that, on average, 24% of the initial input of litter remained as refractory material. Undecomposed material can settle to the stream bed, creating mats. When the organic mat gets thick enough, anaerobic layers will develop in the lower portions. Decomposition continues to occur, with mineralization occurring slowly (Ponnamperuma, 1972). Ammonium builds up in this portion of the sediments and is released to the stream's water column through diffusion. Nitrate is not generated in this zone, as there is no oxygen present (Ponnamperuma, 1972). This sets up the gradient of ammonium within the deeper sediments and nitrate within the water column, which results in movements of ammonium and nitrate between the two zones.

1.1.3 Autochthonous sources

Autochthonous sources are the in-stream production of carbon (through photosynthesis) and nitrogen (through nitrogen fixation) (Triska et al., 1984). Examples of autochthonous sources of nitrogen are filamentous alga, diatoms, and mosses (Figure 1.1) (Triska et al, 1984). All nitrogen from autochthonous sources was reported as organic nitrogen (e.g., Triska et al., 1984; Cooke and Cooper, 1988). Triska et al. (1984) found

autochthonous inputs to the stream to be 5% of the total nitrogen inputs. Phosphorous cannot enter the stream through an autochthonous source.

The roles of these two sources, allochthanous and autochthanous, vary with the stream. In streams draining heavily forested watersheds, the shift is toward almost entirely allochthonous inputs due to little or no light being intercepted by the stream (Teal, 1957; Minshall, 1967; Fisher and Likens, 1973; Sedell et al., 1974; Meyer et al., 1981; Triska et al., 1982). In streams with less canopy cover, autochthonous inputs can play a more important role as a source of fixed carbon and nutrients (Cushing and Wolf, 1982; Horne and Carmiggelt, 1975; Triska and Buckley, 1978).

1.2 Stream Outputs

Nitrogen can be permanently removed from a forested stream in one of three ways; it can be released to the atmosphere via denitrification (Seitzinger, 1988; Triska et al., 1984), lost to emergence drift (Meyer et al., 1981), or discharged at the mouth of the stream (Triska et al., 1989a). Phosphate can be removed via emergence drift or discharged at the mouth of the stream (Meyer et al., 1981).

1.2.1 Denitrification

Denitrification is the reduction of nitrate (NO_3^-) to the gaseous nitrous oxide (N_20) and elemental N (N_2) (Tisdale et al., 1993). It occurs in the anaerobic sediments along the bottom of a river or stream (Figure 1.1) and has been identified as a major pathway of nitrogen loss from a stream or river (van Kessel, 1977; Seitzinger, 1988; Duff et al., 1984; Cooper and Cooke, 1984). Denitrification rates are affected by many factors, such as presence of oxygen, pH, organic carbon supply, temperature, nitrate supply, and denitrifier population levels (van Kessel, 1977; Swank and Caskey, 1982; Tisdale et al., 1993).

Triska et al. (1984) found that in the total nitrogen budget of Watershed 10, there was a loss of 26% in input nitrogen that was unaccounted for. This loss was assumed to be due to denitrification within the stream itself and stream sediments. Meyers' studies at Bear Brook (1981) found a small amount of unaccounted-for losses of nitrogen and assumed that these were due to denitrification. There are very few actual measurements of denitrification in streams prior to the early 1990's (e.g., Duff et al., 1984; Christensen and Sørensen, 1988), of which there are only a handful from forested streams (e.g., Duff et al., 1996; Seitzinger, 1988) (Table 1.7).

1.2.2 Emergent Drift

Emergence drift is the loss of nutrients due to insect emergence from the stream (Figure 1.1). Insects that go through their immature stages within the stream utilize nutrients as they grow and develop (Meyer et al, 1981). As they mature into adults they leave the steam reducing the overall amounts of nutrients by a small amount. The emergence drift losses of total input nitrogen and phosphorous were found to be small in studies conducted by Triska et al., 1984, (0.2% nitrogen loss) and Meyer, et al., 1981, (0.3% nitrogen loss and 1% phosphorous loss).

1.2.3 Outlet Discharge

Nitrogen is discharged at the outlet (Figure 1.1) of a forested watershed in all forms; large particulate organic nitrogen (leaves, needles, twigs, bark, and coarse wood), fine particulate organic nitrogen, dissolved organic nitrogen, nitrate, and ammonium. This composes the nitrogen that was not removed previously from the system (via denitrification or emergent drift) or stored within the stream (plant uptake or sorption). The amount of nitrogen being discharge is greatest under higher flows of winter, roughly half the amount

retained as compared to the lower flows of summer and autumn (Triska et al., 1984). Phosphorous discharged at the outlet is also in both particulate organic and dissolved organic and inorganic forms and represents that which was not removed by emergent drift or stored within the stream (plant uptake or sorption) (Meyer et al., 1981).

Triska et al. (1984) reported that 73.8% of the input nitrogen was discharged at the outlet. He found that the particulate fraction made up 23% with dissolved components making up 77% (73% organic and 4% nitrate with no ammonium present) of the nitrogen outputs by the stream. Meyer et al. (1981) reported 99.7% of the input nitrogen and 99% of the input phosphorous was discharge from the outlet. They, on the other hand, found that the particulate fraction of nitrogen export to be 4% with dissolved components making up 96% (12% organic, 79% nitrate, and 5% ammonium) of the nitrogen output by the stream with phosphorous export being 16% dissolved (no breakdown between organic and inorganic was reported) and 84% particulate. Nitrogen and phosphorus concentrations in outflow from different locations can be found in Table 1.8.

1.2.4 Human Activity

Human activity such as dredging or channel clearing was not addressed by any of the previous studies as they were conducted in mostly undisturbed pristine streams where flow obstructions such as embankment sloughs or debris dams are allowed to either be eroded naturally or alter the flow of the stream. The drainage systems of managed forests, as found in the coastal plain of North Carolina, typically have steeper bank slopes resulting in higher erosion and sloughing from animal movement than in natural streams. The systems are designed for the removal of excess water to improve tree growth as well to provide trafficability on the site at the time of harvest, while taking the least possible amount of land

out of production. To continue to function, field ditches and collector canals need to be periodically cleared of obstructions which impede flow. This is accomplished by using a drag line or backhoe to dig the canals and ditches back to their original depths and slopes. This process removes a thick layer of organic sediment along with the overlying litter layer which accumulates over time in the bottoms of these drainage systems. This layer contains a large amount of organic nitrogen (as well as ammonium within the pore water) and both inorganic phosphate and organic phosphorous. Thus the process of field ditch and collector canal clean-out is a potentially large removal avenue for nitrogen and phosphorous.

Table 1.7. Denitrification rates for forested streams from different locations.

Location	Land use	Stream Type	Method	Denitrification Rate mg NO_3^--N/m^2/day (ρ m/d)[1]	Stream Concentration NO_3-N mg/L	Source
Salto River, Costa Rica	Lowland Rain Forest	Lowland Swamp	C_2H_2 Sediment-Water Flux in Benthic Chamber	7-37 mg/m^2/d *(ρ=0.0045-0.0080)*	1.55-4.65 mg/L	Duff et al., 1996
Little Lost Man[2] Creek, California	Old Growth Redwood Forest	Pristine Creek	C_2H_2 Undisturbed Core	18 mg/m^2/d *(ρ=0.02)*	0.9 mg/L	Duff et al., 1984
Skit, New Jersey	Mixed Forest	Forest Stream	N_2 Flux Undisturbed Core	<29 mg/m^2/d *(ρ<0.483)*	0.06 mg/L	Seitzinger, 1994
Swift Brook, Ontario	Mixed Forest	Perennial Spring Fed Creek	NO_3 Depletion Over Sediment Core	180-449 mg/m^2/d *(ρ=0.36-0.112)*	0.5-4 mg/L	Robinson et al., 1979
Swift Brook, Ontario	Mixed Forest	Perennial Spring Fed Creek	Stream Mass Balance	425-490 mg/m^2/d *(ρ=0.07-0.142)*	3.0-7.0 mg/L	Kaushik and Robinson et al., 1976
Plymouth, North Carolina	Mixed Forest	Drainage Canal	NO_3 Depletion Over Undisturbed Sediment Core	409 mg/m^2/day *(ρ=0.0682)*	6 mg/L (@ 25°C)	This Study
Plymouth, North Carolina	Mixed Forest	Drainage Canal	NO_3 Depletion in In-Stream Tanks	382 mg/m^2/day *(ρ=0.0637)*	6 mg/L (@ 25°C)	This Study
Plymouth, North Carolina	Mixed Forest	Drainage Canal	Modeled Mass Balance	2580 mg/m^2/day *(ρ=0.43)*	6 mg/L (@ 25°C)	This Study

[1] Mass Transfer Coefficient - ρ -in m/d as determined by Kelly's Equation, Removal Rate (mg/m^2/d) = ρ (m/d) * nitrate Concentration (mg/m^3).

[2] Carbon limited stream.

Table 1.8. Average volume weighted concentration of nutrients in stream water from different locations.

Location	Period	Stand Type	NH_4-N mg/L	NO_3-N mg/L	DON mg/L	Total N mg/L	PO_4 -P mg/L	Total P mg/L	Source
Aroostook River Basin, Maine	1994-1996	Mixed Forest	0.08	0.20	-	-	-	-	Cronan et al., 1999
Beaufort, North Carolina	1986-1994	Loblolly Pine Plantation	0.12	0.02	1.08	1.22	0.02	0.05	Lebo and Herrmann, 1998
Carteret County, North Carolina	Feb. 1989-Mar. 1990	Loblolly Pine Plantation	0.08	0.93	1.26	2.27	-	0.03	Amatya et al., 1998
Piedmont, North Carolina	---	Loblolly Pine	0.04	0.80	0.70	1.54	-	0.07	Fromm and Herrmann, 1996
Coastal Plain, Florida	---	Slash Pine	0.1	0.1	0.9	1.1	-	-	Fisher, 1981
Fernow, West Virginia	---	Mixed	0.23	0.76	-	-	-	-	Aubertin et al., 1973
Central Oregon	---	Douglas Fir	0.0	0.0	0.15	0.15	-	0.01	Stay et al., 1979
Soastal Range, Washington	---	Douglas Fir	0.03	0.60	0.20	0.83	-	-	Bisson et al., 1992
Central Sweden	---	Norway Spruce	-	0.02	0.22	-	-	-	Ring and Nohrstedt, 1993
New Zealand	---	Radiata Pine	0.00	0.00	0.32	0.32	-	0.04	Leonard, 1977
Watershed 10, Oregon	Mar. 1874 - April 1975	Douglas Fir		330 g/yr	0.50		-	-	Triska et al., 1984
Hubbard Brook Experimental Forest, New Hampshire	Sept. 1968 - Aug. 1969	Mixed Hardwood	0.02	0.25	0.04	0.31	-	0.01	Meyer et al., 1981
Lye Brook Wilderness, Vermont	June 1994 - October 1995	Mixed Forest	0.10	0.01	0.30	0.41	-	-	Campbell et al., 2000
Plymouth, North Carolina	Jan. 2001 - June 2002	Mixed Forest	0.08	1.80	1.62	1.70	0.01	0.02	This Study[1]

[1] Concentrations at the upstream inflow of the study reach.

1.3 Nutrient Storage (Spiraling)

Meyer et al. (1981) reported an uptake of 1% of the total input nitrogen and 5% of the total input phosphorous by plant roots along the study reach. These were not treated as outputs from the stream in this budget analysis, because these uptakes are balanced over time with releases to the stream as these nutrients are cycled within the stream (see Spiraling Processes, below).

1.4 In-Stream Processes

An in-stream process is the transformation of an element by physical, chemical, or biological process resulting in a change in the physical or chemical state of the element, or a change in the particle size in which it is associated (Meyer et al., 1981; Cummins, 1974; Boling et al., 1981).

1.4.1 Physical Processes

A physical in-stream process changes the physical size or transportational form of an element via physical processes. Leaching and physical fragmentation are examples of this type of process (Triska et al., 1984). The initial conversion of leaf substrates to dissolved organic and inorganic nitrogen and phosphorous compounds occurs through leaching (Boling et al., 1975). Leaching, an abiotic removal of nutrients from particulate organic material via water movement over or through the material, is predominant in the first 24-hour period after the leaf enters the stream. The stream releases 3% to 30% of the leaf's original dry weight as dissolved organic matter (McDowell and Fisher, 1976). In studies by Peterson and Cummins (1974), an average leaching rate for leaf litter is 15% for the first three days in the stream.

Physical fragmentation is the breaking down of large particulate organic matter (litter-sized organic material) to smaller fine particulate organic matter by the physical

abrasion of the material against the stream bed, rocks, or other organic material (Boling et al., 1975). Physical in-stream processes do not result in the direct removal of nutrients from the system but do play a significant role in transforming particulate organic nitrogen into forms more usable in chemical and biological processes.

1.4.2 Chemical Processes

A chemical in-stream process changes the chemical structure or association of an element via chemical processes. Ammonium adsorption and conversion of ammonium to gaseous ammonia are examples of in-stream chemical processes (Owens et al., 1972; Tisdale et al., 1993). Ammonium can be sorbed, or fixed, within the stream bed sediments. Newbold et al. (1983) found that in an ammonium-enriched stream, 21% of the ammonium had been sorbed to the sediments within the reach after 265 minutes of enrichment. Ammonium adsorption to clays is similar to that of potassium. This gives ammonium a lower adsorption strength, which means it can easily be desorbed. The amount of ammonium adsorbed to the stream bed sediments is strongly influenced by water column ammonium concentrations, as well as the concentrations of other cations in the water column and clay surfaces (Tisdale et al., 1993). This process is also influenced by the pH of the water column and sediment. More acidic conditions lead to a higher desorption potential for ammonium, causing most ammonium to remain in solution (Kuwabara and Helliker, 1988; Reported in Tisdale et al., 1993).

Also within the sediments, ammonium can be converted in a chemical process to ammonia gas (Johnson, 1991). The process of converting ammonium to ammonia gas is heavily reliant on temperature, pH, water turbulence, and ammonium concentration (Owens et al., 1972). In the case of ammonium adsorption, nitrogen can leave the system along with

the sediment as it is transported along the stream and expelled at the mouth. Other sorbed ammonium can be released again to the water column as conditions within the water column change, resulting in a temporary removal of stream nitrogen. Ammonia gas generated within the sediment, on the other hand, is lost to the system through volatilization, and as such results in a net reduction in the overall amount of nitrogen within the system.

An example of a chemical process changing the form of phosphorus within the steam is the shift of phosphate ions from $H_3PO_4^0$ to $H_2PO_4^{-1}$ to HPO_4^{-2} to PO_4^{-3} based on the pH (going from pH 0 to pH 14) (Tisdale et al., 1993). Inorganic phosphorous can also be sorbed to stream bed sediments (Meyer and Likens, 1979) and can desorb as solution concentrations decrease (Tisdale et al., 1993). Chemical processes generally relate to equilibriums within the system, resulting in a shift from one form to another (sorbed/desorbed, solid/dissolved, etc.) based on the pH, temperature, and concentration (Tisdale et al., 1993)

1.4.3 Biological Processes

A biological in-stream process is a change in either the physical or chemical form of an element that is directly mediated by biological activity. Some of the most important biologically mediated processes change organic nitrogen to inorganic nitrogen (or vice versa) or the chemical forms. These are the processes of mineralization, immobilization, nitrification, and denitrification. Phosphorous can be mineralized or immobilized.

1.4.3.1 Mineralization

Mineralization is the conversion of organic forms of nutrients to inorganic forms. Nitrogen mineralization is the conversion of organic nitrogen to inorganic nitrogen in the form of ammonium (NH_4) through the processes of aminization (Equation 1.1):

$$\textbf{Proteins} \xrightarrow[\substack{\text{Bacteria}\\\text{Fungi}}]{H_2O} \textbf{Amino Acids + Amines + Urea} \qquad \text{(Equation 1.1)}$$

and ammonification (Equations 1.2 and 1.3):

$$\textbf{Amino Acids + Amines + Urea} \xrightarrow[\substack{\text{Bacteria}\\\text{Fungi}}]{+H_2O} \textbf{NH}_3 \textbf{ + R-OH + energy} \qquad \text{(Equation 1.2)}$$

$$\textbf{NH}_3 \xrightarrow{+H_2O} \textbf{NH}_4 + \textbf{OH}^- \qquad \text{(Equation 1.3)}$$

as a result of heterotrophic activity (Tisdale et al, 1993). Aminization is the decomposition of organic material (primarily proteins) into amines, amino acids, and urea. This process is dominated by bacteria in alkaline environments and fungi under very acidic conditions (Reported in Tisdale et al., 1993). The amines, amino acids, and urea are further broken down during ammonification into ammonium by other heterotrophs (Reported in Tisdale et al, 1993). Heterotrophs use the carbon in the organic material as an energy source. In cases where organic nitrogen is high in relation to carbon, more nitrogen will be released to the surrounding environment (Reported in Tisdale et al., 1993). This process accelerates as temperatures increase (from 5^{o}C to 40^{o}C, optimum being 30^{o}C to 35^{o}C), provided there is sufficient oxygen and carbon. In streams or anaerobic waterlogged conditions, this process still occurs but is slowed (Reported in Tisdale et al., 1993). Phosphorous can also be mineralized via the phosphatase catalyzed reaction (Tisdale et al., 1993). Organic nitrogen and phosphorous can also be converted to inorganic nitrogen and phosphorous by grazing invertebrates that ingest nitrogen-rich organic material and excrete it as ammonia and phosphate (Triska et al.,1984).

1.4.3.2 Immobilization

Immobilization is the reverse of mineralization: inorganic nutrients are converted to organic forms. Microbes take up nutrients and incorporate them into their tissues (Boling et al., 1975). In cases where nitrogen and phosphorous content is low in relation to carbon, organisms will utilize available ammonium and nitrate as a source of nitrogen and phosphate as a source of phosphorous, thus lowering the nitrogen and phosphorous levels in the surrounding environment (Tisdale et al., 1993).

1.4.3.3 Role of Carbon-to-Nitrogen Ratio in Mineralization and Immobilization

The carbon-to-nitrogen ratio (C/N ratio) refers to the amount of carbon relative to the amount of nitrogen present in decomposing residuals. The importance of the C/N ratio in the organic matter of an aquatic environment (in this study, a flowing canal system) is that it controls mineralization and immobilization. If the C/N ratio is high, nitrogen in the forms of ammonium or nitrate in the sediment or water column can be used for further decomposition, resulting in an overall net immobilization (Reported in Tisdale et al., 1993). The nitrogen is utilized in the growth of the microbial population. If the C/N ratio is low, the microbes utilize the nitrogen within the organic matter in the decomposing material to grow, resulting in an overall net mineralization (Reported in Tisdale et al., 1993). Tisdale et al. (1993) reported that in C/N ratios between 20:1 and 30:1, neither a net mineralization nor a net immobilization occurs. Litterfall has an average C/N ratio of 15:1, which would result in net mineralization of its nitrogen (Johnston, 1991; Lorenz et al., 2000; Oelbermann and Gordon, 2000).

1.4.3.4 Role of Carbon-to-Phosphorous Ratio in Mineralization and Immobilization

The carbon-to-phosphorous ratio (C/P ratio) refers to the amount of carbon relative to the amount of phosphorous present in decomposing residuals. As with the C/N ratio, when the C/P ratio is high (>300), immobilization will occur as inorganic phosphate from the environment is consumed to continue decomposition (Reported in Tisdale et al., 1993). If the C/P ration is low (<200), mineralization of a portion of the organic phosphorous within the decomposing material will occur (Reported in Tisdale et al., 1993). C/P ratios between 200 and 300 result in no gain or loss of inorganic phosphorous in the system (Reported in Tisdale et al., 1993).

1.4.3.5 Nitrification

Nitrification is the conversion of ammonium (NH_4) to nitrate (NO_3) via a two-step process that is moderated by nitrifying bacteria (Equations 1.4 and 1.5):

$$2NH_4^+ + 3O_2 \xrightarrow[Nitrosomonas]{} 2NO_2^- + 2H_2O + 4H^+ \qquad \text{(Equation 1.4)}$$

$$2NO_2^- + O_2 \xrightarrow[Nitrobacter]{} 2NO_3^- \qquad \text{(Equation 1.5)}$$

The first step is the biological oxidation of ammonium (NH_4) to nitrite (NO_2). The second step is to further oxidize the nitrite (NO_2) to nitrate (NO_3). Factors affecting this process are the availability of ammonium (Jensen et al., 1994), oxygen availability (Rysgaard et al., 1994), pH (Wyer, 1988), temperature (Tisdale et al., 1993), and population levels of nitrifying bacteria (Tisdale et al., 1983). Nitrification cannot occur without ammonium present because ammonium is the form of nitrogen required for this process to occur. As the ammonium concentration increases, the potential for nitrification also increases. As

temperatures fall below a certain level, the nitrification process will slow. Optimum temperatures for nitrification are between 25°C and 35°C. Nitrification will also slow as the pH falls. The normal pH range for nitrification is 4.5 to 10, with the optimum pH being 8.5 (Reported in Tisdale et al., 1993). Nitrification takes place in the aerobic portion of the soil as well as in the water column when there are high levels of available oxygen (Jensen et al., 1994). The presence of an adequate supply of calcium and $H_2PO_4^-$ phosphate is required for nitrification to occur. The canal used for this study had a pH of between 4 and 6, which resulted in $H_2PO_4^-$ being the only phosphate form present.

1.4.3.6 Denitrification

Denitrification has been identified as the only method that truly removes nitrogen from the system (Chatarpaul et al., 1979; Swank and Caskey, 1982; Hill and Sanmugadas, 1985; Jensen et al.,1994; Seitzinger, 1988). Denitrification refers to the reduction of nitrate (NO_3^-) to the gaseous nitrous oxide (N_2O) and elemental N (N_2) (Equation 1.6) via anaerobic respiration of facultative organisms that make use of the nitrate as an electron acceptor in the absence of oxygen (O_2) (Tisdale et al., 1993).

$$\mathbf{2HNO_3} \xrightarrow[-2H_2O]{+4H} \mathbf{2HNO_2} \xrightarrow[-2H_2O]{+2H} \mathbf{2NO} \xrightarrow[-H_2O]{+2H} \mathbf{N_2O}\uparrow \xrightarrow{+2H,\ -H_2O} \mathbf{N_2}\uparrow \quad \text{(Equation 1.6)}$$

Nitrate Reductase | Nitrite Reductase | Nitric Oxide Reductase | Nitrous Oxide Reductase

Typical denitrificating genera include *Pseudomonas sp., Micrococcus sp., Denitrobacillus sp., Spirillum sp., Achromobacter sp., Bacillus sp.,* and *Paracoccus sp*. (Tisdale et al., 1993; Painter, 1970). As oxygen levels fall, these normally aerobic bacteria shift to an anaerobic respiration relying on nitrates. This is possible due to the enzymes nitrate reductase (reducing

NO_3^- to NO_2), nitrite reductase (reducing NO_2 to NO), nitric oxide reductase (reducing NO to N_2O), and nitrous oxide reductase (reducing N_2O to N_2) (Kloos et al., 2001).

The result of denitrification is the removal of nitrogen from a system by converting it to gaseous forms (N_2O and N_2) that are lost to the atmosphere. In stream ecosystems, denitrification occurs in a zone that encompasses the upper sediments along the bottom of the stream. This zone, the hyporheic zone (Hynes, 1983) (subsurface interstitial flow with 10% or greater channel water present, which runs beneath and parallel to its upper boundary, the stream channel, and over its lower boundary, the groundwater), is divided into two parts, an upper aerobic portion and a lower anaerobic portion (Figure 1.2). Nitrification, the transformation of ammonium (NH_4) to nitrate (NO_3^-), occurs in the aerobic portion, while denitrification (nitrification - denitrification coupling) occurs in the anaerobic portion (Hynes, 1983). Where this zone contacts the groundwater is the boundary of the stream ecosystem (Triska et al., 1989b). The primary transport mechanism between the hyporheic zone and the stream channel is advection in its upper layer, with diffusion due to gradients in the lower layer (Triska et al., 1989b). Higher denitrification rates can occur during summer months when water temperatures are higher (oxygen is less soluble in warmer water, reducing the movement of oxygen to the sediments (Terry and Nelson, 1975; van Kessel, 1977; Hill, 1988)). When water velocity is slower, the time of residency within the reach is increased, allowing the possibility of more nitrate moving into the anaerobic sediment layers, which facilitates the denitrification process (Jansson et al., 1994). Denitrification rates are affected by many factors: molecular diffusion (Jensen et al., 1994), dissolved oxygen concentration (Rysgaard et al., 1994), pH (Waring and Gilliam, 1983), organic carbon supply

(Swank and Caskey, 1982), temperature (Dawson and Murphy, 1972), nitrate supply (van Kessel, 1977), and denitrifier population levels (Tisdale et al., 1993).

Molecular diffusion is defined by Audesirk and Audesirk (1993) as "the net movement of molecules in a fluid from regions of high concentration to regions of low concentration, driven by the concentration gradient". Diffusion of nitrogen species in a system composed of an aerated water column overlaying an anaerobic denitrifying sediment found in most streams and rivers causes nitrate to move from the water column to the sediments and ammonium to move from the sediments to the water column by diffusion (Jensen et al., 1994). Nitrate is denitrified in the denitrifying sector of the hyporheic zone in the sediment, resulting in a lower concentration of nitrate within the hyporheic zone and creating a gradient between the sediments (with lower nitrate concentrations) and the overlaying water column (with higher nitrate concentrations). This creates a net movement of nitrate from the water column into the denitrifying sector within the hyporheic zone.

Ammonium, on the other hand, is rapidly converted to nitrate under aerobic conditions through nitrification, resulting in little to no ammonium in the water column over the sediments. The ammonium originates in the sediments as organic matter that has formed a decomposing organic layer of material on the surface of the sediment or has been buried and decomposed in the sediment. This creates a large reservoir of ammonium in the hyporheic zone in the sediments, which results in relatively high concentrations of ammonium in the sediment pore water. The gradient thus causes movement of ammonium from the sediments (with higher concentrations) toward the water column (with lower concentrations). As the ammonium moves from the anaerobic sediments to the shallower aerobic sediments and the lower portion of the water column, it is nitrified into nitrate and

starts moving in the opposite direction, according to the nitrate gradient. This phenomenon results in nitrification-denitrification coupling—the denitrification of nitrates formed from sediment ammonium that had been nitrified.

In a study by van Kessel (1977), as dissolved oxygen concentrations increased, the denitrification of the nitrates in the water column decreased. When oxygen concentration in the water column increased from 0 mg/L to 2 mg/L, the denitrification rate decreased approximately 13% to 17% in two sediments: from 6.7 mg NO_3-N /m^2/h to 5.8 mg NO^3-N /m^2/h and from 5.0 mg NO^3-N /m^2/h to 4.2 mg NO^3-N /m^2/h respectively. The denitrification rate remained constant as oxygen concentrations increased. Rysgaard et al. (1994) found that the denitrification of water column nitrate decreased by four-fifths, from 2.8 mg NO^3-N /m^2/h to 0.7 mg NO^3-N /m^2/h, as oxygen concentrations increased from 0 mg/L to 6 mg/L, while denitrification of nitrate nitrified in the sediment increased from 0.0 mg NO_3-N /m^2/h to 0.7 mg NO_3-N /m^2/h, resulting in an overall denitrification rate reduction of only around 50%. Rysgaard et al. also found that as oxygen levels increase above 6 mg/L, denitrification of nitrate from the water column continued to decline but at a much reduced rate, and denitrification of nitrates from sediment nitrification slowly increased, resulting in little further change to the overall total denitrification rate of approximately 1.4 mg NO_3-N /m^2/h. This was also the case in other studies (e.g., Anderson, 1977; Christensen et al., 1990).

Waring and Gilliam (1983) found that after four days of incubation, waterlogged soils with a pH higher than approximately 4.0 showed similar nitrate removal, while those with pH values lower than 4.0 showed a decrease in nitrate removal from 100 mg/L loss to around 20 mg/L loss at a pH of 3.0.

Carbon is important to denitrification because it is required in nitrate reduction, as shown in Equation 1.7.

$$\mathbf{5(CH_2O) + 4NO_3^- + 4H^+ \Uparrow 5CO_2 + 2N_2 + 7H_2O} \qquad \text{(Equation 1.7)}$$

Based on Equation 1.7, it takes 1mg/L of available C for the production of 1.17 mg/L of N as nitrite (N_2O) or of 0.99 mg/L of N as dinitrogen gas (N_2) (Tisdale et al., 1993).

Temperatures ranging from 5^{o}C to 27^{o}C were shown by Dawson and Murphy (1972) to have substantial denitrification rates (ranging from 0.0135 mg/L/h to 0.1590 mg/L/h respectively). At temperatures lower than 5^{o}C, denitrification occurs but at a much reduced rate, until freezing, at which point it ceases. At temperatures above 27^{o}C, denitrification increases only slightly, until about 60^{o}C, when denitrification ceases (Reported in Tisdale et al., 1993).

An increase in nitrate concentration in the water column was shown to increase denitrification by both van Kessel (1977) and Rysgaard et al. (1994). Van Kessel (1977) found that denitrification increased from 0.0 mg/m^2/h to 25 mg/m^2/h as nitrate concentrations increased from 0.0mg/L to approximately 200 mg/L in the overlying water column. This rate stayed constant at higher concentrations. Rysgaard et al. (1994) found a 1.2:1 increase in denitrification to concentration of overlying water column concentrations.

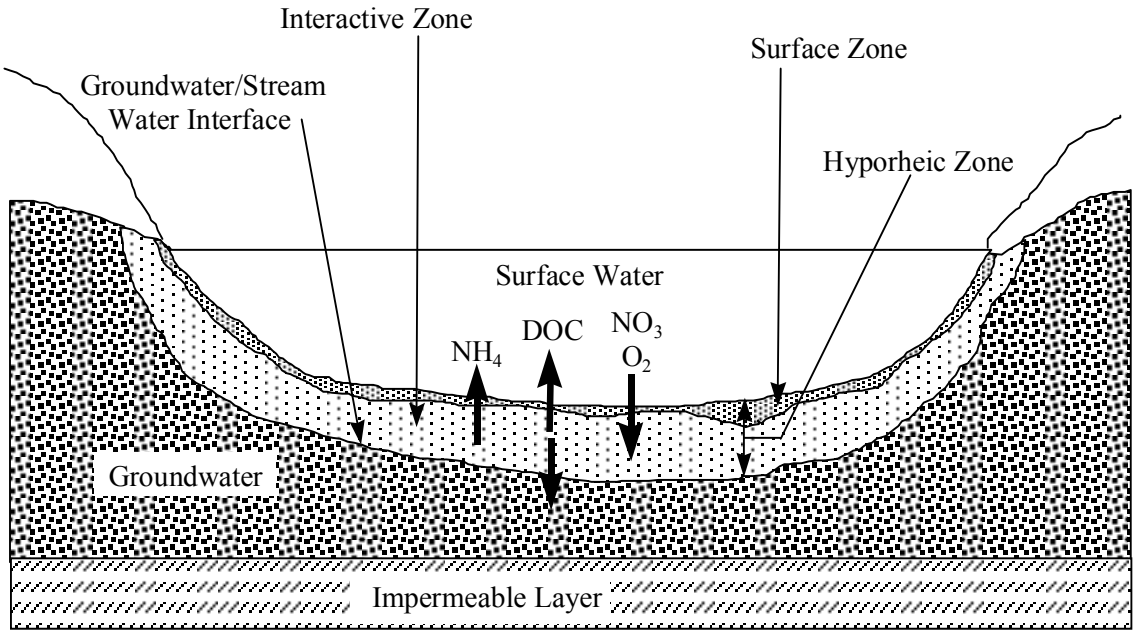

Figure 1.2. Hyporheic Zone.

1.4.4 Spiraling Processes

In-stream spiraling processes, or nutrient recycling, occurs by the transformation of nutrients from one form to another form and back again (Meyer et al., 1981). An example of this is the uptake of nitrogen from the inorganic pool (NH_4 or NO_3) utilized for plant production (conversion to organic nitrogen - immobilization), thus removing it temporarily from the stream system (Jansson et al., 1994; Cooke and Cooper, 1988; Hill, 1988; Owens et al., 1972). In one study, Cooke and Cooper (1988) found that in open agricultural ditches, as much as 75% of the nitrogen in a stream can be retained in aquatic plants. When the plant dies, it is decomposed and the nitrogen is released in a particulate organic form that can remain as particulate organic nitrogen, become dissolved organic nitrogen, or be mineralized

back into inorganic nitrogen form (NH_4) and further nitrified into nitrate (NO_3) within the stream. This also occurs as grazing animals such as crayfish, salamanders, and small invertebrates feed on particulate material within the stream (Woodall, 1975; Cummings, 1974), utilizing the organic forms of nitrogen in their growth. This removes nitrogen from the nitrogen pool until it is excreted as ammonia or as the animal dies and decomposes, releasing the nitrogen as organic or inorganic nitrogen, depending on the level of decomposition. Spiraling processes can be interrupted and result in a permanent removal of nitrogen if the plants or grazing animals are harvested from the stream by terrestrial grazers or predators.

1.5 Summary

Stream nutrients come from many sources—hydrologic, allochthanous, and autochthanous—and have several fates: discharge at the mouth, emergence drift, and denitrification, as well as storage within the stream ecosystem in plant and animal tissues, organic mater, and sediments. The fates of these nutrients are determined by the in-stream processes (physical, chemical, and biological) at work within the stream. Though physical and chemical processes change the forms of stream nutrients (fragmentation of particulate matter or particulate to dissolved) or their availability (sediment adsorption), the only path of nitrogen removal from streams is denitrification (conversion of nitrate to nitrous oxide and nitrogen gas), although minor amounts are lost via emergence (insects developing within the stream and leaving as adults). The only natural path of phosphorus removal from the stream is emergence, though this is minor. Most phosphorous is discharged at the outlet. Nitrogen and phosphorous can also be removed from the system through human activities such as canal dredging and clean-out. Spiraling processes such as plant uptake, adsorption to

sediments, and sedimentation into the stream bed only temporarily store nutrients, re-releasing them at a later time within the system.

This study, located in the lower coastal plain of North Carolina, was conducted on a slow-moving (velocity ≈ 0.04 m/s), heavily forest canopied, high dissolved oxygen (concentrations ranging from 5 mg/L to 9 mg/L during flow), acidic (pH ≈ 4 to 5) canal that has little to no submergent or emergent vegetation typical of the area. This results in long residency times, allochthonous carbon sources, and fungi-dominated mineralization, with little to no plant uptake of nutrients. The relatively high dissolved oxygen content of the stream during the fall and winter restricts the denitrification activity to the lower portion of the hyporheic zone.

References

Amatya, D.M., R.W. Skaggs, and J.D. Gregory. 1996. Effects of controlled drainage on the hydrology of drained pine plantations in the North Carolina coastal plain. J. Hydrology 181:211-232.

Amatya, D.M., J.W. Gilliam, R.W. Skaggs, M.E. Lebo, and R.G. Campbell. 1998. Effects of controlled drainage on forest water quality. J. Environ. Qual. 27(4): 923-935.

Anderson, J.M. 1977. Rates of denitrification of undisturbed sediment from six lakes as a function of nitrate concentration, oxygen and temperature. Arch. Hydrobiol. 80: 147-159.

Aubertin, G.M., D.W. Smith, J.H. Partice, 1973. Quantity and quality of streamflow after urea fertilization on a forested watershed: first year results. In: Forest Fertilization Symposium Proceedings. USDA Forest Service General Technical Report NE-3, pp.88-100.

Audesirk, G. and T. Audesirk. 1993. Biology, Life on Earth. 3rd Ed. Macmillan Publishing Company. New York.

Berg, M.P., H.A. Verhoef. 1998. Ecological characteristics of a nitrogen saturated coniferous forest in The Netherlands. Biol. Fertil. Soils 26: 258-267.

Bisson, P.A., G.G. Ice, C.J. Perrin, and R.E. Bilby. 1992. Effects of forest fertilization on water quality and aquatic resources in the Douglas-fir region. In: Forest Fertilization: Sustaining and Improving Nutrition and Growth of Western Forests. University of Washington, Seattle, pp. 179-193.

Boling, R.H., E.D. Goodman, J.A. Van Sickle, J.O. Zimmer, K.W. Cummins, R.C. Busch, and S.G. Fisher. 1981. Metabolism of a desert stream. Freshwater Biol. 11:301-307.

Boling, R.H., E.D. Goodman, J.A. Van Sickle, J.O. Zimmer, K.W. Cummins, R.C. Petersen, S.R. Reice. 1975. A model of detritus processing in a woodland stream. Ecology 56(1): 141-151.

Callesen, I., K. Raulund-Rasmussen, P. Gundersen, and H. Stryhn. 1999. Nitrate concentrations in soil solutions below Danish forests. For. Ecol. Manage. 114: 71-82.

Campbell, J.L., J.W. Hornbeck, W.H. Mcdowell, D.C. Buso, J.B. Shanley, and G.E. Likens. 2000. Dissolved organic nitrogen budgets for upland, forested ecosystems in New England. Biogeochem. 49: 123-142.

Chatarpaul, L., J.B. Robinson, and N.K. Kaushik. 1979. Role of tubificid worms on nitrogen transformations in stream sediment. J. Fish. Res. Board Can. 36:673-678.

Christensen, P.B. L.P. Nelsen, J. Sörensen, and N.P. Revsbech. 1990. Denitrification in nitrate-rich streams: Diurnal and seasonal variation related to benthic oxygen metabolism. Limnol. Oceanogr. 35. 640-651.

Christensen, P.B. and J. Sørensen. 1988. Denitrification in sediment of lowland streams: regional and seasonal variation in Gelbæk and Rabis Bæk, Denmark. FEMS Microbiol. Ecol. 53: 335-344.

Cooke, J.G., and A.B. Cooper. 1988. Sources and sinks of nutrients in a New Zealand hill pasture catchment III. nitrogen. Hydrol. Proc. 2:135-149.

Cooper, A.B., and J.G. Cooke. 1984. Nitrate loss and transformation in two vegetated headwater streams. N. Z. J. March Freshwater Res. 18:441-450.

Croke, J., P. Hairsine, and P. Fogarty. 2000. Nutrient movement due to overland flow in managed native *Eucalyptus* forests, southeastern Australia. Water, Air, and Air Pollut. 122: 17-35.

Cronan, C.S., J.T. Piampiano, and H.H. Patterson. 1999. Influence of land use and hydrology on exports of carbon and nitrogen in a Maine river basin. J. Envir. Qual. 28(3): 953-961.

Cummins, K.W. 1974. Structure and function of stream ecosystems. BioScience 24:631-641.

Cushing, C.E., and E.G. Wolf. 1982. Organic energy budget of Rattlesnake Springs, WA. American Midland Naturalist 107:404-407.

Dawson, R.N. and K.L. Murphy. 1972. The temperature dependency of biological denitrification. Wat. Res. 6:71-83).

De Schhrijver, A., G. van Hoydonck, L. Nachtergale, L. De Keersmaeker, S. Mussche, and N. Lust. 2000. Comparison of nitrate leaching under Silver Birch (Betula Pendula) and Corsican Pine (Pinus Nigra spp. Laricio) in Flanders (Belgium). Water, Air, and Soil Pollut. 122: 77-91.

Duff, J.H., C.M. Pringle, and F.J. Triska. 1996. Nitrate reduction in sediments of lowland tropical streams draining swamp forest in Costa Rica: an ecosystem perspective. Biogeochem. 33: 179-196.

Duff, J.H., F.J. Triska, and R.S. Oremland. 1984. Denitrification associated with stream periphyton: chamber estimates from undisturbed communities. J. Environ. Qual. 13: 514-518.

Fisher. R.F. 1981. Impact of intensive silviculture on soil and water quality in a coastal lowland. 299-309. In: R. Lal and E.W. Russel, eds. Tropical Agriculture Hydrology. Wiley, New York.

Fisher, S.G., and G.E. Likens. 1973. Energy flow in Bear Brook, New Hampshire: an integrative approach to aquatic ecosystem metabolism. Ecol. Monog. 43:421-439.

Fromm, J.H. and R.B. Herrmann. 1996. Jones-5 fertilizer runoff monitoring - 1992. Weyerhaeuser Research and Development Report, Southern Environmental Field Station, New Bern, NC.

Gosz, J.R., G.E. Likens, F.H. Bormann. 1972. Nutrient content of litterfall on the Hubbard Brook experimental forest, New Hampshire. Ecology 53(5): 769-784.

Gunderson, P. and L. Ramussen. 1995. Nitrogen mobility in a nitrogen limited forest at Klosterhede, Denmark, examined by NH_4NO_3 addition. For. Ecol. Manage. 71: 75-88.

Hamburg, S.P., and T.C. Lin. 1998. Throughfall chemistry of an ecotonal forest on the edge of the Great Plains. Can. J. For. Res. 28: 1456-1463.

Hill, A.R. 1988. Factors influencing nitrate depletion in a rural stream. Hydrobiologia. 160:111-122.

Hill, A.R., and K. Sanmugadas. 1985. Denitrification rates in relation to stream sediment characteristics. Wat Res. 19: 1579-1586.

Horne, A.J., and C.J.W. Carmiggelt. 1975. Algal nitrogen fixation in California streams: seasonal cycles. Freshwat. Biol. 5:461-470.

Hyer, K.E., J.R. Webb, and K.N. Eshleman. 1995. Episodic acidification of three streams in Shenandoah National Park, Virginia, USA. Water, Air, and Soil Pollut. 85: 523-537.

Hynes, H.B.N. 1983. Groundwater and stream ecology. Hydrobiologia 100: 93-99.

Jansson, M., L. Leonardson, and J. Fejes. 1994. Denitrification and nitrogen retention in a farmland stream in southern Sweden. Am. Bio. 23(6): 326-331.

Jewel, W.J. 1971. Aquatic weed decay: dissolved oxygen utilization and nitrogen and phosphorous regeneration. J. Wat. Pollut. Control Fed. 43(7): 1457-1467.

Jensen. K., N.P. Sloth, N. Risgaard-Petersen, S. Rysgaard, and N.P. Revsbech. 1994. Estimation of nitrification and denitrification from microprofiles of oxygen and nitrate in model sediment systems. Appl. Environ. Microbiol. 60(6): 2094-2100.

Johnston, C.A. 1991. Sediment and nutrient retention by freshwater wetlands: effects on surface water quality. CRC Crit. Rev. Environ. Control. 21: 491-565.

Johnson, D.W., D. Todd. 1988. Nitrogen fertilization of poplar and pine plantations. Soil Sci. Soc. Am. 52: 1468-1477.

Kloos, K., A. Mergel, C. Rösch, and H. Bothe. 2001. Denitrification within the genus *Azospirillum* and other associative bacteria. Aust. J. Plant Physiol. 28: 991-998.

Kuwabara, J.S., and P. Helliker. 1988. Trace contaminants in streams. Civil Engineering Practice, Environmental 5(26):739-765.

Leanard, J.H. 1977. Nitrogen run-off from radiata pine forest fertilization with urea. NZ. J. For. Sci. 22: 64-80.

Lebo, M.E. and R.B. Herrmann. 1998. Harvest impacts on forest outflow in coastal North Carolina. J. Environ. Qual. 27(6): 1382-1395.

Lorenz, K., C.M. Preston, S. Raspe, I.K. Morrison, K.H. Feger. 2000. Litter decomposition and humus characteristics in Canadian and German spruce ecosystems: information from tannin analysis and ^{13}C CPMAS NMR. Soil Biology and Biochemistry 32: 779-792.

McClurkin, D.C. and P.D. Duffy. 1975. Evaluating Impact of Forest Site Preparation on Soil and Water Quality in the Gulf Coastal Plain. In: B. Bernier and C.H. Winget, eds. Forest Soils and Forest Land Management. Les Presses de l'Université Laval, Quebec, Canada, pp. 315-321.

McDonald, M.A., and J.R. Healey. 2000. Nutrient cycling in secondary forests in the Blue Mountains of Jamaica. For. Ecol. and Manage. 139: 257-278.

McDowell, W.H. and S.G. Fisher. 1976. Autumnal processing of dissolved organic matter in a small woodland stream ecosystem. Ecology 57: 561-569.

Meyer, J.L. and G.E. Likens. 1979. Transport and transformations of phosphorous in a forest stream ecosystem. Ecology 60(6): 1255-1269.

Meyer, J.L., G.E. Likens, and J. Sloane. 1981. Phosphorous, nitrogen and organic carbon flux in a headwater stream. Arch. Hydrobiol. 91(1): 28-44.

Miller, P., A. Bytnerowiez, M. Fenn, M. Poth, P. Temple, S. Schilling, D. Jones, D. Johnson, J. Chow, and J. Watson. 1998. Multidisciplinary study of ozone, acidic deposition and climate effects on a mixed conifer forest in California, USA. Chemosphere 36(4-5): 1001-1006.

Minshall, G.W. 1967. Role of allochthonous detritus in the trophic structure of a woodland spring brook community. Ecology 48:139-149.

Muzika, R.M., J.B. Gladden, and J.D. Haddock. 1987. Structural and functional aspects of succession in southeastern floodplain forests following a major disturbance. Am. Midl. Nature 117: 1-9.

Newbold, J.D., J.W. Elwood, M.S. Schulze, R.W. Stark, and J.C. Barmeier. 1983. Continuous ammonium enrichment of a woodland stream: uptake kinetics, leaf decomposition, and nitrification. Freshwater Biol. 13: 193-204.

Nohrstedt, H.Ö. 1992. Soil water chemistry as affected by liming and N fertilization at two Swedish coniferous forest sites. Scand. J. For. Res. 7: 143-153.

Oelbermann, M., and A.M. Gordon. 2000. Quality and quantity of autumnal litterfall into a rehabilitated agricultural stream. J. Environ. Qual. 29:603-611.

Owens, M., J.H.N. Garland, I.C. Hart, and G. Wood. 1972. Nutrient budgets in streams. Symp. Zool. Soc. Lond. 29: 21-40.

Painter, H.A. 1970. A review of literature on inorganic nitrogen metabolism in micro-organisms. Wat. Res.. 4: 393-450.

Peterson, R.C. and K.W. Cummings. 1974. Leaf processing in a woodland stream. Freshwat. Biol. 4: 343-368.

Ponnamperuma, F.N. 1972. The chemistry of submerged soils. Adv. Agron. 24: 29-96.

Ring, E. and H.Ö. Nohrstedt. 1993. Stream water chemistry after two forest fertilizations with Skog Vital in central Sweden. Skogforsk Report #3. Forest Research Institute of Sweden, Uppsala.

Robertson, S.M.C., M. Hornung, V.H. Kennedy. 2000. Water chemistry of throughfall and soil water under four tree species at Gisburn, northwest England, before and after felling. For. Ecol. Manage. 129: 101-117.

Robinson, J.B., H.R. Whiteley, W. Stammers, N.K. Kaushik, and P. Sain. 1979. The fate of nitrate in small streams and its management implications, p. 247-259. In: Proc. 10th Annu. Agric. Waste Manage. Conf. Cornell University, Ithaca, NY.

Rysgaard, S., N. Rysgaard-Petersen, N.P. Sloth, K. Jensen, and L.P. Nielsen. 1994. Oxygen regulation of nitrification and denitrification in sediments. Limnol. Oceanogr. 39(7): 1643-1652.

Sauer, T.J., T.C. Daniel, D.J. Nichols, C.P. West, P.A. Moore Jr., and G.L. Wheeler. 2000. Runoff water quality from litter-treated pasture and forest soils. J. Environ. Qual. 29: 515-521.

Schroth, G., M.E.A. Elias, K. Uguen, R. Seixas, and W. Zech. 2001. Nutrient fluxes in rainfall, throughfall and stemflow in tree-based land use systems and spontaneous tree vegetation of central Amazonia. Agric. Ecosys. and Environ. 87: 37-49.

Sedell, J.R., F.J. Triska, J.D. Hall, N.H. Anderson, and J.H. Lyford. 1974. Sources and fates of organic inputs in coniferous forest streams. 57-69 In: R.H. Waring, ed. Integrated Research in the Coniferous Forest Biome. Proceedings, AIBS Symposium Coniferous Forest Ecosystem. Bulletin Number 5, Coniferous Forest Biome, University of Washington AR-10, Seattle.

Seely, B., K. Lajtha, and G.D. Salvucci. 1998. Transformation and retention of nitrogen in a coastal forest ecosystem. Biogeochem. 42: 325-343.

Seitzinger, S.P. 1988. Denitrification in freshwater and coastal marine ecosystems: ecological and geochemical significance. Limnol. Oceanogr. 33(4):702-704.

Seitzinger, S.P. 1994. Linkages between organic matter mineralization and denitrification in eight riparian wetlands. Biogeochem. 25: 19-39.

Stay, E.S., A. Katko, K.W. Malueg, M.R. Crouse, S.E. Dominguez, and R.E. Austin. 1979. Effects of forest fertilization with urea on major biological components of small Cascade streams, Oregon. EPA-600/3-79-099. USEPA Environmental Research Lab. Corvallis, Oregon. p. 60.

Suberkropp, K., G.L. Godshalk, and M.J. Klug. 1976. Changes in the chemical composition of leaves during processing in a woodland stream. Ecology 57(4): 720-727.

Swank, W.T., and W.H. Caskey. 1982. Nitrate depletion in a second-order mountain stream. J. Environ. Qual. 11:581-584.

Teal, J.M. 1957. Community metabolism in a temperate cold spring. Ecol. Monog. 27:283-302.

Terry, R.E., and D.W. Nelson. 1975. Factors influencing nitrate transformations in sediments. J. Envir. Qual. 4:549-554.

Tisdale, S.L., W.L. Nelson, J.D. Beaton, and J.L. Havlin. 1993. Soil Fertility and Fertilizers. 5th ed. Macmillan Publishing Company, New York.

Triska, F.J., and B.M. Buckley. 1978. Patterns of nitrogen uptake and loss in relation to litter disappearance and associated invertebrate biomass in six streams in the Pacific Northwest, USA. Internationale Veeinigung fur theoretische und Angewandte Limnologie, Verhandlungen. 20:324-332.

Triska, F.J., V.C. Kennedy, R.J. Avanzino, G.W. Zellweger, and K.E. Bencala. 1989a. Retention and transport of nutrients in a third order stream: channel process. Ecology 70(6): 1877-1892.

Triska, F.J., V.C. Kennedy, R.J. Avanzino, G.W. Zellweger, and K.E. Bencala. 1989b. Retention and transport of nutrients in a third order stream: hyporheic processes. Ecology 70(6): 1893-1905.

Triska, F.J., J.R. Sedell, and S.V. Gregory. 1982. Coniferous forest streams. 292-332. In: R.L. Edmonds, ed. Analysis of Coniferous Forest Ecosystems in the Western United States. Hutchinson Ross, Stroudsberg, PA.

Triska, F.J., J.R. Sedell, K. Cromack Jr., S.V. Gregory, and F.M. McCorison. 1984. Nitrogen budget for a small coniferous forest stream. Ecol. Monog. 54(1): 119-140.

van Kessel, J.F., 1977. Factors affecting the denitrification rate in two water sediment systems. Wat. Res. 11:259-267.

van Miegroet, H., R.J. Norby, T.J. Tschaplinski. 1994. Nitrogen fertilization strategies in a short-rotation sycamore plantation. For. Ecol. Manage. 64: 13-24.

Waring, S.A. and J.W. Gilliam. 1983. The effect of acidity on nitrate reduction and denitrification in lower coastal plain soils. J. Soil Sci. 47(2): 246-251.

Webb, J.R., B.J. Cosby, F.A. Deviney, K.N. Eshleman, and J.N. Galloway. 1995. Change in the acid-base status of an Appalachian mountain catchment following forest defoliation by the gypsy moth. Water, Air, Soil Pollut. 85: 535-544.

Wells, C.G., C.E. Murphy, C. Davis, D.M. Stone, and G.J. Hollod. 1985. Effect of sewage sludge from two sources on element flux in soil solution of loblolly pine plantations. In: Cole, D., C. Henry, and W. Nutter, eds. The Forest Alternative for Treatment and Utilization of Municipal and Industrial Wastes. University of Washington Press, Seattle, pp. 154-165.

Wetzel, R.G., and B.A. Manny. 1972. Decomposition of dissolved organic carbon and nitrogen compounds from leaves in an experimental hard water stream. Limnol. Oceanogr. 17(6): 927-931.

Wollum, A.G., and C.B. Davey. 1975. Nitrogen Accumulation, Transformation, and Transport in Forest Soils. In: B. Bernier and C.H. Winget, eds. Forest Soils and Forest Land Management. Les Presses de l'Université Laval, Quebec, Canada, pp. 67-106.

Woodall, W. 1975. Mineral pathways in small Appalachian streams. 408-422. In: F.G. Howell, J.B. Gentry, and M.H. Smith, eds. Mineral Cycling in Southeastern Ecosystems. Energy Research and Development Administration Symposium Series (CONF-740513), Washington, D.C.

Wyer, M.D. 1988. Nitrification in Ontario stream sediments. Wat. Res. 22(3): 287-292.

Chapter 2

Field Evaluated Values of Inputs, Outputs from Surface Waters in Forested Watersheds

2.1 Site Description

This study was located in Washington County, near Plymouth, in the coastal plain of North Carolina (Figure 2.1). The 10,000 ha watershed drains into Albemarle Sound through a five-mile stretch of Kendrick's Creek. The portion of the watershed used for this study, the Parker Tract, is owned and managed by Weyerhaeuser Company and consists of approximately 4,000 ha of managed forest.

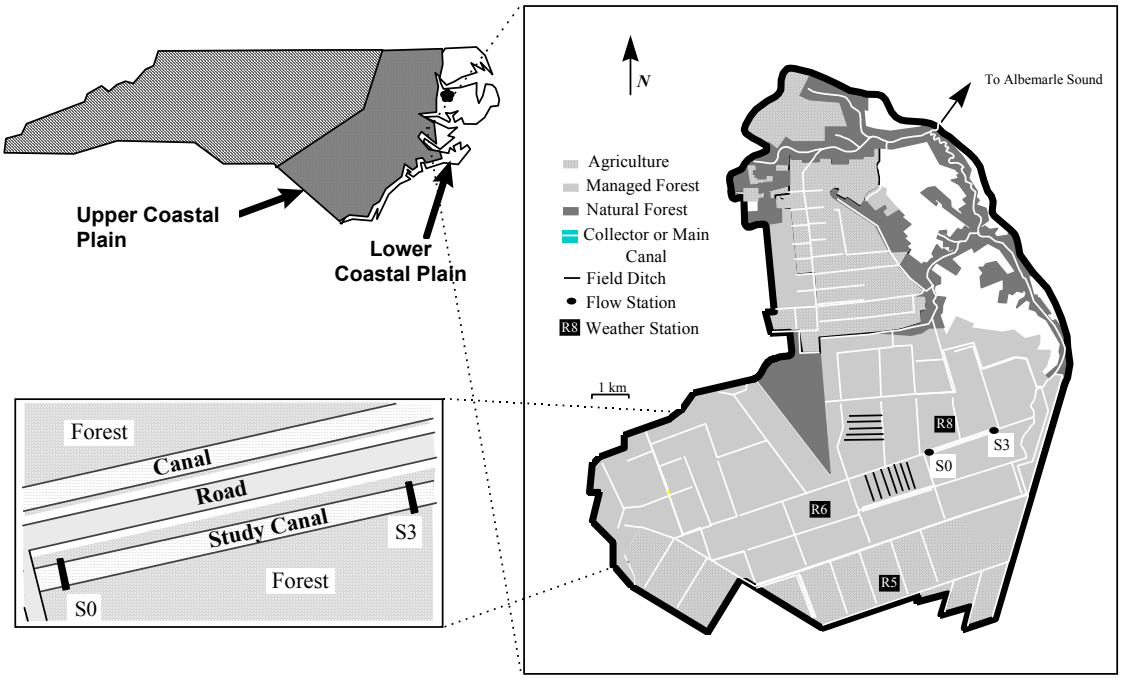

Figure 2.1. Location of Parker Tract watershed and canal study site.

The soils in the watershed are primarily organic soils of the Belhaven series (Loamy, mixed, dysic, thermic Terric Medisaprists) and Pungo series (Dysic, thermic Typic Medisaprists) with some mineral soils of the Portsmouth series (Fine-loamy over sandy or sandy-skeletal, mixed, thermic Typic Umbraquults) and Cape Fear series (Clayey, mixed, thermic Typic Umbraquults) being present to a lesser extent (SCS Soil Survey of Washington County, North Carolina, 1981). These soil series are characterized as very poorly drained with loamy subsoil.

2.2 Field description

A 1900 meter section of a forest drainage canal, from S0 to S3 (Figure 2.2), averaging four meters in top width, 1.4 meters in depth, average side slope of 1:1, and an overall bottom slope of 0.0003, was selected for the study. A litter layer (≈ 4 cm thick) and organic layer (≈ 20 cm thick) cover the bottom of the canal. Below ≈ 20 cm there is a thick sand layer underlain by an impermeable layer. All lateral field ditches were plugged and rerouted to the opposite end of their respective fields to create a continuous section of ditch with no surface water sources except at the upstream inflow (S0). The canal was constructed in the 1960's to lower ground water levels and improve trafficability and soil conditions for timber production. The canal is maintained as needed to manage drainage. The soil removed during construction was placed on the north side of the canal and made into a forest access road. The south side of the canal is composed of a combination of planted pine, mixed natural pine and hardwood, and natural hardwood stands (50%, 25%, and 25% of the canal study length respectively, Figure 2.2). The canal itself has a several-meter-wide strip of hardwoods along both banks that overhang the canal and shade the ditch during most of the year. During cleaning operations (usually during site prep prior to planting or as needed

between planting and harvest), these overhanging trees are removed as the canals are dredged to maintain flow. This allows light to penetrate the canals during the spring, summer, and fall. During the winter months, after the hardwoods have lost their leaves, there is a potential for sunlight to enter and strike the water's surface, but the sun at this time of year is low in the southern sky and is blocked by the forests along the southern bank of the canal. This canal normally has flow from the late fall (normally December) through the winter until mid-spring (normally April to May). In some years, flow will occur during the summer and early fall in response to heavy rains from tropical storms or repeated convective showers. The soil in the study area is composed of Belhaven series.

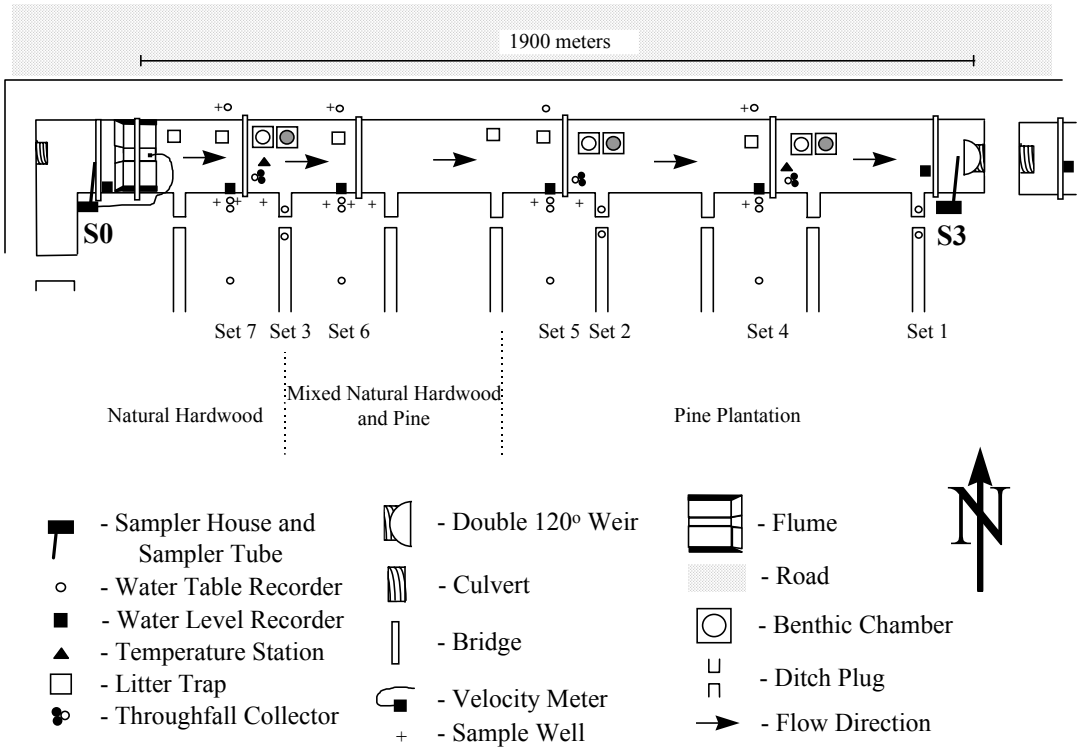

Figure 2.2. Study canal and equipment location.

2.3 Atmospheric Deposition

2.3.1 Rainfall

2.3.1.1 Methods

Rainfall data were collected within one kilometer of the study canal using a Hobo tipping bucket rain gauge (R8 in Figure 2.1). Rainfall samples were taken at a wetland site approximately 4 kilometers from the study site. Samples were analyzed for ammonium, nitrate, organic nitrogen, total phosphorous, phosphate, and chloride. Samples were taken as part of a larger watershed scale study and used here with permission. No statistical analysis was conducted on the rainfall water quality data due to the small number of samples taken per season.

Water samples were placed in a freezer immediately after collection and kept frozen until analysis. All samples were filtered through a 0.45 micron filter (Gelman Laboratory, Supor®-450) to remove particulate material. Each sample was analyzed for nitrate, ammonium, and phosphate, and dissolved organic, inorganic, and total carbon (Standard Methods, 1989).

2.3.1.2 Results and Discussion

The greatest rainfall occurred in the summer, when daily thunderstorms occur, with potentially high rainfall amounts(Table 2.1). The second greatest rainfall occurred in the spring, as thunderstorms begin during the latter part of that season. Rainfall was less in winter than in spring and summer. Although rainfall events during winter are normally much longer in duration, they are less frequent. These events are normally generated as cold fronts move through the area. The fall is normally a drier period, because cooling temperatures cause a decrease in thunderstorms, but the wintertime progression of cold fronts has not yet

started. The years presented here are three drought years, so annual rainfall was less than for an average rainfall year.

Table 2.1. Average seasonal rainfall amounts recorded at rain gauge R8 (2000-2002).

Season	Average Rainfall Amount (mm)
Spring (Mid-March – Mid-June)	265
Summer (Mid-June – Mid-September)	433
Fall (Mid-September – Mid-December)	132
Winter (Mid-December – Mid-March)	196
Total	1026

The nutrient content of the rainfall (Table 2.2) is similar to other studies summarized in Table 1.1. The nitrogen species are most prevalent in the organic form, followed by nitrates and then ammonium. Total phosphorous and phosphate are both at the lower end of detection.

Chloride is fairly constant throughout the year. The average concentration, approximately 2.62 mg/L, is due to the proximity of the site to the coast (approximately 100 km). As one moves further from the coast, the chloride content of rainfall decreases, typically ranging from approximately 2 mg/L near the coast to 0.1 mg/L in the Great Plains region (Reported in Tisdale et al., 1993).

Table 2.2. Average seasonal rainfall nutrient concentrations (1998-2001).

Season	Nutrient					
	NO_3-N	NH_4-N	Organic Nitrogen	Total Phosphorous	PO_4-P	Chloride
	Average Concentration (mg/L)					
Spring (Mid-Mar. – Mid-June)	0.36	0.43	0.77	0.06	0.02	2.89
Summer (Mid-June – Mid-Sept.)	0.08	0.25	1.12	0.10	0.02	2.12
Fall (Mid-Sept. – Mid-Dec.)	0.10	0.50	1.07	0.07	0.05	2.68
Winter (Mid-Dec. – Mid-Mar.)	0.41	0.34	0.27	0.08	0.03	3.30
Yearly Average	0.24	0.38	0.81	0.08	0.03	2.74
Volume Weighted Yearly Average	0.22	0.35	0.86	0.08	0.03	2.62

2.3.2 Throughfall

2.3.2.1 Methods

Throughfall inputs were measured using three throughfall collectors (Figure 2.3). The three collectors were located along the length of the study canal on posts approximately two meters above the midpoint of the canals. Each collector consisted of a pair of 15 cm diameter funnels, which directed throughfall into two separate 2 liter sample bottles. The funnels were screened with a 0.7 mm fiberglass mesh to remove larger material (which was collected in litter traps as described in the "Allochthonous Inputs" section) from the sample. The two sample bottles were located in separate, insulated, dark chambers to help preserve the sample until collected. A manual rainfall gauge was placed on the collector to record the total throughfall amounts for the sample period. Throughfall samples were taken from the collectors on a weekly basis after mixing the contents of each sample bottle. During periods of low throughfall, the contents of the two sample bottles from each collector were combined

into a single sample for each collector. Any throughfall remaining after sampling was discarded, and the sample bottle was rinsed prior to being reinstalled into the collector.

Water samples were placed in a freezer immediately after collection and kept frozen until analysis. All samples were filtered through a 0.45 micron filter (Gelman Laboratory, Supor®-450) to remove particulate material. Each sample was analyzed for nitrate, ammonium, and phosphate, and dissolved organic, inorganic, and total carbon (Standard Methods, 1989).

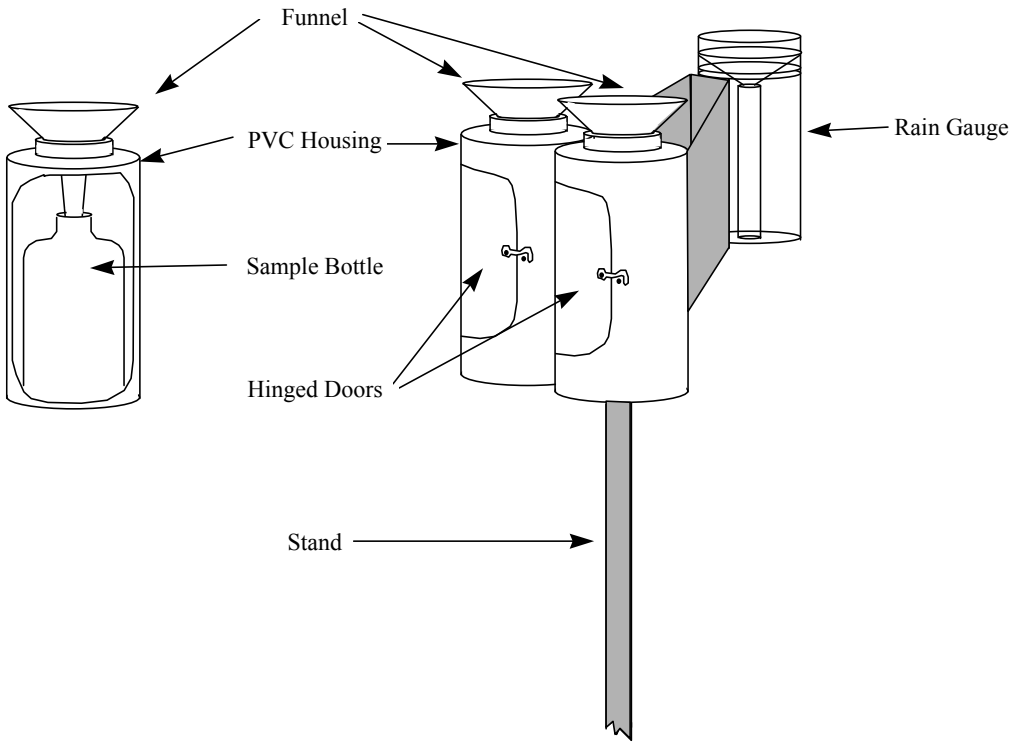

Figure 2.3. Throughfall collector.

2.3.2.2 Statistical Analysis

Statistical analysis was conducted on the average event chemical concentrations to determine seasonal and location main effects for each chemical of interest in the throughfall. Both event and volume weighted seasonal, annual, and location averages are presented for each chemical analyzed. A general linear model for the ammonium concentration of the throughfall is shown in Equation 2.1.

$$\text{Model: } Y = \mu + \alpha_i + \beta_j + (\alpha\beta)_{ij} + \varepsilon_{ij} \quad \text{Equation 2.1}$$

where: Y = the throughfall ammonium concentration
μ = the average throughfall ammonium concentration
α_i represents the main effects of season on the throughfall ammonium concentration (i = spring, summer, fall, winter)
β_j represents the main effects of location on the throughfall ammonium concentration (j = 1, 2, 3)
$(\alpha\beta)_{ij}$ represents the interactions between season and location on the throughfall ammonium concentration
ε_{ij} = error term.

The constraints of $\sum_i\alpha_i = 0$, $\sum_j\beta_j = 0$, $\sum_i\alpha_i\beta_j = 0$, $\sum_j\alpha_i\beta_j = 0$. The hypotheses being tested are: H_o: $\alpha_i = 0$ - no main effect of season, H_o: $\beta_j = 0$ - no main effect of location, and H_o: = 0 - no interactive effects between season and location on the ammonium concentration of the throughfall (Steel and Torrie, 1980). The same statistical model and constraints were used for analyzing the nitrate, organic nitrogen, phosphate, total phosphorous, dissolved organic carbon, and chloride concentrations of the throughfall from the different seasons and locations. The same hypotheses were tested on each of these different throughfall components. The data were transformed using a square root transformation to stabilize the variance. There was a slight non-homogeneity in the data. The individual least squares means

analysis were adjusted for multiple comparisons using Tukey's test (a pairwise comparison method) for a more conservative comparison (Steel and Torrie, 1980).

2.3.2.3 Results and Discussion

There was no interaction between season and location in throughfall for any of the parameters investigated (volume, ammonium, nitrate, organic nitrogen, phosphate, total phosphorous, dissolved organic carbon, and chloride). This means each main effect can be looked at separately.

2.3.2.3.1 Daily Throughfall Amount

Seasonal and total throughfall amounts are given in Table 2.3. The throughfall amounts follow the same pattern as rainfall as far as seasonal variation is concerned (see Section 2.3.1, Rainfall). The percentage of rainfall intercepted by the canopy is the highest in the spring (Table 2.4). The spring interception is the highest due to the new flush creating a full canopy. Summer has a lower interception percentage, even though trees have a full canopy. This is because summer rainfall events are normally thunderstorm events of medium to high intensity, which cause the canopy to reach its maximum holding capacity rapidly and lose water to throughfall after saturation. The winter has the lowest interception percentage, as the leaves have fallen from the canopy, resulting in less surface area for interception.

Table 2.3. Seasonal throughfall amounts per season and location (2001-2002).

Season	Average Seasonal Throughfall Amount by Location (mm)			Average Seasonal Throughfall Average (mm)
	East	Central	West	
Spring (Mid-March – Mid-June)	157	131	172	153
Summer (Mid-June – Mid-September)	340	267	353	320
Fall (Mid-September – Mid-December)	101	100	88	96
Winter (Mid-December – Mid-March)	170	178	174	174
Total	768	676	787	743

Table 2.4. Percentage of rainfall intercepted by the canopy.

Season	Average Rainfall Interception by the Canopy (%)
Spring (Mid-March – Mid-June)	42
Summer (Mid-June – Mid-September)	26
Fall (Mid-September – Mid-December)	27
Winter (Mid-December – Mid-March)	11
Yearly Average	27

Canopy interception from other studies ranged from 12% to 36% (Table 1.2). Lower interception occurred in broadleaf forests, while higher interception occurred in pine forests. This is due to the higher ratio of surface area to leaf mass of pine needles as compared to broadleaf leaves, which allows pine needles to intercept more rainfall than broadleaf leaves. The yearly average canopy interception found in this study, 27%, is approximately the interception midpoint of broadleaf and pine forests. This is due to the mixed pine and hardwood overstory found at the study site.

2.3.2.3.2 Throughfall Ammonium Concentration

The statistical analysis indicated that there was no main effect for either season or location on the average ammonium concentration on an event basis ($R^2 = 0.07$, RMSE = 0.48). The ammonium concentration averages (event and volume weighted) for each season can be found in Table 2.5. Average throughfall ammonium concentration (event and volume weighted) per location can be found in Table 2.6.

Table 2.5. Average throughfall ammonium concentration per season.

Season	Average Event Ammonium Concentration (mg/L)	Volume Weighted Average Ammonium Concentration (mg/L)
Spring (Mid-March – Mid-June)	0.44 A[1]	0.45
Summer (Mid-June – Mid-September)	0.45 A	0.49
Fall (Mid-September – Mid-December)	0.35 A	0.37
Winter (Mid-December – Mid-March)	0.30 A	0.20
Yearly Average	0.39	0.37

[1] Different letters indicate significant difference using the Least Squares Means adjusted for multiple comparisons using the Tukey adjustment at $\propto = 0.05$.

Table 2.6. Yearly average throughfall ammonium concentration per location.

Location	Yearly Average Event Ammonium Concentration (mg/L)	Volume Weighted Yearly Average Ammonium Concentration (mg/L)
East Location	0.28 A[1]	0.33
Central Location	0.61 A	0.45
West Location	0.28 A	0.33
Location Average	0.39	0.37

[1] Different letters indicate significant difference using the Least Squares Means adjusted for multiple comparisons using the Tukey adjustment at $\propto = 0.05$.

Ammonium concentrations in throughfall vary mostly with the ammonium concentration in the atmosphere. During this study, ammonium concentrations were relatively constant throughout the year, as can be seen by the similar yearly average and volume weighted yearly average concentrations. The volume weighted average ammonium concentration determined during this study, 0.37 mg/L, is similar to the lower concentrations of the studies shown in Table 1.2 (e.g., Seely et al, 1988; McDonald et al., 2000). The high ammonium concentrations found in the studies in Table 1.2 are due to high-intensity livestock production near the study site (e.g., De Schrijver et al., 2000; Berg and Verhoef, 1998). Livestock production results in large amounts of water-soluble ammonia being released to the atmosphere, which causes large increases in rainfall ammonium concentrations downwind of the farms. The high concentration of hog farms to the east of this study site did not seem to influence the ammonium concentrations of either rainfall or throughfall. The ammonium concentration did slightly increase as it passed through the canopy during the spring and summer periods, but was reduced slightly during the fall and winter periods, which resulted in a similar volume weighted yearly average for both rainfall and throughfall (0.35 mg/L to 0.37 mg/L respectively). The increase in the spring and summer is most likely due to leaching of the leaves of the canopy, whereas the decrease in the fall and winter is most likely due to uptake by algae and lichens on the bare branches and trunks of the trees as it is intercepted. There was a slight increase in ammonium concentration at the central location of the study. This is assumed to be a natural spatial variability.

2.3.2.3.3 Throughfall Nitrate Concentration

The statistical analysis indicated that there was a main effect for both season and location on the average nitrate concentration on an event basis ($R^2 = 0.30$, RMSE = 0.33). Individual comparisons of season averages showed that summer concentrations were significantly lower than both spring and winter concentrations (Table 2.7). Fall throughfall nitrate concentrations were not significantly different from the other three seasons. The average throughfall nitrate concentration at the three locations showed a significantly lower nitrate concentration at the central location as compared to the eastern and western locations (Table 2.8).

Table 2.7. Average throughfall nitrate concentrations per season.

Season	Average Nitrate Concentration (mg/L)	Volume Weighted Average Nitrate Concentration (mg/L)
Spring (Mid-March – Mid-June)	0.74 A[1]	0.60
Summer (Mid-June – Mid-September)	0.15 B	0.20
Fall (Mid-September – Mid-December)	0.33 AB	0.34
Winter (Mid-December – Mid-March)	0.65 A	0.41
Yearly Average	0.63	0.40

[1] Different letters indicate significant difference using the Least Squares Means adjusted for multiple comparisons using the Tukey adjustment at $\propto = 0.05$.

Table 2.8. Yearly average throughfall nitrate concentrations per location.

Location	Yearly Average Nitrate Concentration (mg/L)	Volume Weighted Yearly Average Nitrate Concentration (mg/L)
East Location	0.67 A[1]	0.41
Central Location	0.38 B	0.32
West Location	0.85 A	0.47
Location Average	0.63	0.40

[1] Different letters indicate significant difference using the Least Squares Means adjusted for multiple comparisons using the Tukey adjustment at $\propto = 0.05$.

The throughfall nitrate concentrations also have the same pattern as the rainfall. The highest concentrations occur in the spring and winter while summer has the lowest concentration of all four seasons. The seasonal throughfall nitrate concentrations all are elevated from the rainfall values with the exception of the winter period indicating that there was an enrichment of the throughfall as it passed through the canopy while the leaves were present. This is due to the dry deposition on the canopy. When the leaves are present there is a larger surface area for dry deposition to occur. These increases are similar to those seen in the studies presented in Tables 1.1 and 1.2, although the concentrations found during this study are substantially lower than those located near livestock production. The differences in the nitrate concentrations between locations is opposite of what was measured for ammonium concentrations where the central location had the highest concentration. In the case of nitrate, the central location had the lowest concentration of the three locations. This indicates that nitrification may be occurring to a lesser extent in the canopy at the central location than at the other two locations.

2.3.2.3.4 Throughfall Dissolved Organic Nitrogen Concentration

The statistical analysis indicated that there was a main effect for both season and location on the average dissolved organic nitrogen concentration ($R^2 = 0.39$, RMSE = 0.57). The individual comparisons of the season averages showed that only the spring and winter had statistically different dissolved organic nitrogen concentrations (Table 2.9). The fall and summer concentrations were not significantly different from each other nor from the spring and winter concentrations. Average throughfall dissolved organic nitrogen per location again showed statistical difference between the central location and the other two locations (Table 2.10).

Table 2.9. Average throughfall dissolved organic nitrogen concentrations per season.

Season	Average Dissolved Organic Nitrogen Concentration (mg/L)	Volume Weighted Average Dissolved Organic Nitrogen Concentration (mg/L)
Spring (Mid-March – Mid-June)	3.23 A[1]	2.09
Summer (Mid-June – Mid-September)	1.56 AB	1.57
Fall (Mid-September – Mid-December)	3.32 AB	3.29
Winter (Mid-December – Mid-March)	1.45 B	1.36
Yearly Average	2.31	1.71

[1] Different letters indicate significant difference using the Least Squares Means adjusted for multiple comparisons using the Tukey adjustment at $\propto = 0.05$.

Table 2.10. Yearly average throughfall dissolved organic nitrogen concentration per location.

Location	Yearly Average Dissolved Organic Nitrogen Concentration (mg/L)	Volume Weighted Yearly Average Dissolved Organic Nitrogen Concentration (mg/L)
East Location	1.72 A[1]	1.39
Central Location	3.78 B	2.51
West Location	1.42 A	1.41
Location Average	2.31	1.71

[1] Different letters indicate significant difference using the Least Squares Means adjusted for multiple comparisons using the Tukey adjustment at $\propto = 0.05$.

Throughfall dissolved organic nitrogen is highest during the spring and fall. High concentrations during the spring are due to the large amount of pollen generated in the spring. Pollen is blown across the forest and deposited on the canopy, where it is subsequently washed off during a rainfall event, adding dissolved organic nitrogen to the throughfall. The high dissolved organic nitrogen concentrations found in the fall are due to leaching and fragmentation of the canopy leaves as they prepare to fall. Winter has the lowest average dissolved organic nitrogen concentration in throughfall because there are no leaves to leach and no pollen in the atmosphere. This results in less organic nitrogen enriching the throughfall. These variables can cause variations between locations, as seen in Table 2.10. The higher volume weighted yearly average concentration at the central location indicates that factors causing readily transported organic nitrogen (such as higher pollen production or higher leachability of leaves) are more prevalent at the central location.

The throughfall dissolved organic nitrogen concentration found in this study, 1.71 mg/L, is substantially higher than the two studies referenced in Table 1.2, which report

dissolved organic nitrogen of 0.44mg/L and 0.03 mg/L. A possible explanation is the higher organic nitrogen content of the rainfall (0.86 mg/L) as compared to the other studies shown in Table 1.2 (0.21 mg/L and 0.11 mg/L).

2.3.2.3.5 Throughfall Phosphate Concentration

The statistical analysis indicated that there was a main effect of location but not of season (Table 2.11) on the average phosphate concentration ($R^2 = 0.32$, RMSE = 0.29). The individual comparisons of the location averages showed that the throughfall phosphate concentrations at the central location were significantly higher than at the other two locations (Table 2.12).

Table 2.11. Average throughfall phosphate concentrations per season.

Season	Average Phosphate Concentration (mg/L)	Volume Weighted Average Phosphate Concentration (mg/L)
Spring (Mid-March – Mid-June)	0.32 A[1]	0.19
Summer (Mid-June – Mid-September)	0.36 A	0.25
Fall (Mid-September – Mid-December)	0.12 A	0.12
Winter (Mid-December – Mid-March)	0.09 A	0.06
Yearly Average	0.24	0.16

[1] Different letters indicate significant difference using the Least Squares Means adjusted for multiple comparisons using the Tukey adjustment at $\propto = 0.05$.

Table 2.12. Yearly average throughfall phosphate concentration per location.

Location	Yearly Average Phosphate Concentration (mg/L)	Volume Weighted Yearly Average Phosphate Concentration (mg/L)
East Location	0.14 A[1]	0.09
Central Location	0.51 B	0.33
West Location	0.06 A	0.08
Location Average	0.24	0.16

[1] Different letters indicate significant difference using the Least Squares Means adjusted for multiple comparisons using the Tukey adjustment at $\propto = 0.05$.

Throughfall phosphate and phosphorous originate in the canopy from dry deposition. This can be seen in the differences in the phosphorous and phosphate concentrations in the rainfall and throughfall reported in this study. Phosphate and phosphorous concentrations are highly variable from event to event. Longer time periods between rainfalls allows more deposition and results in higher throughfall concentrations as compared to frequent events. These concentrations are greater than those of the studies presented in Table 1.2. This is due to a combination of a drought that occurred during the study and the presence of an unsurfaced road along the study canal. The drought resulted in longer than normal periods between rainfall events, allowing phosphate and phosphorous to accumulate in the canopy. The presence of the road provided a readily available source of phosphorous and phosphate, which is blown into the air with passing vehicles. For both phosphate and phosphorous, the highest concentrations occurred at the central location. This is most likely due to a higher content of phosphate and phosphorous in the road material along the side of the study canal.

2.3.2.3.6 Throughfall Total Phosphorous Concentration

The statistical analysis indicated that there was a main effect of location but not of season on the average total phosphorous concentration ($R^2 = 0.28$, RMSE = 0.29). The total phosphorous concentration averages for each season are given in Table 2.13. The individual comparisons of the location averages showed that the eastern location was not statistically different from the other two locations. However, the central and western locations were statistically different from each other (Table 2.14).

Table 2.13. Average throughfall total phosphorous concentration per season.

Season	Average Total Phosphorous Concentration (mg/L)	Volume Weighted Average Total Phosphorous Concentration (mg/L)
Spring (Mid-March – Mid-June)	0.49 A[1]	0.33
Summer (Mid-June – Mid-September)	0.18 A	0.20
Fall (Mid-September – Mid-December)	0.24 A	0.25
Winter (Mid-December – Mid-March)	0.21 A	0.17
Yearly Average	0.35	0.23

[1] Different letters indicate significant difference using the Least Squares Means adjusted for multiple comparisons using the Tukey adjustment at $\propto = 0.05$.

Table 2.14. Yearly average throughfall total phosphorous concentration per location.

Location	Yearly Average Total Phosphorous Concentration (mg/L)	Volume Weighted Yearly Average Total Phosphorous Concentration (mg/L)
East Location	0.32 AB[1]	0.27
Central Location	0.62 A	0.31
West Location	0.12 B	0.12
Location Average	0.35	0.23

[1] Different letters indicate significant difference using the Least Squares Means adjusted for multiple comparisons using the Tukey adjustment at $\propto = 0.05$.

See previous discussion in Section 2.3.2.3.5, Throughfall Phosphate Concentration.

2.3.2.3.7 Throughfall Dissolved Organic Carbon Concentration

The statistical analysis indicated that there was a main effect for both season and location on the average dissolved organic carbon concentration ($R^2 = 0.45$, RMSE = 1.19). The individual comparisons of the season averages showed that dissolved organic carbon concentrations in the fall are significantly greater than those in winter, spring, and summer (Table 2.15). The individual comparisons of the location averages showed that the central location had a statistically higher dissolved organic carbon concentration than the other two locations (Table 2.16). The east and west locations were not statistically different.

Table 2.15. Average throughfall dissolved organic carbon concentrations per season.

Season	Average Dissolved Organic Carbon Concentration (mg/L)	Volume Weighted Average Dissolved Organic Carbon Concentration (mg/L)
Spring (Mid-March – Mid-June)	19.3 B[1]	14.3
Summer (Mid-June – Mid-September)	22.4 B	22.8
Fall (Mid-September – Mid-December)	59.8 A	58.7
Winter (Mid-December – Mid-March)	16.4 B	12.7
Yearly Average	20.0	18.7

[1] Different letters indicate significant difference using the Least Squares Means adjusted for multiple comparisons using the Tukey adjustment at $\propto = 0.05$.

Table 2.16. Yearly average throughfall dissolved organic carbon concentration per location.

Location	Yearly Average Dissolved Organic Carbon Concentration (mg/L)	Volume Weighted Yearly Average Dissolved Organic Carbon Concentration (mg/L)
East Location	17.7 A[1]	17.5
Central Location	28.0 B	23.2
West Location	14.4 A	15.4
Location Average	20.0	18.7

[1] Different letters indicate significant difference using the Least Squares Means adjusted for multiple comparisons using the Tukey adjustment at $\propto = 0.05$.

The large value of the average dissolved organic carbon concentration in throughfall during the fall is expected. This is due to the highly leachable organic carbon present in the dying leaves as they senesce. The winter values are small because there is no easily leached material available. The leaves have already fallen from the trees by this time. Leachable organic carbon comes from any dry deposition in the branches of the trees. The spring also has small values, as the leaves are in an active state of growth and are not prone to leaching as they expand. There was a slight increase in the summer season. This is due to the shedding of some leaves, which can be leached prior to dropping.

The central location has statistically higher dissolved organic carbon concentrations than the other two locations. This is assumed to be due to natural spatial variability.

2.3.2.3.8 Throughfall Chloride Concentration

Statistical analysis indicated that there was a main effect of season but not of location on the average chloride concentration ($R^2 = 0.19$, RMSE = 1.07). The individual comparisons of the season averages showed that only the spring and winter had statistically

different chloride concentrations (Table 2.17). Fall and summer concentrations were not significantly different from each other, or from the spring and winter concentrations. Average throughfall chloride concentration (event and volume weighted) per location can be found in Table 2.18.

Table 2.17. Average throughfall chloride concentrations per season.

Season	Average Chloride Concentration (mg/L)	Volume Weighted Average Chloride Concentration (mg/L)
Spring (Mid-March – Mid-June)	3.55 A[1]	2.02
Summer (Mid-June – Mid-September)	0.74 AB	0.76
Fall (Mid-September – Mid-December)	2.01 AB	2.07
Winter (Mid-December – Mid-March)	0.84 B	0.46
Yearly Average	2.25	1.10

[1] Different letters indicate significant difference using the Least Squares Means adjusted for multiple comparisons using the Tukey adjustment at $\propto = 0.05$.

Table 2.18. Yearly average throughfall chloride concentration per location.

Location	Yearly Average Chloride Concentration (mg/L)	Volume Weighted Yearly Average Chloride Concentration (mg/L)
East Location	1.96 A[1]	1.37
Central Location	2.80 A	0.96
West Location	1.99 A	0.93
Location Average	2.25	1.10

[1] Different letters indicate significant difference using the Least Squares Means adjusted for multiple comparisons using the Tukey adjustment at $\propto = 0.05$.

Chloride variations in throughfall by season are most likely due to variations in the dry deposition on the canopy throughout the year. Chloride in the atmosphere comes primarily from salt spray carried aloft by winds and transported inland (Tisdale et al., 1993). The rainfall chloride concentration remains relatively constant over the seasons (Table 2.2), suggesting that variations in the throughfall are due to dry depositions being greater during the spring and fall. The lower frequency of rainfall events during the spring results in more buildup on in the canopy, which causes higher concentrations in throughfall during a rainfall event. The average rainfall concentrations for the summer and winter, 2.12mg/L and 3.30 mg/L respectively, are higher than their throughfall counterparts, 0.74 mg/L and 0.84 mg/L respectively. The lower concentrations during the summer and winter months are unexplained at this point. Uptake by the leaves could account for some, but not all, of the loss during the summer months. Hamburg and Lin (1998) also reported an unexplained loss of chloride to the canopy in their study during the dormant season. The lack of a statistical difference between different locations indicates that chloride is deposited in a relatively uniform manner over the area.

2.3.2.4 Conclusion

Atmospheric and canopy interactions determine the nutrient concentrations in throughfall. Nutrients in rainfall entering the canopy in rainfall can be either lost to the canopy or enriched by the canopy. During this study, the concentration of all but one nutrient studied increased as it passed through the canopy (average annual changes in mg/L: ammonium +0.02 , nitrate +0.18, dissolved organic nitrogen +0.85, phosphate +0.13, total phosphorous +0.15, chloride -1.52). The increases are primarily due to dry deposition and

leaching within the canopy. The reason for the loss of chloride to the canopy is unexplained, though a similar loss of chloride has been noted in another study during the dormant season.

2.4 Groundwater

2.4.1 Methods

Groundwater was sampled using 12 groundwater sampling wells, four within each of the three forest types (three to the south of the study canal and one along the road to the north) (Figure 2.2). Each of the wells was located three meters from the edge of the canal. The wells were installed to a depth of two meters, with the bottom one and a half meters screened. Samples were taken once a week in conjunction with throughfall samples. Each well was bailed twice and allowed to refill prior to sampling. Water level recorders were placed one, five, 10, and 50 meters from the canal edge on the south side, one within the canal, and one one meter from the canal edge on the north side (Figure 2.4).

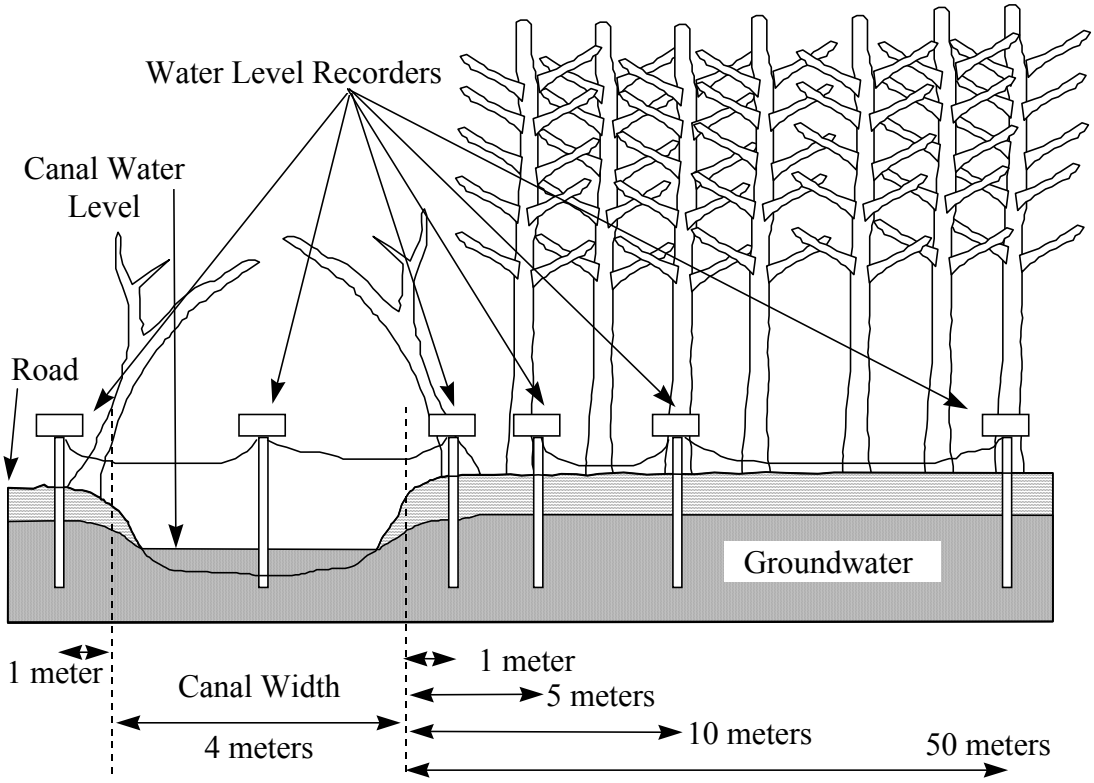

Figure 2.4. Water level recorder locations at each monitoring location.

The water level recorders within the canal and one meter from the canal edge on the south side were used to measure water level differences between surface water in the canal and groundwater in the forested fields. These data allowed the flow rate of groundwater from or to the fields, or to or from the canal, to be calculated using Darcy's Equation (Equation 2.2):

$$Q=KA\triangle h/L \qquad \text{(Equation 2.2)}$$

where: Q = the flow rate (m^3/s)
$\triangle h$ = the head loss (m)
L = the length of travel (m)
A = the cross-sectional area of flow (m^2)
K = the hydraulic conductivity (m/s).

In the same manner, data from two water level recorders, one within the canal and one one meter from the canals' edge along the north side of canal, were used to estimate subsurface flow between the study canal and the canal located on the northern side of the road, parallel to the study canal. Determination of hydraulic conductivity by calibrating the field hydrology model DRAINMOD (Skaggs, 1991) to measured data was attempted. Using known parameters from the site, hydraulic conductivity can be varied until the modeled midpoint water table depth matched measured midpoint water table depth at the water level recorder located 50 meters from the canal. The 50 meter distance was chosen because it is the midpoint between the original field ditches. This method failed because water tables were lower than the field ditches due to extended drought. The auger hole method (van Beers, 1970) was also attempted. However, the presence of root canals caused the measured hydraulic conductivities to be unreasonably large. This problem, plus unstable auger holes, resulted in the abandonment of this method. Hydraulic conductivities determined from two neighboring fields (Table 2.19) (Diggs, 2004) were used for calculating flow from the fields bordering the study canal section.

Table 2.19. Hydraulic conductivities used for determining flow from bordering fields (Diggs, 2004).

Field F5		Field F6	
Depth (cm)	Hydraulic Conductivity (cm/hr)	Depth (cm)	Hydraulic Conductivity (cm/hr)
0-45	650	0-30	700
45-55	400	30-45	350
55-68	10	45-60	10
68-250	5	60-240	5

Water movement through the field ditch plugs was estimated at three locations in the same manner as groundwater flow. Water surface elevations measured by two water level recorders (one placed on either side of the plug) were used in the Darcy's equation to determine flow volume and direction through the plug (Figure 2.5).

Water samples were placed in a freezer immediately after collection and kept frozen until analysis. All samples were filtered through a 0.45 micron filter (Gelman Laboratory, Supor®-450) to remove particulate material. Each sample was analyzed for nitrate, ammonium, and phosphate, and dissolved organic, inorganic, and total carbon (Standard Methods, 1989).

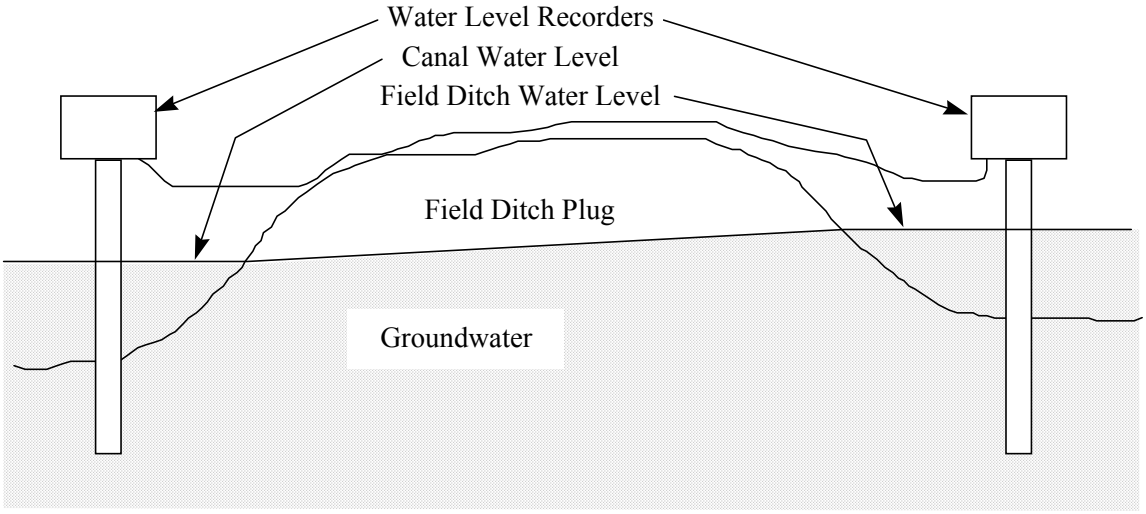

Figure 2.5. Field ditch plugs.

2.4.2 Statistical Analysis

A general linear model for the differences in the ammonium concentration of the groundwater entering the canal is shown in Equation 2.3.

$$\text{Model: } Y = \mu + \alpha_i + \beta_j + (\alpha\beta)_{ij} + \varepsilon_{ij} \quad \text{Equation 2.3}$$

where: Y = the ammonium concentration of the groundwater
μ = the average ammonium concentration of the groundwater
α_i represents the main effects of season on the ammonium concentration of the groundwater (i = spring, summer, fall, winter)
β_j represents the main effects of location on the ammonium concentration of the groundwater (j = 1, 2, 3, 4, 5)
$(\alpha\beta)_{ij}$ represents the interactions between season and location on the ammonium concentration of the groundwater
ε_{ij} = error term.

The constraints of $\sum_i\alpha_i = 0$, $\sum_j\beta_j = 0$, $\sum_i\alpha_i\beta_j = 0$, $\sum_j\alpha_i\beta_j = 0$. The hypothesis being tested are: H_o: $\alpha_i = 0$ - no main effect of season, H_o: $\beta_j = 0$ - no main effect of location, and H_o: $(\alpha\beta)_{ij} = 0$ - no interactive effects between season and location on the ammonium concentration of the groundwater (Steel and Torrie, 1980). The same statistical model and constraints were used for analyzing nitrate, organic nitrogen, total phosphorous, phosphate, chloride, and total organic carbon content of groundwater for different seasons and locations. The same hypotheses were tested on each of the different groundwater components. The data were transformed using a square root transformation to stabilize the variance. The individual least squares means analysis were adjusted for multiple comparisons using Tukey for a more conservative comparison.

2.4.3 Results and discussion

There were no interactions between season and location in groundwater for any of the parameters investigated (ammonium, nitrate, organic nitrogen, phosphate, total phosphorous,

dissolved organic carbon, and chloride). This means each main effect can be examined separately. During the fall, the water table was below the sample well depth, so no samples were taken.

2.4.3.1 Groundwater Ammonium Concentration

The statistical analysis indicated that there was a main effect of season but not of location on the average groundwater ammonium concentration entering the canal ($R^2 = 0.14$, RMSE = 0.23). The individual comparisons of seasonal averages showed that the average groundwater ammonium concentration during the winter season was statistically different from the summer season. Spring season concentrations were not statistically different from either the summer or the winter concentrations (Table 2.20). The individual comparisons of locations among the average groundwater ammonium concentrations are given in Table 2.21.

Table 2.20. Average groundwater ammonium concentration per season.

Season	Average Daily Ammonium Concentration (mg/L)	Volume Weighted Average Ammonium Concentration (mg/L)[1]
Spring (Mid-March – Mid-June)	0.34 AB[2]	0.47
Summer (Mid-June – Mid-September)	0.51 A	-
Fall (Mid-September – Mid-December)	-	-
Winter (Mid-December – Mid-March)	0.28 B	0.62
Yearly Average	0.33	0.53

[1] Volume weighted averages only include measurements when flow is from the field to the canal.
[2] Different letters indicate significant difference using the Least Squares Means adjusted for multiple comparisons using the Tukey adjustment at $\propto = 0.05$.

Table 2.21. Average groundwater ammonium concentration per location.

Location	Yearly Average Daily Ammonium Concentration (mg/L)	Volume Weighted Yearly Average Ammonium Concentration (mg/L)[1]
Eastern Location - Forested side of canal	0.39 A[2]	1.06
Central Location - Forested side of canal	0.27 A	0.59
Western Location - Forested side of canal	0.37 A	0.10
Eastern Location - Road side of canal	0.16 A	0.24
Central Location - Road side of canal	0.21 A	0.01
Western Location - Road side of canal	0.30 A	-
Yearly Average	0.33	0.53

[1] Volume weighted averages only include measurements when flow is from the field to the canal.
[2] Different letters indicate significant difference using the Least Squares Means adjusted for multiple comparisons using the Tukey adjustment at $\propto = 0.05$.

Ammonium concentrations were similar to those found in throughfall. Ammonium concentrations remain low, because ammonium is nitrified in the soils as well as being potentially adsorbed by the soil (Tisdale et al., 1993). The ammonium concentration found during this study was low, as expected in forested lands, and is similar to that found in other studies (e.g., De Schrijver et al., 2000; Campbell et al., 2000; Nohrstedt, 1992, Table 1.3).

2.4.3.2 Groundwater Nitrate Concentration

The statistcal analysis indicated there was a main effect of season with a strong main effect of location on the average groundwater nitrate concentration entering the canal (R^2 = 0.61, RMSE = 0.59). The individual comparisons of seasonal averages showed the average groundwater nitrate concentration during the spring season was statistically different from the summer season. The winter season concentration was not statistically different from either the summer or spring season concentrations (Table 2.22). Individual comparisons of groundwater nitrate concentrations showed statistical differences due to location (Table

2.23). There was also a statistical difference in the average groundwater nitrate concentrations between the forested side of the canal at the central location and the forested side of the canal at the eastern and western locations.

Table 2.22. Average groundwater nitrate concentration per season.

Season	Average Daily Nitrate Concentration (mg/L)	Volume Weighted Average Nitrate Concentration (mg/L)[1]
Spring (Mid-March – Mid-June)	2.53 A[2]	1.41
Summer (Mid-June – Mid-September)	0.11 B	-
Fall (Mid-September – Mid-December)	-	-
Winter (Mid-December – Mid-March)	1.83 AB	0.94
Yearly Average	2.14	1.21

[1] Volume weighted averages only include measurements when flow is from the field to the canal.
[2] Different letters indicate significant difference using the Least Squares Means adjusted for multiple comparisons using the Tukey adjustment at $\propto = 0.05$.

Table 2.23. Average groundwater nitrate concentration per location.

Location	Yearly Average Daily Nitrate Concentration (mg/L)	Volume Weighted Yearly Average Nitrate Concentration (mg/L)[1]
Eastern Location - Forested side of canal	0.50 AB[2]	0.47
Central Location - Forested side of canal	2.85 BC	2.69
Western Location - Forested side of canal	1.02 AB	1.16
Eastern Location - Road side of canal	1.41 ABC	1.87
Central Location - Road side of canal	5.38 D	7.39
Western Location - Road side of canal	14.22 E	-
Yearly Average	2.14	1.21

[1] Volume weighted averages only include measurements when flow is from the field to the canal.
[2] Different letters indicate significant difference using the Least Squares Means adjusted for multiple comparisons using the Tukey adjustment at $\propto = 0.05$.

The lower groundwater nitrate concentration during the summer months is due to a combination of the increased denitrification rate caused by higher summer temperatures and lower flow due to lower water tables during the summer, resulting in longer residence times for denitrification to occur. The average seasonal groundwater nitrate concentrations were higher than in most of the studies reported in the literature (see review section, Table 1.3) because of the high average volume recorded at the road side of the canal at the central and western locations (4.95 mg/L and 14.22 mg/L respectively). There is currently no explanation for these two high averages. The groundwater nitrate concentrations of the forested side of the canal are closer to the range of studies reported in the literature (Table 1.3).

2.4.3.3 Groundwater Organic Nitrogen Concentration

The statistical analysis indicated that there was a main effect of season and a main effect of location on the average groundwater organic nitrogen concentration entering the canal ($R^2 = 0.19$, RMSE = 0.25). The individual comparisons of seasonal averages showed the average groundwater organic nitrogen concentrations during the spring season were statistically different from those during of the winter season (Table 2.24). There was no statistical difference in the average groundwater organic nitrogen concentration between winter and summer and between spring and summer. The individual comparisons of the average groundwater organic nitrogen concentrations at the different locations showed a statistical difference between the forested side of the canal at the central location and at the other locations, with the exception of the road side at the central location (Table 2.25). No other differences were significant.

Table 2.24. Average groundwater organic nitrogen concentration per season.

Season	Average Daily Organic Nitrogen Concentration (mg/L)	Volume Weighted Average Organic Nitrogen Concentration (mg/L)[1]
Spring (Mid-March – Mid-June)	1.54 A[2]	2.27
Summer (Mid-June – Mid-September)	1.11 AB	-
Fall (Mid-September – Mid-December)	-	-
Winter (Mid-December – Mid-March)	1.34 B	1.68
Yearly Average	1.45	2.02

[1] Volume weighted averages only include measurements when flow is from the field to the canal.
[2] Different letters indicate significant difference using the Least Squares Means adjusted for multiple comparisons using the Tukey adjustment at $\propto = 0.05$.

Table 2.25. Average groundwater organic nitrogen concentration per location.

Location	Average Daily Organic Nitrogen Concentration (mg/L)	Volume Weighted Yearly Average Organic Nitrogen Concentration (mg/L)[1]
Eastern Location - Forested side of canal	1.18 A[2]	2.14
Central Location - Forested side of canal	2.01 B	3.51
Western Location - Forested side of canal	1.23 A	1.47
Eastern Location - Road side of canal	1.18 A	1.29
Central Location - Road side of canal	1.55 AB	1.99
Western Location - Road side of canal	1.05 A	-
Yearly Average	1.45	2.02

[1] Volume weighted averages only include measurements when flow is from the field to the canal.
[2] Different letters indicate significant difference using the Least Squares Means adjusted for multiple comparisons using the Tukey adjustment at $\propto = 0.05$.

The higher average groundwater organic nitrogen concentrations found during the spring are due to the high concentrations found in throughfall and the organic nitrogen content in litterfall during this period. The higher organic nitrogen concentration at the central location is most likely due to the elevated throughfall concentrations of organic

nitrogen found at this location. However, the seasonal organic nitrogen values found in this study were higher than those found in the few studies that report them in the literature (Table 1.3). This is most likely due to the organic soils found at the study location.

2.4.3.4 Groundwater Total Phosphorous Concentration

The statistical analysis indicated that there was a main effect of season with no main effect of location on the average groundwater total phosphorous concentration entering the canal ($R^2 = 0.61$, RMSE = 0.03). The individual comparisons of seasonal averages showed the average groundwater total phosphorous concentrations during the spring season were statistically greater than during the summer and winter seasons (Table 2.26). There was no statistical difference in the average groundwater total phosphorous concentration during the winter and summer seasons. The individual comparisons of average groundwater total phosphorous concentrations between the locations can be found in Table 2.27.

Table 2.26. Average groundwater total phosphorous concentration per season.

Season	Average Daily Total Phosphorous Concentration (mg/L)	Volume Weighted Average Total Phosphorous Concentration (mg/L)[1]
Spring (Mid-March – Mid-June)	0.03 A[2]	0.04
Summer (Mid-June – Mid-September)	0.01 B	-
Fall (Mid-September – Mid-December)	-	-
Winter (Mid-December – Mid-March)	0.01 B	0.02
Yearly Average	0.02	0.03

[1] Volume weighted averages only include measurements when flow is from the field to the canal.
[2] Different letters indicate significant difference using the Least Squares Means adjusted for multiple comparisons using the Tukey adjustment at $\propto = 0.05$.

Table 2.27. Average groundwater total phosphorous concentration per location.

Location	Average Daily Total Phosphorous Concentration (mg/L)	Volume Weighted Yearly Average Total Phosphorous Concentration (mg/L)[1]
Eastern Location - Forested side of canal	0.02 A[2]	0.03
Central Location - Forested side of canal	0.02 A	0.03
Western Location - Forested side of canal	0.02 A	0.03
Eastern Location - Road side of canal	0.02 A	0.01
Central Location - Road side of canal	0.02 A	0.01
Western Location - Road side of canal	0.03 A	-
Yearly Average	0.02	0.03

[1] Volume weighted averages only include measurements when flow is from the field to the canal.
[2] Different letters indicate significant difference using the Least Squares Means adjusted for multiple comparisons using the Tukey adjustment at $\propto = 0.05$.

All values of groundwater phosphorous are at the limit of detection using today's methods. This is to be expected, as the phosphorous in decaying organic material in this system is immobilized, and any remaining phosphate readily adsorbs to the soil. Most organic phosphorous remains in the upper layers of the soils (Reported in Tisdale et al., 1993). Organic phosphorous in this study was immobilized rather than mineralized due to the high C/P ratio (370+) as discussed in Section 1.4.3.4 (Role of Carbon-to-Phosphorous Ratio in Mineralization and Immobilization). Any phosphates not immobilized are readily adsorbed to the soil, particularly in acidic soils like those found around the study canal (Reported in Tisdale et al., 1993). Soil adsorption of phosphates, along with the low inputs of phosphorous and phosphate through litterfall (0.07 g/m^2/day) and throughfall (0.23 mg/L and 0.16 mg/L respectively) result in little to no phosphorous or phosphate entering the groundwater. These results are similar to those shown in Table 1.3.

2.4.3.5 Groundwater Phosphate Concentration

The statistical analysis indicated that there was a main effect of season with no main effect of location on the average groundwater phosphate concentration entering the canal (R^2 = 0.34, RMSE = 0.04). The individual comparisons of seasonal averages showed the average groundwater phosphate concentrations during the spring season were statistically greater than during the summer and winter seasons (Table 2.28). There was no statistical difference in the average groundwater phosphate concentration between the summer and winter seasons. The individual comparisons of the average groundwater phosphate concentrations at different locations can be found in Table 2.29.

Table 2.28. Average daily groundwater phosphate concentration per season.

Season	Average Daily Phosphate Concentration (mg/L)	Volume Weighted Average Phosphate Concentration (mg/L)[1]
Spring (Mid-March – Mid-June)	0.01 A[2,3]	0.01
Summer (Mid-June – Mid-September)	0.01 B	-
Fall (Mid-September – Mid-December)	-	-
Winter (Mid-December – Mid-March)	0.01 B	0.01
Yearly Average	0.01	0.01

[1] Volume weighted averages only include measurements when flow is from the field to the canal.
[2] Different letters indicate significant difference using the Least Squares Means adjusted for multiple comparisons using the Tukey adjustment at $\propto = 0.05$.
[3] Similar values for each season are due to rounding.

Table 2.29. Average daily groundwater phosphate concentration per location.

Location	Average Daily Phosphate Concentration (mg/L)	Volume Weighted Yearly Average Phosphate Concentration (mg/L)[1]
Eastern Location- Forested side of canal	0.01 A[2]	0.01
Central Location- Forested side of canal	0.01 A	0.02
Western Location- Forested side of canal	0.01 A	0.01
Eastern Location- Road side of canal	0.01 A	0.00
Central Location- Road side of canal	0.01 A	0.00
Western Location- Road side of canal	0.01 A	-
Yearly Average	0.01	0.01

[1] Volume weighted averages only include measurements when flow is from the field to the canal.
[2] Different letters indicate significant difference using the Least Squares Means adjusted for multiple comparisons using the Tukey adjustment at $\propto = 0.05$.

See Section 2.4.3.4 above, Average Groundwater Phosphorous Concentration, for discussion.

2.4.3.6 Groundwater Organic Carbon Concentration

The statistical analysis indicated that there was a main effect of location but not with season (Table 2.30) on the average groundwater organic carbon concentration entering the canal ($R^2 = 0.27$, RMSE = 1.26). The individual comparisons of the average groundwater organic carbon concentrations between locations showed a statistical difference between the forested side of the canal at the most central location and the other five locations (Table 2.31).

Table 2.30. Average groundwater organic carbon concentration per season.

Season	Average Daily Organic Carbon Concentration (mg/L)	Volume Weighted Average Organic Carbon Concentration (mg/L)[1]
Spring (Mid-March – Mid-June)	33.1 A[2]	44.3
Summer (Mid-June – Mid-September)	31.1 A	-
Fall (Mid-September – Mid-December)	-	-
Winter (Mid-December – Mid-March)	28.4 A	35.7
Yearly Average	31.3	40.7

[1] Volume weighted averages only include measurements when flow is from the field to the canal.
[2] Different letters indicate significant difference using the Least Squares Means adjusted for multiple comparisons using the Tukey adjustment at $\propto = 0.05$.

Table 2.31. Average groundwater organic carbon concentration per location.

Location	Average Daily Organic Carbon Concentration (mg/L)	Volume Weighted Yearly Average Organic Carbon Concentration (mg/L)[1]
Eastern Location- Forested side of canal	25.9 A[2]	48.9
Central Location- Forested side of canal	45.6 B	77.8
Western Location- Forested side of canal	25.6 A	22.8
Eastern Location- Road side of canal	25.0 A	27.9
Central Location- Road side of canal	26.1 A	29.7
Western Location- Road side of canal	21.3 A	-
Yearly Average	31.3	40.7

[1] Volume weighted averages only include measurements when flow is from the field to the canal.
[2] Different letters indicate significant difference using the Least Squares Means adjusted for multiple comparisons using the Tukey adjustment at $\propto = 0.05$.

The seasonal similarity of the dissolved organic carbon can be traced to the layer of litterfall covering the ground continuously throughout the year. As the litterfall continues to be broken down throughout the year, dissolved organic carbon is leached and migrates to the groundwater. The similarity of the groundwater organic carbon concentrations at the different locations is again due to the constant supply of organic carbon from the always-

present litter layer. The high average organic carbon concentration seen at the central location of the forested side of the canal is unexplained at this time.

2.4.3.7 Groundwater Chloride Concentration

The statistical analysis indicated that there was a main effect of location but not of season (Table 2.32) on the average groundwater chloride concentration entering the canal (R^2 = 0.42, RMSE = 1.29). The individual comparisons of the average groundwater chloride concentrations between locations showed a statistical difference between the forested side of the canal at the central location and all other locations (Table 2.33). A significant difference in the average groundwater chloride concentration was also found between the forested side of the canal and the road side of the canal, with the exception of the eastern road side location, which was not statistically different from the eastern and western locations on the forested side of the canal.

Table 2.32. Average groundwater chloride concentration per season.

Season	Average Daily Chloride Concentration (mg/L)	Volume Weighted Average Chloride Concentration (mg/L)[1]
Spring (Mid-March – Mid-June)	18.2 A[2]	34.6
Summer (Mid-June – Mid-September)	9.8 A	-
Fall (Mid-September – Mid-December)	-	-
Winter (Mid-December – Mid-March)	15.4 A	29.6
Yearly Average	16.7	32.5

[1] Volume weighted averages only include measurements when flow is from the field to the canal.
[2] Different letters indicate significant difference using the Least Squares Means adjusted for multiple comparisons using the Tukey adjustment at $\propto = 0.05$.

Table 2.33. Average groundwater chloride concentration per location.

Location	Average Daily Chloride Concentration (mg/L)	Volume Weighted Yearly Average Chloride Concentration (mg/L)[1]
Eastern Location - Forested side of canal	13.7 ABE[2]	37.4
Central Location - Forested side of canal	27.3 C	71.8
Western Location - Forested side of canal	15.9 AE	16.3
Eastern Location - Road side of canal	6.4 ABD	2.8
Central Location - Road side of canal	1.8 BD	1.3
Western Location - Road side of canal	2.3 BD	-
Yearly Average	16.7	32.5

[1] Volume weighted averages only include measurements when flow is from the field to the canal.
[2] Different letters indicate significant difference using the Least Squares Means adjusted for multiple comparisons using the Tukey adjustment at $\propto = 0.05$.

Groundwater chloride concentrations are expected to be higher than throughfall (by as much as threefold—Peters and Ratcliffe, 1998) due to the chloride found in the parent material of the soil (Reported in Tisdale et al., 1993). Seasonal variations in groundwater chloride concentration, although not significant from season to season, are due to natural variation (Peters and Ratcliffe, 1998; Reported in Tisdale et al., 1993; Russo et al., 2003). Concentration variations were greater on the forested side of the canal than on the road side, and are similar to other studies. Lischeid et al. (1998) found large variations in chloride groundwater, ranging from a low of 1.64 mg/L to a high of 16.1 mg/L in a 25 m X 25 m grid pattern. They found no adequate explanation for these variations. The results found in this study are somewhat higher than those reported by Lischeid et al. (1998). This is probably due to the closer proximity of this study to the coast.

2.4.4 Conclusions

The yearly average ammonium, nitrate, phosphate, and total phosphorous concentrations (0.28 mg/L, 1.48 mg/L, 0.01 mg/L, and 0.01 mg/L respectively) of the groundwater found in this study are similar to values reported in other studies. The dissolved organic nitrogen concentration (1.35 mg/L) was greater than reported in other studies, where dissolved organic nitrogen concentrations were 0.04 mg/L to 0.50 mg/L. This may be due to the high organic content of the canal sediments. The dissolved organic carbon concentrations found in this study (averaging 24.9 mg/L for all plots except the central location on the forested side, which averaged 45.2 mg/L) are adequate to provide the energy required for all biologically mediated nutrient transformations (mineralization and nitrification) within the system and removals (denitrification) from the system. Chloride concentrations in groundwater were elevated on the forested side (18.8 mg/L) of the study canal as compared to the road side (3.49 mg/L) but were within ranges found in other studies (1.64 mg/L to 16.1 mg/L). The elevated chloride values found in this study are most likely due to the study site's close proximity to the coast.

2.5 Upstream Canal Inflow

2.5.1 Methods

Upstream inflow to the study canal section was estimated using a flume structure instrumented with a Doppler flow meter (Straflow, Unidata^{TM}, Australia) (Figure 2.6). The structure was constructed to give a known cross-sectional area for calculating flow as well as an unobstructed flow path for the Doppler flow meter to take measurements (Figure 2.7). This is required because the presence of rocks and plant material near the Doppler flow

meter can cause differing velocities within the view of the meter's acoustic beam. This may distort the actual velocity indicated by the meter (STARFLOW Owners Manual, 1998).

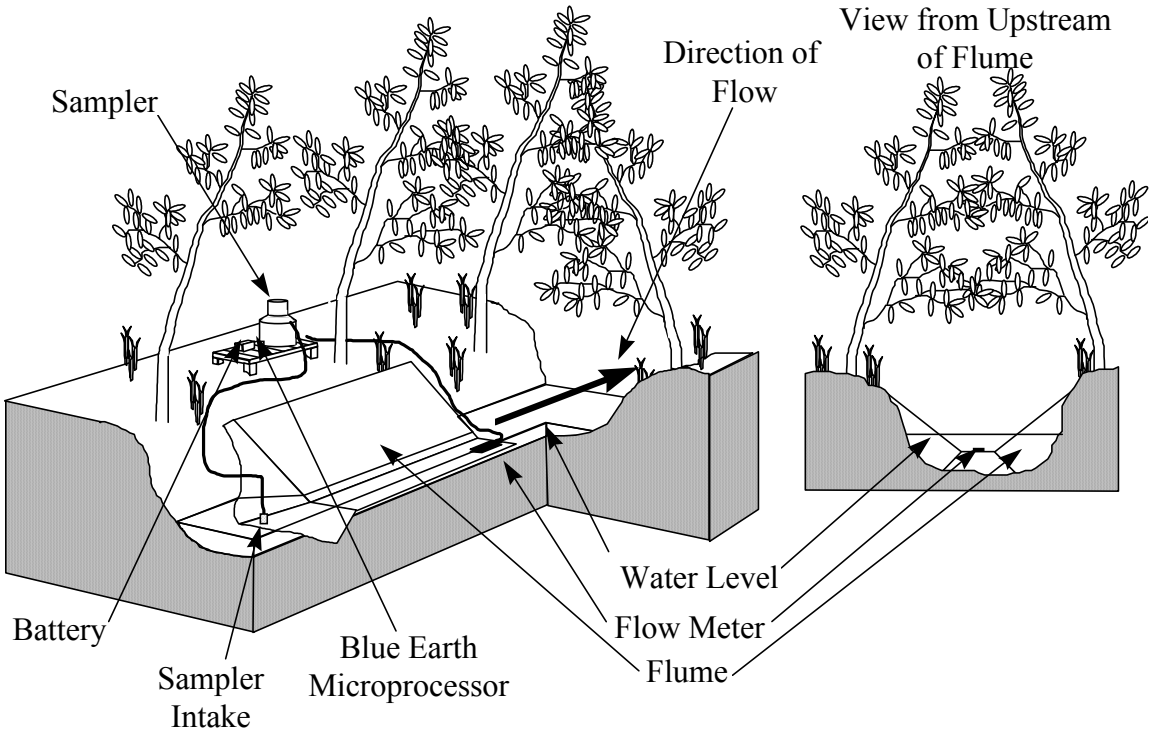

Figure 2.6. Flume structure at upstream end of canal study section.

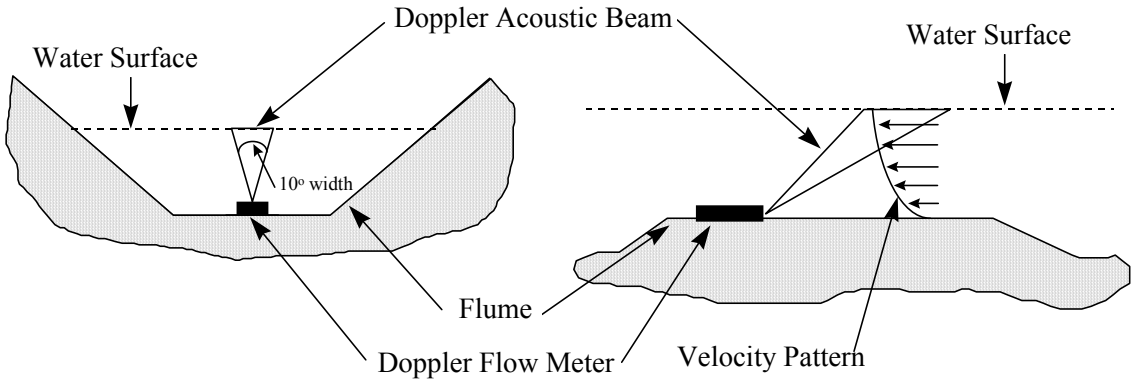

Figure 2.7. Doppler flow meter.

The structure generated turbulent flow (Reynold's Numbers ranging from 2,000 to 600,000 during measurable flows), which results in nutrient mixing with a more uniform velocity distribution across the cross-sectional area of flow (Nelson, 1976). The Reynold's Number is a criterion for determining whether flow is laminar or turbulent. Equation 2.4, from Roberson et al. (1988), was used to determine the range of Reynold's Numbers occurring in the flume structure during the study:

$$Re = V*R/v \qquad \text{(Equation 2.4)}$$

Where: Re = the Reynold's Number (unitless)
V = the average velocity (m/s)
R = the hydraulic radius (m)
v = kinematic viscosity of water
($1.31*10^{-6}$ m^2/s @ 10^oC)

(An average temperature of 10^oC was chosen to determine the kinematic viscosity, as this was close to the average temperature of the canal waters during flow events). Average stage and velocity readings at the center of the channel were automatically taken and recorded every ten minutes by the Doppler flow meter. The Doppler flow meter velocities that usually

contain “signal noise,” especially at low velocities, were “smoothed” using two methods. The first method was the removal of large spikes caused by power surges or other factors of unknown origin. This was accomplished using a computer program that removed excessively large peaks by eliminating all points above or below threshold values (based on the possible maximum and minimum values for the flow), as well as sudden increases or decreases in velocity based on a threshold value for changes in velocities (again based on the possibilities of occurrence within the flow). The second method averaged the velocities over a one-and-a-half-hour period surrounding each reading (50 minutes prior and 50 minutes after). This was done to remove small spikes and irregularities caused by sudden small increases or decreases in velocities to achieve a more averaged velocity for the period.

As previously stated, the Doppler flow meter emits an acoustic beam. This beam has a width of about 10^{o} (Figure 2.7) (STARFLOW User’s Manual, 1998). Locating the meter in the center of a stream gives cleaner, more reliable data in most cases but results in a velocity higher than the actual average velocity for the whole channel (STARFLOW User’s Manual, 1998). This means Doppler flow meter velocities need to be converted to average channel velocities for use in determining total flow. This was accomplished by comparing the Doppler flow meter velocities to average flow velocities that were calculated using manual velocity measurements and the Velocity-Area-Integration method (Equation 2.5) (Roberson et al., 1988) for the same time periods:

$$V = Q/A = (\sum V_i * A_i) / A \qquad \text{(Equation 2.5)}$$

where: V = average flume velocity (m/s)
Q = flow through flume (m^3/s)
A = cross sectional area of flume flow (m^2)
V_i = Measured velocity of flow section (m/s)
A_i = cross sectional area of flow section (m^2)
i = 1 to n (the number of cross sections)

Manual measurements were taken using a MARSH MCBIRNEY Model 201 portable water current meter, at 0.60 the flow depth from the water surface during shallower flow depths (<1 m) and at 0.20 and 0.8 the flow depth at deeper flow depths (>1 m), at equally spaced locations across the flume during different flow rates (Figure 2.8). The manual velocity measurements for each section of the flume were then multiplied by the known cross-sectional area of each flume section, resulting in a flow volume per unit time for each flume section. The flow volumes for all the flume sections were then summed and divided by the total cross-sectional area of flow within the flume, giving an overall average flow velocity.

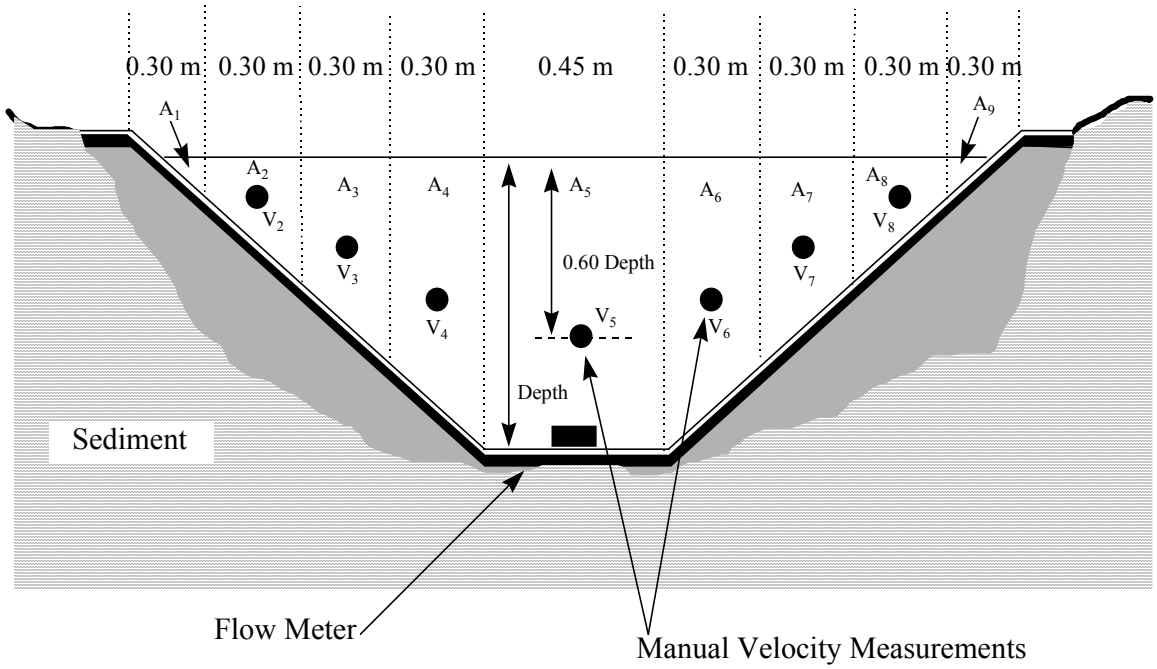

Figure 2.8. Locations and cross sectional areas for each manual velocity measurement and associated volume calculation.

The "smoothed" Doppler flow meter velocities were then plotted against their associated calculated average velocities from the manual measurements (Figure 2.9). A linear model, originating at the origin (0,0), was overlaid on the plot. The resultant linear model, Y =0.7893*X, is the relationship between the Doppler flow meter velocity (X) and the calculated average velocity (Y) within the flume structure. The high coefficient of determination (R^2 = 0.96) implies that the linear model Y=0.7893*X, based on the Doppler flow meter velocities, explains 96.1% of the total sample variation of the calculated average velocity. This means there is a strong relationship between the two velocities, and the model is a good fit with the data (McClave and Dietrich, 1979).

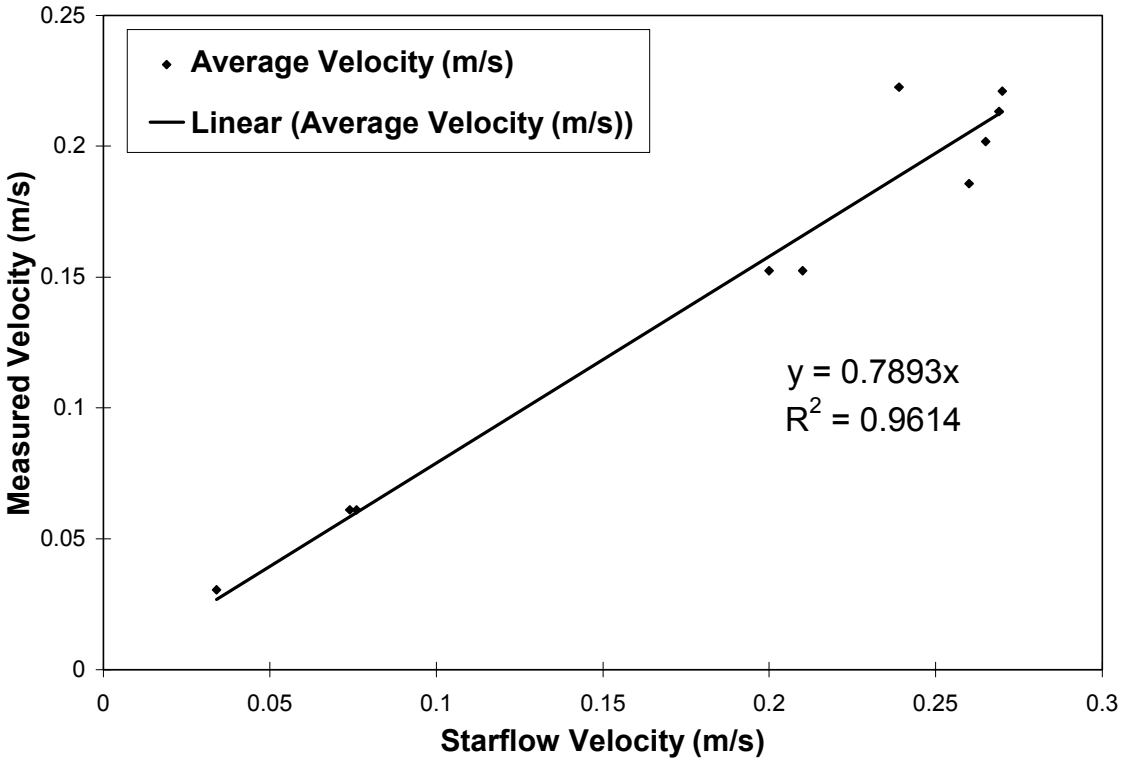

Figure 2.9. STARFLOW velocity calibration curve.

Missing Doppler flow meter velocity data were extrapolated from depth data using a water level recorder, located alongside the flume, connected to a BLUE EARTH® microprocessor that was used to trigger the water quality sampler described later in this section. This was accomplished by comparing calibrated flow volumes per unit time to their associated stages (the calibrated Doppler flow meter velocities (as described above) were multiplied by their associated depths to determine their total flow volumes per unit time) (Figure 2.10). A hysteretic effect was found when plotting the data. The rising limb data gave much higher velocities than did the falling limb data. This is due to the lack of water in the canal to slow the flow as the stage rises. The empirical quadratic relationship for the rising limb relationship is expressed in Equation 2.6:

$$Q = -0.4263*D^2 + 0.4734*D - 0.0267 \quad \text{Equation 2.6}$$

Where: Q = flow volume (m^3/s)
D = stage (m)
(R^2=0.99)

where the falling limb relationship is expressed in Equation 2.7:

$$Q = 0.3044*D^2 + 0.1256*D - 0.0177 \quad \text{Equation 2.7}$$

Where: Q = flow volume (m^3/s)
D = stage (m)
(R^2=0.99).

Equations 2.6 and 2.7 were used to model the higher flow volumes during rising and falling parts of the hydrograph while an empirical power function relationship, Equation 2.8:

$$Q = 1.7065*D^{2.7778} \quad \text{Equation 2.8}$$

Where: Q = flow volume (m^3/s)
D = stage (m)
(R^2=0.8015)

was used to model the lower volumes. The point of switching from the power function model to the quadratic model was determined to be at a stage of 0.1340 m (the point at which the three models are equal). Below this depth, the quadratic models underestimate the flow and become negative while the stage is still positive. Above this depth, the power function overestimates the flow. The predicted discharges are then converted to flow velocities by dividing them by their associated cross-sectional areas. A comparison of the predicted velocities to measured velocities can be seen in Figure 2.11.

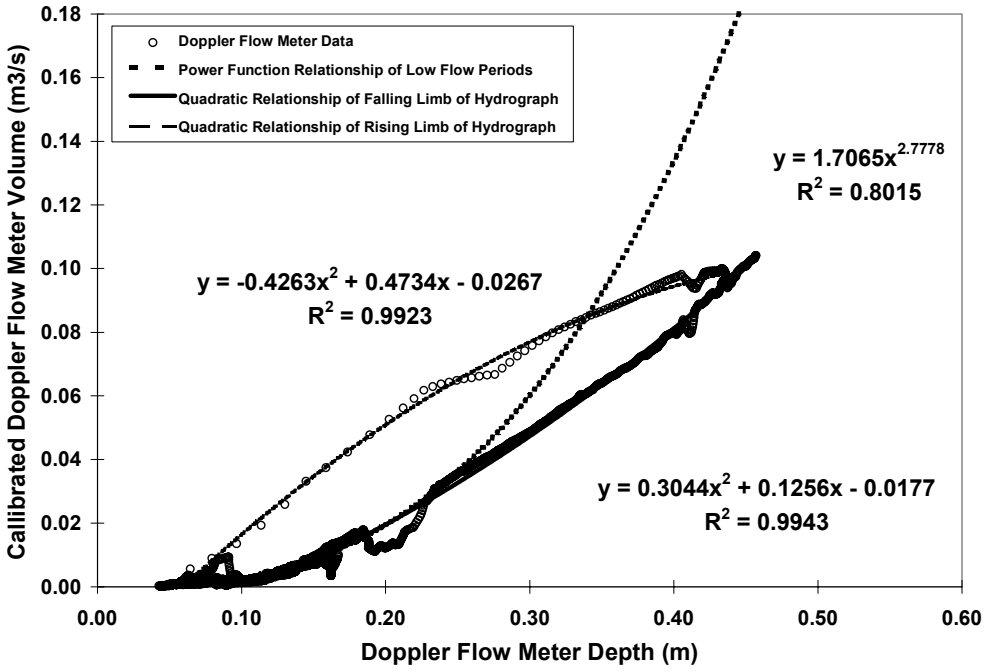

Figure 2.10. Model development for use during periods of missing Doppler flow meter data.

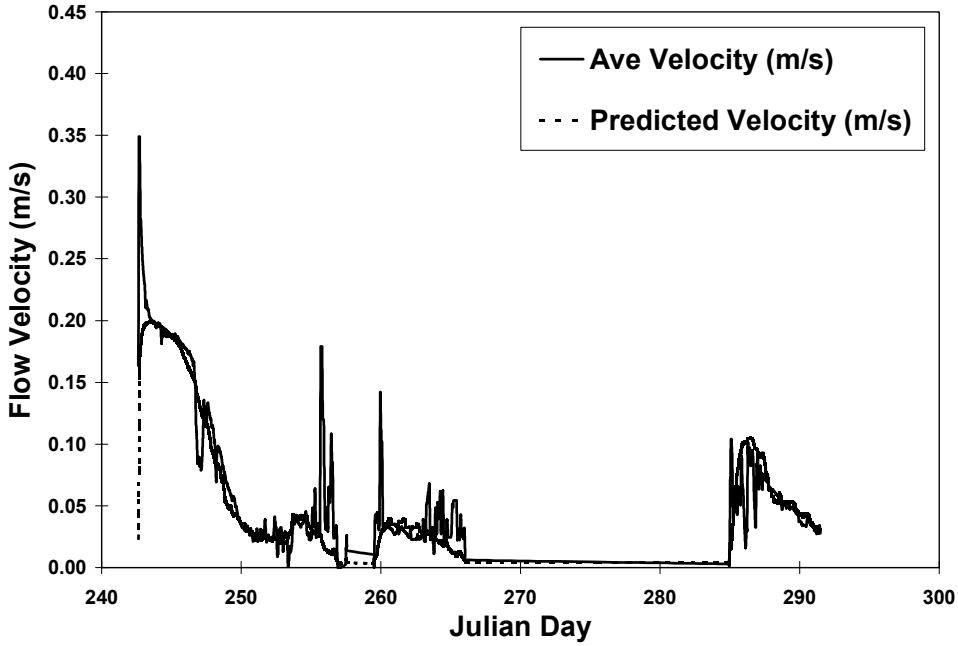

Figure 2.11. Comparison of predicted velocities to measured velocities using flow data from S0 during early Fall 2002.

Discrete water quality samples were taken using a Sigma 900® automatic sampler. The sampler was connected to a BLUE EARTH® microprocessor and a water level recorder to make calculations to trigger the sampler and record real time, stage, and time of sample. Samples were taken on a flow-proportional basis during normal flow periods. During events, the sampling regime switched to a timed mode based on the time to peak, taking samples every two hours on the rising limb of the hydrograph and every six hours on the falling limb until flow returned to a threshold level. The more intense sampling regime during events is used to ensure that nutrient flushes which occur during events are adequately sampled. Samples were removed from the sampler on a weekly basis. After collection, water samples were placed in a freezer immediately and kept frozen until analysis. All samples were filtered through a 0.45 micron filter (Gelman Laboratory, Supor®-450) to remove particulate material. Each sample was analyzed for nitrate, ammonium, phosphate, and dissolved organic, inorganic, and total carbon (Standard Methods, 1989).

Dissolved oxygen, pH, and temperature at mid-depth of the water column of the inflow were also taken on a weekly basis using a YSI Model 610-D Multi-Parameter Water Quality Monitor when the water sampler was emptied.

2.5.2 Results and Discussion

Upstream inflow depth, velocity, volume, and nutrient concentrations (Figures 2.12 and 2.13) are dependent on the inputs from their associated rainfall, throughfall, litterfall, and groundwater, along with their in-stream processes, which may vary the nutrient concentrations as described in those sections.

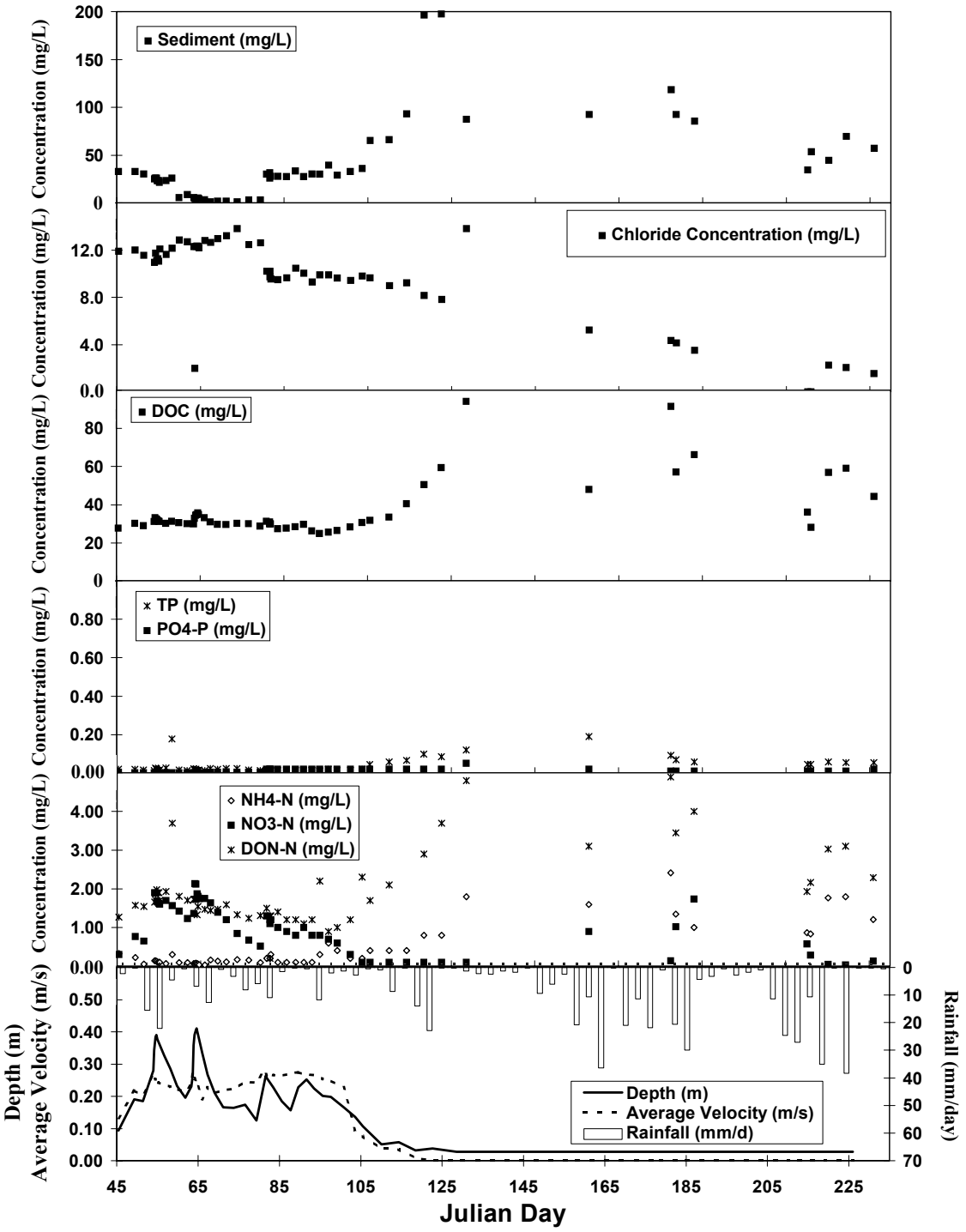

Figure 2.12. Flow velocity, depth, daily rainfall, ammonium, nitrate, dissolved organic nitrogen, phosphate, total phosphate, dissolved organic carbon, chloride, and sediment concentrations measured at the upstream inflow during the 2001 flow season.

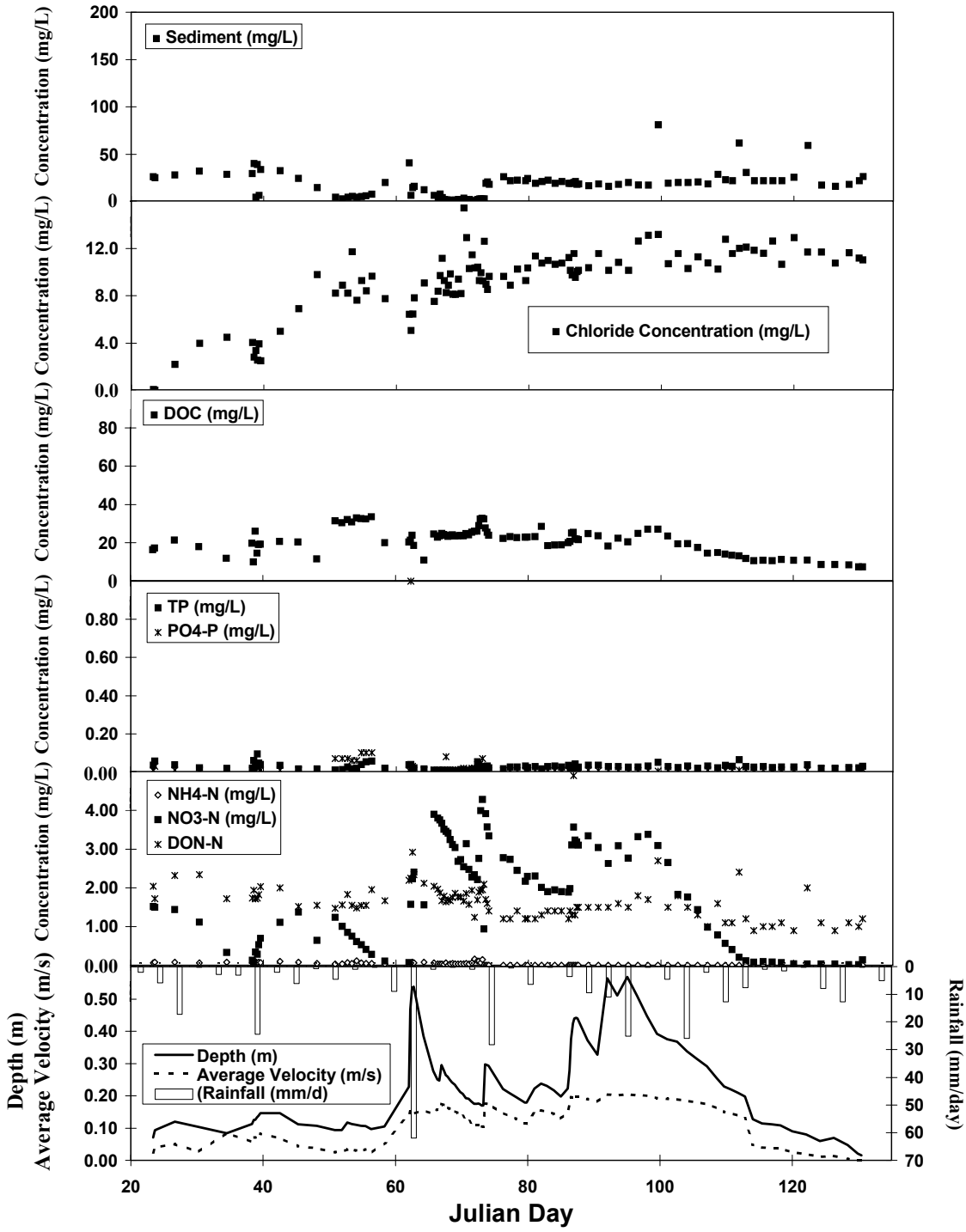

Figure 2.13. Flow velocity, depth, daily rainfall, ammonium, nitrate, dissolved organic nitrogen, phosphate, total phosphate, dissolved organic carbon, chloride, and sediment concentrations measured at the upstream inflow during the 2002 flow season.

Volume weighted average inflow concentrations of ammonium, nitrate, dissolved organic nitrogen, total phosphorous, phosphate, dissolved organic carbon, chloride, and sediment can be found in Table 2.34. Average concentrations of these nutrients during the period of no flow in 2001 can be found in Table 2.35.

Table 2.34. Volume weighted average inflow concentrations of ammonium, nitrate, dissolved organic nitrogen, total phosphorous, phosphate, dissolved organic carbon, chloride, and sediment for 2001 and 2002.

Nutrient	Volume Weighted Average Concentration (mg/L)		
	2001	2002	Overall
Ammonium	0.16	0.01	0.08
Nitrate	1.14	2.36	1.80
Dissolved Organic Nitrogen	1.56	1.68	1.62
Total Phosphorous	0.02	0.03	0.02
Phosphate	0.01	0.02	0.01
Dissolved Organic Carbon	29.7	21.2	25.1
Chloride	11.2	10.3	10.7
Sediment	21.2	24.4	21.3

Table 2.35. Average concentrations of ammonium, nitrate, dissolved organic nitrogen, total phosphorous, phosphate, dissolved organic carbon, chloride, and sediment at S0 during period of no flow (2001).

Nutrient	Average Concentration (mg/L)
Ammonium	1.40
Nitrate	0.46
Dissolved Organic Nitrogen	3.31
Total Phosphorous	0.08
Phosphate	0.01
Dissolved Organic Carbon	58.3
Chloride	4.07
Sediment	84.8

2.5.2.1 Ammonium

Ammonium concentrations in the inflow waters at S0 remain low, at levels ranging from 0.4 mg/L to 0.01 mg/L (volume weighted average of 0.08 mg/L over the two years) during the flow period. A majority of the readings were at the lower end of the range. During the non-flow period (from day 120 to the end of sampling during 2001), ammonium levels increase to an average of 1.4 mg/L. The low values for the ammonium concentrations during the flow period are similar to those from other studies (Table 1.8). The relatively constant concentrations found in the inflow waters is due to the constant concentrations from the groundwater entering the canal. The canal values are slightly lower due to the occurrence of some nitrification within the canal. The increase in the ammonium concentration during the period of no flow (from day 120 of 2001) is most likely due to reduction in nitrification because of a drop in dissolved oxygen to below 1.0 mg/L (0.37 mg/L measured on day 181) as the flow stops. Mineralization, on the other hand, continued to add ammonium to the system.

2.5.2.2 Nitrate

Nitrate concentrations in the inflow water at S0 show a close correlation to the depth of the water in the canal; as the depth increases due to rainfall events, the nitrate concentration increases, and as the depth decreases, the nitrate concentration decreases. After flow stopped (from day 120 of 2001), the nitrate concentration decreased to the detection limit, except during large rainfall events (average 0.46 mg/L). The close correlation between the depth in the canal and the nitrate concentration is due to the flush effect that occurs at these times. As a rainfall event occurs, nitrates that have been formed in the soil are leached from the soil and into the drainage water in the canal. This causes an increase in the

concentration as the canal deepens due to the increases in groundwater flow into the canal. As the water flows through the canal drainage system, it takes the excess nitrates with it, and concentrations return to normal levels after a short period. This is why the decrease in depth correlates with the reduction in nitrate concentration. This effect is most evident during a drought, as occurred during this study. During a drought, there is a larger zone in the soil for nitrification to occur, as well as a longer period between rainfall events for the nitrate to accumulate. This may explain the higher-than-average nitrate concentrations (volume weighted average of 1.80 mg/L over the two years) found in this study, as compared to other studies on discharge from forested watersheds (Table 1.8). Low concentrations during the no-flow periods (averaging 0.46 mg/L) are due to the low dissolved oxygen in the water column, little or no nitrification in the canal, and accelerated denitrification rates. The sudden increases in nitrate (approximately day 155 and 165) are due to the large rainfall events that flushed nitrates into the canal waters. These nitrates were rapidly denitrified in the anaerobic canal waters, as there was no flow during this period.

2.5.2.3 Dissolved Organic Nitrogen

The organic nitrogen concentrations of the upstream inflow at S0 show a relatively constant concentration over the two flow periods studied. During the study, concentrations remained between 1.0 mg/L and 2.0 mg/L (volume weighted average of 1.62 mg/L over the two years), with exceptions occurring during some of the rainfall events. When flow ceased (approximately day 105 of 2001), the dissolved organic nitrogen concentrations increased to an average of 3.31 mg/L, with a high of 4.9 mg/L and a low of 1.7 mg/L. The relatively constant dissolved organic nitrogen concentrations of the inflow are due to the relatively constant concentrations of dissolved organic nitrogen from the groundwater inputs to the

drainage water. During the period of no flow (after day 120 of 2001), dissolved organic nitrogen concentrations continued to increase as nitrogen leached from the organic material in the bottom sediment. Also, as the water evaporates, the dissolved organic nitrogen is concentrated, increasing concentrations within the canal. Mineralization is also slowed during times of no flow due to lack of oxygen in the water column, resulting in higher levels of dissolved organic nitrogen. Shortly after flow ends, dissolved oxygen levels drop to 1.0 mg/L or less. The results are similar to those of other studies (Table 1.8).

2.5.2.4 Total Phosphorous and Phosphate

Throughout the study, total phosphorous and phosphate concentrations remained low (< 0.1 mg/L, with volume weighted averages of 0.02 mg/L and 0.01 mg/L respectively over the two years) in the waters flowing into the study canal from upstream of flume structure S0. Average concentrations during the no flow period were 0.08 mg/L for total phosphorous and 0.01 mg/L for phosphate. These results are similar to those studies reporting total phosphorous and phosphate found in Table 1.8. The source of organic phosphorous in the surface water of the canal is from litterfall (directly entering the canal and as leachate and particulate from litterfall on the forest floor), throughfall, and groundwater. Phosphorous in the groundwater along with a portion of the inorganic phosphate was likely immobilized due to the high C/P ratio (>370) as discussed in Section 1.4.3.4 (Role of Carbon-to-Phosphorous Ratio in Mineralization and Immobilization). Phosphates not immobilized are readily adsorbed by the soil, particularly in acidic soils like those found around the study canal (Tisdale et al., 1993). This results in little to no phosphorous or phosphate entering the groundwater, which in turn results in little to no phosphorous and phosphate entering the canal drainage water.

2.5.2.5 Dissolved Organic Carbon

The dissolved organic carbon concentrations remained relatively constant during periods of flow (volume weighted average of 25.1 mg/L over the two years). The dissolved organic carbon concentrations increase during the no-flow period (from day 120 of 2001) to an average of 58.3 mg/L. The constant concentrations during the periods of flow are due to the constant inputs from the groundwater entering the canal from upstream of S0. The higher values during the no-flow period of 2001 are due to continuous leaching from organic material at the bottom of the canal and the concentrating action of evaporation. Another contributing factor is slower carbon utilization due to low dissolved oxygen levels present during no-flow conditions.

2.5.2.6 Chloride

The chloride concentrations found over the length of the study show an increase over the first part of the season, leveling off during the central portion (peaking at around 12 to 14 mg/L), and declining during the latter portion of the study (volume weighted average for the two years was 10.7 mg/L). This shows the same general trend as the groundwater chloride concentrations but is lower in overall range. This seasonal variation follows the natural seasonal variations in chloride concentration suggested by Peters and Ratcliffe, 1998; Russo et al., 2003; and reported by Tisdale et al., 1993. Though variable with season, chloride can still be used as a conservative tracer in mass balance studies (Peters and Ratcliffe, 1998).

2.5.2.7 Sediment

The sediment concentrations (volume weighted average of 21.3 mg/L over the two years) found throughout this study during normal flow periods were similar to those found by Appelboom (2000) in previous years in other locations (ranging from 32.4 mg/L to 7.0 mg/L)

within the Parker Tract, where this study was conducted. These concentrations are low due to the low gradient and velocities characteristic of this flat coastal area. After flow ceased (after day 120 of 2001), sediment concentrations increased above the normal range (84.8 mg/L). This is most likely due to the purging of the sampler line. Prior to each sample being taken, the sampler flushes the tube with water by drawing water up and expelling it again. When the water is expelled, it would disturb the sediment in the shallow canal water. There was no current to move the sediment-laden water away from the sampler intake, resulting in higher-than-normal sediment concentrations.

2.5.3 Conclusions

The inflow to the study canal at S0 showed similar streamwater volume weighted concentrations to those of other studies (Table 8) for ammonium (0.08 mg/L), dissolved organic nitrogen (1.6 mg/L), total phosphorous(0.02 mg/L), and sediment (21.3 mg/L). Nitrate concentrations (1.8 mg/L) averaged slightly higher than those in other studies.

2.6 Surface Runoff

Surface runoff is not considered, as all rainfall either infiltrates immediately or is stored as surface storage until infiltration without generating runoff.

2.7 Allochthonous Inputs (Litterfall and Lateral Movement)

2.7.1 Methods

Litter inputs and lateral inputs (wind-blown litterfall from the surrounding forest floor) were measured as one input. This made it easier to ensure that lateral inputs were accurately represented. Samples were collected at five locations along the study canal in 0.5 m by 0.5 m litter traps floating on the water surface within the study canal (Figure 2.14). This method intercepted litter as well as lateral material just prior to entering the canal. Material was removed from the litter traps on a weekly basis, placed in brown paper bags, and allowed to air dry. Samples were then oven-dried, weighed, and analyzed for nutrient content (nitrogen and carbon (Perkins Elmer, 1988) and phosphate (Analytical Service Laboratory, 1976)).

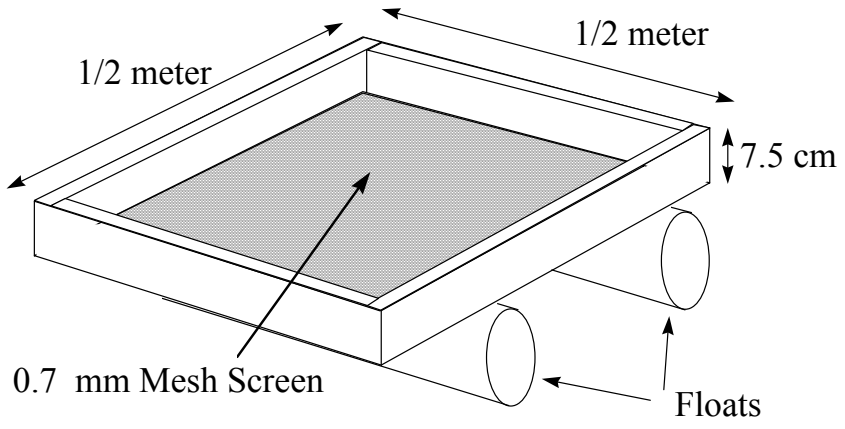

Figure 2.14. Floating litter trap.

2.7.2 Statistical Analysis

A general linear model for the litterfall entering the canal is shown in Equation 2.9.

$$\text{Model: } Y = \mu + \alpha_i + \beta_j + (\alpha\beta)_{ij} + \varepsilon_{ij} \qquad \text{Equation 2.9}$$

where: Y = the mass of litterfall
μ = the average mass of litterfall
α_i represents the main effects of season on the mass of litterfall
(i = spring, summer, fall, winter)
β_j represents the main effects of location on the mass of the litterfall
(j = 1, 2, 3, 4, 5)
$(\alpha\beta)_{ij}$ represents the interactions between season and location on the mass of the litterfall
ε_{ij} = error term.

The constraints of $\sum_i\alpha_i = 0$, $\sum_j\beta_j = 0$, $\sum_i\alpha_i\beta_j = 0$, $\sum_j\alpha_i\beta_j = 0$. The hypotheses being tested are: H_o: $\alpha_i = 0$ - no main effect of season, H_o: $\beta_j = 0$ - no main effect of location, and H_o: $(\alpha\beta)_{ij} = 0$ - interactive effects between season and location on the mass of litterfall (Steel and Torrie, 1980). The same statistical model and constraints were used for analyzing the nitrogen, phosphate, and carbon content as well as the carbon-to-nitrogen ratio of the litterfall from the different seasons and locations. The same hypotheses were tested on each of the different litterfall components. The data were transformed using a square root transformation to stabilize the variance. There was a slight non-homogeneity in the data. The individual least squares means analyses were adjusted for multiple comparisons using Tukey for a more conservative comparison.

2.7.3 Results and discussion

2.7.3.1 Average Daily Litterfall Mass

The statistical analysis indicated that there was a main effect of season on the average daily litterfall mass but not of location ($R^2 = 0.59$, RMSE = 0.19). There was no interactive effect of season with location. The individual comparisons showed the average daily litterfall amount during the fall season to be statistically larger than during the winter, spring, and summer (Table 2.36). There was also a statistical difference between the summer and winter average daily litterfall amounts. Average daily litterfall mass per location is given in Table 2.37.

Table 2.36. Average daily litterfall mass per season.

Season	Average Daily Litterfall Mass ($g/m^2/day$)
Spring (Mid-March – Mid-June)	0.60 BC[1]
Summer (Mid-June – Mid-September)	1.20 B
Fall (Mid-September – Mid-December)	3.04 A
Winter (Mid-December – Mid-March)	0.52 C
Yearly Average	1.33

[1] Different letters indicate significant difference using the Least Squares Means adjusted for multiple comparisons using the Tukey adjustment at $\propto = 0.05$.

Table 2.37. Average daily litterfall mass per location.

Location	Average Daily Litterfall Mass ($g/m^2/day$)
Planted Pine Location 1	1.45 A[1]
Planted Pine Location 2	1.52 A
Mixed Stand Location 1	0.82 A
Natural Hardwood Location 1	1.15 A
Natural Hardwood Location 2	1.70 A
Average	1.33

[1] Different letters indicate significant difference using the Least Squares Means adjusted for multiple comparisons using the Tukey adjustment at $\propto = 0.05$.

Seasonal differences were due to the life cycles of the trees along and overhanging the canal, hardwoods in this case. In the fall, most of the trees shed their leaves, becoming completely defoliated as they go into dormancy for the winter. This generates a maximum amount of litterfall. This material can enter the canal by either falling into, or by being blown into the canal. During the winter most leaves have already fallen leaving only twigs and branches to make up the litterfall for this season. This results in the smallest mass of litterfall among the seasons. The amount of litterfall during the spring was only slightly larger than the winter. This is due to the active flushing out of the new leaves. The trees are growing new foliage with no leaf loss. The slight increase is due to flowering, fruit, and seed set in some of the trees. The increase in the amount of litterfall during the summer as compared to the winter and spring months is due to the loss of flower, seed and fruit by the trees in the earlier part of summer, leaf loss latter in the summer, and natural pruning of twigs and branches over the entire summer due to wind, storms, etc. (Gosz et al, 1972). The seasonal litterfall distribution found in this study is similar to those found by Gosz et al. (1972). The average yearly litterfall, 4855 kg/ha/yr, is similar to that of the studies presented in Table 1.5.

2.7.3.2 Average Daily Litterfall Percentage Organic Carbon

The statistical analysis indicated that there was a main effect of season on the average litterfall percentage organic carbon but not for location ($R^2 = 0.18$, RMSE = 0.07). There was no interactive effect of season with location. The individual comparisons showed the average daily percentage organic carbon during the fall season to be statistically less than during the spring, and summer seasons (Table 2.38). There was no statistical difference in the average daily percentage organic carbon during the winter, summer, and spring seasons. The

difference between the average daily percentage organic carbon of the fall and winter season was also not significant. Average daily litterfall percentage organic carbon per location can be found in Table 2.39.

Table 2.38. Average daily litterfall percentage organic carbon per season.

Season	Average Daily Litterfall Percentage Organic Carbon
Spring (Mid-March – Mid-June)	48.2 B[1]
Summer (Mid-June – Mid-September)	48.4 B
Fall (Mid-September – Mid-December)	47.2 A
Winter (Mid-December – Mid-March)	47.9 AB
Weighted Yearly Average	47.9

[1] Different letters indicate significant difference using the Least Squares Means adjusted for multiple comparisons using the Tukey adjustment at $\propto = 0.05$.

Table 2.39. Average daily litterfall percentage organic carbon per location.

Location	Average Daily Litterfall Percentage Organic Carbon
Planted Pine Location 1	48.0 A[1]
Planted Pine Location 2	48.0 A
Mixed Stand Location 1	48.1 A
Natural Hardwood Location 1	47.6 A
Natural Hardwood Location 2	48.0 A
Average	47.9

[1] Different letters indicate significant difference using the Least Squares Means adjusted for multiple comparisons using the Tukey adjustment at $\propto = 0.05$.

Even though there was a slight statistical difference in the average daily litterfall percentage organic carbon, the averages are very similar. The carbon content of litterfall varied little throughout the year. The amount here is very similar to the year-long average litterfall percentage organic carbon (47%) found by Meyer et al. (1981) in their study of Bear Brook. Most studies shown in Table 1.5 did not present carbon content data.

2.7.3.4 Average Daily Litterfall Percentage Total Nitrogen

The statistical analysis indicated that there was a main effect of season on the average litterfall percentage total nitrogen but not of location ($R^2 = 0.34$, RMSE = 0.17). There was no interactive effect of season with location. The individual comparisons showed the average daily percentage total nitrogen during the spring season to be statistically larger than during the summer, fall, and winter seasons, which were not statistically different from each other (Table 2.40). Average daily litterfall percentage total nitrogen per location can be found in Table 2.41.

Table 2.40. Average daily litterfall percentage total nitrogen per season.

Season	Average Daily Litterfall Percentage Total Nitrogen
Spring (Mid-March – Mid-June)	1.71 A[1]
Summer (Mid-June – Mid-September)	1.28 B
Fall (Mid-September – Mid-December)	1.08 B
Winter (Mid-December – Mid-March)	1.26 B
Weighted Yearly Average	1.34

[1] Different letters indicate significant difference using the Least Squares Means adjusted for multiple comparisons using the Tukey adjustment at $\propto = 0.05$.

Table 2.41. Average daily litterfall percentage total nitrogen per location.

Location	Average Daily Litterfall Percentage Total Nitrogen
Planted Pine Location 1	1.28 A[1]
Planted Pine Location 2	1.36 A
Mixed Stand Location 1	1.48 A
Natural Hardwood Location 1	1.29 A
Natural Hardwood Location 2	1.27 A
Average	1.34

[1] Different letters indicate significant difference using the Least Squares Means adjusted for multiple comparisons using the Tukey adjustment at $\propto = 0.05$.

The seasonal differences in the percentage total nitrogen are due to the life cycles of the vegetation surrounding the canal. During the fall season, leaves dominate the litterfall. These leaves have greatly reduced nitrogen due to translocation of the nitrogen prior to senescing, as the trees go into dormancy for the winter (Berg and Verhoef, 1998). Nitrogen content is highest in the leaves (proteins and chlorophyll), branches, flowers, and fruit of the trees during spring, when growth is most active. Large amounts of pollen produced and released during this period also contribute to litterfall having a high nitrogen content (Starr and Taggart, 1995). The yearly average nitrogen content, 1.34% or 13.4 mg/g, is similar to the nitrogen content in the studies presented in Table 1.5.

2.7.3.5 Average Daily Litterfall Percentage Total Phosphorous

The statistical analysis indicated that there was a main effect of season on the average litterfall percentage total phosphorous but not of location ($R^2 = 0.32$, RMSE = 0.08). There was no interactive effect of season with location. The individual comparisons showed the average daily percentage total phosphorous during the spring season to be statistically larger than during the summer, fall, and winter seasons, which were not statistically different from each other (Table 2.42). Average daily litterfall percentage total phosphorous per location

can be found in Table 2.43.

Table 2.42. Average daily litterfall percentage total phosphorous per season.

Season	Average Daily Litterfall Percentage Total Phosphorous
Spring (Mid-March – Mid-June)	0.13 A[1]
Summer (Mid-June – Mid-September)	0.07 B
Fall (Mid-September – Mid-December)	0.05 B
Winter (Mid-December – Mid-March)	0.08 B
Weighted Yearly Average	0.08

[1] Different letters indicate significant difference using the Least Squares Means adjusted for multiple comparisons using the Tukey adjustment at $\propto = 0.05$.

Table 2.43. Average daily litterfall percentage total phosphorous per location.

Location	Average Daily Litterfall Percentage Total Phosphorous
Planted Pine Location 1	0.08 A[1]
Planted Pine Location 2	0.08 A
Mixed Stand Location 1	0.09 A
Natural Hardwood Location 1	0.08 A
Natural Hardwood Location 2	0.08 A
Average	0.08

[1] Different letters indicate significant difference using the Least Squares Means adjusted for multiple comparisons using the Tukey adjustment at $\propto = 0.05$.

Phosphorous content of the litterfall showed a similar pattern to that of nitrogen. This is due to both nutrients being mobile within the vegetation and transportable into or out of the leaves during the different seasons (Palma et al, 2000). Phosphorous content is lowest during the fall due to translocation from the leaves prior to senescence. High phosphorous levels are found in the spring due to the flowering and fruiting of the trees. The yearly average phosphorous content, 0.08% or 0.80 mg/g, is similar to the phosphorous content in the study conducted by Gosz et al., 1972 (Table 1.5).

2.7.3.6 Average Daily Litterfall Carbon-to-Nitrogen Ratio

The statistical analysis indicated there was a main effect of season on the average litterfall carbon-to-nitrogen ratio but not of location ($R^2 = 0.32$, RMSE = 0.88). There was no interactive effect of season with location. The individual comparisons showed the average daily carbon-to-nitrogen ratio during the spring season to be statistically lower than during the summer, fall, and winter, which were not statistically different from each other (Table 2.44). Average daily litterfall carbon-to-nitrogen ratio can be found in Table 2.45.

Table 2.44. Average daily litterfall carbon-to-nitrogen ratio per season.

Season	Average Daily Litterfall Carbon-to-Nitrogen Ratio
Spring (Mid-March – Mid-June)	31.4 A[1]
Summer (Mid-June – Mid-September)	39.5 B
Fall (Mid-September – Mid-December)	44.7 B
Winter (Mid-December – Mid-March)	40.6 B
Weighted Yearly Average	39.1

[1] Different letters indicate significant difference using the Least Squares Means adjusted for multiple comparisons using the Tukey adjustment at $\propto = 0.05$.

Table 2.45. Average daily litterfall carbon to nitrogen ratio per location.

Location	Average Daily Litterfall Carbon-to-Nitrogen Ratio
Planted Pine Location 1	40.9 A[1]
Planted Pine Location 2	38.2 A
Mixed Stand Location 1	36.0 A
Natural Hardwood Location 1	39.7 A
Natural Hardwood Location 2	40.6 A
Average	39.1

[1] Different letters indicate significant difference using the Least Squares Means adjusted for multiple comparisons using the Tukey adjustment at $\propto = 0.05$.

Although the carbon-to-nitrogen ratio varies throughout the four seasons, the ratio remains high enough to indicate net immobilization of nitrogen as it is decomposed in the canal network (reported by Tisdale et al., 1993). Tisdale et al. (1993) also reported that nitrogen content in litterfall between 1.5% and 1.7% is enough to minimize immobilization under aerobic conditions (0.5% nitrogen content for anaerobic conditions). This indicates there is a net mineralization of nitrogen from litterfall in this system due to the nitrogen content (ranging from 1.08 in the fall to 1.71 in the spring, Table 2.40) being higher in the anaerobic zones than the minimum for mineralization (0.5%) discussed by Tisdale et al., 1993. The lower carbon-to-nitrogen ratio in the spring is due to the presence of higher-nitrogen-content pollen, seeds, and fruits during this period. It is not possible to compare this average with results of other studies because carbon and nitrogen data were rarely presented in those studies.

2.7.3.7 Average Daily Litterfall Carbon-to-Phosphorous Ratio

Statistical analysis indicated there was a main effect of season on the average litterfall carbon to phosphorous ratio but not of location ($R^2 = 0.30$, RMSE = 5.66). There was no interactive effect of season with location. The individual comparisons showed the average daily carbon-to-phosphorous ratio during the spring season to be statistically lower than during the summer, fall, and winter, which were not statistically different from each other (Table 2.46). Average daily litterfall carbon-to-phosphorous ratio can be found in Table 2.47.

Table 2.46. Average daily litterfall carbon-to-phosphorous ratio per season.

Season	Average Daily Litterfall Carbon-to-Phosphorous Ratio
Spring (Mid-March – Mid-June)	540 A[1]
Summer (Mid-June – Mid-September)	801 B
Fall (Mid-September – Mid-December)	906 B
Winter (Mid-December – Mid-March)	694 B
Weighted Yearly Average	735

[1] Different letters indicate significant difference using the Least Squares Means adjusted for multiple comparisons using the Tukey adjustment at $\propto = 0.05$.

Table 2.47. Average daily litterfall carbon-to-phosphorous ratio per location.

Location	Average Daily Litterfall Carbon-to-Phosphorous Ratio
Planted Pine Location 1	720 A[1]
Planted Pine Location 2	701 A
Mixed Stand Location 1	670 A
Natural Hardwood Location 1	743 A
Natural Hardwood Location 2	843 A
Average	735

[1] Different letters indicate significant difference using the Least Squares Means adjusted for multiple comparisons using the Tukey adjustment at $\propto = 0.05$.

Both the carbon-to-phosphorous ratio (greater than 300 – reported by Tisdale et al., 1993) and the phosphorous content of the litter (less than 0.2% – reported by Tisdale et al., 1993) indicate immobilization of phosphorous in this system. This results in no additions of phosphorous or phosphate to the system through litterfall. As with the carbonp-to-nitrogen ratio, the lower carbon-to-phosphorous ratio in the spring is due to the presence of higher-phosphorous-content pollen, seeds, and fruits during this period. It is not possible to compare this average with results of other studies because carbon and phosphorous data were rarely presented in those studies.

2.7.4 Conclusions

There is a large influx of litterfall into the canals of the coastal plain of North Carolina. This litterfall has high carbon-to-nitrogen and carbon-to-phosphorous ratios. Nitrogen and phosphorous from litterfall and lateral movement are primarily organic but are converted to inorganic forms through mineralization. Though the carbon-to-nitrogen ratio of the litterfall is high (greater than 30), there is a net mineralization due to the percentage nitrogen being high enough to minimize immobilization (greater than 1.5% for aerobic conditions and 0.5% for anaerobic conditions, reported by Tisdale et al., 1993). Both the high carbon-to-phosphorous ratio and the lower-than-threshold phosphorous content (less than 0.2%, reported by Tisdale et al., 1993) indicate that phosphorous is immobilized in the system rather than mineralized. Litterfall occurring in autumn has a higher carbon-to-nitrogen ratio (averaging 44.7) and carbon-to-phosphorous ratio (906) due to the translocation of nutrients (nitrogen and phosphorous) from the leaves to the stem and trunk prior to leaf drop. Litterfall occurring during the spring has lower carbon-to-nitrogen and carbon-to-phosphorous values (averaging 31.4 and 540 respectively) than the other seasons due to large amount of pollen, seeds, and fruit in the litterfall. The nitrogen from litterfall inputs results in an overall mineralization of nitrogen, which agrees with the results in Appendix D (Mineralization and Nitrification). The phosphorous from litterfall inputs results in an overall immobilization of phosphorous, resulting in a sink for phosphorous in this system.

2.8 Autochthonous Inputs

Autochthonous inputs were not determined, as this canal had little to no light interception at the stream's surface, which discouraged plant growth. Other studies (Meyer et

al., 1981; Triska et al., 1982; Fisher and Likens, 1973) found that forested streams are almost entirely devoid of autochthonous inputs.

2.9 Emergent Drift Outputs

Emergent drift outputs were not determined in this study, as other studies found that the nutrient losses from this vector in forested streams were negligible (Triska et al., 1984; Meyer et al., 1981).

2.10 Downstream Canal Discharge

2.10.1 Methods

Outflow from the study canal was estimated using a double 120^{o} V-notch weir structure instrumented with a Blue Earth microprocessor, and both stages from upstream and downstream water level recorders (Figure 2.15). The bottom of the weir was located at an elevation to minimize the amount of water held back by the structure as well as to reduce the potential for submergence. The upstream water level recorder measures the head (or elevation of the water surface) above the bottom of the V-notch for flow calculations, and the downstream recorder measures the head above the V-bottom (to water surface elevation) behind the weir in case submergence calculations are needed.

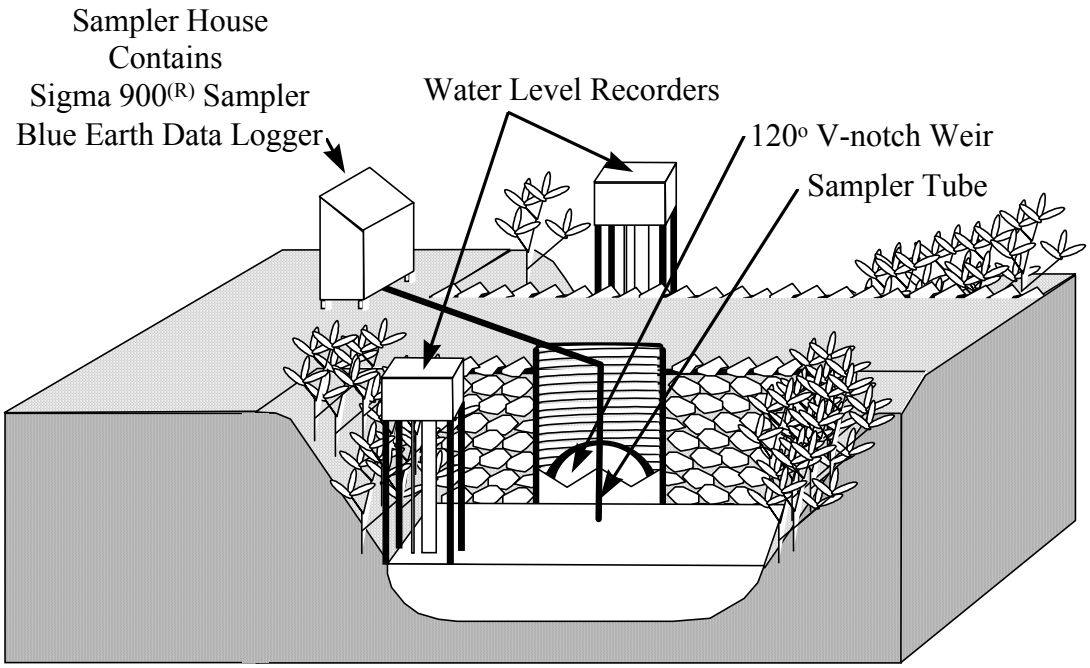

Figure 2.15. Canal study section double weir outlet structure.

Flow was estimated using the basic weir equation (Equation 2.10) (Roberson et al., 1988):

$$Q = 8/15*K*(2*g)^{0.5}*\tan(\theta/2)*H^{2.5} \qquad \text{Equation 2.10}$$

where: Q = discharge (ft^3/sec)
K = flow discharge coefficient (unitless)
g = acceleration due to gravity (ft/sec^2)
θ = weir angle (degrees)
H =head (ft)

Equation 2.10 in S.I. units converts to Equation 2.10a.

$$Q = 2.39*H^{2.5} \qquad \text{Equation 2.10a}$$

where: Q = discharge (m^3/sec)
H = head (m)

As there are two weirs (a double span), flow was calculated for each weir using Equation 2.10. Flows over both weirs were calculated, as the southernmost weir in the structure is 8 mm lower than the other weir.

The flow discharge coefficient, K=0.58, was determined by calibration of the weir. This value is in the range of K (0.60 to 0.57) described by Roberson et al., 1988. To calibrate the weir, a STARFLOW® Doppler flow meter was placed in the pipe downstream of the weir (Figure 2.16). Discharges over the weir were compared to discharges through the outflow pipe. The discharge coefficient, K, was varied until the two instantaneous flows were equal.

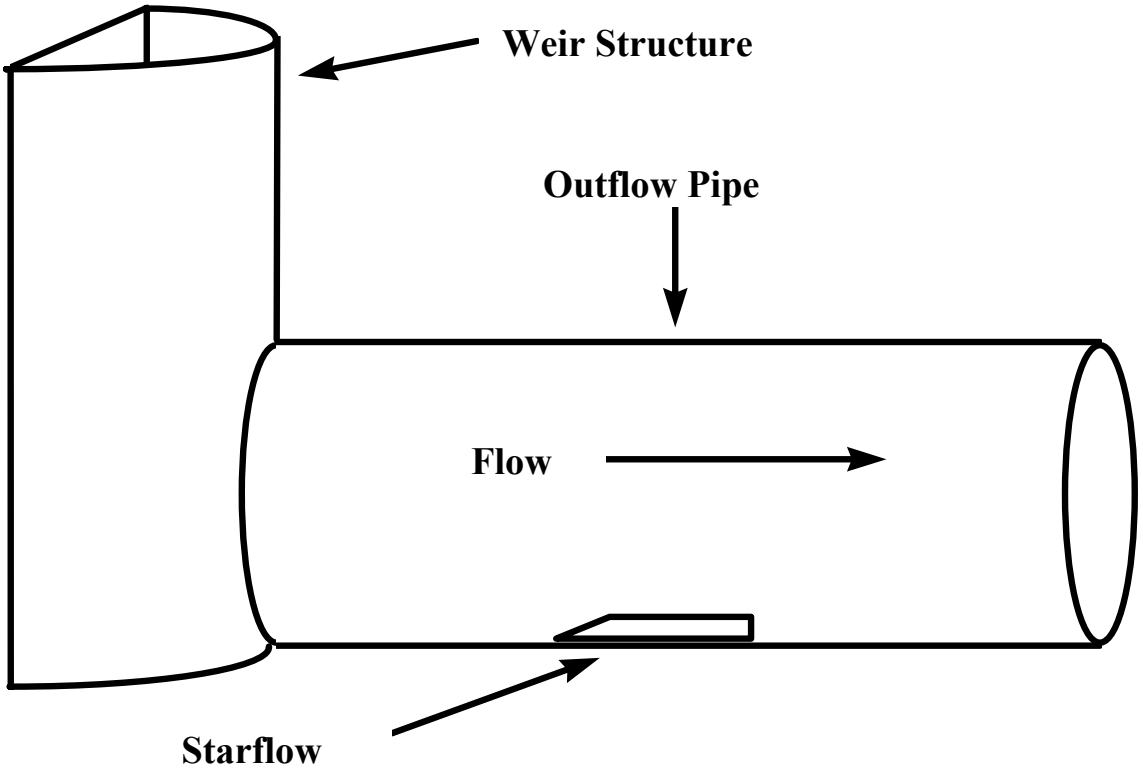

Figure 2.16. Location of STARFLOW® Doppler flow meter in outflow pipe of weir structure.

Velocity and depth were measured over time within the pipe. Discharges were determined by multiplying the velocity by the cross-sectional area of flow. The cross-sectional area of flow was determined by subtracting the area of the triangle formed by the water surface (ABD) from the area of the sector (ACD) and multiplying by two for both halves of the pipe as shown in Equation 2.11 (Figure 2.17).

$$A_{flow} = 2 * (A_{ACD} - A_{ABD}) \qquad \text{Equation 2.11}$$

where: A_{flow} = cross sectional area of flow BCD (m^2)
A_{ACD} = area of the section ACD (m^2)
A_{ABD} = area of the triangle ABD (m^2)

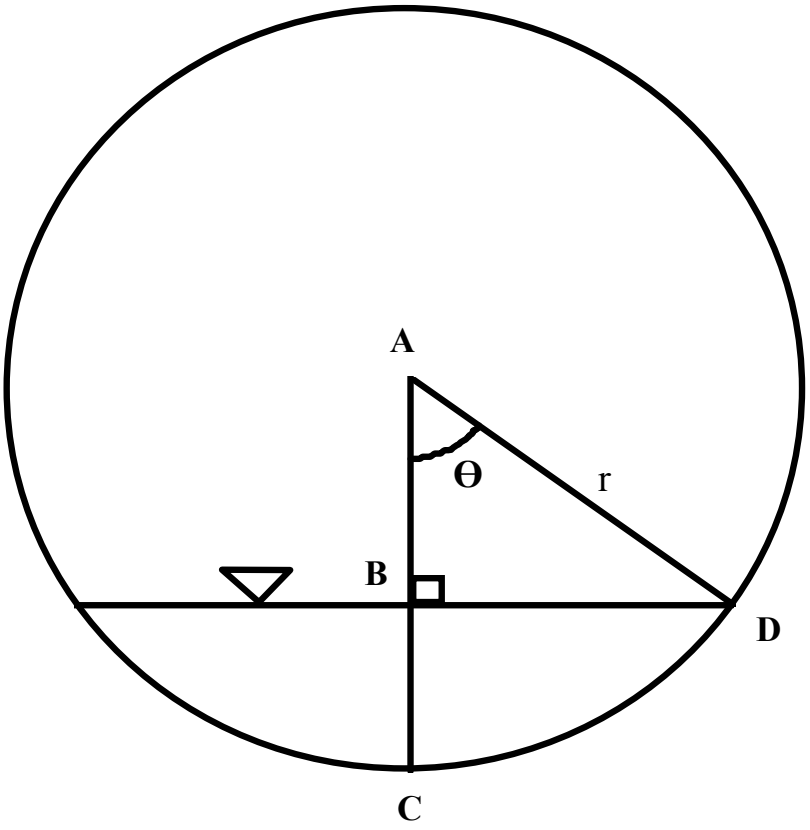

Figure 2.17. Geometry of pipe used for determining cross-sectional area of flow in outflow pipe.

The area of the sector was determined using Equation 2.12 (Person, 1970).

$$A_{ACD} = \frac{1}{2} * r^2 * \theta \qquad \text{Equation 2.12}$$

where: A_{ACD} = area of the sector ACD (m^2)
r = radius of the pipe (m)
θ = angle CAD (radians)

The angle CAD, θ, was determined for each velocity and depth recorded by the velocity meter using Equation 2.13.

$$\theta = A^{*}\cos AB / r \qquad \text{Equation 2.13}$$

where: θ = angle CAD (radians)
AB = the pipe radius minus the depth of the water in the pipe (m)
r = the pipe radius (m)

The area of the triangle formed by the water surface, ABD, was determined by Equation 2.14.

$$A_{ABD} = \tfrac{1}{2} * AB * BD \qquad \text{Equation 2.14}$$

where: A_{ABD} = the area of the triangle ABD (m^2)
BD = the length of the opposite side of the triangle from θ (m)
AB = the radius of the pipe minus the depth of the water in the pipe (m)

The length BD was determined using Equation 2.15.

$$BD = \text{Tan}\ \theta * AB \qquad \text{Equation 2.15}$$

where: BD = the length of the opposite side of the triangle from ? (m)
θ = angle CAD (radians)
AB = the radius of the pipe minus the depth of the water in the pipe (m)

The resulting comparison between the flow calculated from the downstream pipe using the STARFLOW® Doppler flow meter and the flow calculated using the standard weir equation (Equation 1) can be seen in Figure 2.18.

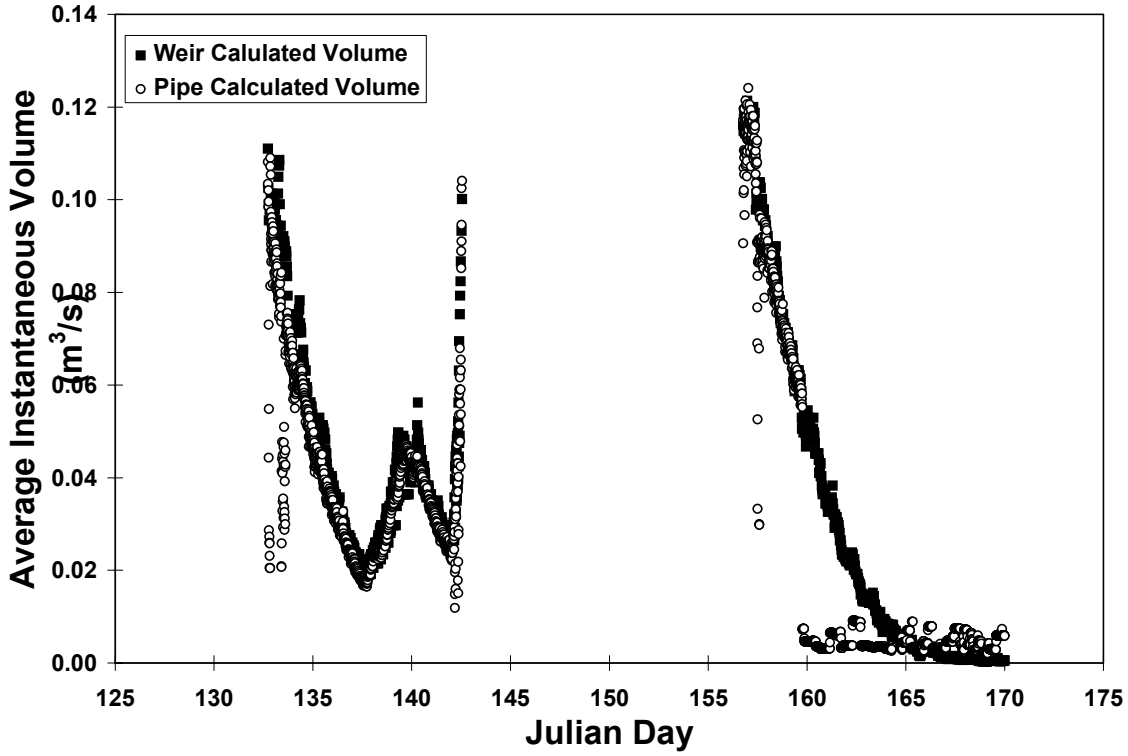

Figure 2.18. Comparison of portion of calibrated weir equation calculated flow and STARFLOW® calculated flow in the downstream pipe at the outlet. Missing portions of data due to flow outside of needed calibration volumes.

Discrete water quality samples were taken using a Sigma 900® automatic sampler. The sampler and two water level recorders were connected to the BLUE EARTH microprocessor, which makes calculations to trigger the sampler and record real time, upstream and downstream stage, and time of sample. Samples were taken on a flow-proportional basis during normal flow periods. During events, the sampling regime switched to a timed mode based on the time to peak, taking samples every two hours on the rising limb of the hydrograph and every six hours on the falling limb. Samples were removed from the sampler on a weekly basis. Water samples were placed in a freezer immediately after collection and kept frozen until analysis. All samples were filtered through a 0.45 micron

filter (Gelman Laboratory, Supor®-450) to remove particulate material. Each sample was analyzed for nitrate, ammonium, and phosphate, and dissolved organic, inorganic, and total carbon (Standard Methods, 1989).

2.10.2 Results and Discussion

Outflow stage and nutrient concentrations can be found in Figures 2.19 and 2.20. The outflow hydrograph and nutrient concentrations give the same trends as the inflow data. This is due to the inflow being by far the dominant source of drainage water, nitrate, ammonium, dissolved organic nitrogen, phosphate, total phosphorous, dissolved organic carbon, and chloride.

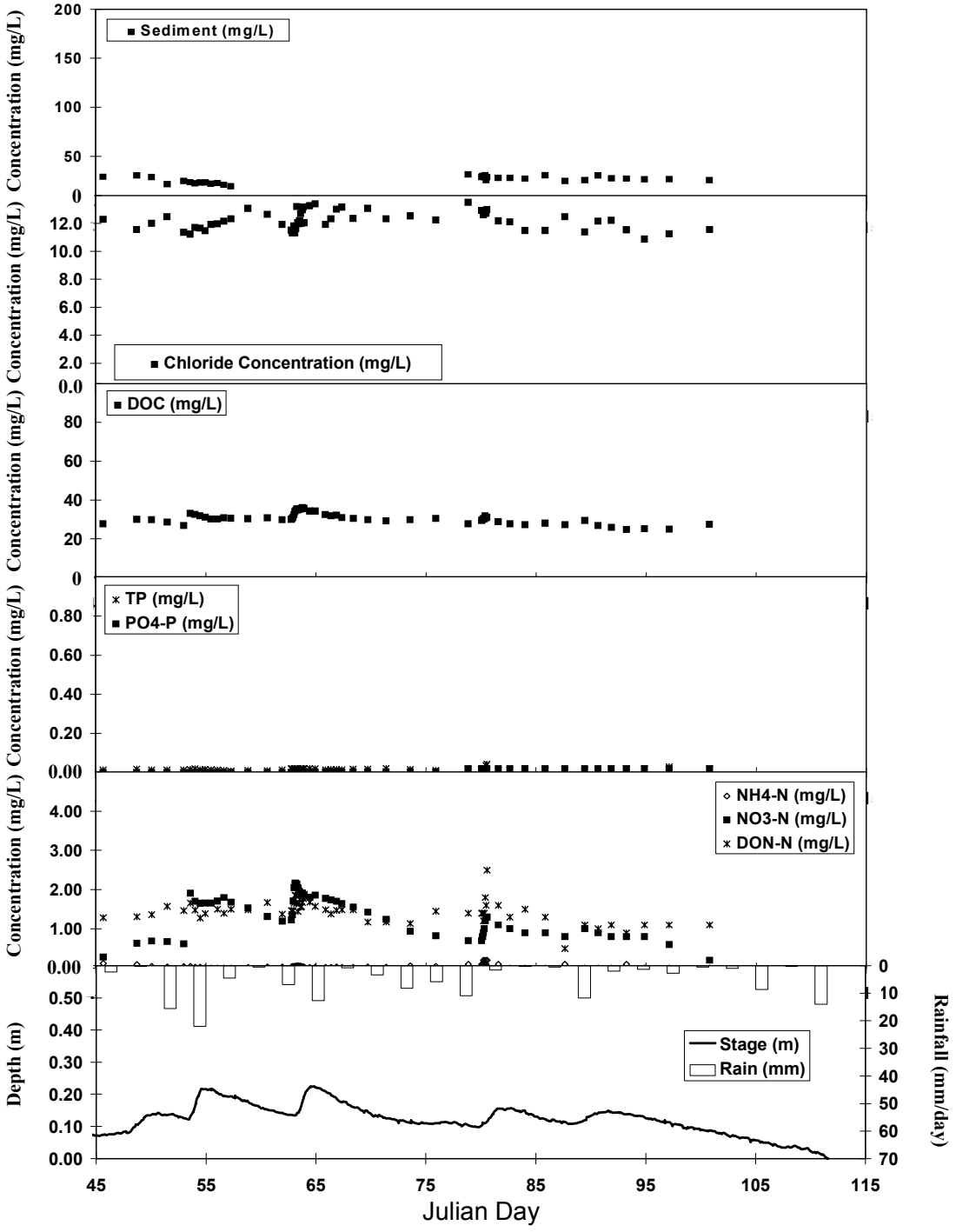

Figure 2.19. Flow depth, daily rainfall, ammonium, nitrate, dissolved organic nitrogen, phosphate, total phosphorous, dissolved organic carbon, chloride, and sediment concentrations measured at the outflow during the 2001 flow season.

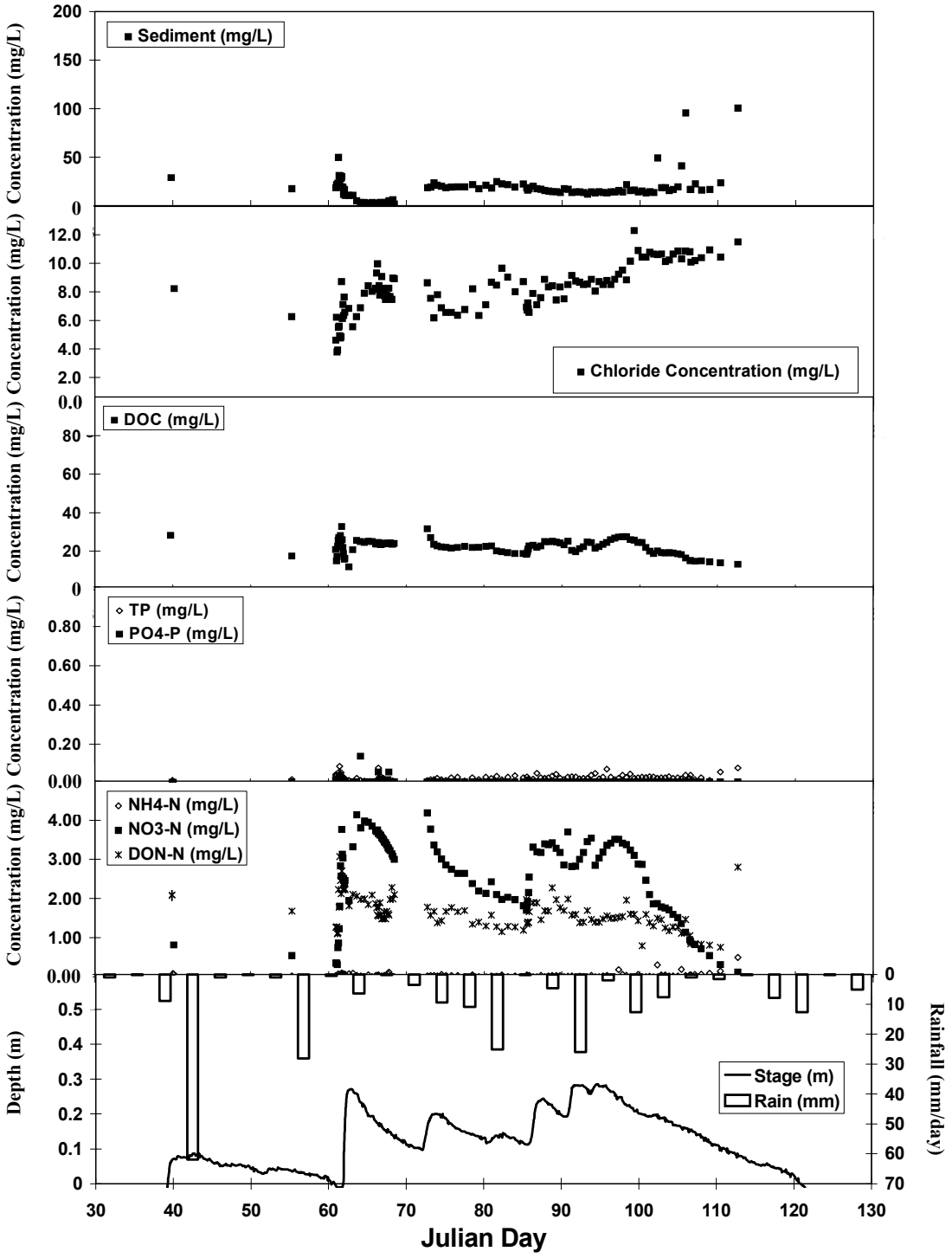

Figure 2.20. Flow depth, daily rainfall, ammonium, nitrate, dissolved organic nitrogen, phosphate, total phosphorous, dissolved organic carbon, chloride, and sediment concentrations measured at the outflow during the 2002 flow season.

Volume weighted average discharge concentrations of ammonium, nitrate, dissolved organic nitrogen, total phosphorous, phosphate, dissolved organic carbon, chloride, and sediment can be found in Table 2.48.

Table 2.48. Volume weighted average discharge concentrations of ammonium, nitrate, dissolved organic nitrogen, total phosphorous, phosphate, dissolved organic carbon, chloride, and sediment for 2001 and 2002.

Nutrient	Volume Weighted Average Concentration (mg/L)		
	2001	2002	Overall[1]
Ammonium	0.03	0.03	0.03
Nitrate	1.26	2.64	2.41
Dissolved Organic Nitrogen	1.52	1.58	1.57
Total Phosphorous	0.02	0.03	0.03
Phosphate	0.01	0.01	0.01
Dissolved Organic Carbon	29.9	24.4	25.3
Chloride	12.2	9.26	9.74
Sediment	16.0	15.9	15.9

[1] The average volume weighted concentration of both years of the study.

The overall volume weighted concentrations (averaged over the two years of the study) found at the outlet (S3 in Figure 2.1) of the canal study section were slightly higher for nitrate (+0.61 mg/L), slightly lower for chloride (-0.97 mg/L), much lower for sediment (-5.40 mg/L), and similar for dissolved organic nitrogen (-0.05 mg/L) and dissolved organic carbon (+0.15 mg/L) as compared to the overall volume weighted concentrations of the inflow at S0. The volume weighted concentrations were similar for ammonium (-0.05 mg/L), total phosphorous (+0.01 mg/L), and phosphate ($\pm$0.00 mg/L) as compared to the overall volume weighted concentrations of the inflow at S0, but were below the accurate detection levels of the laboratory analysis equipment used in this study. The concentrations at the

outlet (S3 in Figure 2.1) are determined by the same input, output, and transformations described in Section 2.5, Upstream Canal Inflow.

The large difference in the inflow and outflow sediment concentrations of the canal section is due to the differences in the structures used at each end of the study section. Upstream, a flume structure was used that did not particularly hinder the flow within the channel. This resulted in little to no change in flow velocity across the structure, allowing the sediment already in suspension to continue moving with the flow. At the outflow (S3 in Figure 2.1), a weir structure was used. This structure increases the cross-sectional area of flow and reduces the velocity immediately upstream, which allows for settling and the loss or deposition of sediment being held in suspension.

2.11 Mass Balance

2.11.1 Methods

A mass balance was used to account for flow volume, different nitrogen and phosphorous species, dissolved organic carbon, and chloride for the canal's study section. The water balance was determined using Equation 2.16.

$$\text{Output} = \sum\text{Inputs} - \text{Losses} \qquad \text{Equation 2.16}$$

where: Output = volume at the outlet (m^3)
Inputs = upstream inflow, rainfall/throughfall, and groundwater (m^3)
Losses = water loss from the fields from the canal during dry periods

The nutrient mass balances were determined using Equation 2.17.

$$\text{Output} = \sum\text{Inputs} + \text{Transformations} \qquad \text{Equation 2.17}$$

where: Output = load at the outlet (kg)
Inputs = upstream inflow, rainfall/throughfall, groundwater, and litterfall (kg)
Transformations = Mineralization (+), nitrification (+), and denitrification (-).

To complete the mass balance, concentrations of each of the nutrients were multiplied by their respective volumes on a half-hour basis (the stream section's calculated inflow, outflow, subsurface flow, and rainfall/throughfall), and the overall litterfall entering the canal section was summed for an overall balance. Cumulative graphs show the sum of the inputs (upstream inflow, rainfall/throughfall, groundwater, and litterfall) as inflow and outflow at the outlet as outflow. Nutrients (nitrogen, phosphorous, and carbon) in the litterfall were assumed to be all in organic form. The amount of litterfall nutrients entering the study canal were assumed to be equal to the amount of dissolved organic nutrients released to the canal water from the litter layer.

2.11.2 Results and Discussion

2.11.2.1 Flow Volume

Balances for the flow volumes closed to within 0.1% for 2001 and 3.5% for 2002 (Table 2.49). These results were well within the potential error in measuring flows in the canal. Figures 2.21 and 2.22 show the cumulative volume of water over the study period for the years 2001 and 2002 respectively. They show a similar net inflow and outflow over time, indicating that the mass balance is achieved throughout the flow season, not only as an overall sum. This indicates that all the inputs and outputs to the system were accounted for and measured accurately.

A drought occurred during both years of this study. The drought of 2001 was more severe than that of 2002. This resulted in a large net loss of water to the fields and under the road to the north from the canal (26,600 m^3) for 2001. During 2002, there was a net inflow (5,010 m^3) to the canal from the fields.

Table 2.49. Input and output of flow volume to the study canal section during the 2001 and 2002 flow periods.

Input/Output	2001 Flow Volume (m^3)	2002 Flow Volume (m^3)
Inflow at S0	213,000	313,000
Throughfall	804	1,270
Flow to/from Fields	-26,600	5,010
Litterfall	-	-
Outflow at S3	187,000	308,000
Difference (input-output)	204	11,280
% Difference (output/input)	-0.1%[1]	-3.5%[1]

[1] Negative percentages indicate less output at the outlet than the sum of the inputs or a loss within the system. A positive percentage indicates more output at the outlet than the sum of the inputs or a gain within the system.

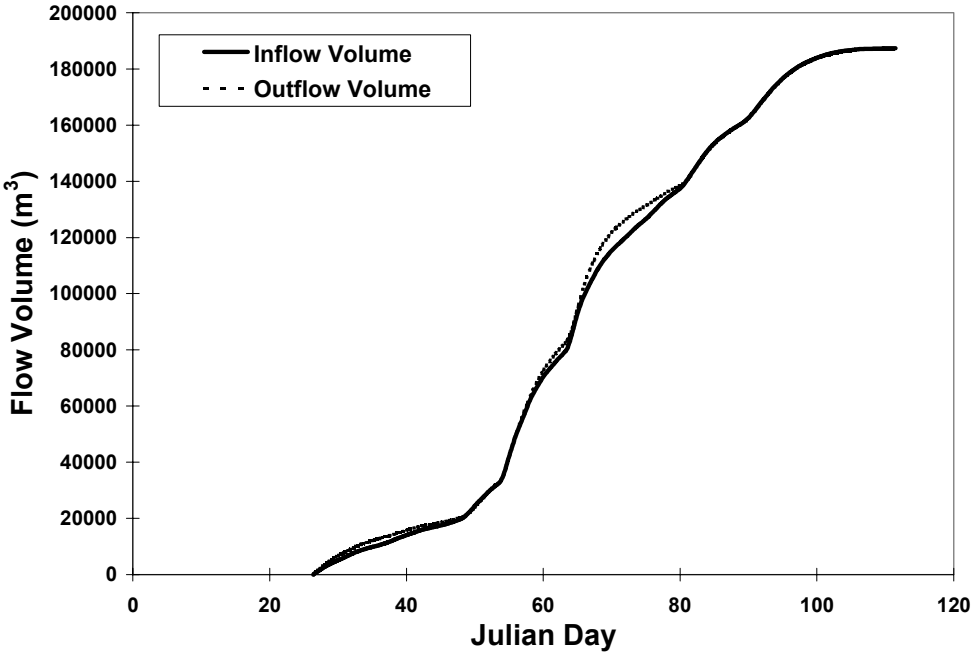

Figure 2.21. Cumulative flow volume inputs to the canal section and output at the outlet for the flow period from day 26 to day 111 during 2001.

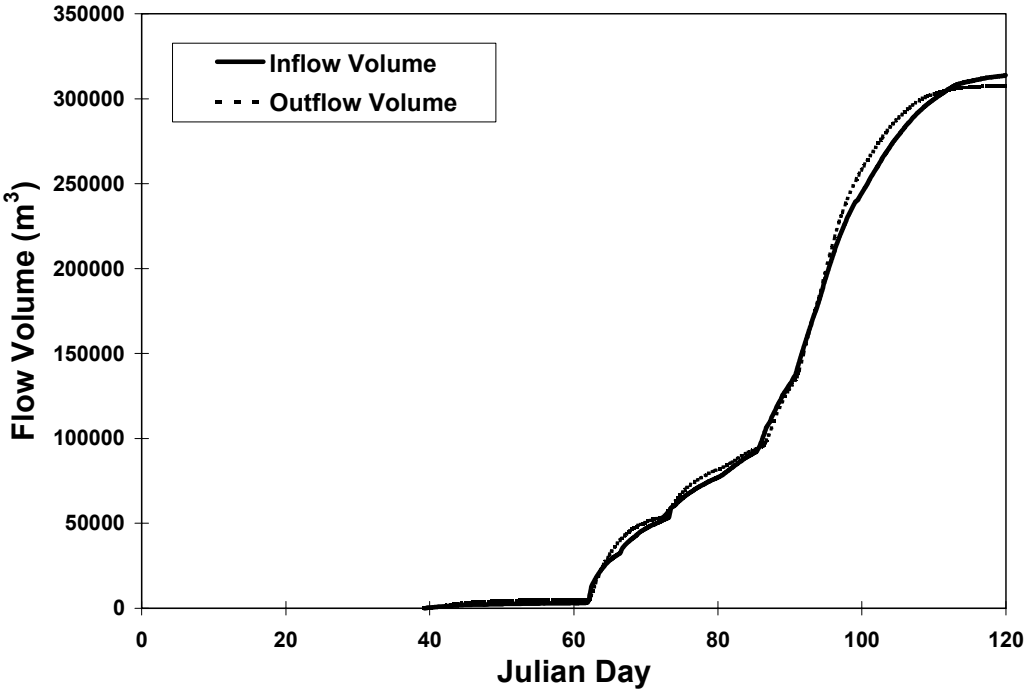

Figure 2.22. Cumulative flow volume inputs to the canal section and output at the outlet for the flow period from day 39 to day 120 during 2002.

2.11.2.2 Chloride

Chloride was used as a conservative tracer, and concentrations were measured for all hydrologic inputs and outputs during the study. Chloride was used because it is highly mobile and not readily adsorbed onto surfaces or incorporated into secondary minerals (Peters and Ratcliffe, 1998). However, chloride concentrations can be altered in the environment by biological reactions, plant uptake (Tisdale et al., 1993), evaporation, and exchanges within the soil (Peters and Ratcliffe, 1998). Inputs from different sources have different concentrations, and they vary over time and under differing environmental conditions. Peters and Ratcliffe (1998) found that chloride concentrations varied in

throughfall, rainfall, soil water, and groundwater between rainfalls of differing intensity and amount. They also found that stream water concentrations of chloride were threefold higher than throughfall. Regardless of these variables, chloride can be used in mass balance calculations as a check for all other nutrients of interest, if all the inputs are measured as they enter the surface water (Hill, 1988; Owens et al., 1972; Peters and Ratcliffe, 1998) and are not subject to removal by physical or biological processes during stream transport (Hill, 1988).

Closure of the chloride mass balance indicates that all the inputs and outputs have been accurately estimated. The chloride mass balance for 2001 closed to within 2.7% (Table 2.50). This difference between the inflow and outflow mass of chloride is within the potential error of measuring flows in the field and nutrient concentrations in the lab, and it indicates that the inflows and outflows were accurately measured for the 2001 flow period. The loss of chloride to the fields (173 kg) is due to the net flow loss to the fields during the 2001 drought. Figure 2.23 shows that the inflow and outflow chloride curves are similar throughout the 2001 flow period, meaning the mass balance holds throughout the year.

The chloride mass balance for the 2002 flow period showed a large percentage (7.5%) of unaccountable loss of chloride from the canal section (Table 2.50). The difference is most likely due to the difference in flow volume as described above. The difference occurs in the last portion of the flow season (Figure 2.24), which is similar to the unaccountable flow loss that occurred (Figure 2.22). As with the 2001 flow period, the inflow and outflow chloride curves are similar throughout the 2002 flow period, showing that the mass balance holds throughout the year.

Table 2.50. Input and output mass of chloride to the study canal section during the 2001 and 2002 flow periods.

Input/Output	2001 Chloride Mass (kg)	2002 Chloride Mass (kg)
Inflow at S0	2400	3320
Rain	2.8	1.8
Flow to/from Fields	-173	73
Litterfall	-	-
Outflow at S3	2290	3140
Difference (input-output)	-60.2	255
% Difference (output/input)	2.7%[1]	-7.5%[1]

[1] Negative percentages indicate less output at the outlet than the sum of the inputs or a loss within the system. A positive percentage indicates more output at the outlet than the sum of the inputs or a gain within the system.

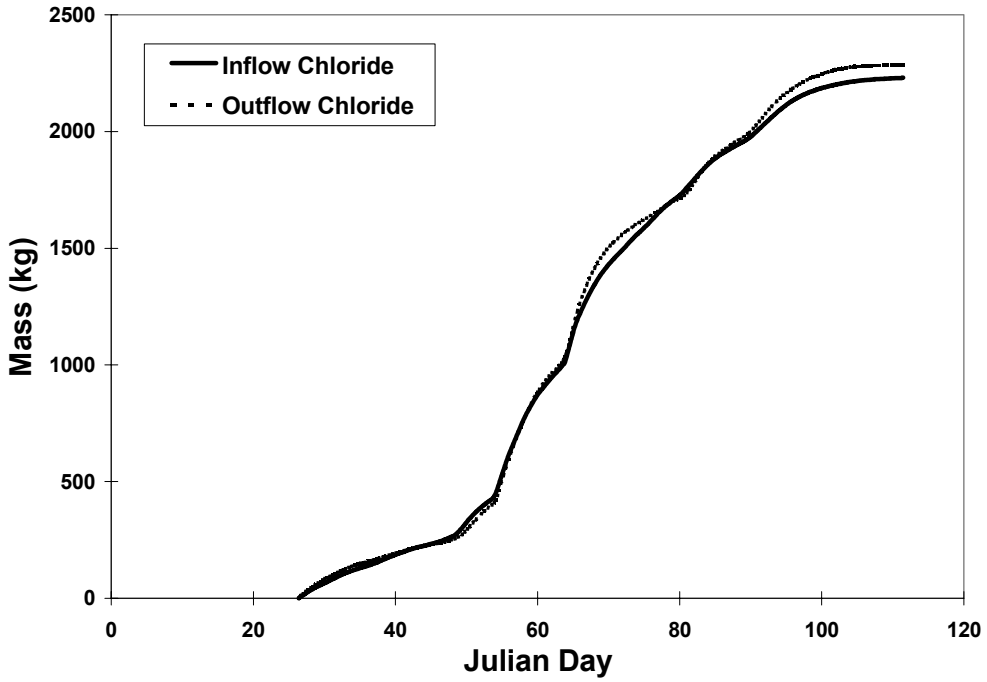

Figure 2.23. Cumulative chloride mass inputs to the canal section and output at the outlet for the flow period from day 26 to day 111 during 2001.

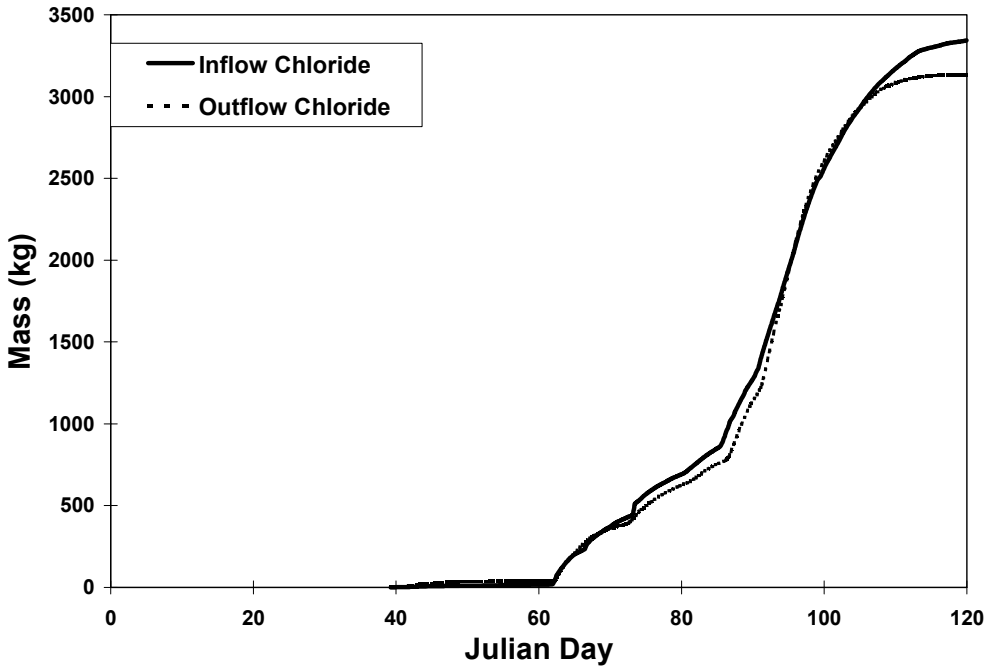

Figure 2.24. Cumulative chloride mass inputs to the canal section and output at the outlet for the flow period from day 39 to day 120 during 2002.

2.11.2.3 Ammonium

The ammonium mass balance for both years, 2001 and 2002, resulted in a large percentage (80.5% and 43.2% respectively, Table 2.51) decrease in the amount of ammonium leaving at the outlet vs. the sum of the inputs to the study canal section. Figure 2.25 shows the cumulative ammonium mass balance for the 2001 flow season over time. The inflow ammonium mass is always higher and continually increases compared to the outflow. Figure 2.26 shows the cumulative ammonium mass of inflow and outflow over time for the year 2002. The two lines are similar until approximately day 70, where the outflow ammonium mass stops increasing, while the inflow continues to increase. These cumulative values are in reality too low to accurately determine the effects. The most plausible explanation for the large difference in the mass of ammonium input vs. output is that the low

concentrations usually found within the drainage network (0.03 mg/L) are close to or below the accuracy level of the equipment used for analyzing the water samples. This results in analysis variations from 0.001 mg/L to 0.01 mg/L due to these low sample concentrations. When multiplied by the flow volumes, the error is multiplied, resulting in the potential for large differences in the ammonium input and output, as seen here.

Table 2.51. Input and output mass of ammonium to the study canal section during the 2001 and 2002 flow periods.

Input/Output	2001 Ammonium Mass (kg)	2002 Ammonium Mass (kg)
Inflow at S0	38.5	3.2
Rain	0.2	1.0
Flow to/from Fields	-4.9	0.2
Litterfall	-	-
Outflow at S3	6.6	2.5
Difference (input-output)	27.2	1.9
% Difference (output/input)	-80.5%[1]	-43.2%[1]

[1] Negative percentages indicate less output at the outlet than the sum of the inputs or a loss within the system. A positive percentage indicates more output at the outlet than the sum of the inputs or a gain within the system.

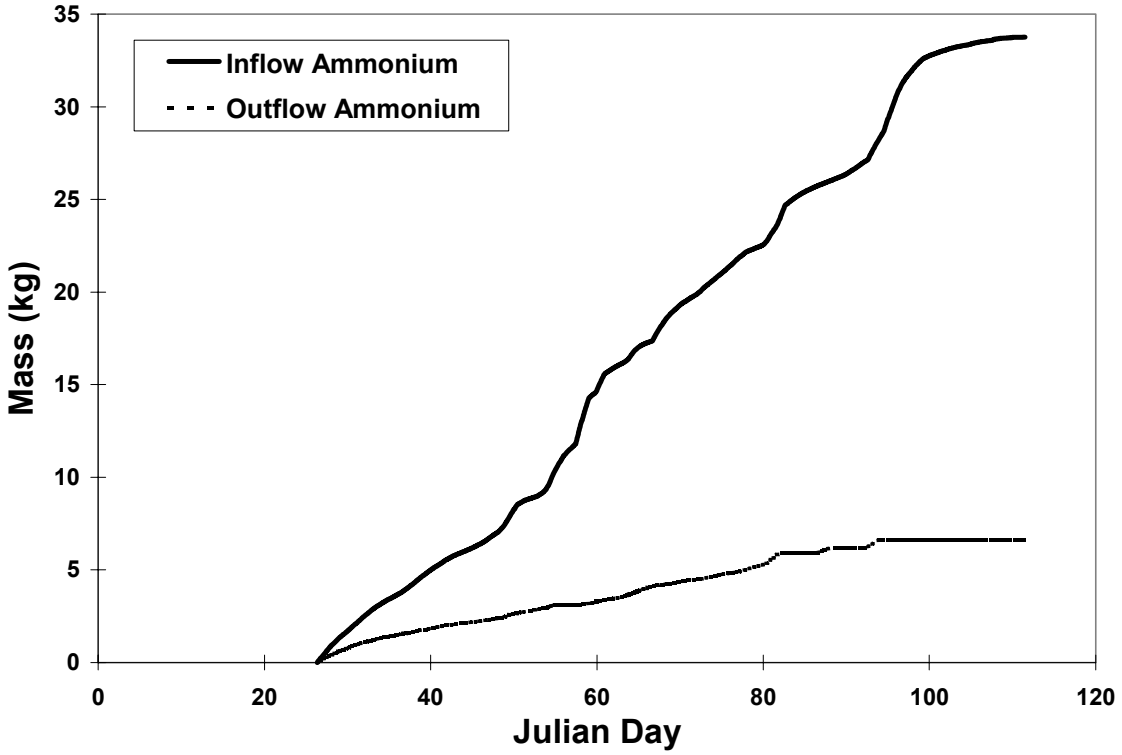

Figure 2.25. Cumulative ammonium mass inputs to the canal section and output at the outlet for the flow period from day 26 to day 111 during 2001.

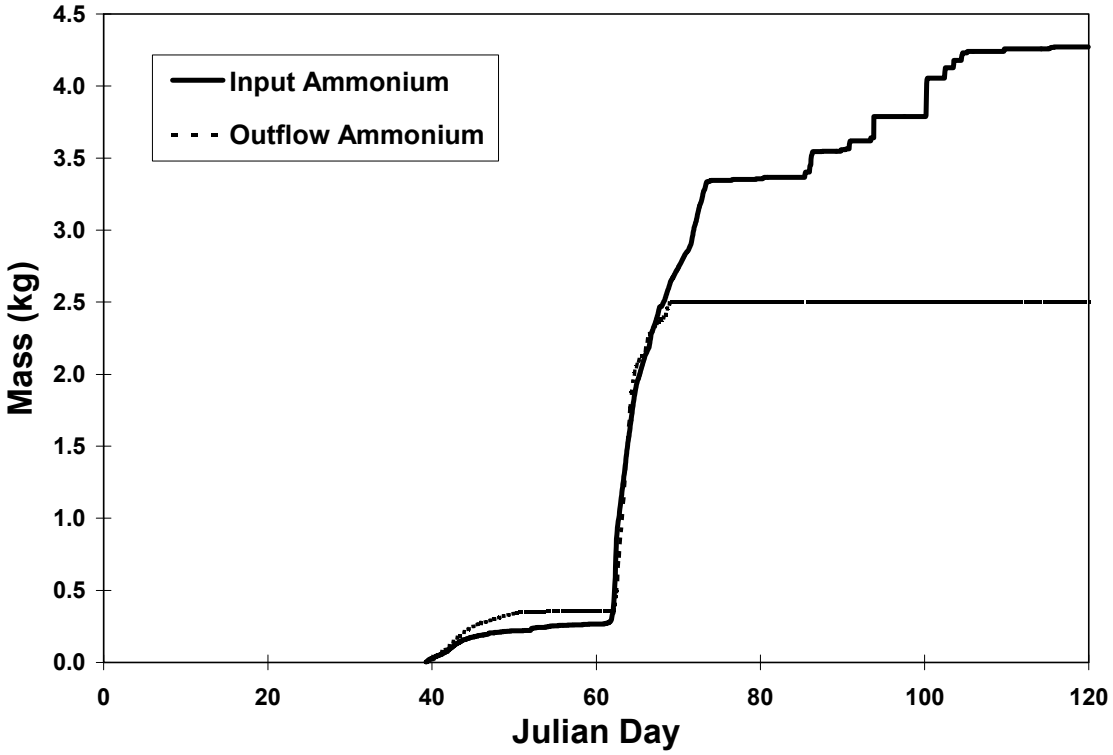

Figure 2.26. Cumulative ammonium mass inputs to the canal section and output at the outlet for the flow period from day 39 to 120 during 2002.

2.11.2.4 Nitrate

The nitrate mass balance resulted in a 1.3% increase of nitrate for the 2001 flow period along the study canal's length (Table 2.52). The 2001 value is well within the potential error of field and lab measurements. The cumulative amount of nitrate input and output over time shows curves similar to those for cumulative flow volume and chloride with respect to accumulation as time progresses, with accumulation occurring more rapidly during rainfall events (Figure 2.27). The sudden increase seen around days 55 and 65 of 2001 relates to the two larger rainfall events. This results in higher discharge from the fields to the canal as well as higher nitrate concentrations (2.0 mg/L as compared to an average of 0.7 mg/L during normal flow). This effect can be seen in Figure 2.12 of Section 2.5, Upstream Canal

Inflow. Higher nitrate concentrations are due to the dry period prior to the rainfall event. During this period, the soil has more air-filled pores that allow nitrification to occur, which results in more nitrate being generated. Also, the nitrates are not leached out of the soil due to the lack of moving pore water. When the rainfall event occurs, the nitrates are flushed from the soil to the canal, resulting in higher nitrate concentrations in the canal.

During the 2002 flow season, there is a more dramatic difference in the cumulative nitrate mass. There was a 10.7% increase in the amount of nitrate leaving the study canal section at the outlet over the total inputs to the canal section (Table 2.52). This difference occurs over two periods of time during the 2002 flow period, around day 70 and day 90, where the outflow mass increases more rapidly than the inflow mass (Figure 2.28 and 2.29). These differences are due to the small number of samples taken at these times at one of the locations. During the period between day 70 and day 75, the inflow station took more samples than did the outflow station, resulting in the inflow station capturing the decrease in concentration that the outflow station missed. Accordingly, there was an overestimation of nitrate at the outflow during this period (Figure 2.29). During the period between day 90 and day 100, the inflow station took fewer samples than did the outflow station, causing the outflow station to capture the increase in concentration that the inflow station missed (the inflow station actually took samples at the lowest concentrations during this period). Therefore, nitrate was underestimated at the inflow during this period (Figure 2.29). These two sampling errors resulted in an overestimation of 18.3 kg at the outflow location during the period between day 70 and day 75 and an underestimation of 70.1 kg at the inflow location between days 90 and 100, resulting in a total error of 100 kg of nitrate between the inflow and outflow cumulative nitrate during the 2002 flow period. This error caused the

total cumulative nitrate outflow to be 92.1 kg higher than the total cumulative nitrate inflow for the whole flow period. When this error is taken into consideration, the difference between the total inflow and outflow becomes +4.8 kg (-0.6%) rather than the -83.2 kg (10.7%) found in Table 2.52. (The previous figure was calculated by subtracting the overestimated 18.3 kg from the outflow and adding the underestimated 70.1 kg to the inflow.) This result brings the mass balance of the 2002 nitrate balance to within 0.6%, which is well within the potential error of field and lab measurements.

Table 2.52. Input and output mass of nitrate to the study canal section during the 2001 and 2002 flow periods.

Input/Output	2001 Nitrate Mass (kg)	2002 Nitrate Mass (kg)
Inflow at S0	234	767
Rain	0.6	0.6
Flow to/from Fields	-19.4	7.2
Litterfall	-	-
Outflow at S3	218	858
Difference (input-output)	-2.8	-83.2
% Difference (output/input)	1.3%[1]	10.7%[1]

[1] Negative percentages indicate less output at the outlet than the sum of the inputs or a loss within the system. A positive percentage indicates more output at the outlet than the sum of the inputs or a gain within the system.

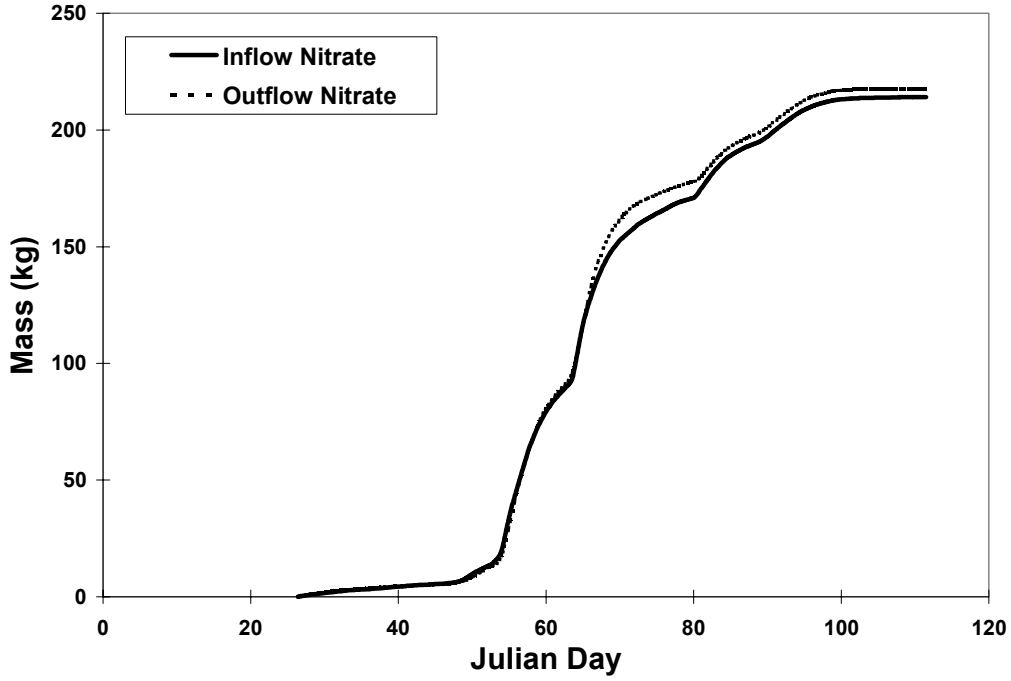

Figure 2.27. Cumulative nitrate mass inputs to the canal section and output at the outlet for the flow period from day 26 to day 111 during 2001.

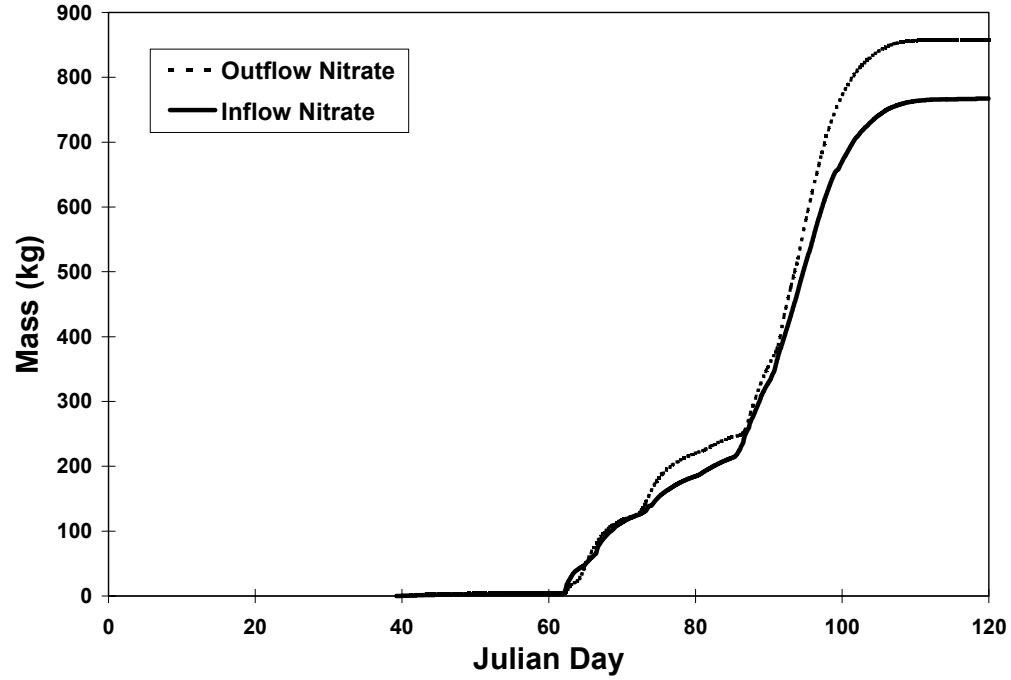

Figure 2.28. Cumulative nitrate mass inputs to the canal section and output at the outlet for the flow period from day 39 to day 120 during 2002.

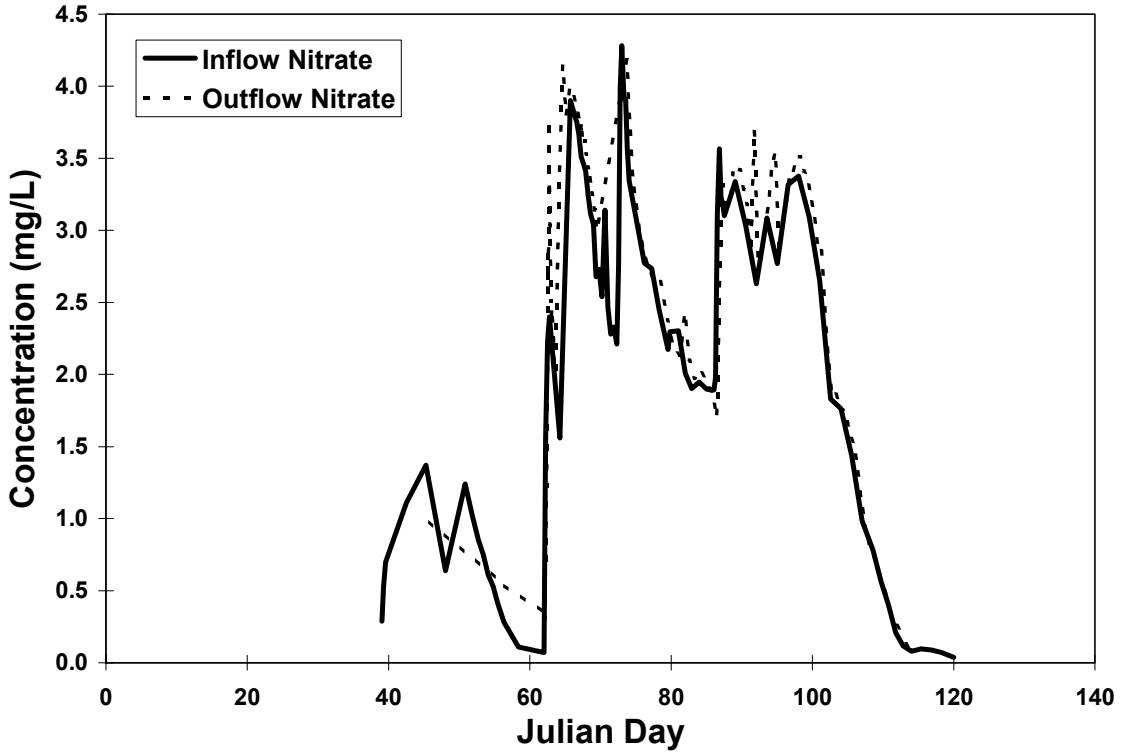

Figure 2.29. Sample nitrate concentrations at the inflow and outflow of the canal study section for the 2002 flow period.

2.11.2.5 Dissolved Organic Nitrogen

The dissolved organic nitrogen mass balance resulted in a decrease of 9.1% during the 2001 flow period and a decrease of 6.0% during the 2002 flow period along the study canal's length (Table 2.53). Though the percentage difference is different between the two years, the amount lost is similar, 28.6 kg for 2001 and 32.9 kg for 2002.

During the two years of the study, the sums of the inflow and outflow of dissolved organic nitrogen are similar. Figures 2.30 and 2.31 show the cumulative mass of dissolved organic nitrogen over time. Both years show similar increases with time, demonstrating that

the mass balance nearly closes throughout each flow season. Small variations that could lead to the divergences may be due to mineralization within the study canal section.

Table 2.53. Input and output mass of dissolved organic nitrogen to the study canal section during the 2001 and 2002 flow periods.

Input/Output	2001 Dissolved Organic Nitrogen Mass (kg)	2002 Dissolved Organic Nitrogen Mass (kg)
Inflow at S0	337	526
Rain	1.0	2.7
Flow to/from Fields	-33.9	8.1
Litterfall	8.5	8.1
Outflow at S3	284	512
Difference (input-output)	28.6	32.9
% Difference (output/input)	-9.1%[1]	-6.0%[1]

[1] Negative percentages indicate less output at the outlet than the sum of the inputs or a loss within the system. A positive percentage indicates more output at the outlet than the sum of the inputs or a gain within the system.

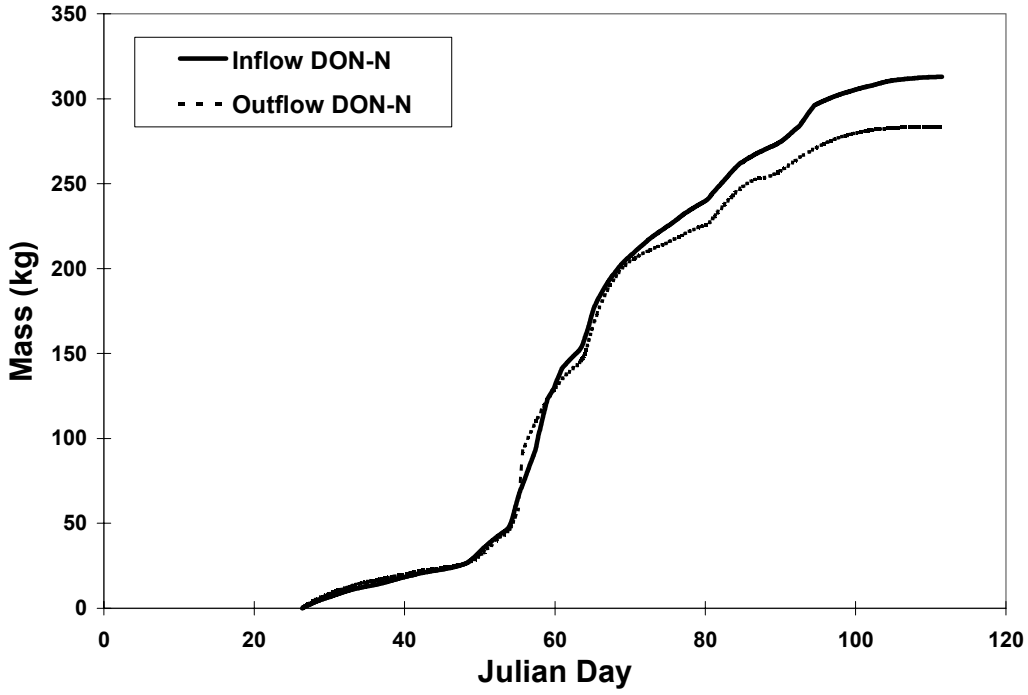

Figure 2.30. Cumulative dissolved organic nitrogen mass inputs to the canal section and output at the outlet for the flow period from day 26 to day 111 during 2001.

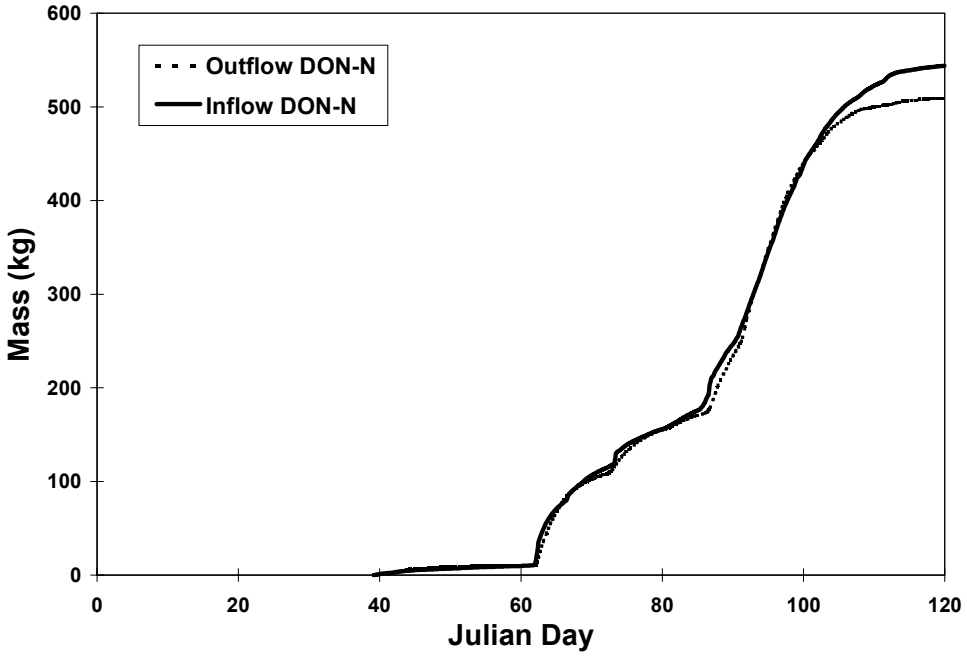

Figure 2.31. Cumulative dissolved organic nitrogen mass inputs to the canal section and output at the outlet for the flow period from day 39 to day 120 during 2002.

2.11.2.6 Total Nitrogen

The mass balance for the total dissolved nitrogen resulted in an overall decrease in total nitrogen of 9.6% for the 2001 flow period along the study canal's length (Table 2.54). This loss is similar to the percentage loss of dissolved organic nitrogen found over the same period. The cumulative amount of total dissolved nitrogen input and output over time (Figure 2.32) shows the same pattern as the cumulative amount of dissolved organic nitrogen (Figure 2.30). Inflows and outflows are about the same until approximately day 70, when the inflow curve increases faster than the outflow curve.

During the 2002 flow season, the mass balance of total dissolved nitrogen closed fairly well, with an increase of 5.4%. Figure 2.33 shows a comparison of the inputs vs. the

outflow for cumulative total dissolved nitrogen for the 2002 flow period. The close closure of the mass balance in 2002 is due to the decrease in the dissolved organic nitrogen (33.3 kg) being offset by the increase in nitrate (84.2 kg) within the system. The 2002 results indicate that not only is mineralization occurring, but that nitrification may also be occurring in the canal, even though the pH is very low (pH ≈ 4 Appendix F). Nitrification may be occurring in small pockets in the upper sediments, where the pH could be higher than that of the water column. The pH of the sediment was not recorded in this study.

Table 2.54. Input and output mass of total dissolved nitrogen to the study canal section during the 2001 and 2002 flow periods.

Input/Output	2001 Dissolved Organic Nitrogen Mass (kg)	2002 Dissolved Organic Nitrogen Mass (kg)
Inflow at S0	610	1300
Rain	1.8	4.3
Flow to/from Fields	-58.2	15.5
Litterfall	8.5	8.1
Outflow at S3	508	1400
Difference (input-output)	54.1	72.1
% Difference (output/input)	-9.6%[1]	5.4%[1]

[1] Negative percentages indicate less output at the outlet than the sum of the inputs or a loss within the system. A positive percentage indicates more output at the outlet than the sum of the inputs or a gain within the system.

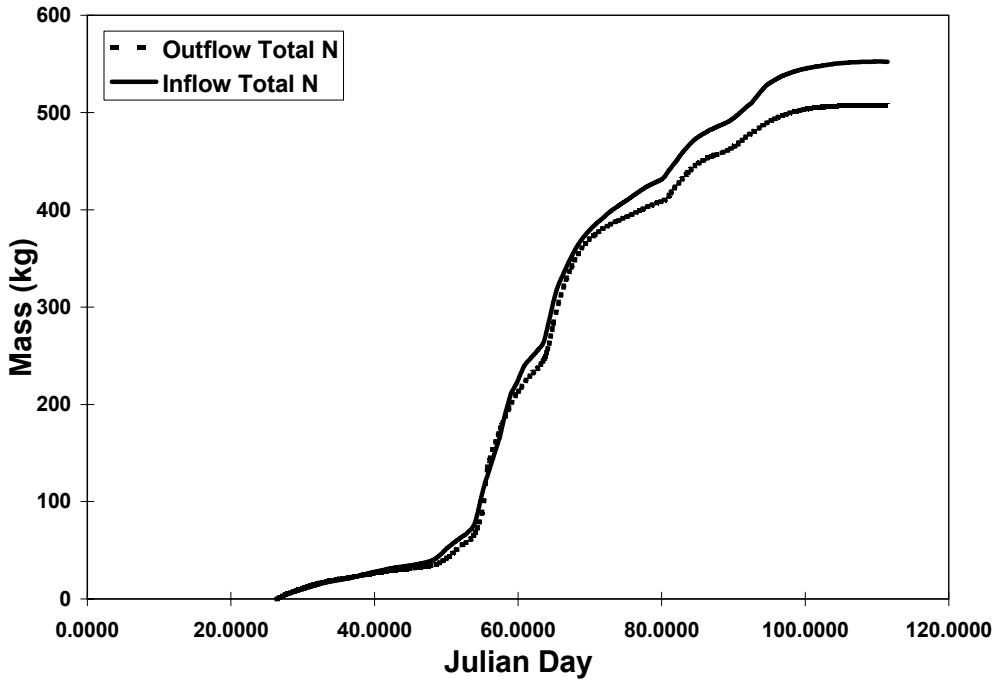

Figure 2.32. Cumulative total dissolved nitrogen mass inputs to the canal section and output at the outlet for the flow period from day 26 to day 111 during 2001.

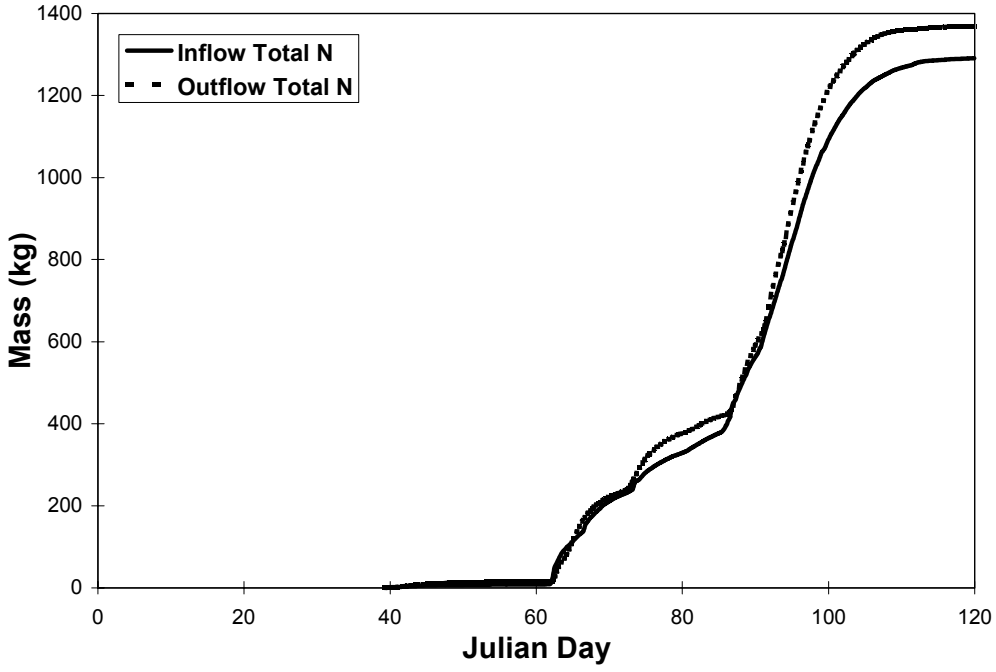

Figure 2.33. Cumulative total dissolved nitrogen mass inputs to the canal section and output at the outlet for the flow period from day 39 to day 120 during 2002.

2.11.2.7 Phosphate

The phosphate mass balance resulted in all the phosphate being accounted for during the 2001 flow period and a 11.4% loss during the 2002 flow period within the study canal (Table 2.55).

During the 2001 flow season, the phosphate concentrations are extremely low, averaging 0.01 mg/L. This value is below the range of accuracy of the laboratory instrumentation used in this study. This fairly constant concentration results in similar mass balance of the flow volume, which is a well-closed mass balance of 0.0% (Figure 2.34).

During the 2002 flow period, the average concentration of phosphate was in the range of 0.01 mg/L and as such is below the detection level of the instrumentation used. The difference noticed at the end of the 2002 flow period is due to the concentration differences (0.01 mg/L for both inflow and outflow prior to separation of the two curves, and 0.02 mg/L for the inflow after the separation) in phosphate between the inputs and outflow at the outlet (Figure 2.35). When dealing with very small values, small differences (0.4 kg) result in large percentage differences.

The dissolved organic phosphorous (total phosphorous - phosphate) resulted in very low concentrations (0.001 mg/L), such that very small variations were amplified during multiplication by the flow volumes. The percentage difference in the dissolved organic phosphorous is large but in reality is due to the small amounts of the inflow and outflow masses (2.6 kg and 1.5 kg respectively), whose actual difference is small (2.3 kg).

Table 2.55. Input and output mass of phosphate to the study canal section during the 2001 and 2002 flow periods.

Input/Output	2001 Phosphate Mass (kg)	2002 Phosphate Mass (kg)
Inflow at S0	2.0	3.2
Rain	0.1	0.2
Flow to/from Fields	-0.6	0.1
Litterfall	-	-
Outflow at S3	1.5	3.1
Difference (input-output)	0.0	0.4
% Difference (output/input)	0.0%[1]	-11.4%[1]

[1] Negative percentages indicate less output at the outlet than the sum of the inputs or a loss within the system. A positive percentage indicates more output at the outlet than the sum of the inputs or a gain within the system.

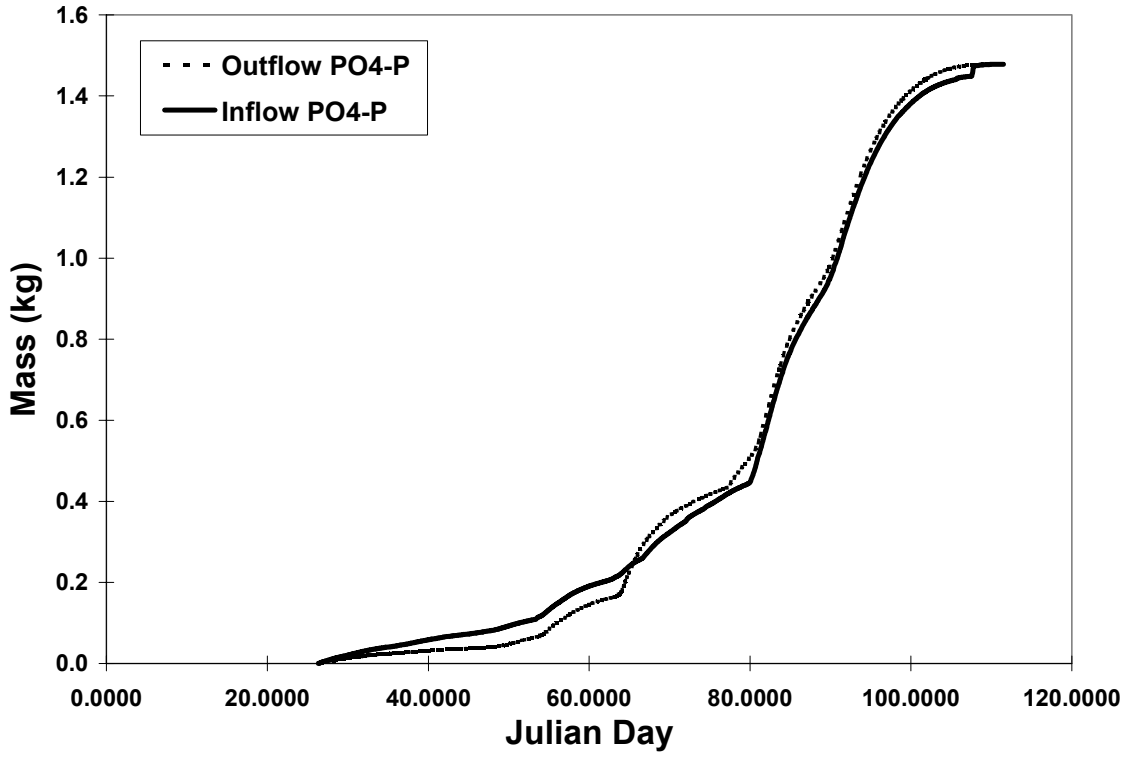

Figure 2.34. Cumulative phosphate mass inputs to the canal section and output at the outlet for the flow period from day 26 to day 111 during 2001.

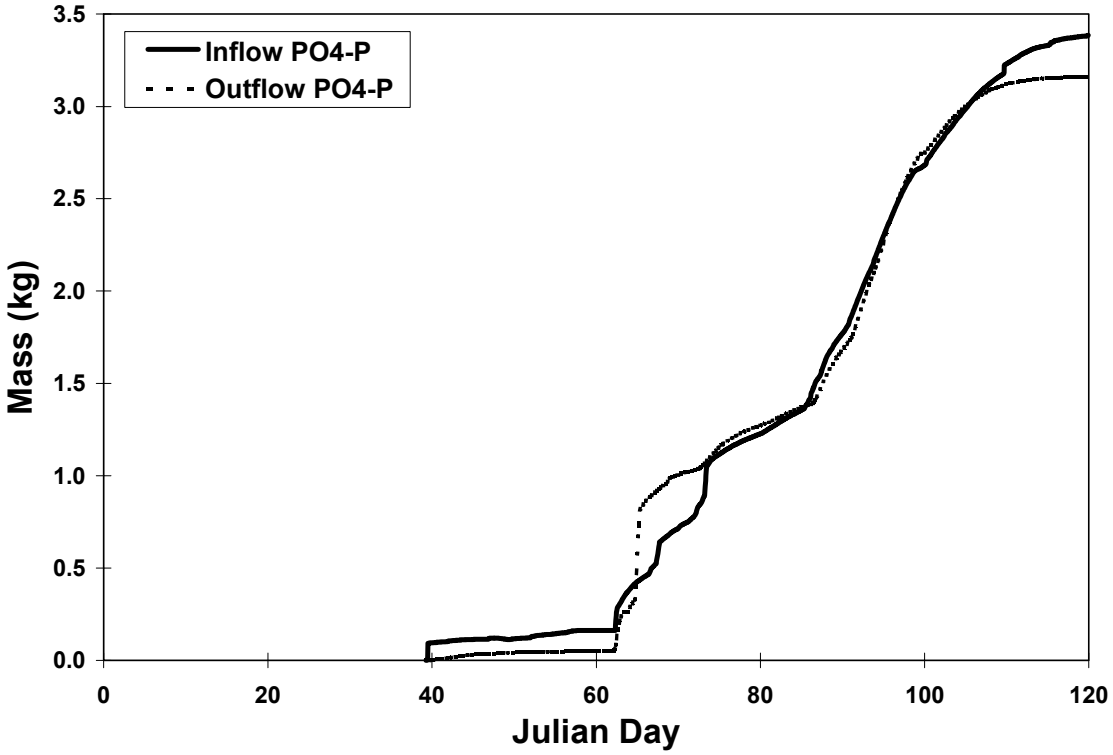

Figure 2.35. Cumulative phosphate mass inputs to the canal section and output at the outlet for the flow period from day 39 to day 120 during 2002.

2.11.2.8 Dissolved Organic Phosphorous

Dissolved organic phosphorous (total phosphorous - phosphate) was present in very low concentrations (0.001 mg/L) for both flow periods (2001 and 2002). As described in the previous section, these values are too low for accurate measurement by the instrumentation used in this study. Very small variations were amplified during multiplication by the flow volumes, resulting in large percentage differences (42.3% and 16.4% for 2001 and 2002 respectively, Table 2.56). In reality, the small amounts of the inflow and outflow masses (2.6 kg and 1.5 kg respectively for 2001 and 5.5 kg and 6.4 kg respectively for 2002) have actual differences that are small, 1.1 kg in 2001 and 0.9 kg in 2002. Figures 2.36 and 2.37 show the

inflow and outflow dissolved organic phosphorous loads over time for the two flow periods (2001 and 2002 respectively).

Table 2.56. Input and output mass of dissolved organic phosphorous to the study canal section during the 2001 and 2002 flow periods.

Input/Output	2001 Dissolved Organic Phosphorous Mass (kg)	2002 Dissolved Organic Phosphorous Mass (kg)
Inflow at S0	1.8	4.8
Rain	0.1	0.1
Flow to/from Fields	0.1	0.1
Litterfall	0.6	0.5
Outflow at S3	1.5	6.4
Difference (input-output)	1.1	-0.9
% Difference (output/input)	-42.3%[1]	16.4%[1]

[1] Negative percentages indicate less output at the outlet than the sum of the inputs or a loss within the system. A positive percentage indicates more output at the outlet than the sum of the inputs or a gain within the system.

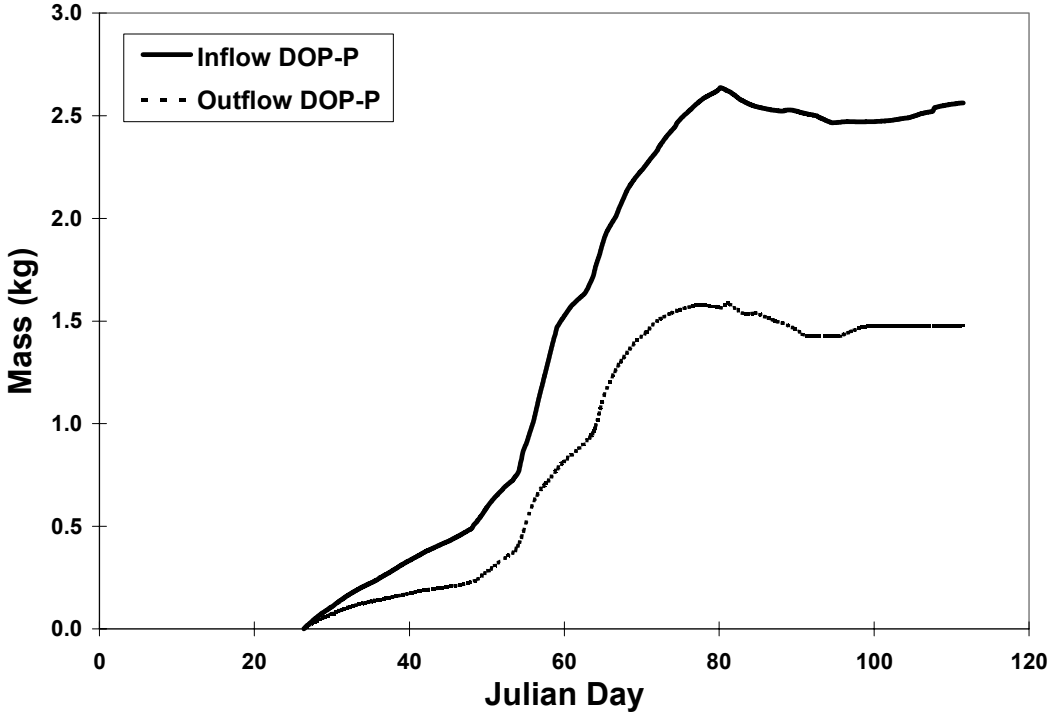

Figure 2.36. Cumulative dissolved organic phosphorous mass inputs to the canal section and output at the outlet for the flow period from day 26 to day 111 during 2001.

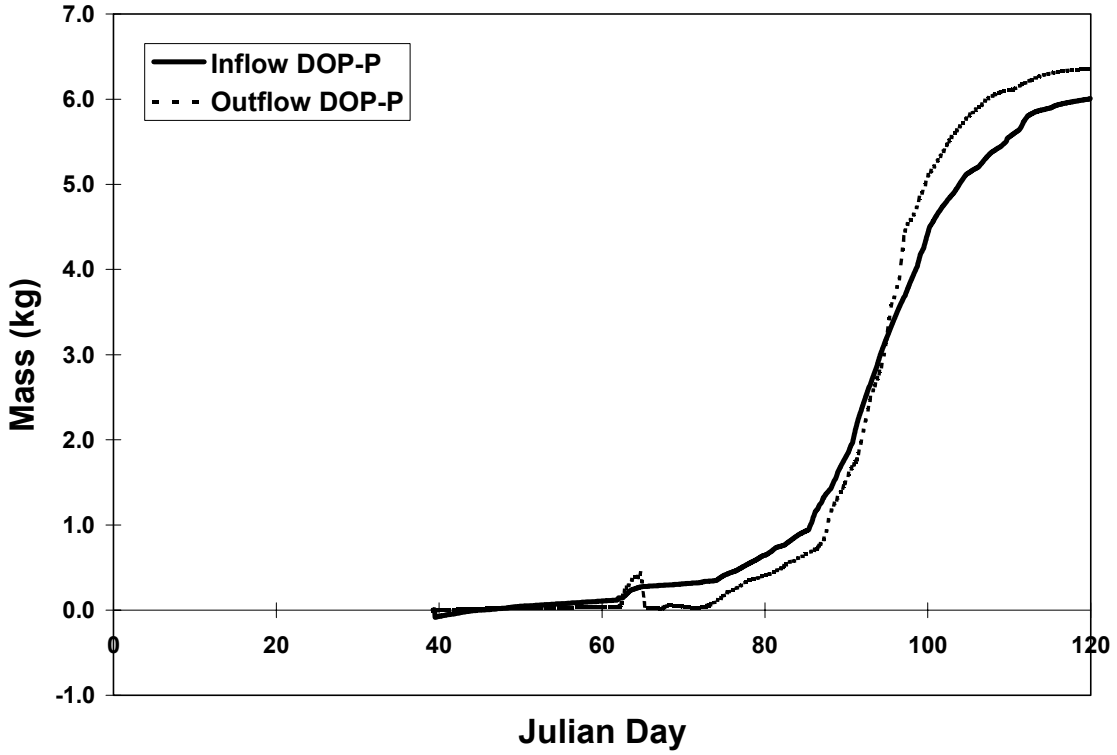

Figure 2.37. Cumulative dissolved organic phosphorous mass inputs to the canal section and output at the outlet for the flow period from day 39 to day 120 during 2002.

2.11.2.9 Dissolved Organic Carbon

The dissolved organic carbon mass balance resulted in a decrease of 6.4% during the 2001 flow period and an increase of 0.3% in the 2002 flow period along the study canal's length (Table 2.57). This value is well within the potential error of field and lab measurements.

The 2001 cumulative mass of dissolved organic carbon shows very close agreement between the inflow and outflow of the study canal section (Figure 2.38). Though carbon drives the biological transformations within the canal, there is no noticeable change in the inflow and outflow amounts until approximately day 70, when water and sediment temperatures start to increase (see Figures E.3 and E.5 of Appendix E, Temperature). After

day 70, the inflow line and outflow line of Figure 2.38 start to diverge, but only minimally. This divergence may be due to the increase in microbial activity caused by rising temperatures. Differences between the inflow and outflow dissolved organic carbon load were small (6.4%) compared to that of the total load. The high organic content of the litter layer and sediment within the canal may have acted to buffer any losses due to microbial activity through leaching of carbon from the litter layer or sediment.

During the 2002 flow season, the dissolved organic carbon mass balance closed well (within 0.3%) (Table 2.57). The cumulative masses of dissolved organic carbon are similar throughout the 2002 flow season (Figure 2.39). This again indicates that the dissolved organic carbon levels (21.2 mg/L) within the canal as well as the thick organic litter layer and upper sediment are able to offset any carbon usage by the microorganisms within the canal, resulting in a stable concentration of carbon within the canal throughout the flow period.

Table 2.57. Input and output mass of dissolved organic carbon to the study canal section during the 2001 and 2002 flow periods.

Input/Output	2001 Dissolved Organic Carbon Mass (kg)	2002 Dissolved Organic Carbon Mass (kg)
Inflow at S0	6320	6,750
Rain	12.0	16.7
Flow to/from Fields	-708	13.2
Litterfall	306	292
Outflow at S3	5550	7050
Difference (input-output)	380	22
% Difference (output/input)	-6.4%[1]	0.3%[1]

[1] Negative percentages indicate less output at the outlet than the sum of the inputs or a loss within the system. A positive percentage indicates more output at the outlet than the sum of the inputs or a gain within the system.

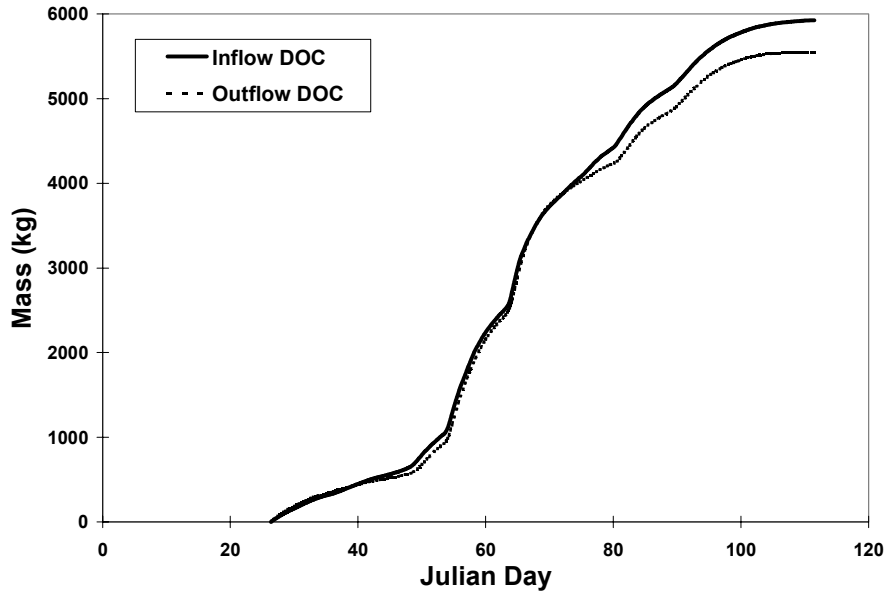

Figure 2.38. Cumulative dissolved organic carbon mass inputs to the canal section and output at the outlet for the flow period from day 26 to day 111 during 2001.

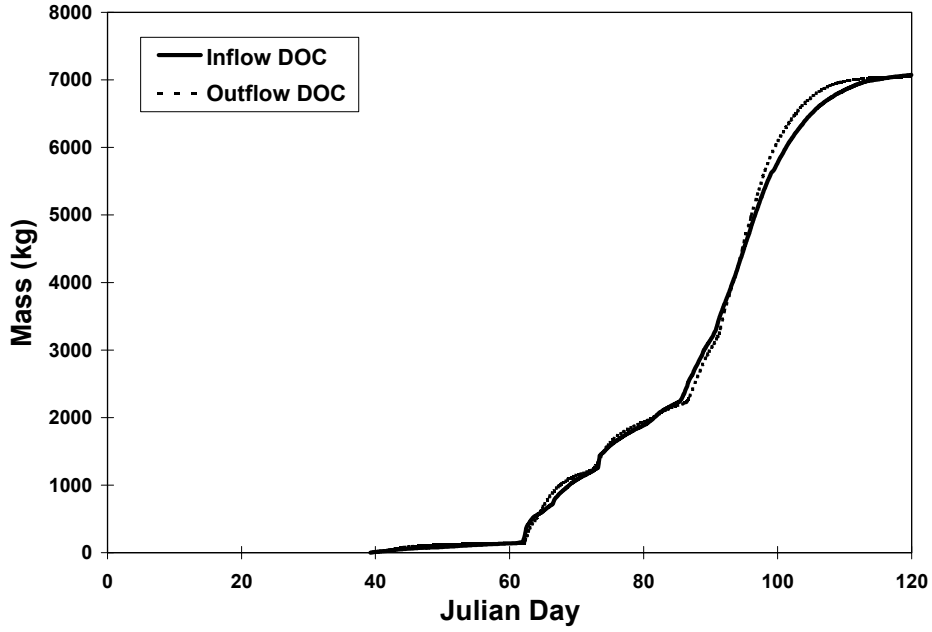

Figure 2.39. Cumulative dissolved organic carbon mass inputs to the canal section and output at the outlet for the flow period from day 39 to day 120 during 2002.

2.11.3 Conclusions

During the two flow periods, 2001 and 2002, the mass balance of chloride closed well (within 2.7% for 2001 and 7.5% for 2002). As chloride is a conservative tracer, this indicates that all the inflows and outflows of water and nutrients were accounted for and calculated accurately. This closure is also seen in the water balance for the two flow periods (within 0.1% for 2001 and 5.5% for 2002) and the dissolved organic carbon mass balance, which closed within 6.4% in 2001 and 0.3% in 2002.

The mass balance for nitrate closed well for the 2001 flow period (within 1.3%) but was off by 10.7% during the 2002 flow period. The large difference in the 2002 nitrate balance was traced to two periods (days 70 to 75 and days 90 to 100) where the samples at either the inflow location or the outflow location were taken at larger intervals than the other location, resulting in one location capturing the large variation in nitrate concentration when the other location did not. These two periods resulted in 10.2% of the difference in the inflow and outflow. This leaves only 0.5% difference in the nitrate mass balance unaccounted for.

The mass balance of the dissolved organic nitrogen closed within 9.1% in 2001 and 6.0% in 2002. These were both decreases over the flow period, which is most likely due to increased mineralization within the canal study section as warmer periods occur. There was not a buildup of ammonium during this period, as nitrification, though reduced, was still occurring and also increased due to the warming periods.

The phosphate and dissolved organic phosphorous mass balances seem to close relatively closely, judging by the mass difference (ranging from 0.0 kg to 1.3 kg), even though the percentage differences are large (ranging from 0.0% to 42.3%). The large percentage differences are due to the very small total masses for each flow period. The near-

closure based on the difference in the masses is due to the relatively constant, extremely low concentrations found throughout the study (usually rounding to the same concentration, but usually below the accurate measurement by the instruments used in this study). This near-closure of the mass balances for phosphate and phosphorous is more influenced by the flow volume.

The ammonium mass balance did not close well during either flow period (80.5% during the 2001 flow period and 43.2% during the 2002 flow period). This is due to the larger variations in concentrations than found with the phosphate and dissolved organic phosphorous, but these variations are still usually below the accurate levels of measurement by the instruments used in this study.

References

Analytical Service Laboratory, NCSU, Raleigh, NC. Modification of Molybdovanandophosphoric Acid Method of Greweling, T., Chemical Analysis of Plant Tissue, 1976, Vol.6, No.8, Search Agricultural Experiment Station, Cornell University, Ithaca, NY.

Appelboom, T.W. 2000. Evaluation of Forest Road Management Practices for Reducing Sediment Production and Transport from Forested Watersheds. MS Thesis. 87 pp, North Carolina State University, Raleigh, 2000.

Berg, M.P., H.A. Verhoef. 1998. Ecological characteristics of a nitrogen saturated coniferous forest in The Netherlands. Biol. Fertil. Soils 26: 258-267.

Campbell, J.L., J.W. Hornbeck, W.H. Mcdowell, D.C. Buso, J.B. Shanley, and G.E. Likens. 2000. Dissolved organic nitrogen budgets for upland, forested ecosystems in New England. Biogeochem. 49: 123-142.

De Schhrijver, A., G. van Hoydonck, L. Nachtergale, L. De Keersmaeker, S. Mussche, and N. Lust. 2000. Comparison of nitrate leaching under Silver Birch (Betula Pendula) and Corsican Pine (Pinus Nigra spp. Laricio) in Flanders (Belgium). Water, Air, and Soil Pollut. 122: 77-91.

Diggs, J. 2004. Simulation of hydrology and nitrogen loading of forested fields in eastern North Carolina using Drainmod-N-II. Masters Thesis. North Carolina State University, Raleigh, 2004.

Fisher, S.G., and G.E. Likens. 1973. Energy flow in Bear Brook, New Hampshire: an integrative approach to aquatic ecosystem metabolism. Ecol. Monog. 43:421-439.

Gosz, J.R., G.E. Likens, and F.E. Bormann. 1972. Nutrient content of litterfall on the Hubbard Brook experimental forest, New Hampshire. Ecology 53(5): 769-784.

Hamburg, S.P., and T.C. Lin. 1998. Throughfall chemistry of an ecotonal forest on the edge of the Great Plains. Can. J. For. Res. 28:1456-1463.

Hill, A.R. 1988. Factors influencing nitrate depletion in a rural stream. Hydrobiologia 160: 111-122.

Lischeid, G., C. Alewell, J. Bittersohl, A. Göttlein, C. Jungnickel, H. Lange, B. Manderscheid, K. Mortz, B. Ostendorf, and H. Sager. 1998. Investigating soil and groundwater quality at different scales in a forested catchment: the Waldstein case study. Nutrient Cycling in Agroecosystems. 50:109-118.

McClave, J.T. and F.H. Dietrich. 1979. Statistics. Dellen Pub. San Francisco.

McDonald, M.A., and J.R. Healey. 2000. Nutrient cycling in secondary forests in the Blue Mountains of Jamaica. For. Ecol. and Manage. 139: 257-278.

Meyer, J.L., G.E. Likens, and J. Sloane. 1981. Phosphorous, nitrogen, and organic carbon flux in a headwater stream. Arch. Hydrobiol. 91(1): 28-41.

Nelson, S.B. 1976. Water Engineering. In: M.S. Frederick, ed. Standard Handbook of Civil Engineering, 2nd ed. McGraw-Hill Book Co. New York.

Nohrstedt, H.Ö. 1992. Soil water chemistry as affected by liming and N fertilization at two Swedish coniferous sites. Scand. J. For. Res. 7: 143-153.

Owens, M., J.H.N. Garland, I.C. Hart, and G. Wood. 1972. Nutrient budgets in streams. Symp. Zool. Soc. Lond. 29: 21-40.

Palma, R.M., R.L. Defrieri, M.F. Tortarolo, J. Prause, and J.F. Gallardo. 2000. Seasonal changes of bioelements in the litter and their potential return to green leaves in four species of the Argentine subtropical forest. Annals of Botany 85: 181-186.

Perkin Elmer PE 2400 CHN Elemental Analyzer Users Manual, Perkin Elmer Corp., Norwalk, Conn., 1988.

Person, R.V. 1970. Calculus with Analytic Geometry. Rinehart Press, San Francisco.

Peters, N.E. and E.B. Ratcliffe. 1998. Tracing hydrologic pathways using chloride at the Panola Mountain Research Watershed, Georgia, USA. Water, Air, and Soil Pollut. 105: 263-275.

Roberson, J.A., J.J. Cassidy, and M.H. Chaudhry. 1988. Hydraulic Engineering. Houghton Mifflin Co., Boston.

Russo, S.L., L. Zavattaro, M. Acutis, and G.M. Zuppi. 2003. Chloride profile technique to estimate water movement through unsaturated zone in a cropped area in subhumid climate (Po Valley-NW Italy). J. Hydrology 270: 65-74.

SCS. 1981. Soil Survey of Washington County, North Carolina, United States Department of Agriculture, Soil Conservation Service.

Seely, B., K. Lajtha, and G.D. Salvucci. 1998. Transformation and retention of nitrogen in a coastal forest ecosystem. Biogeochem. 42: 325-343.

Skaggs, R.W. 1991. Chapter 10 Drainage. In: Modeling Plant and Soil Systems. Agronomy Monograph No. 31. Madison, Wis.

Standard Methods for the Examination of Water and Waste Water. 17th ed. 1989. American Public Health Association, American Waterworks Association, and Water Pollution Control Federation.

Starflow Owners Manual. 1998. STARFLOW: Ultrasonic Doppler Instrument Owner's Manual, Model 6526B. Revision E. Lynn MacLaren Pub. Australia.

Starr, C. and R. Taggart. 1995. Biology: The Unity and Diversity of Life. 7th Ed. Wadsworth Publishing Company, Belmont, California.

Steel, R.G.D. and J.H. Torrie. 1980. Principles and Procedures of Statistics: A Biomedical Approach. 2nd Ed. McGraw-Hill, Inc., New York.

Tisdale, S.L, W.L. Nelson, J.D. Beaton, and J.L. Havlin. 1993. Soil Fertility and Fertilizers. 5th Edition. Macmillan Publishing Company, New York.

Triska, F.J., J.R. Sedell, K.Cromack Jr., S.V. Gregory, and F.M. McCorison. 1984. Nitrogen budget for a small coniferous forest stream. Ecol. Monog. 54(1): 119-140.

Triska, F.J., J.R. Sedell, and S.V. Gregory. 1982. Coniferous forest streams. 292-332. In: R.L. Edmonds, ed. Analysis of Coniferous Forest Ecosystems in the Western United States. Hutchinson Ross, Stroudsberg, Penn.

Van Beers, W.F.J. 1970. The Auger-Hole Method: a field measurement of the hydraulic conductivity of soil below the water table. Rev. ed. International Institute for Land Reclamation and Improvement. Bulletin 1. Wageningen, 32 pp.

Chapter 3

Denitrification in Surface Waters of Forested Watersheds

The mass transfer coefficient (ρ) (derived in Chapter 4) was determined using seven methods: 1. nitrate depletion in in-stream tanks, 2. nitrate depletion in undisturbed cores, 3. naturally occurring background N^{15} and O^{18} in the canal waters, 4. N^{15} addition to in-stream tanks, 5. diffusion calculations, 6. mass balance, and 7. modeling.

Information on the statistical models used in the denitrification portion of the study can be found in Appendix A.

Water samples taken during the denitrification studies were placed in a freezer immediately after collection and kept frozen until analysis. All samples were filtered through a 0.45 micron filter (Gelman Laboratory, Supor®-450) to remove particulate material. Each sample was analyzed for nitrate, ammonium, phosphate, and dissolved organic, inorganic, and total carbon (Standard Methods, 1989). N^{15} and O^{18} samples were filtered prior to freezing using a 0.7 micron filter (Environmental Express, Borosilicate Microfiber Filter #FG75047MM). Each sample was analyzed for N^{15} and O^{18} proportions (Chang et al., 1999).

3.1 Nitrate Depletion in In-Stream Tanks

3.1.1 Methods

Nitrate depletion in in-stream tanks was measured in three tanks, constructed of a section of PVC pipe 43.2 cm in diameter (Figure 3.1), positioned in the center of the canal, one each at three locations (marked as benthic chamber locations in Figure 2.2). A base for each tank was installed into the sediment during the dry season. An extension of the same diameter as the tanks was inserted into the sediment to a depth of 23 cm. An attached base

plate at the top of the base rested on the sediment surface to keep the tanks from sinking into the sediment. A ring of the same diameter as the base protruded 7.5 cm above the sediment to serve as an attachment site for the tanks as they were placed in the canal, as well as to hold the tank in place and produce a seal between the tank and the base. A piece of neoprene rubber was attached to the base to ensure that water inside the tank would not mix with water outside the tank. The base allowed for the installation and removal of the tanks without disturbing the sediments. Tanks were not continuously circulated due to the absence of a power source at the site. The tanks were placed in the canal after a rainfall event to take advantage of the naturally occurring nitrate peak following each rainfall event. After the tanks were set in the canal, samples were taken on days one, two, three, four, seven, 10, and 17 after tank placement. All three tanks were sampled at the same time.

Dissolved oxygen, pH, and temperature were measured at mid-depth in the water column within the tank and in the open canal at each sampling.

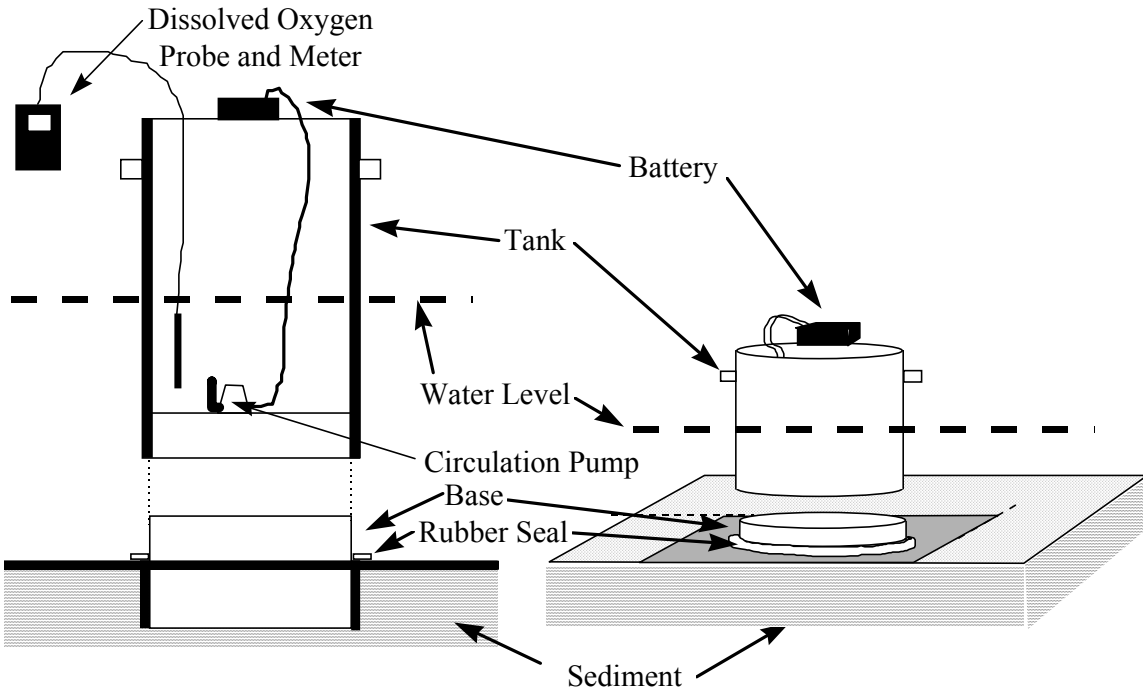

Figure 3.1. In-stream denitrification tank.

3.1.2 Results and Discussion

Measurement of nitrate depletion in in-stream tanks indicated the variability of the mass transfer coefficient in the field. Only two of the five runs were used from each location. Three runs were omitted due to increases in depth caused by subsequent rainfall events occurring during these runs, which resulted in water entering the tank through the deep sediments with an undeterminable amount of nitrates, rendering them unsuitable for this study.

3.1.2.1 Ammonium:

During the first run of the three tanks (22 days), the ammonium level remained low (approximately 0.05 mg/L) and constant within the water column (Figure 3.2). This indicates that any mineralization of organic nitrogen producing ammonium was being offset by nitrification of ammonium, resulting in neither a net gain or loss of ammonium within the water column. Tisdale et al. (1993) noted that nitrification, though reduced, will still occur at pH levels around pH 4, as were those measured during this run (Table 3.1). This indicates that nitrification occurs. Low ammonium levels are consistent with the forested watershed drainage waters of this area.

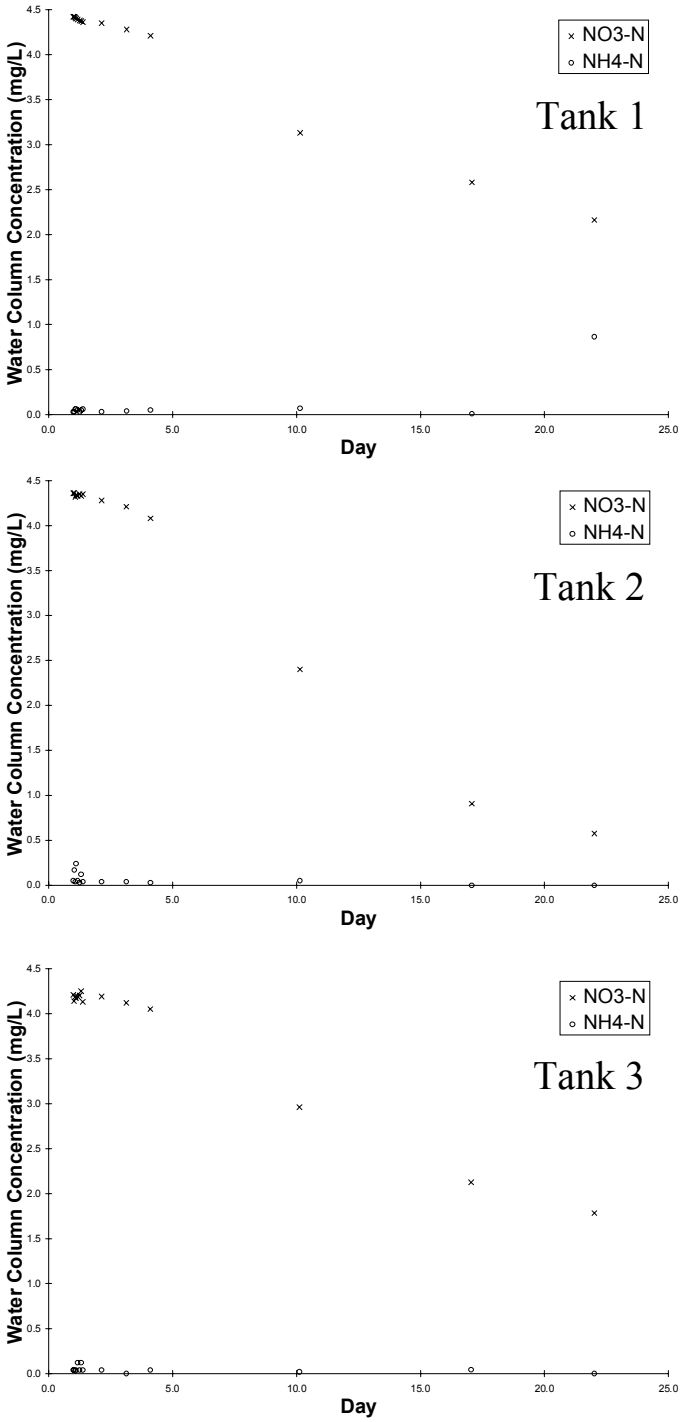

Figure 3.2. Nitrate and ammonium concentrations over time in Tanks 1, 2, and 3 for the first run of the field study.

The second run resulted in an increase in ammonium concentration over the 14-day run (Tank 1: 0.02 to 0.17 mg/L, Tank 2: 0.04 to 0.438 mg/L, and Tank 3: 0.02 mg/L to 0.10 mg/L) (Figure 3.3). This indicates that mineralization is occurring at a faster rate than nitrification. The lower pH of run 2, approximately 3.5 (Table 3.1), is in the range where Tisdale et al. (1993) indicates that nitrification would be reduced (a natural nitrification inhibitor), while mineralization is increased to a small degree due to the higher temperatures of the second run (13^{O}C to 20^{O}C) as compared to the first run (6^{O}C to 14^{O}C). This gives evidence that nitrification is not occurring to a measurable amount during either run.

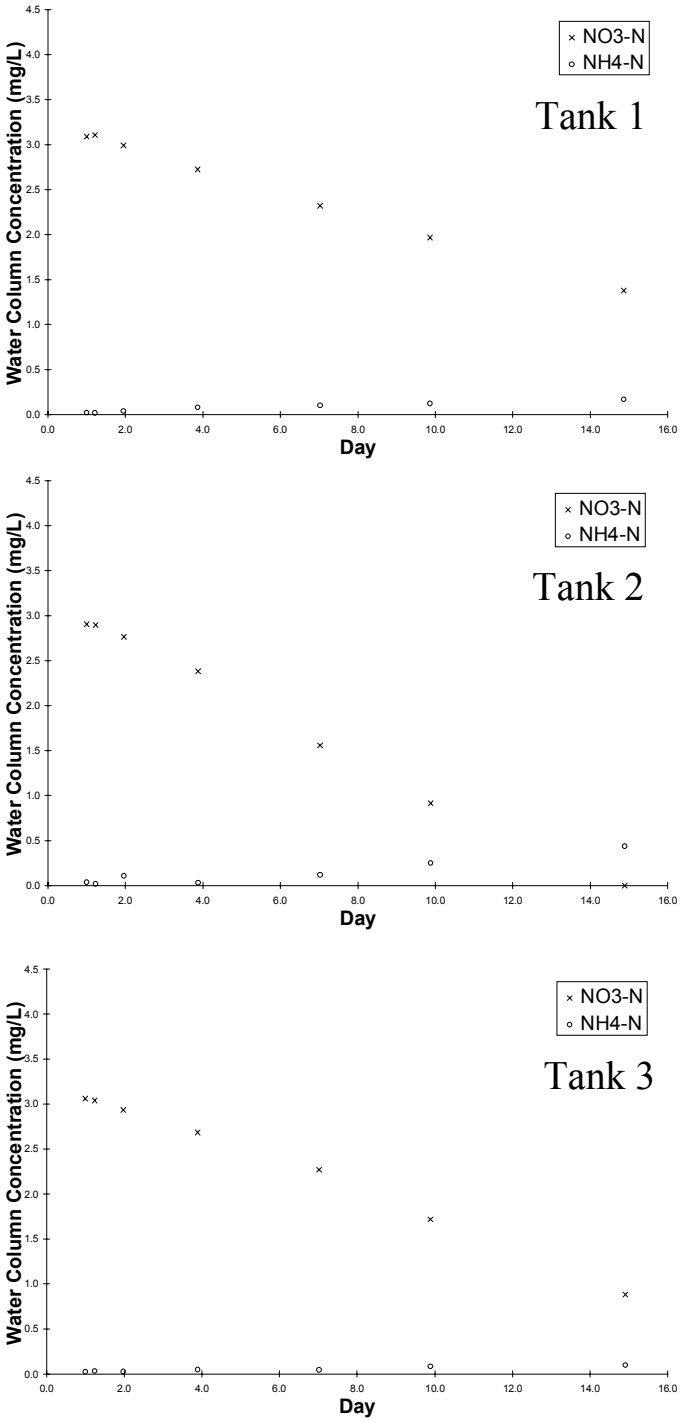

Figure 3.3. Nitrate and ammonium concentrations over time in Tanks 1, 2, and 3 for the second run of the field tank study.

Table 3.1. Environmental conditions during each run of field tank study.

	Tank 1		Tank 2		Tank 3	
	Run 1	**Run 2**	**Run 1**	**Run 2**	**Run 1**	**Run 2**
pH	4.0	3.5	4.0	3.5	4.0	3.5
Dissolved Oxygen (mg/L)	7-8	6-7	7-8	6-7	7-8	6-7
Temperature (^{o}C)	6-14	13-20	6-14	13-20	6-14	13-20
Total Organic Carbon (mg/L)	27	25	24	21	24	20

3.1.2.2 Nitrate:

At all three locations, the nitrate removal rate was greater during the second run than during the first run (Table 3.2). Consequently, the mass transfer coefficient was larger during the second run. This can be explained by a combination of two factors: temperature and pH differences between the two runs (Table 3.1).

Table 3.2. Mass Transfer Coefficients for field tank study at measured rate.

	Mass Transfer Coefficient (m/day)		
	Tank 1	**Tank 2**	**Tank 3**
Run 1	0.015	0.042	0.018
Run 2	0.022	0.056	0.031
% Increase Between Run 1 and Run 2	48%	35%	71%

The temperature range of the second run is higher than that of the first run. Higher temperatures increase both nitrification and denitrification. Using the temperature relationship for denitrification proposed by Dawson and Murphy (1972), one would expect the denitrification rate to roughly double with the average increase in temperature between these two runs. The measured mass transfer coefficients actually increased by 1.5, 1.4, and

1.7 times for Tank 1, Tank 2, and Tank 3 respectively (Table 3.2), indicating that either nitrification has also occurred or that denitrification did not follow the temperature relationship. Evidence from the ammonium concentrations discussed above indicate that nitrification occurred during the first run but not the second run. Theoretically, this would lead to more than a doubling of the net nitrate removal rate, due to nitrification reducing the net removal rate during the first run.

The pH value for the first run (pH 4.0) is at the level at which Waring and Gilliam (1983) reported that denitrification starts to become inhibited. Below this level, the denitrification rate decreases at an appreciable rate. This indicates that denitrification has been inhibited by the lower pH (approximately 3.5) of the second run, explaining why nitrate removal is lower than would be expected given the increase in temperature.

An interesting phenomenon found in the field tanks was an initial delay (lasting around a day or two) in the start of the removal of nitrate from the water column (Figures 3.2 and 3.3). This is due to the conversion in the sediment profile of nitrate from a circulated system to a non-circulated system. Because circulation is stopped by the placement of the tank over the selected sediment section, the deeper nitrates within the sediment are removed from the sediment as the depth of the aerobic zone is decreased. The different profiles are described in Appendix C, Nitrate, Ammonium, and Phosphorous Distribution in Sediment Pore Water and Water Column. These portions of the data were not used in the analysis, as they did not represent a steady-state system.

Statistical analysis (See Appendix A) was conducted on the mass transfer coefficients after they were normalized to values for a temperature of $8^{o}C$ (Table 3.3).

Table 3.3. Mass Transfer Coefficients for field tank study converted to 8°C.

	Mass Transfer Coefficient (m/day)		
	Tank 1	**Tank 2**	**Tank 3**
Run 1	0.011	0.022	0.014
Run 2	0.011	0.024	0.014
Average	0.011	0.023	0.014

To normalize the data, the mass of nitrate removed at each measured concentration was calculated using the method described in Appendix B.

The statistical analysis on the data in Table 3.3 showed there were significant differences in the mass transfer coefficients at the three locations. According to individual tank comparisons using t-tests, all three tanks are significantly different from each other. The differences between the three tanks is most likely due to variations in sediment porosity (assumed to be equal to the average porosity of the undisturbed cores at each location of a field tank) as total organic carbon and dissolved oxygen levels remain relatively uniform between the three Tanks (Table 3.1). The porosity of Tank 2 (porosity of 0.97) was higher than that of Tanks 1 and 3 (porosity of 0.91 and 0.91 respectively), resulting in a higher diffusion rate into the sediment and thus a higher potential nitrate removal rate than in Tanks 1 and 3.

An improvement to this method would have been to install a circulating system that can operate continuously via a solar panel and battery system. Even though the results of method 2 showed that the circulation was not statistically significant, the better the natural system is mimicked, the lower the chance of variability will be introduced to the study.

3.2 Nitrate Depletion in Undisturbed Cores

3.2.1 Methods

Nitrate depletion was determined on nine undisturbed cores (approximately 42 cm in diameter and approximately 20 cm deep) taken from the canal bottom sediment and placed in nine separate tanks located in the lab (Figure 3.4) (three cores were taken from each field tank location). The thickness of each core was determined using a sediment pore water sampler (Appendix C, Nitrate, Ammonium, and Phosphate Distribution in Sediment Pore Water and Water Column). The depth at which the concentration of ammonium became undetectable was chosen as the bottom of the cores. This thickness corresponded with the bottom of the organic layer that overlies a sand layer in which there was no organic material. It also marks the bottom of the hyporheic zone for this canal and the total depth from which ammonium for nitrification can be formed through mineralization.

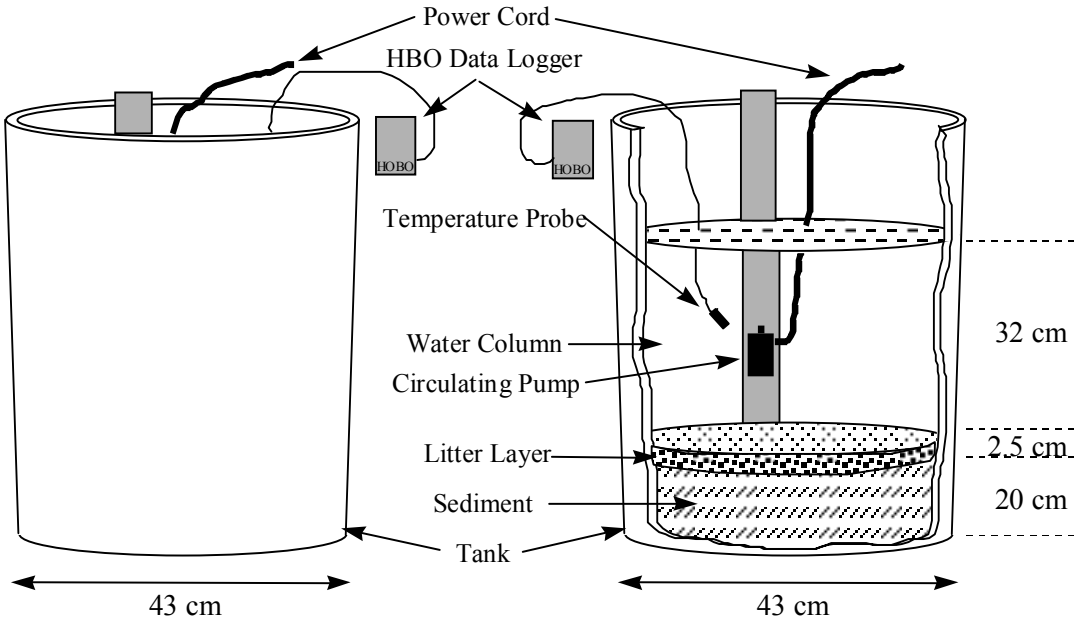

Figure 3.4. Lab tanks with undisturbed sediment cores.

The tanks were separated into three treatments, each with the three locations represented (Figure 3.5). The first treatment was uncirculated without a nitrification inhibitor, the second treatment was circulated without a nitrification inhibitor, and the third treatment was circulated with a nitrification inhibitor (Nitrification Inhibitor Formula 2533 from HACH Company). Circulation was generated using a 0.53 m^3/hr pump that was run continuously throughout the study. The non-circulated and circulated tank study was conducted to determine whether stratification of nutrients (nitrate, ammonium, and phosphate) occurred when the tanks were not circulated. This would affect the overall nitrate removal rates and thus the mass transfer coefficients. Comparison between the two circulated

tanks (with and without the nitrification inhibitor) was used to estimate a mineralization rate, a nitrification rate, a mass transfer coefficient (ρ_d) for the gross nitrate removal rate (the true denitrification rate), and a mass transfer coefficient (ρ_{d+n}) for the net nitrate removal rate (when nitrification and denitrification are occurring). This was done by assuming that the nitrification inhibitor stopped all nitrification within the tank, resulting in a buildup of ammonium within the tank. The slope of the line relating the ammonium buildup over time corresponds to the mineralization rate. The slope of the line relating the difference in the ammonium concentrations between the tanks (with and without nitrification inhibitor) over time would correspond to the nitrification rate (addition of ammonium minus the conversion to nitrate). In the tanks with nitrification inhibitor, all nitrates removed by denitrification originate from the water column, giving a gross nitrate removal rate (the true denitrification rate), which allows for determination of its associated mass transfer coefficient (ρ_d). The loss of nitrate from the water column in the tanks without the nitrification inhibitor represented a net nitrate removal rate, as it includes denitrification of the nitrate from the water column as well as the nitrate produced via nitrification in the sediment within the tank (nitrification-denitrification coupling), which allows for the determination of its associated mass transfer coefficient (ρ_{d+n}).

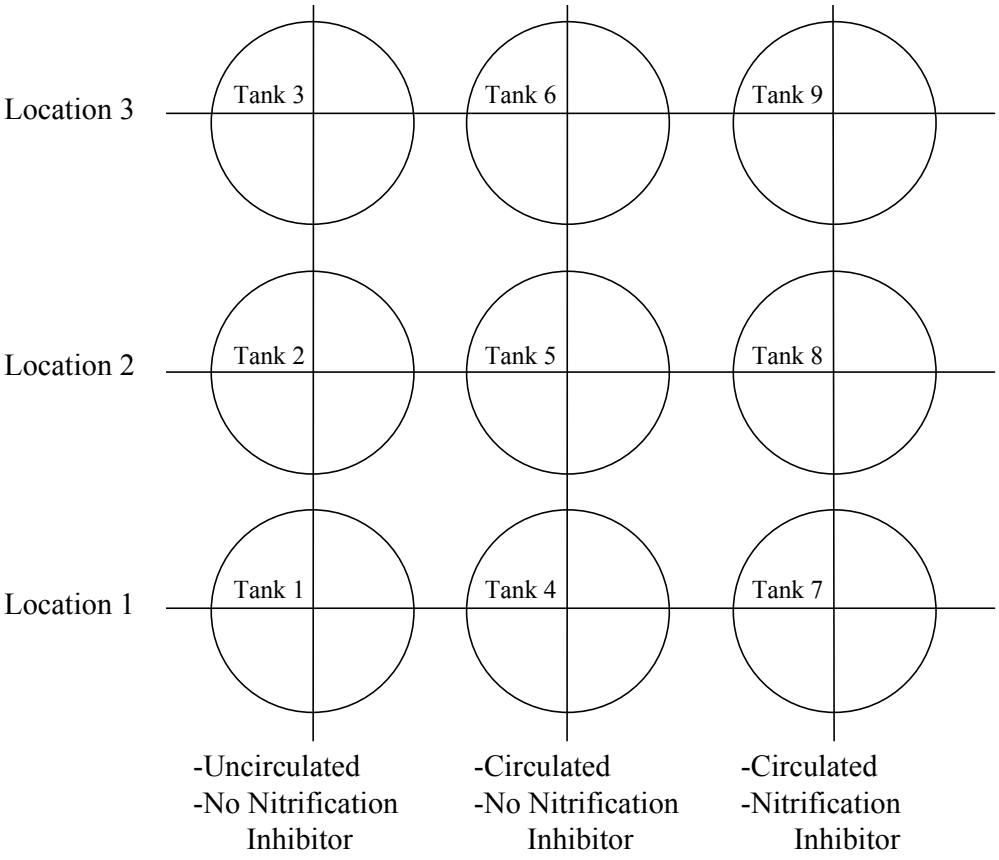

Figure 3.5. Tank layout for undisturbed core study.

The tanks were drained to the sediment surface and allowed to sit for approximately 48 hours between runs. At the start of a run, the tanks were filled with water to a depth of 20 cm or 30 cm above the sediment, depending on the run. Nitrate concentrations were increased at the time of filling to desired levels (6 mg/L for runs 1, 2, and 3 at 8^{o}C and run 1 at 21^{o}C, and 3 mg/L for run 4 at 8^{o}C) by the addition of calcium nitrate ($Ca(NO_3)_2\ nH_2O$). The calcium nitrate (2 gm/tank for 6 mg/L and 1 gm/tank for 3 mg/L) was placed in 900 ml of distilled water and mixed thoroughly. After mixing, 100 ml was dispensed in each tank. This was done to ensure that the enrichment would produce similar starting concentrations for each tank. The form of nitrate used, $Ca(NO_3)_2\ nH_2O$, though marketed as 15% nitrogen,

varied with respect to individual pellets in the batch due to their variable water content - nH_2O (M. Burchell, 2002, personal communication).

The runs included two temperatures (21°C and 8°C), two water column depths (20 cm and 30 cm), and two initial concentrations (3 mg/L and 6 mg/L). The 21°C run was conducted in a room with large windows allowing for a natural light-and-dark cycle, whereas the subsequent runs at 8°C were conducted in a cold room where the lighting system was regulated to try to mimic the natural light cycle.

Samples were taken daily for the first week, every other day for the second week, and every third day for the third week. The small amounts of evaporated water were replaced with water at the same temperature but lacking in nitrate. This was done because only water was lost through evaporation (this occurred rarely and only in minimal volumes).

Dissolved oxygen and pH were measured mid-depth in the water column within each tank at the time of sampling. Temperature was measured on a 0.5 hour interval throughout the study.

3.2.2 Results and Discussion

Nitrate depletion in the undisturbed cores method examined the influence of water column depth, initial water column nitrate concentration, temperature, circulation of the water column, presence of a nitrification inhibitor, and location within the study reach on the mass transfer coefficient. It also allowed for an estimation of an overall nitrate removal rate, denitrification rate, mineralization rate, and nitrification rate within the study canal section under the more controlled environment of a lab study. Table 3.4 gives the environmental conditions during each run of the lab tank study.

Table 3.4. Environmental conditions during each run of lab tank study.

		Initial $[NO_3\text{-}N]$	Depth (cm)	DO (mg/L)	pH	Total Organic Carbon (mg/L)
Tank 1						
8°C	Run 1	6	30	4.9-8.4	5.8	19-19
	Run 2	6	30	7.3-6.7	6.21	9-11
	Run 3	6	20	7.2-8.7	-	10-14
	Run 4	3	30	7.4-9.9	-	10-15
21°C	Run 1	6	30	4.5-5.3	5.5	22-40
Tank 2						
8°C	Run 1	6	30	5.6-8.4	5.6	19-20
	Run 2	6	30	7.0-5.9	6.0	10-15
	Run 3	6	20	7.8-9.5	-	11-15
	Run 4	3	30	7.5-9.5	-	11-16
21°C	Run 1	6	30	4.6-3.5	5.0	19-33
Tank 3						
8°C	Run 1	6	30	8.6-9.1	6.0	9-11
	Run 2	6	30	8.3-6.6	6.5	5-8
	Run 3	6	20	8.7-9.6	-	6-9
	Run 4	3	30	7.8-10.2	-	8-12
21°C	Run 1	6	30	5.2-4.8	5.2	17-51
Tank 4						
8°C	Run 1	6	30	11.9-11.9	6.5	10-19
	Run 2	6	30	10.2-8.5	6.7	6-15
	Run 3	6	20	11.0-11.0	-	8-21
	Run 4	3	30	10.6-10.8	-	9-28
21°C	Run 1	6	30	8.5-8.2	5.3	18-26
Tank 5						
8°C	Run 1	6	30	11.7-11.5	5.6	19-21
	Run 2	6	30	9.83-10.6	6.0	10-19
	Run 3	6	20	10.3-10.4	-	12-22
	Run 4	3	30	9.9-10.4	-	18-35
21°C	Run 1	6	30	7.5-6.9	5.1	32-37

Table 3.4 (continued)						
Tank 6						
8°C	Run 1	6	30	12.2-11.8	6.0	9-19
	Run 2	6	30	10.0-11.7	6.7	6-16
	Run 3	6	20	11.0-10.9	-	8-25
	Run 4	3	30	10.6-10.8	-	10-37
21°C	Run 1	6	30	8.8-8.8	5.3	17-28
Tank 7						
8°C	Run 1	6	30	11.9-11.6	6.3	16-22
	Run 2	6	30	10.1-11.5	7.0	9-17
	Run 3	6	20	11.3-11.0	-	9-23
	Run 4	3	30	11.1-11.2	-	13-31
21°C	Run 1	6	30	8.0-8.6	5.6	38-63
Tank 8						
8°C	Run 1	6	30	11.7-11.6	6.3	15-24
	Run 2	6	30	10.1-11.5	6.9	9-22
	Run 3	6	20	11.0-11.1	-	13-25
	Run 4	3	30	11.1-11.3	-	13-36
21°C	Run 1	6	30	7.8-8.1	5.1	32-33
Tank 9						
8°C	Run 1	6	30	11.9-11.6	6.3	11-20
	Run 2	6	30	x-11.5	-	8-17
	Run 3	6	20	11.2-11.1	-	10-22
	Run 4	3	30	11.1-11.3	-	11-30
21°C	Run 1	6	30	8.4-8.6	5.2	26-30

3.2.2.1 Ammonium:

The average starting water column ammonium concentrations (approximately 1.5 mg/L) for all of the runs of all of the tanks at both temperatures (8°C and 21°C) of the lab study were much higher than those found in the canal reach during the study (<.1 mg/L). This is a function of the design of the study. In the field, during periods of no flow, ammonium generated through mineralization is converted to nitrate through nitrification, because the hyporheic zone is unsaturated and aerobic. This keeps the ammonium concentration at a lower equilibrium level in the sediments between periods of flow. In the

lab study, the tanks were drained to the sediment surface, resulting in a saturated anaerobic environment. This gives rise to continued mineralization without nitrification, leading to an elevation of ammonium in the sediments. As the tanks were filled, the ammonium in the upper sediment mixed with the incoming water, immediately elevating the water column ammonium concentration to an average of 1.5 mg/L.

Tanks 1, 2, and 3 (uncirculated) demonstrated a slow increase in ammonium concentration average over time during each of the four runs at 8^{o}C (Figures 3.6-3.8). This slow increase is due to the reduced nitrification potential of the sediment without circulation. In the absence of circulation, the movement of dissolved oxygen into the sediment is restricted to diffusion, a much slower process than the advection generated by circulation. The result is less oxygen entering the sediment. The oxygen that does enter the sediment is consumed closer to the surface of the sediment, as the anaerobic zone moves upward in the sediment (Appendix C, Nitrate, Ammonium, and Phosphorous Distribution in Sediment Pore Water and Water Column). This results in the nitrifying zone being restricted to a thinner zone in the uppermost layer of the sediment. At 8^{o}C, the mineralization rate and unrestricted nitrification rate (not limited by ammonium concentration) are approximately equal in this system (Appendix D, Mineralization and Nitrification). This means when the nitrification zone is reduced in size, mineralization will outproduce nitrification, resulting in the increase in ammonium in the system that is expressed in the slow increase in water column ammonium concentration over time.

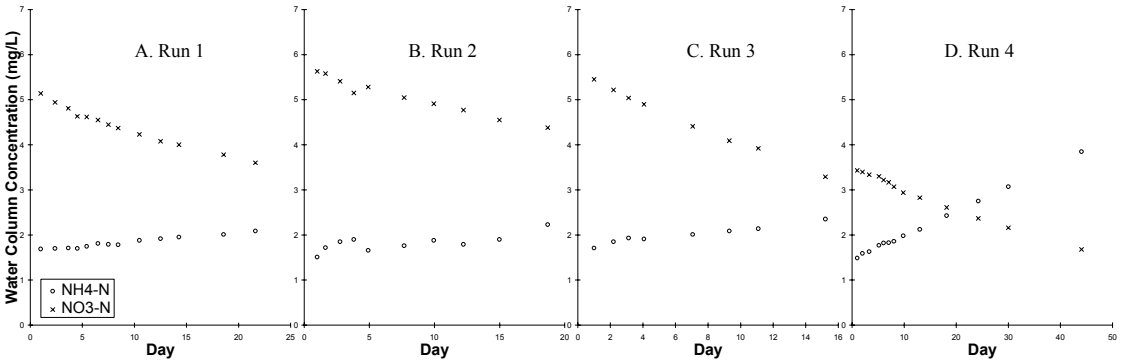

Figure 3.6. Nitrate and ammonium concentrations over time in Tank 1 for initial concentrations and depths of: A.) 5.14 mg/L, 30.48 cm depth, B.) 5.63 mg/L, 30.48 cm depth, C.) 5.45 mg/L, 20.32 cm depth, and D.) 3.43 mg/L, 30.48 cm depth at a temperature of 8^{o}C, in the undisturbed core study.

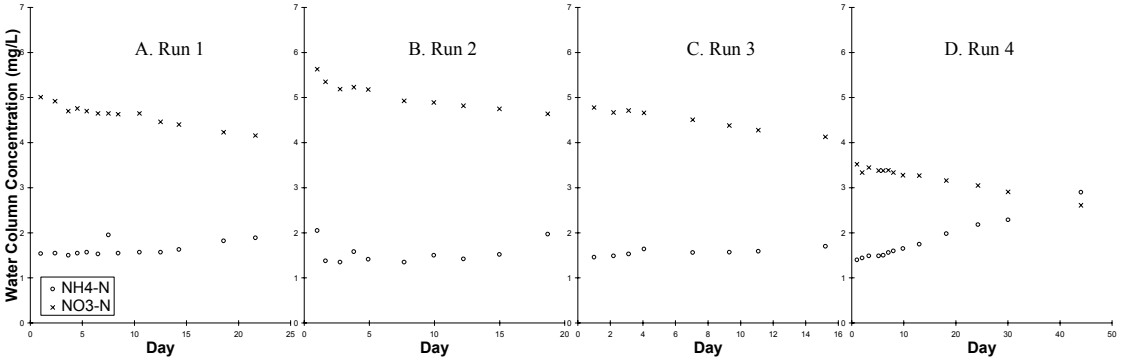

Figure 3.7. Nitrate and ammonium concentrations over time in Tank 2 for initial concentrations and depths of: A.) 5.01 mg/L, 30.48 cm depth, B.) 5.63 mg/L, 30.48 cm depth, C.) 4.78 mg/L, 20.32 cm depth, and D.) 3.52 mg/L, 30.48 cm depth at a temperature of 8^{o}C, in the undisturbed core study.

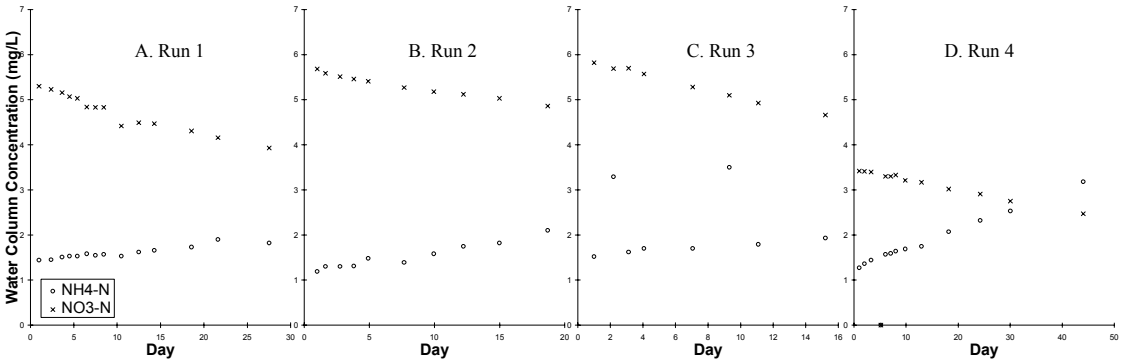

Figure 3.8. Nitrate and ammonium concentrations over time in Tank 3 for initial concentrations and depths of: A.) 5.30 mg/L, 30.48 cm depth, B.) 5.68 mg/L, 30.48 cm depth, C.) 5.82 mg/L, 20.32 cm depth, and D.) 3.42 mg/L, 30.48 cm depth at a temperature of 8^{o}C, in the undisturbed core study.

At 21^{o}C, the ammonium concentrations for Tanks 1, 2, and 3 remain relatively constant with time over the run (Figure 3.9). The higher temperature of this run offsets the reduction of the nitrification zone in the previous runs by virtue of the concomitant increase in both the oxygen diffusion rate (from 1.446 x 10^{-6} cm^2/sec at 8^{o}C to 2.055 x 10^{-6} cm^2/sec at 21^{o}C) and the nitrification rate. The mineralization rate, on the other hand, does increase but not dramatically (Appendix D, Mineralization and Nitrification). This creates an equilibrium between the mineralization rate and nitrification rate, which is expressed as the water column's relatively constant ammonium concentration, approximately 1 mg/L.

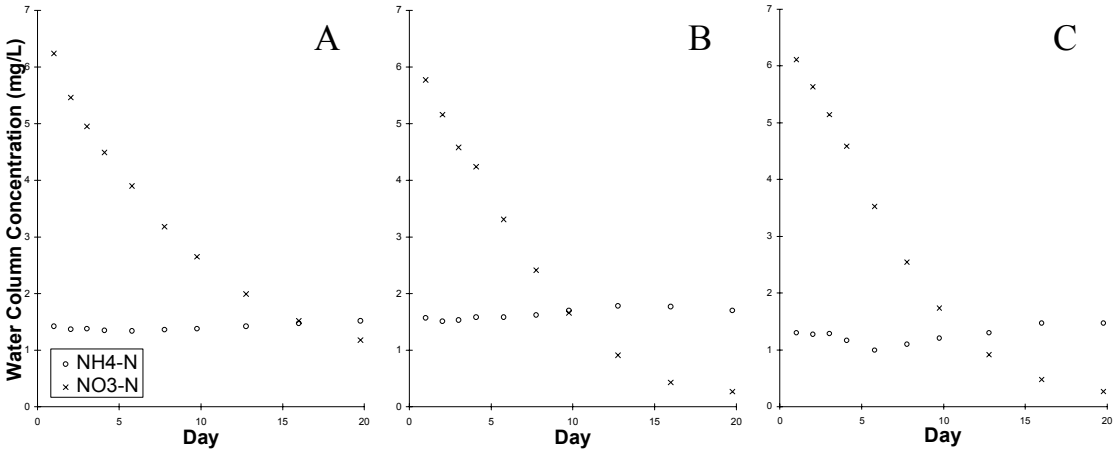

Figure 3.9. Nitrate and ammonium concentrations over time in A) Tank 1, B) Tank 2, and C) Tank 3 for initial concentrations of 6.24 mg/L, 5.77 mg/L, and 6.11 mg/L respectively at a depth of 30.48 cm and temperature of 21^{o}C.

Tanks 5, 6, and 7 (circulated) demonstrated a relatively constant average ammonium concentration over time for each of the first three runs at 8^{o}C (Figures 3.10-3.12). This can be directly linked to the circulation of the water column above the sediment surface. As the water column is circulated, advective movement through the sediment starts to occur, bringing water with high levels of dissolved oxygen into the upper layers of the sediment, creating a thicker aerobic layer. This thicker aerobic zone now allows nitrification to occur in a larger portion of the sediment, resulting in mineralization and nitrification to be more in equilibrium to each other at 8^{o}C. This closer equilibrium results in a relatively constant ammonium concentration over time. The fourth run of Tanks 4, 5, and 6 at 8^{o}C resulted in an increase in ammonium over time (Figures 3.10-3.12). This may be due to the continued cold temperature during the four runs (8^{o}C). Some of the nitrifiers may be able to withstand this temperature, while others can only tolerate it for a short period of time.

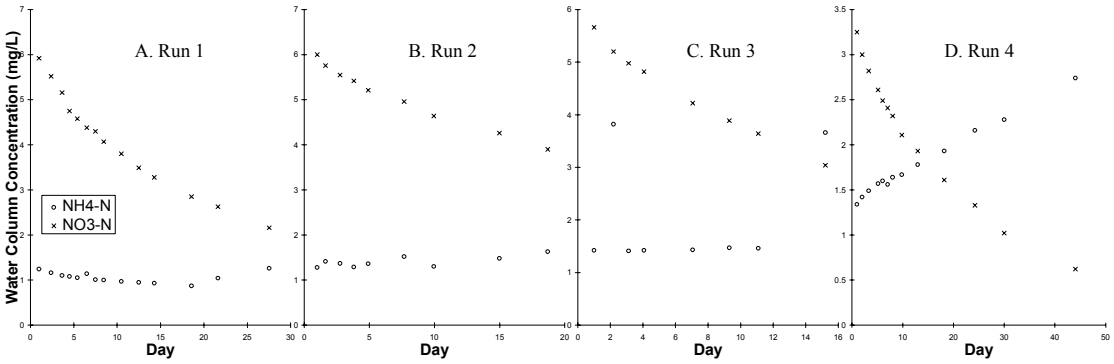

Figure 3.10. Nitrate and ammonium concentrations over time in Tank 4 for initial concentrations and depths of: A.) 5.92 mg/L, 30.48 cm depth, B.) 6.00 mg/L, 30.48 cm depth, C.) 5.66 mg/L, 20.32 cm depth, and D.) 3.25 mg/L, 30.48 cm depth at a temperature of 8^{o}C, in the undisturbed core study.

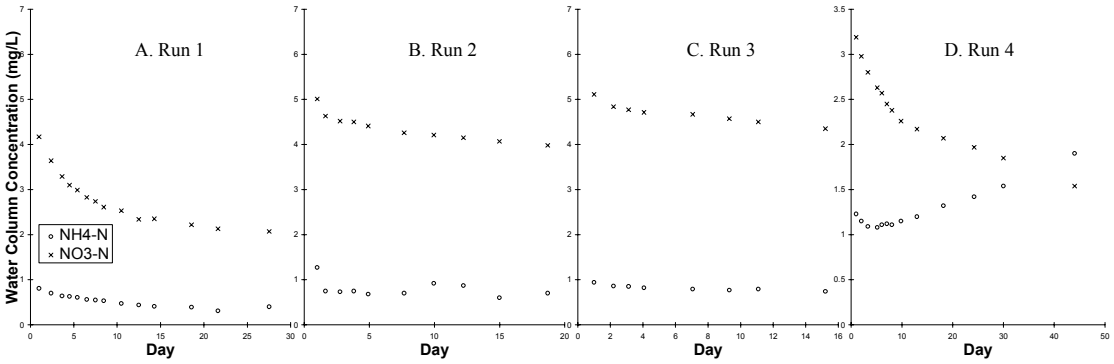

Figure 3.11. Nitrate and ammonium concentrations over time in Tank 5 for initial concentrations and depths of: A.) 4.17 mg/L, 30.48 cm depth, B.) 5.01 mg/L, 30.48 cm depth, C.) 5.11 mg/L, 20.32 cm depth, and D.) 3.19 mg/L, 30.48 cm depth at a temperature of 8^{o}C, in the undisturbed core study.

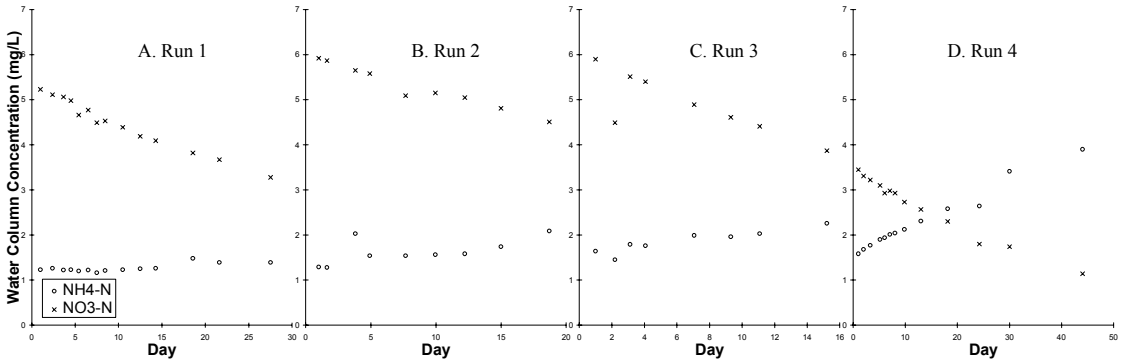

Figure 3.12. Nitrate and ammonium concentrations over time in Tank 6 for initial concentrations and depths of: A.) 5.23 mg/L, 30.48 cm depth, B.) 5.92 mg/L, 30.48 cm depth, C.) 5.90 mg/L, 20.32 cm depth, and D.) 3.45 mg/L, 30.48 cm depth at a temperature of 8^{o}C, in the undisturbed core study.

At 21^{o}C, the ammonium concentrations for Tanks 4, 5, and 6 decrease relatively rapidly with time over the run (Figure 3.13). As previously stated, the increase in temperature increases the nitrification rate, resulting in a higher potential for nitrification. This factor combines with the thicker nitrifying zone to cause the nitrification rate to exceed the mineralization rate in the sediment, resulting in a net reduction of ammonium from the system. This loss of ammonium is expressed in the decrease in the ammonium concentration in the water column over time.

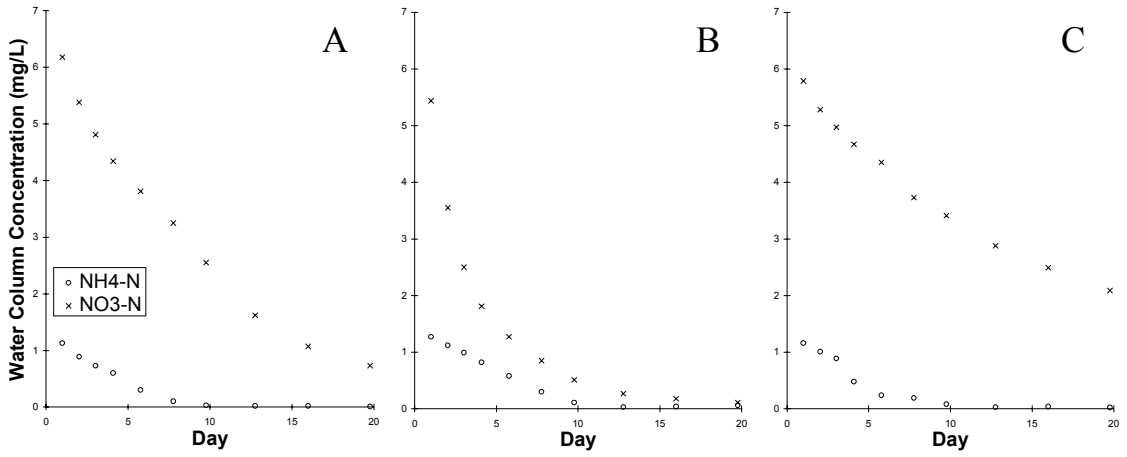

Figure 3.13. Nitrate and ammonium concentrations over time in A) Tank 4, B) Tank 5, and C) Tank 6 for initial concentrations of 6.18 mg/L, 5.44 mg/L, and 5.79 mg/L respectively at a depth of 30.48 cm and temperature of 21^{o}C.

Tanks 7, 8, and 9 (circulated with nitrification inhibitor) demonstrated a larger increase in ammonium concentrations over time for all four runs at 8^{o}C than did Tanks 1, 2, and 3 (Figures3.14-3.16). This is due to the presence of the nitrification inhibitor. Mineralization proceeded as before, but without nitrification converting the ammonium to nitrate, resulting in a more rapid buildup of ammonium within the system. This accelerated ammonium buildup is reflected in the increasing ammonium concentrations in the water column over time.

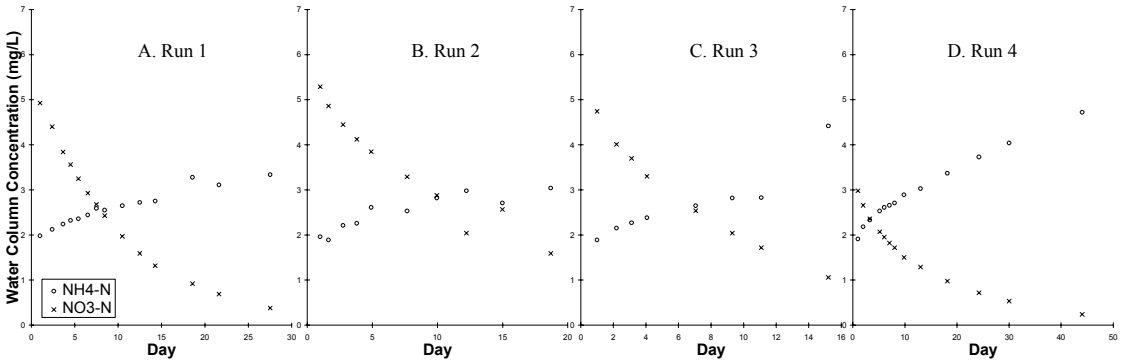

Figure 3.14. Nitrate and ammonium concentrations over time in Tank 7 for initial concentrations and depths of: A.) 4.93 mg/L, 30.48 cm depth, B.) 5.29 mg/L, 30.48 cm depth, C.) 4.74 mg/L, 20.32 cm depth, and D.) 2.98 mg/L, 30.48 cm depth at a temperature of 8^{o}C, in the undisturbed core study.

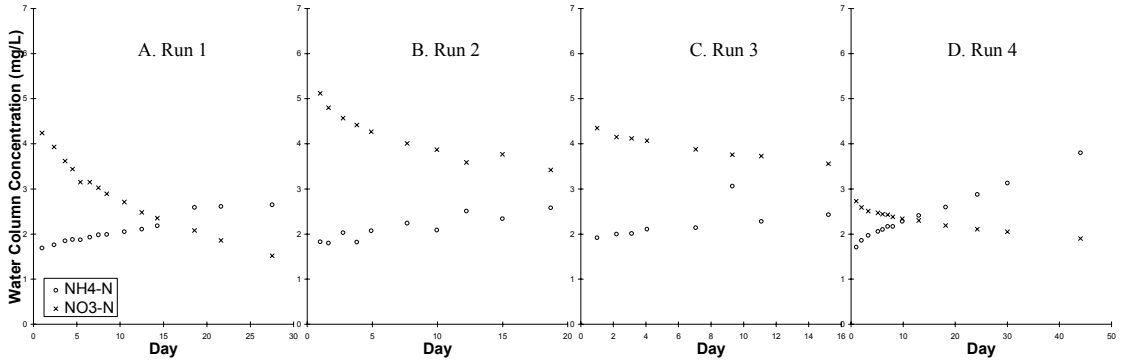

Figure 3.15. Nitrate and ammonium concentrations over time in Tank 8 for initial concentrations and depths of: A.) 4.24 mg/L, 30.48 cm depth, B.) 5.12 mg/L, 30.48 cm depth, C.) 4.35 mg/L, 20.32 cm depth, and D.) 2.73 mg/L, 30.48 cm depth at a temperature of 8^{o}C, in the undisturbed core study.

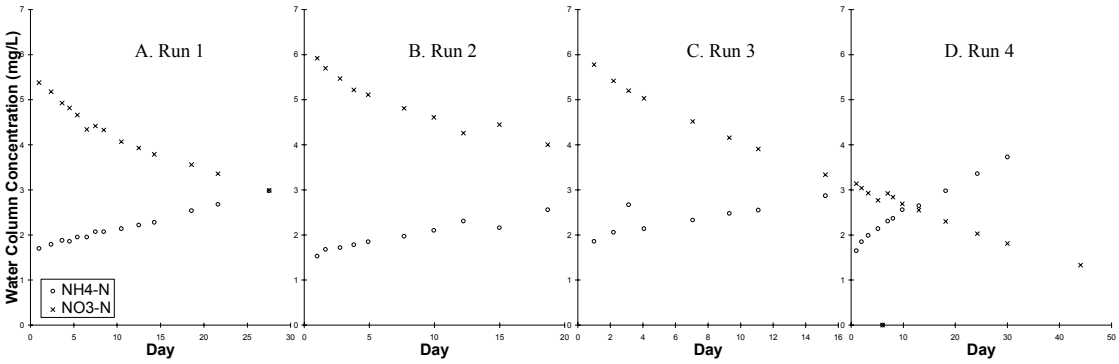

Figure 3.16. Nitrate and ammonium concentrations over time in Tank 9 for initial concentrations and depths of: A.) 5.38 mg/L, 30.48 cm depth, B.) 5.92 mg/L, 30.48 cm depth, C.) 5.78 mg/L, 20.32 cm depth, and D.) 3.14 mg/L, 30.48 cm depth at a temperature of 8^{o}C, in the undisturbed core study.

At 21^{o}C, ammonium concentrations increased over time, as they did during the runs at 8^{o}C in Tanks 7, 8, and 9 (Figure 3.17). The buildup of ammonium in the system at 21^{o}C is slightly higher than at 8^{o}C, due to the increased mineralization rate at the higher temperature. Again, the ammonium present in the system is not converted to nitrate, as the nitrification inhibitor stops nitrification from occurring. The slower buildup of ammonium in Tanks 8 and 9 may be due to a lower mineralization due to a smaller population of mineralizers present in the sediment. The buildup of ammonium is again reflected in the increase in the water column ammonium concentrations over time.

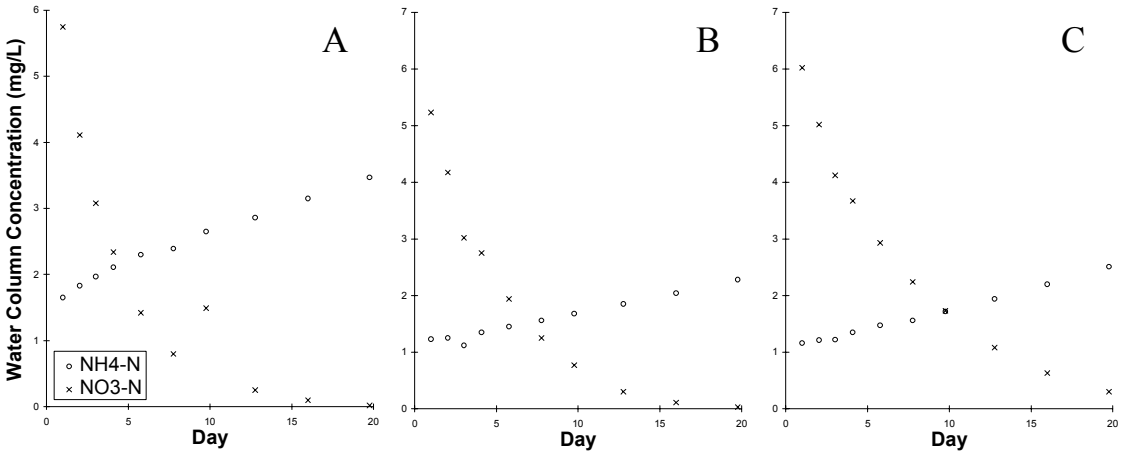

Figure 3.17. Nitrate and ammonium concentrations over time in A) Tank 7, B) Tank 8, and C) Tank 9 for initial concentrations of 5.75 mg/L, 5.23 mg/L, and 6.02 mg/L respectively at a depth of 30.48 cm and temperature of 21^{o}C.

3.2.2.2 Nitrate:

Figures 3.6 to 3.17 show plots of the measured nitrate concentrations over time for all runs of Tanks 1-9. Tables 3.5, 3.6, and 3.7 contain the mass transfer coefficients for each run of each of the tanks of the study. Under each tank, two columns appear, 1st and 2nd. These indicate points where the mass transfer coefficient suddenly changes to a new value. The 1st column indicates the initial mass transfer coefficient that occurred for the first several days (no entry in the 1st column indicates that the mass transfer coefficient did not change during the run). This 1st column's initial mass transfer coefficient is the result of the system attaining an equilibrium within the system after refilling the tanks and adding the nitrate. The 2nd column indicates the mass transfer for the duration of the run (the 2nd column was used for the statistical analysis).

Table 3.5. Mass transfer coefficients for uncirculated tanks.

			Mass Transfer Coefficient (m/day)					
Temperature (^oC)	**Depth (cm)**	**Initial $[NO^3]$ (mg/L)**	**Tank 1**		**Tank 2**		**Tank 3**	
			1^{st}	2^{nd}	1^{st}	2^{nd}	1^{st}	2^{nd}
8	30	6	0.007	0.005	0.005	0.003	-	0.004
8	30	6	-	0.004	0.012	0.002	-	0.003
8	20	6	-	0.007	-	0.002	-	0.003
8	30	3	-	0.005	-	0.002	-	0.002
21	30	6	-	0.029	0.035	0.039	0.028	0.059

Table 3.6. Mass transfer coefficients for circulated tanks.

			Mass Transfer Coefficient (m/day)					
Temperature (^oC)	**Depth (cm)**	**Initial $[NO^3]$ (mg/L)**	**Tank 4**		**Tank 5**		**Tank 6**	
			1^{st}	2^{nd}	1^{st}	2^{nd}	1^{st}	2^{nd}
8	30	6	0.012	0.010	0.002	0.004	-	0.006
8	30	6	0.008	0.006	0.004	0.002	-	0.005
8	20	6	-	0.008	-	0.002	-	0.006
8	30	3	-	0.012	0.014	0.004	-	0.008
21	30	6	0.029	0.043	0.124	0.070	-	0.017

Table 3.7. Mass transfer coefficients for circulated tanks containing nitrification inhibitor.

			Mass Transfer Coefficient (m/day)					
Temperature (^oC)	**Depth (cm)**	**Initial $[NO^3]$ (mg/L)**	**Tank 7**		**Tank 8**		**Tank 9**	
			1^{st}	2^{nd}	1^{st}	2^{nd}	1^{st}	2^{nd}
8	30	6	-	0.031	0.020	0.011	0.010	0.006
8	30	6	-	0.021	-	0.007	0.014	0.008
8	20	6	-	0.021	-	0.003	-	0.007
8	30	3	-	0.019	0.013	0.002	-	0.007
21	30	6	-	0.089	-	0.070	-	0.046

Depth was analyzed using the data subset of temperature at 8^{o}C and initial concentration of 6 mg/L, resulting in three levels of location, three levels of treatment, and two levels of depth. The analysis showed that the depth of the water column had no main effect nor interactive effects with location and treatment on the mass transfer coefficient (R^2=0.94 and an MSE=0.003). When the water column is shallower, nitrate concentrations decline at a more rapid rate, due to the smaller overall mass of nitrate in the water column. The mass transfer coefficient used here (developed by Birgand, 2003, personal communication) is independent of the depth; thus, this result is expected. Based on this result, depth was omitted from the overall statistical model in this study.

Initial nitrate concentration was analyzed using the data subset of temperature at 8^{o}C, resulting in three levels of location, three levels of treatment, and two levels of initial concentration. The statistical analysis of initial water column nitrate concentration showed no main effect nor interactive effects with location and treatment on the mass transfer coefficient (R^2=0.92 and an MSE=0.003). This was expected, as nitrate removal is expected to follow a first-order exponential decay curve. Different starting concentrations would not influence the decay rate and thus would not affect the mass transfer coefficient. Based on this result, initial concentration was also omitted from the overall statistical model.

Location, treatment, and temperature were analyzed using the full data set, as depth and initial concentration were found to have no effect on the mass transfer coefficients (see Appendix A). This resulted in three levels of location, three levels of treatment, and two levels of temperature. Location and treatment were found to be significant, while temperature was found to be very significant (R^2=0.99 and an MSE=0.003). The interaction between

treatment and location and the three-way interaction between treatment, location, and temperature were not found to be significant and can be ignored. Interactions between treatment and temperature and between location and temperature were found to be significant. This means temperature affects the nitrate removal rate, and thus the mass transfer coefficient, differently at the different locations. Similarly, temperature and treatment interact in the same way: temperature affects the mass transfer coefficient to a different degree in each treatment.

A comparison of the mass transfer coefficients shows that the combined effect of temperature and location both have the same direction, becoming greater as the temperature is increased, but by different amounts (Table 3.8). At the east and west location, the temperature-induced increases in the mass transfer coefficient (0.036 m/day and 0.038 m/day respectively) are much less than at the central location, where the temperature-induced increase in mass transfer coefficient (0.063 m/day) is almost double that of the other locations. This is most likely due to the higher porosity of the undisturbed cores from the central location. Denitrification is regulated by the amount of nitrate present to be denitrified. The higher porosity allows for more nitrate to penetrate to the denitrification zone at a faster rate, thus increasing the mass transfer coefficient. This factor, combined with the increase in temperature, results in a larger increase in the mass transfer coefficient compared to the other locations.

Table 3.8. Comparison of the mass transfer coefficients (m/day) based on temperature and location.

	Temperature		Difference
Location	**8°C**	**21°C**	
East	0.005	0.041	0.036
Central	0.004	0.067	0.063
West	0.016	0.054	0.038

When the mass transfer coefficients are compared, the combined effect of temperature and treatment also have the same direction. The results for the circulated tank with the nitrification inhibitor had the greatest difference (0.056 m/day), followed by the uncirculated treatment (0.046 m/day) and then the circulated treatment (0.037 m/day) (Table 3.9). The combined effect of temperature and treatment (uncirculated, circulated, and circulated with a nitrification inhibitor) on the mass transfer coefficient can be explained by the treatment differences (Table 3.9). The larger effect of temperature on the nitrification inhibitor treatment is expected. As the temperature is increased in the treatments without the nitrification inhibitor, nitrification increases along with denitrification. The increase in nitrification offsets the increase in denitrification, resulting in a smaller increase in the net nitrate removal as compared to the treatment containing the nitrification inhibitor.

The difference in the temperature response of the mass transfer coefficient between the circulated and uncirculated treatments without the nitrification inhibitor was not expected. This may be due to the increased diffusion rate of nitrates into the sediment, the reduction of dissolved oxygen within the water and sediment column, and higher metabolic rates within the sediment. In the uncirculated treatment, the dissolved oxygen was consumed near the sediment surface, reducing the nitrification layer to a very thin band along the surface of the sediment. The increase in denitrification caused by the increase in temperature

resulted in a higher mass transfer coefficient. The circulated treatment compensated for the lower dissolved oxygen levels and increased demand by advectively supplying dissolved oxygen deeper into the sediment. This maintained thicker nitrifying zone, as was determined with the lower temperature. This resulted in a larger increase in the nitrification rate with temperature compared to the noncirculated treatment. This caused a smaller increase of the mass transfer coefficient with temperature.

Table 3.9. Comparison of the mass transfer coefficients (m/day) based on temperature and treatment.

	Temperature		Difference
Treatment	**8°C**	**21°C**	
Uncirculated	0.004	0.049	0.46
Circulated	0.006	0.044	0.037
Circulated with Nitrification Inhibitor	0.012	0.068	0.056

Effects of circulation were analyzed by using the data subset obtained for tanks without a nitrification inhibitor. This resulted in three levels of location, two levels of circulation, and two levels of temperature. The analysis showed that the circulation of the water column had no main effect on the mass transfer coefficient (R^2=0.99 and an MSE=0.001). There was a significant interaction between circulation and temperature, indicating that temperature and circulation together increase the mass transfer coefficient by more than a simple additive effect as described above.

The effect of the nitrification inhibitor was analyzed using the data subset where water column was circulated, resulting in three levels of location, two levels of nitrification inhibitor, and two levels of temperature. The analysis showed a significant main effect for

the presence of the nitrification inhibitor but not the interactions with location and temperature (R^2=0.99 and an MSE=0.003). The presence of a main effect of the inhibitor is simply due to the effect that the inhibitor stopped nitrification from occurring. The increase in the mass transfer coefficient was not similar in both treatments as the temperature increased (Table 3.10). In the treatment without the inhibitor, the increased denitrification rate is offset by the increase in the nitrification rate with temperature, resulting in a smaller net increase in the mass transfer coefficient.

Table 3.10. Comparison of the mass transfer coefficients based on temperature and presence of nitrification inhibitor.

	Temperature		Difference
Inhibitor	**8°C**	**21°C**	
No	0.006	0.044	0.037
Yes	0.012	0.068	0.056

Several improvements could be made to this method. First, the tanks should be drained completely between runs to avoid ammonium buildup in the sediment. This would better mimic natural field conditions and eliminate some of the variability in the mass transfer coefficients that results from the high nitrification caused by abnormally high ammonium concentrations at the start of each run (as described previously in this section). The second improvement would be to use potassium nitrate rather than the calcium nitrate used in this study. The use of calcium nitrate introduces large amounts of calcium, which, reported by Tisdale et al. (1993), can result in an increase in nitrification. This effect was not observed in this study, most likely due to the lower temperature (8°C). At 21°C, this could

have affected the nitrification effect until the water column ammonium was removed, after which point the nitrification rate was controlled by the mineralization rate.

3.3 In-Stream Background N^{15} and O^{18}

3.3.1 Methods

The use of in-stream background nitrate-N^{15} and nitrate-O^{18} consisted of sampling the canal flow during different flow velocities and measuring the proportion of the naturally occurring nitrate -N^{15} and nitrate-O^{18} present in comparison to nitrate -N^{14} and nitrate -O^{16} present. N^{15}, N^{14}, O^{18}, and O^{16} are the naturally occurring stable isotopes of nitrogen and oxygen found in the environment and are reported as $\delta^{15}N$ ($^0/_{00}$) and $\delta^{18}O$ ($^0/_{00}$), measures of N^{15} and O^{18} relative to the atmospheric concentrations and a standard V-SMOW respectively, generally reported in per mil ($^0/_{00}$) (Kendall and Arvena, 2000). Flow velocities, dissolved oxygen, pH, and temperature were recorded at the time of sampling. Different velocities are measured because the retention time within the stream determines the exposure time of the nitrates to the denitrifying organisms within the sediments. During denitrification, the heavier nitrate (N^{15}) and nitrate (O^{18}) react slower than the lighter nitrate (N^{14}) and nitrate (O^{16}) (Kendall and Aravena, 2000; Farrell et al., 1996). This difference would result in the reactant pool (NO_3) becoming enriched with N^{15} and O^{18}, while the products (N_2O and N_2) become richer in N^{14} and O^{16}. Eventually, all the nitrates in the reactive pool are converted to N_2O and N_2, resulting in the same ratio of N^{15} to N^{14} and O^{18} to O^{16} in the products as were originally in the reactants (Kendall and Aravena, 2000; Farrell et al., 1996). This process is described by the Rayleigh Equation (Equation 3.1).

$$\delta \approx \delta_o + \varepsilon_{p\text{-}s} \ln(f) \qquad \text{Equation 3.1}$$

where: δ_o = is the initial concentration of the substrate
f = is the remaining fraction of the substrate
$\varepsilon_{p\text{-}s}$ = the isotopic enrichment factor, <0

(Kendall and Aravena, 2000).

The isotopic enrichment factor is calculated by Equation 3.2.

$$\varepsilon_{p\text{-}s} = 1000 \text{ x } (\alpha - 1) \qquad \text{Equation 3.2}$$

where: $\varepsilon_{p\text{-}s}$ = the isotopic enrichment factor, <0
α = the kinetic fractionation factor

(Kendall and Aravena, 2000).

Irreversible kinetic fractionation effects such as denitrification α can be defined by Equation 3.3.

$$\alpha_{p\text{-}s} = R_p/R_s \qquad \text{Equation 3.3}$$

where: $R_p = N^{15}/N^{14}$ ratio of the products
$R_s = N^{15}/N^{14}$ ratio of the reactant

(Kendall and Aravena, 2000).

A plot of the δN^{15} vs. Ln[NO^3] produces a straight-line relationship of the effect of denitrification (Kendall and Aravena, 2000).

Kendall and Aravena (2000) also describe a "distinctive isotopic signature" when plotting δN^{15} vs. δO^{18} when denitrification is occurring (a slope of approximately 0.5). This process is useful in making initial determinations of whether or not denitrification is occurring in a large system such as a watershed.

3.3.2 Results and Discussion

The use of naturally occurring background O^{18} and N^{15} in nitrate gave interesting results. The $\delta^{18}O$ ($^{0}/_{00}$) values were dominated by rainfall contributions of nitrate, which range from $\delta^{18}O$ ($^{0}/_{00}$)= +25 to +65 where soil nitrate contributions (baseflow) range from $\delta^{18}O$ ($^{0}/_{00}$)= -4 to 10 (Figure 3.18). The high conductivity of the soils within the area allowed the rainfall to rapidly move into the soil and to the canal, raising the $\delta^{18}O$ ($^{0}/_{00}$) value of the canal waters. Most of the samples inadvertently were taken within 24 hours of a rainfall event, which resulted in artificially high $\delta^{18}O$ ($^{0}/_{00}$) values. The $\delta^{18}O$ ($^{0}/_{00}$) values declined over time regardless of flow velocities in the canal, as the rainfall moved through the soil to the canal. The $\delta^{18}O$ ($^{0}/_{00}$) value fell to the anticipated values between -4 and +10 only once in the six samples.

The $\delta^{15}N$ ($^{0}/_{00}$) tended to become smaller as the velocity in the flume increased (Figure 3.19). This is an expected result as velocity decreases and the residence time of the water increases, increasing the amount of nitrate removed through denitrification. As denitrification increases, the proportion of N^{14} -nitrate decreases and the proportion of N^{15} -nitrate increases due to the natural preference of the denitrifiers for the lighter N^{14} -nitrate. This is an indicator of denitrification. A stronger indicator is shown in Figure 3.20, when the data are plotted as $\delta^{15}N$ ($^{0}/_{00}$) vs. $\ln[NO_3]$. This yields a straight line that can be described by the Rayleigh equation (an exponential equation) (Kendall and Aravena, 2000). The negative slope of this line indicates denitrification is occurring.

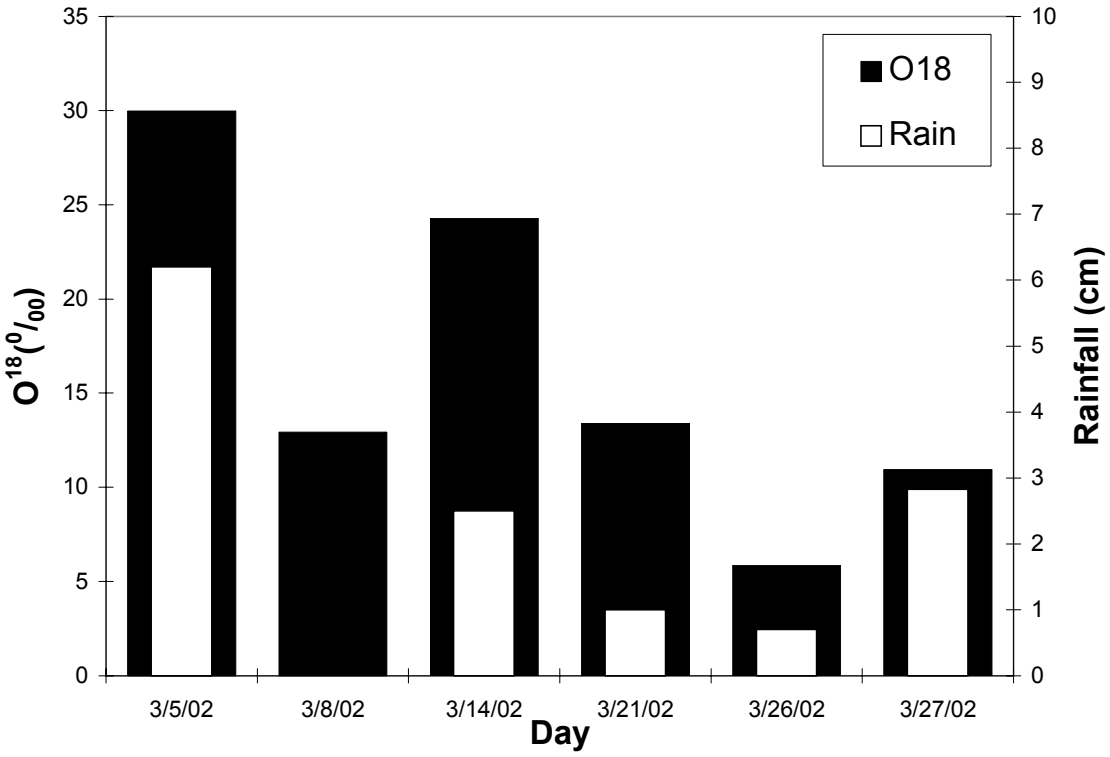

Figure 3.18. Rainfall and $\delta^{18}O$ ($^0/_{00}$) vs. time.

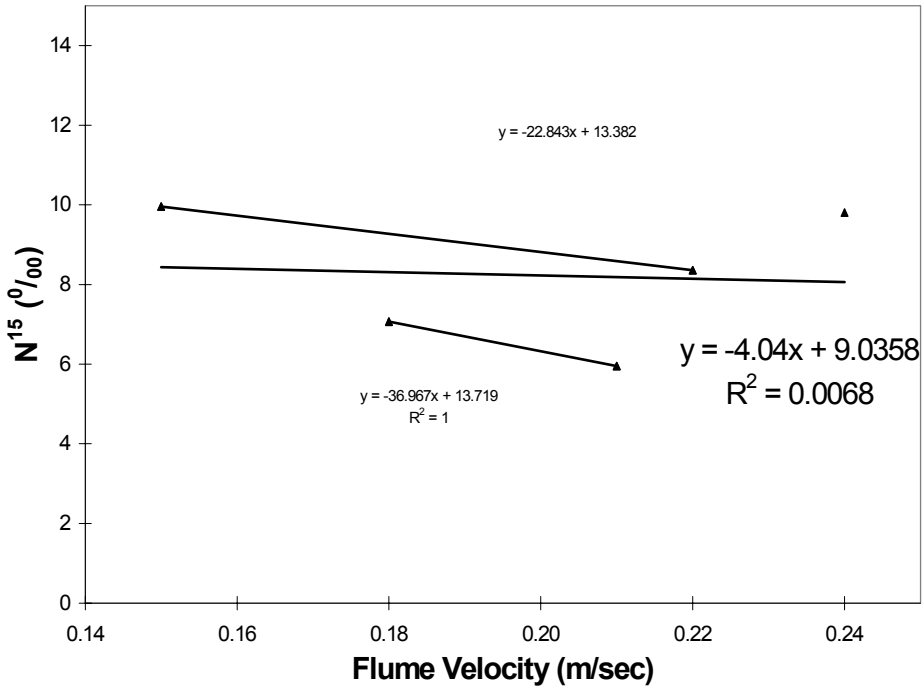

Figure 3.19. $\delta^{18}N$ ($^0/_{00}$) vs. flume velocity.

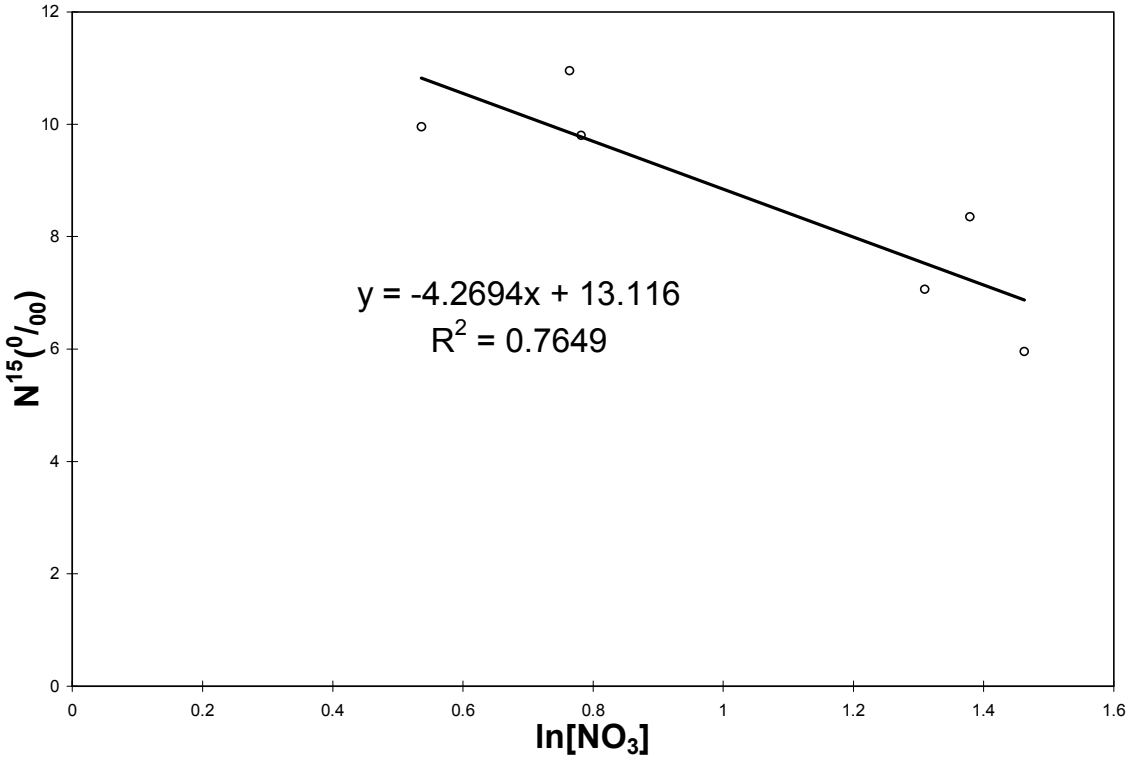

Figure 3.20. $\delta^{15}N$ ($^{0}/_{00}$) vs. ln[NO_3] showing an increase in the $\delta^{15}N$ ($^{0}/_{00}$) as the concentration of nitrate is reduced, indicating the occurrence of denitrification.

Improvements to this method would include a close monitoring of the weather and the avoidance of sampling after a rainfall event, which would facilitate the proper collection of the O^{18} water samples. This would make it possible to generate the δN^{15} vs δO^{18} plot which, if denitrification is occurring, will result in the distinctive isotopic signature (a slope of approximately 0.5) (Kendall and Aravena. 2000).

3.4 N^{15} Enrichment

3.4.1 Methods

N^{15} enrichment method for determining the mass transfer coefficient was performed in conjunction with nitrate depletion method in the field tanks. After the tanks were installed, 2.4 mg of 99 atom % N^{15} in the form of potassium nitrate (KNO_3) was added, resulting in approximately 1% enrichment within the tank. A 0.90 m^3/h pump was added to each tank to mix the tanks for several hours initially to ensure the added N^{15} was thoroughly mixed within the tank. This method operates under the same premise as the background N^{15}, O^{18} method. Samples were collected from the tanks used in field study.

Parkin et al. (1985) present the following equation (Equation 3.4) for determining denitrification rates from N^{15} plot results.

$$\Delta t * r_d = \frac{\Delta[NO_3\text{-}] * 0.003665 - \Delta[^{15}NO_3\text{-}]}{R - 0.003665} \qquad \text{Equation 3.4}$$

where: Δt = length of the incubation period (day)
r_d = average denitrification rate over the incubation period ($mg/m^3/day$)
$\Delta[NO_3\text{-}]$ = change in the nitrate pool (mg/m^3)
$\Delta[^{15}NO_3\text{-}]$ = Change in the N^{15} pool (mg/m^3)
R = average ratio of $N^{15}/(N^{15} + N^{14})$ in NO_3- over the period (unitless)

3.4.2 Results and Discussion

The use of N^{15} -nitrate enrichment in the field tanks resulted in the reverse of expected results. As denitrification progresses, the percentage of N^{15} -nitrate remaining should increase as described by the Rayleigh equation (Kendall and Arvena, 2000). In this study, both the N^{14} -nitrate and N^{15} -nitrate decreased similarly. These results can be explained by the lack of circulation in the tanks. This method works best when circulation brings nitrate into and out of the sediment via advective transport, allowing the selective use

of the lighter N^{14} nitrate. In this study, a gradient is formed due to anaerobic conditions within the sediments. This results in nitrate diffusion into the sediment from the water column. As the nitrate enters the sediment, it starts to be denitrified. The N^{14} -nitrate is denitrified first, as it is preferred by the denitrifiers. The N^{15} -nitrate, however, continues to diffuse deeper into the sediment, where it becomes the only nitrate available and is thus denitrified. This results in same rate of decrease for both isotopes within each chamber.

To overcome these problems, the tank should be circulated to the point that advection is the major transport of nitrate into the sediment. This would result in water from the water column being moved through the sediment and would allow for the selectivity by the organisms of the lighter N^{14} nitrate, resulting in the expected increase in the N^{15} nitrate percentage. This would better mimic the natural system of advection of water from the water column in and out of the upper sediments, as seen in flowing surface waters.

3.5 Nitrate Diffusion Calculations

3.5.1 Methods

Nitrate removal determined by diffusion is based on the molecular movement of nitrates into the sediment from the water column and ammonium from the sediment to the aerobic zones, where they can be nitrified and then denitrified as described previously in the literature review. Molecular movement can be described by Fick's law (Equation 3.5), and in an aqueous nonporous system can be stated as:

$$J = -D_d * \text{grad}(C) \qquad \text{Equation 3.5}$$

where: J = mass flux ($mg/m^2/sec$)
D_d = diffusion coefficient (m^2/sec)
grad = grad operator (m^{-1})
C = concentration (mg/m^3)

(Domenico and Schwartz, 1990). The negative sign indicates movement in the direction of decreasing concentration. The grad operator takes into account the three gradients (in the X, Y, and Z directions) of a molecular concentration possible in a three-dimensional environment (Equation 3.6).

$$\text{grad}(C) = dC_x/dx + dC_y/dy + dC_z/dz \qquad \text{Equation 3.6}$$

where: grad = grad operator (m^{-1})
C = concentration (mg/m^3)
dC_x = the change in concentration in the x direction (mg/m^3)
dx = the change in distance in the x direction (m)
dC_y = the change in concentration in the y direction (mg/m^3)
dy = the change in distance in the y direction (m)
dC_z = the change in concentration in the z direction (mg/m^3)
dz = the change in distance in the z direction (depth) (m)

In the case of stream sediments, the grad operator can be simplified (by assuming a homogeneous concentration in the horizontal plain - X and Y directions at each depth, $dC_x/dx = 0$ and $dC_y/dy = 0$ - with concentrations varying only in the Z direction) to a one-dimensional term dependent on the vertical direction aligned with sediment depth, resulting in Equation 3.7.

$$\text{grad}(C) = dC_z/dz \qquad \text{Equation 3.7}$$

where: grad = grad operator (m^{-1})
C = concentration (mg/m^3)
dC_z = the change in concentration in the z direction (mg/m^3)
dz = the change in distance in the z direction (depth) (m)

Substituting Equation 3.7 into Equation 3.5, a simplified one-dimensional equation (Equation 3.8) is derived:

$$J = -D_d * dC_z/dz \qquad \text{Equation 3.8}$$

where: J = mass flux ($mg/m^2/sec$)
D_d = diffusion coefficient (m^2/sec)
dC_z = the change in concentration in the z direction (mg/m^3)
dz = the change in distance in the z direction (depth) (m)

Diffusion coefficients were corrected for temperature using Equation 3.9 presented by Li and Gregory, 1974.

$$D_{T2}/D_{T1} = n_{T1}/n_{T2} \qquad \text{Equation 3.9}$$

where: D_{T1} = diffusion coefficient at T1 (cm^2/sec)
D_{T2} = diffusion coefficient at T2 (cm^2/sec)
n_{T1} = viscosity of water at T1 ($N*sec/m^2$)
n_{T2} =viscosity of water at T2 ($N*sec/m^2$)
T1 = temperature 1 (^oC)
T2 = temperature 2 (^oC)

Equation 3.8 still does not take into account the changes in molecular movement found in sediment pore water due to the tortuosity and reduced liquid volume caused by the presence of solid particles (porosity). Domenico and Schwartz (1990) defined a bulk diffusion coefficient D_d^*, a function of both tortuosity and porosity, that allows Equation 3.6 to be written as what is referred to as Fick's law of diffusion in sediments in one dimension (Equation 3.10).

$$J = -D_d^* * f * dC_z/dz \qquad \text{Equation 3.10}$$

where: J = mass flux ($mg/m^2/sec$)
D_d^* = bulk diffusion coefficient (m^2/sec)
dC_z = the change in concentration in the z direction (mg/m^3)
dz = the change in distance in the z direction (depth) (m)
f = porosity (unitless).

Because D_d^* * f is an unknown, it can be estimated by D_d`, the effective diffusion coefficient (Domenico and Schwartz, 1990). According to Helfferich (1966), $D_d$` falls in the range of:

$$D_d` = (f/2) * D_d \quad \text{to} \quad D_d` = D_d * [f/(2-f)]^2$$

where: D_d` = the effective diffusion coefficient (m^2/sec)
f = porosity (unitless)
D_d = diffusion coefficient in pure liquid (m^2/sec).

Upper and lower values of the effective coefficients of diffusion (D_d`) for nitrate at 8°C and 21°C for this study are found in Table 3.11.

Table 3.11. Upper and lower values for effective coefficients of diffusion (D_d') for NO^3 for 8°C and 21°C and porosity values for different locations.

Location	Porosity (f)	8°C		21°C	
		D_d` $(f/2) * D_d$ ($*10^{-6}cm^2$/sec)	D_d` $D_d * [f/(2-n)]^2$ ($*10^{-6}cm^2$/sec)	D_d` $(f/2) * D_d$ ($*10^{-6}cm^2$/sec)	D_d` $D_d*[f/(2-n)]^2$ ($*10^{-6}cm^2$/sec)
Field Tank 1	0.91	5.57	8.53	7.91	12.1
Field Tank 3	0.95	5.81	10.0	8.26	14.2
Field Tank 3	0.91	5.57	8.53	7.91	12.1

By substituting the effective diffusion coefficient into Equation 3.8, a relatively easy one-dimensional equation (Equation 3.11) is created to determine diffusion-related movement of molecules into and out of the sediments.

$$J = -D_d` * dC/dz \qquad \text{Equation 3.11}$$

where: J = mass flux (mg/m^2/sec)
D_d` = effective diffusion coefficient (m^2/sec)
dC = the change in concentration (mg/m^3)
dz = the change in depth (m)

Porosity was determined using undisturbed sediment cores. The cores were weighed saturated and after oven-drying. The difference in the weights is the weight of the water

(g/core volume) present during saturation. One cubic centimeter of water weighs one gram; thus, the weight of water removed during drying in grams is equal numerically to the volume of water removed and thus the volume of the pore space in cubic centimeters (Equation 3.12).

$$A - B = C = V_p \qquad \text{Equation 3.12}$$

where: A = weight of the saturated core (g)
B = weight of the oven dried core (g)
C = weight of the water filling the pore spaces in the core (g)
V_p = Volume of water filled pore spaces in the core (cm^3)

The porosity is determined using Equation 3.13 (Hillel, 1982):

$$f = V_p/V_t \qquad \text{Equation 3.13}$$

where: f = porosity (unitless)
V_p = volume of the cores pore space (cm^3)
V_t = total core volume (cm^3).

In the case of the study using the undisturbed cores in the lab, porosity for each tank was determined as an average of three undisturbed cores per field tank location.

Nitrate and ammonium concentrations within the sediment and water column were measured at different depths using the sediment pore water sampler described in Appendix C - Nitrate, Ammonium, and Phosphorous Distribution in Sediment Pore Water and Water Column. The concentration gradients (dC/dz) were determined using these concentration profiles. A gradient was determined for each 1 cm change in depth using Equation 3.14.

$$dC/dz = (C_i - C_{i+1})/(z_i - z_{i+1}) \qquad \text{Equation 3.14}$$

where: dC/dz = concentration gradient over 1 cm interval (mg/m^2)
C_i = concentration at upper interface of 1 cm interval (mg/m^3)
C_{i+1} = concentration at lower interface of 1 cm interval (mg/m^3)
z_i = depth at upper interface of 1 cm interval (m)
z_{i+1} = depth at lower interface of 1 cm interval (m)

The highest concentration gradient per profile was used as that most representative of the actual gradient present at each profile (Birgand, 2000). A relationship was developed between the water column nitrate concentrations and its respective concentration gradients by plotting water column nitrate concentration vs. the highest calculated nitrate concentration gradient within the sediment, dC/dz (Figure 3.21).

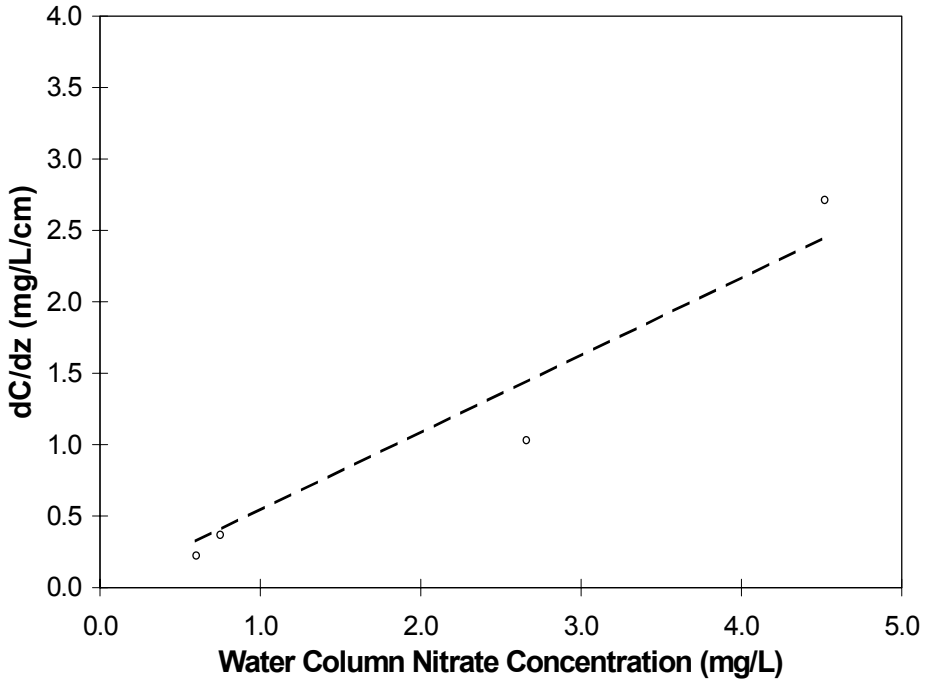

Figure 3.21. Relationship of water column nitrate concentration to sediment nitrate concentration gradient (dC/dz=0.5423*C, R^2=0.9358. C=water column nitrate concentration with dz=1cm, dC/dz=54.23*C for dz=1m).

Using Equation 3.11 developed earlier, the rate of diffusion of nitrate into the sediments can be calculated. From the decay curve generated by the diffusion calculations, a mass transfer coefficient (ρ) can be calculated using Equation 4.12. An example of these calculations can be found in Appendix H.

3.5.2 Results and Discussion

Analysis of the diffusion-calculated mass transfer coefficients was based on the porosity values of each core (Table 3.12), which resulted in no significant differences between the cores from the three locations (R^2=0.05 and an MSE=0.001). The differences between the mass transfer coefficients are due to the effective coefficient of diffusion (D_d'), which is based on the porosity values, which vary little in this study (Table 3.12). The difference between the lower mass transfer coefficient values obtained from Tanks 1 through 3 and the value obtained from the other six tanks is due to the use of a lower concentration gradient (Figure 3.21). This method does not take into account the nitrification-denitrification coupling that may occur. Again, pH, dissolved oxygen, temperature, and ammonium concentration have a great effect on the processes involved, making it difficult to predict with a model as simple as proposed here.

Table 3.12. Diffusion-calculated mass transfer coefficients based on the undisturbed cores in the lab.

Location	Core	Porosity	Mass Transfer Coefficient (m/day)	
			8°C	21°C
West	Tank 1	0.90 A	0.001	0.002
Central	Tank 2	0.93 A	0.002	0.002
East	Tank 3	0.89 A	0.002	0.002
West	Tank 4	0.91 A	0.003	0.005
Central	Tank 5	0.98 A	0.004	0.006
East	Tank 6	0.95 A	0.004	0.005
West	Tank 7	0.92 A	0.003	0.005
Central	Tank 8	0.99 A	0.004	0.006
East	Tank 9	0.88 A	0.003	0.004

This method would be improved by developing a better way of determining the sediment nitrate gradients (dC/dz), and by using the sediment ammonium profile data to determine the flux of ammonium to the nitrifying zone. This ammonium could then be added to the overall nitrate pool. (This was not done in this study due to the abnormally high ammonium levels, which caused a uniform ammonium concentration throughout the sediment profile.)

3.6 Mass Balance

3.6.1 Methods

The mass balance method consisted of summing all nitrate inputs to the system (upstream inflow, field inflows, rainfall/throughfall, and litterfall) over the flow periods and comparing inputs to outflow nitrate load. Here the total outflow nitrate load was subtracted from the sum of nitrate inflows for the two flow periods (2001 and 2002). Outflow was subtracted from inflows because the sum of the inflows was expected to be larger;

denitrification, if occurring, would decrease total nitrates leaving the system. The decrease in total nitrates between inflows and outflow assumed equal to denitrification.

3.6.2 Results and Discussion

The mass balance method of determining denitrification is based on the summation of all the nitrate inputs to the system and subtracting the sum of all the nitrate outputs of the system, the difference being the nitrate lost/gained due to denitrification/nitrification. The mass balance performed on the two years of this study is considered accurate to within the precision of the sampling method and analytical equipment used, as the chloride mass balance closed within 2.5% for 2001 and 5.5% for 2002 (see Section 2.11, Mass Balance). Chloride is considered a conservative tracer. The fact that it balaces indicates that inflows and outflows to the system were accurately determined.

For 2001, total inputs of nitrate to the canal study section were 215 kg and outputs were 218 kg, a gain of 2.7 kg over the 85-day flow period. For 2002, total inputs to the study section were 774 kg and outputs were 858 kg, a gain of 83.6 kg over the 81-day flow period. This translates to an average gain of 55.7 mg/m^2/day of nitrate during the 2001 flow period and an average gain of 181 mg/m^2/day of nitrate during the 2002 flow period. For both years, 2001 and 2002, denitrification rates cannot be determined, as there was a net increase in nitrate occurring based on the mass balance.

This method has several drawbacks. First, it cannot account for the in-stream transformations within the canal. This means only a net denitrification or nitrification can be determined. The second problem is that in sampling, one sample is used to represent the average concentration over a period of time. This may lead to an under- or over-estimation of the nitrate concentration for the time period. The third problem is that the method attempts to

estimate a small number by subtracting two large numbers, each of which are composed of the sums of several calculated values, which are each subject to error. In forested watersheds, denitrification has been found on average to be very small (see Section 3.2, Denitrification). An example of the errors associated with these measurements is the time-based water quality sampling. One sample is used to represent a time period of continually changing concentrations. This results in the possibility that, even if all measurements are done as precisely as possible, the sum of the errors might be larger than the difference that is being determined. In cases where denitrification rates are larger, as in agricultural drainage systems (Birgand, 2000), it may be possible to use a mass balance approach to more accurately estimate the denitrification rate within waterways.

Improvements to this method are difficult. They include increased water quality sampling over time of all inflows and outflows to improve estimation of the nitrate loads. This method as it is normally conducted is very costly in terms of time and money. To increase the water quality sampling for all the inputs and outputs would be cost-prohibitive.

3.7 Modeling

3.7.1 Methods

Models can be used to simulate the effects different environmental conditions (temperature, rainfall, nutrient uptake and transformations, etc.), as well as human activities (harvesting, fertilization, drainage, etc.), have on natural systems. The cost is fraction that of instrumenting and monitoring the many different scenarios that may occur. Models can also be used to determine the effect that one particular aspect (such as nutrient transformations like nitrification, denitrification, etc.) has on the system. In this study, denitrification will be examined by comparing the modeled system output with denitrification excluded from the

model to the measured system output. The difference should be an estimation of the denitrification occurring within the system.

The hydrology and nitrate components of the study canal section, from S0 to S3 (Figure 2.1), were modeled using the DUFLOW model (a one-dimensional, unsteady state, flow and water quality model for open channel systems developed in the Netherlands (Duflow, 1992)) for the years 2001 and 2002. The study canal was broken into smaller sections using a system of nodes and sections (Figure 3.22). Node 1 represents the upstream inflow (the flume structure) to the canal section, Nodes 2 through 18 represent points of inflow from each of the 18 fields, Node 19 represents the outlet (the weir structure), and node 20 represents the downstream boundary condition. Sections 1 through 18 are 105.5 meters long each. The distance between node 19 and 20 (Section 19) is 200 meters to give a long distance between the outlet and the downstream boundary condition. The inputs to the model were the measured inputs of rainfall, upstream inflow, and groundwater as measured in the previous sections. The model was calibrated using the hydrological portion of the model, comparing the modeled results at the outlet (node 19) to the total of the measured inflows. The total of the measured inflows was used for calibration, as the model only routes the inflows (which are measured for each inflow, as was done with the mass balance) through the network, resulting in what should be a close match between the cumulative modeled outflow and combined total inflows. Calibration consisted of varying the Preismann coefficient Theta for flow (0.67) and quality (1.00) and the Apha correction for velocity distribution (1.00). The input files were delineated with a one-hour time step. The model was also run on a one-hour time step to reduce instability in the model. Model outputs were used after the simulations were started to allow the results to “settle” from their initial conditions.

After hydrologic calibration, the nutrient portion of the model was run, neglecting any transformations of nitrate through biological or chemical processes.

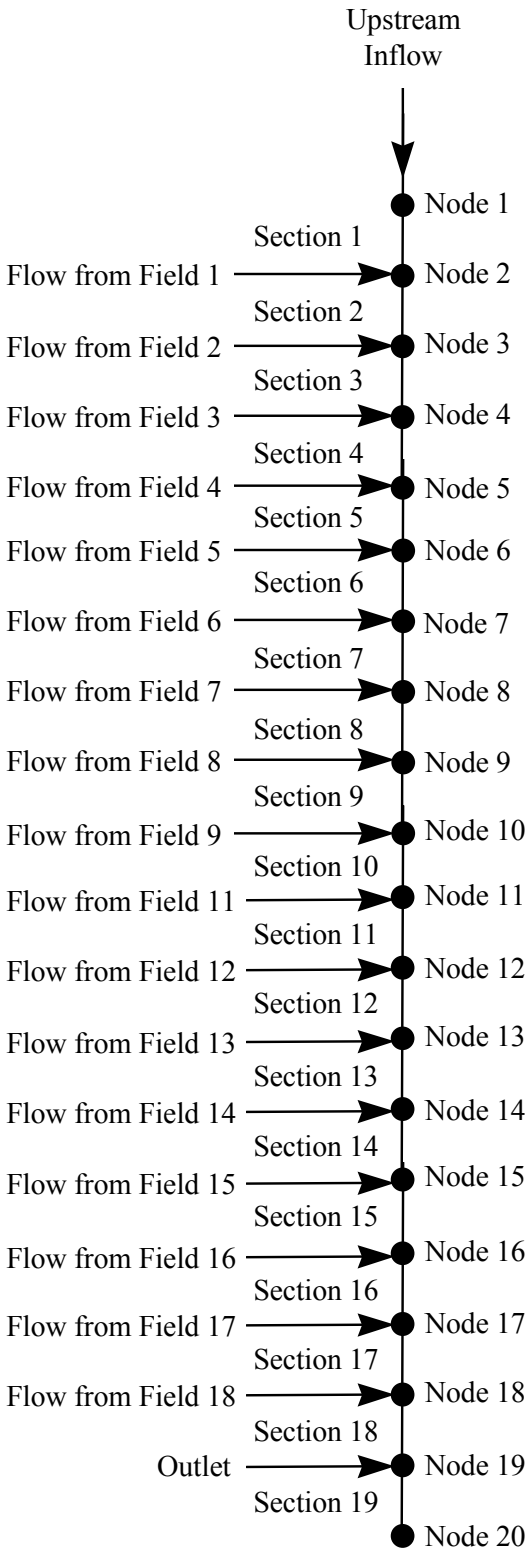

Figure 3.22. Network overlay of the canal study section.

3.7.2 Results and Discussion

Calibration of the model resulted in an acceptable comparison between the modeled outflows and measured inflows for the two flow periods (2001 and 2002) (Figures 3.23 and 3.24). Both hourly and cumulative flows matched well for both years. The small variations are due to the calculations conducted by the routing portion of the program as well as rounding errors.

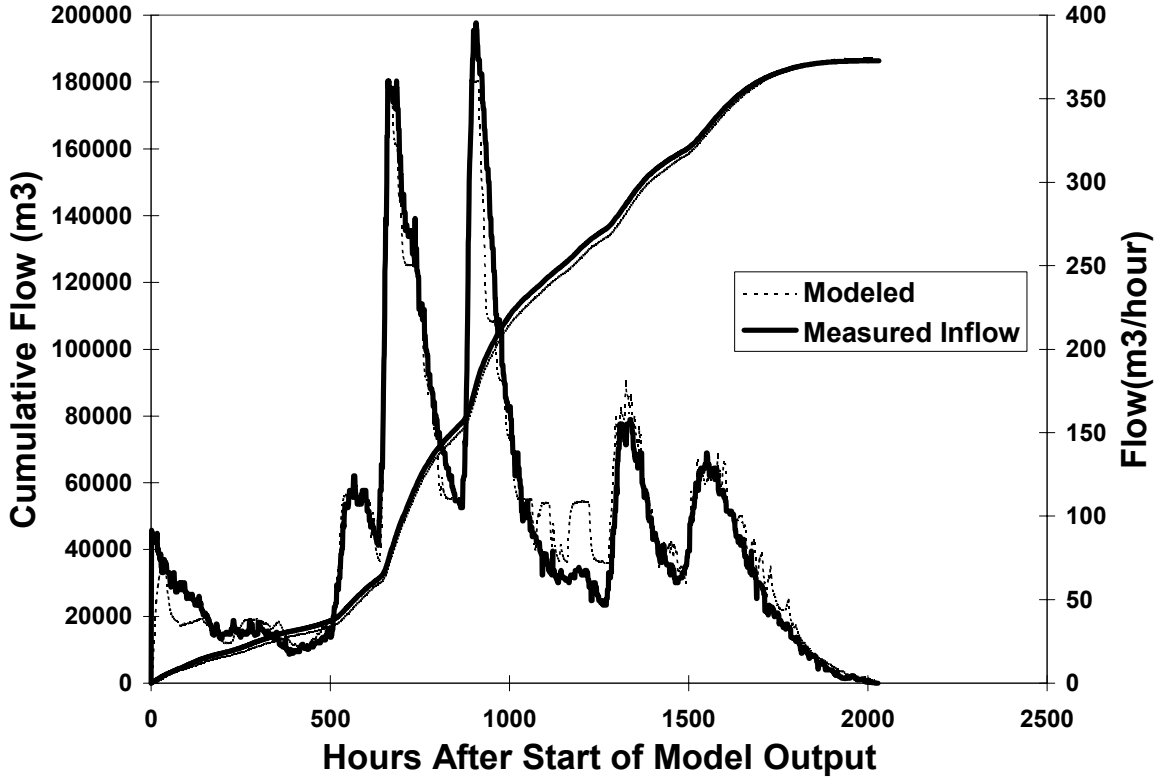

Figure 3.23. DUFLOW calibration using modeled output vs. measured inflow for the year 2001.

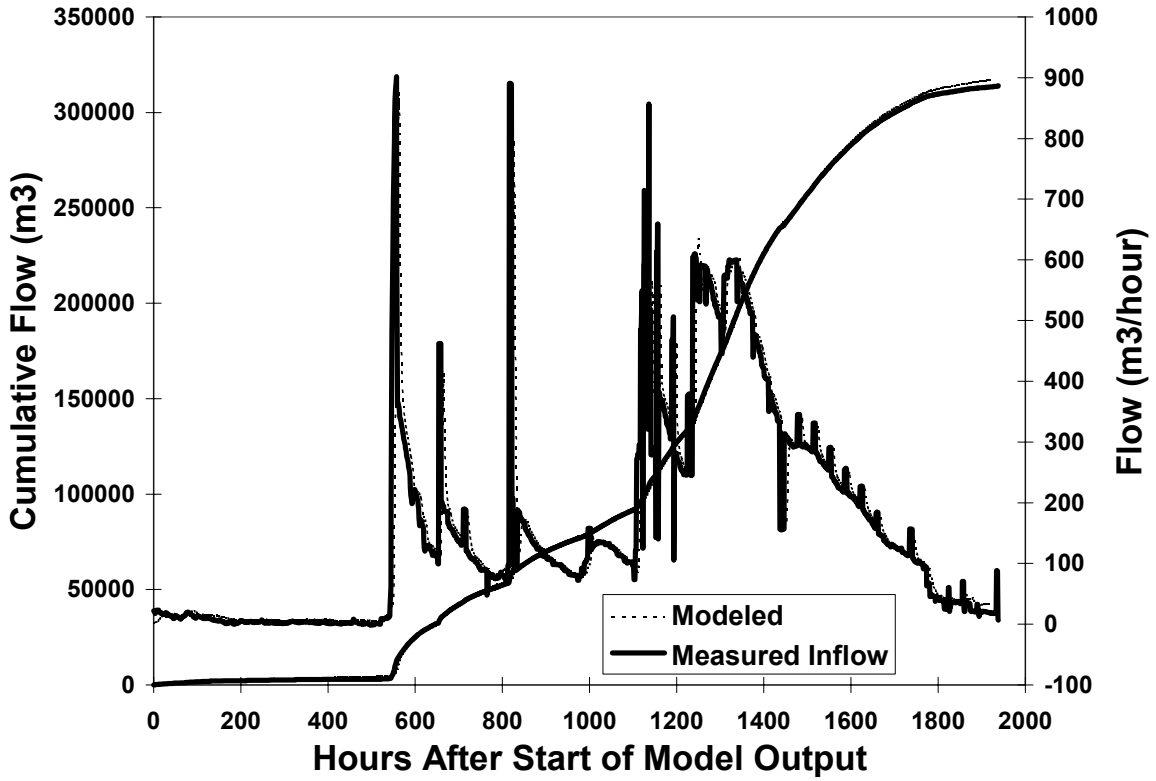

Figure 3.24. DUFLOW calibration using modeled output vs. measured inflow for the year 2002.

The comparisons of the measured and modeled nitrate outflow for the two flow periods, 2001 and 2002 (Figures 3.25 and 3.27), are similar to the results found in the mass balance portion of this study (Section 2.11, Mass Balance). The modeled outflows are based on the measured inflows, resulting in the same problems as described in the mass balance section. One problem is the possibility of missing changes in the nitrate contributions to the canal as rainfall events leach larger amounts of nitrates from the adjacent fields, due to the long periods (weekly) between well sampling. Another problem is the possible error in calculating nitrate loads at the inlet or outlet due to the different sampling intervals, where less frequent sampling at one location may not capture the concentration variation as well as

it was defined by more frequent sampling at the other location (see Section 2.11, Mass Balance). These errors add up during the flow period, resulting in a potential for missing small differences in the two large values of inflows and outflows from the system. This can be seen in the higher measured nitrate load at the outlet as compared to the modeled nitrate load. This indicates a gain in nitrate rather than the loss expected from denitrification (see Section 3.2, Denitrification).

In the mass balance study, an overall average denitrification rate was sought. In the modeling study, the overall cumulative nitrate loads (measured and modeled) were divided into sections, each for differing time periods (Figure 3.26 and 3.28). The idea is to try to eliminate the errors in the determination of nitrate from the fields during and following rainfall events by looking at smaller time periods of "base flow" during each of the flow periods (2001 and 2002). Three suitable periods occurred during the 2001 flow period (Figure 3.26), and four periods occurred during the 2002 flow period (Figure 3.28). Table 3.13 shows the calculated removal rates, water column concentrations, and mass transfer coefficients based on the seven periods of base flow. The removal rate is the slope of the line representing the difference of the cumulative modeled and measured nitrate load over time (here the difference is the modeled load minus the measured load due to the assumption that the modeled load, with no denitrification, will be a larger value than the measured load with denitrification occurring). The water column concentration is the flow-weighted average nitrate concentration for the period of interest, and the mass transfer coefficient (ρ) was calculated using Kelly's equation (Equation 1) (Kelly et al., 1987). Table 3.14 shows the calculated mass transfer coefficients converted to $8^{o}C$ and $21^{o}C$ using Dawson and Murphy's relationship (Dawson and Murphy, 1972).

Table 3.13. Water column temperature, removal rate, water column concentration, and mass transfer coefficient for the periods of base flow during the 2001 and 2002 flow periods.

	Water Column Temperature (^oC)	Removal Rate ($mg/m^2/day$)	Water Column Concentration[1] (mg/L)	Mass Transfer Coefficient (ρ)[2] (m/day)
2001				
Period 1	10.5	168	1.01	0.17
Period 2	10.6	129	0.99	0.13
Period 3	13.8	61.5	0.66	0.09
2002				
Period 1	6.2	64.8	1.53	0.04
Period 2	11.0	815	2.56	0.32
Period 3	13.0	243	1.77	0.13
Period 4	18.2	563	1.39	0.40
Average		292 $\pm$ 287	1.42 $\pm$ 0.63	0.18 $\pm$ 0.13

[1] Water column concentrations are volume weighted averages for the period.

[2] The mass transfer coefficient was calculated using Kelly's equation (ρ = RR/[C], Equation 4.1).

Table 3.14. Mass transfer coefficients converted to 8^oC and 21^oC.

	Mass Transfer Coefficient (ρ)[1] (m/day)	
	8^oC	21^oC
2001		
Period 1	0.13	0.52
Period 2	0.10	0.39
Period 3	0.05	0.19
2002		
Period 1	0.05	0.19
Period 2	0.23	0.89
Period 3	0.08	0.30
Period 4	0.14	0.54
Average	0.11 $\pm$ 0.06	0.43 $\pm$ 0.25

[1] The mass transfer coefficients were converted to 8^oC and 21^oC using Dawson and Murphy's relationship (Equation 4.28).

The calculated mass transfer coefficient ranged from 0.05 m/day to 0.23 m/day with an average of 0.11 $\pm$ 0.06 m/day at 8^{o}C, and ranged from 0.19 m/day to 0.89 m/day with an average of 0.43 $\pm$ 0.25 m/day at 21^{o}C. The relatively large standard deviations (0.06 m/day at 8^{o}C and 0.25 m/d at 21^{o}C) are due to differences in nitrate concentration and the difficulty in accurately estimating nitrate loads in flowing systems when there are many inflows. These values, though, are within the range of mass transfer coefficients reported in Table 1.7 (ranging from 0.0045 to 0.483) of the Denitrification Section (Section 1.4.3.6) for streams in forested watersheds.

The large increases in the differences in the nitrate loads between the measured and modeled outflows (Figures 3.26 and 3.28) are due to the measured cumulative nitrate loads increasing faster than the modeled loads. This is due to the nitrate concentrations from the field used in the modeling effort being based on weekly well sampling, one sample representing an average nitrate concentration for the week. This sampling scheme allows for variation of groundwater nitrate concentrations due to rainfall event flushes (as described in Section 2.5, Upstream Canal Inflow) to be missed. This results in an under- or overestimation of nitrates entering the canal from the fields (assumed to be an underestimation in this study).

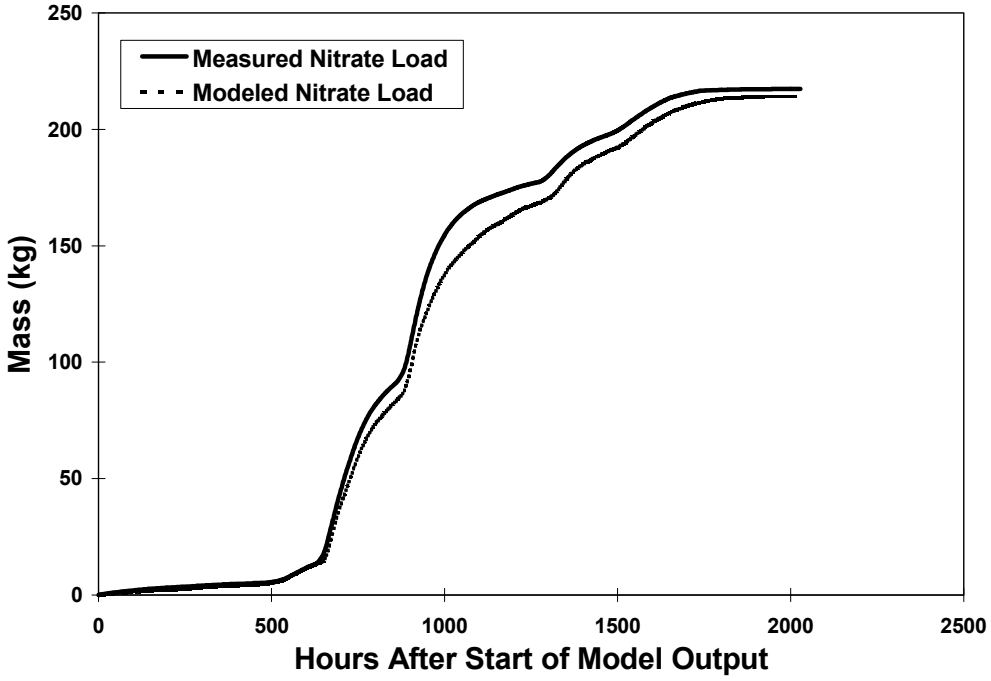

Figure 3.25. Modeled and measured nitrate loads for flow period 2001.

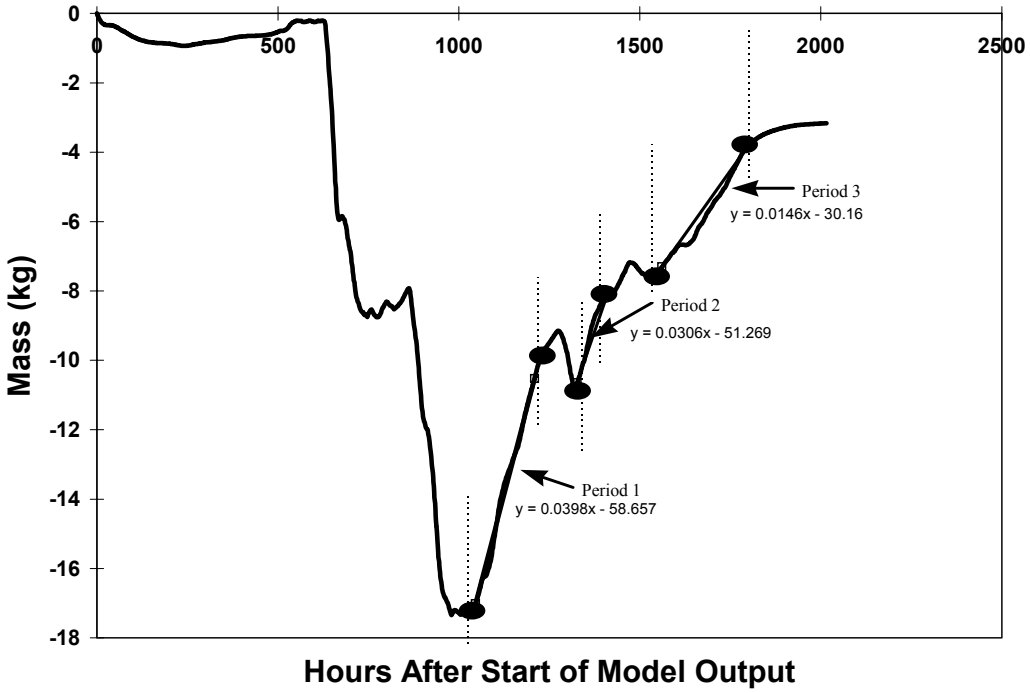

Figure 3.26. Mass difference between modeled and measured nitrate loads (modeled - measured) for flow period 2001.

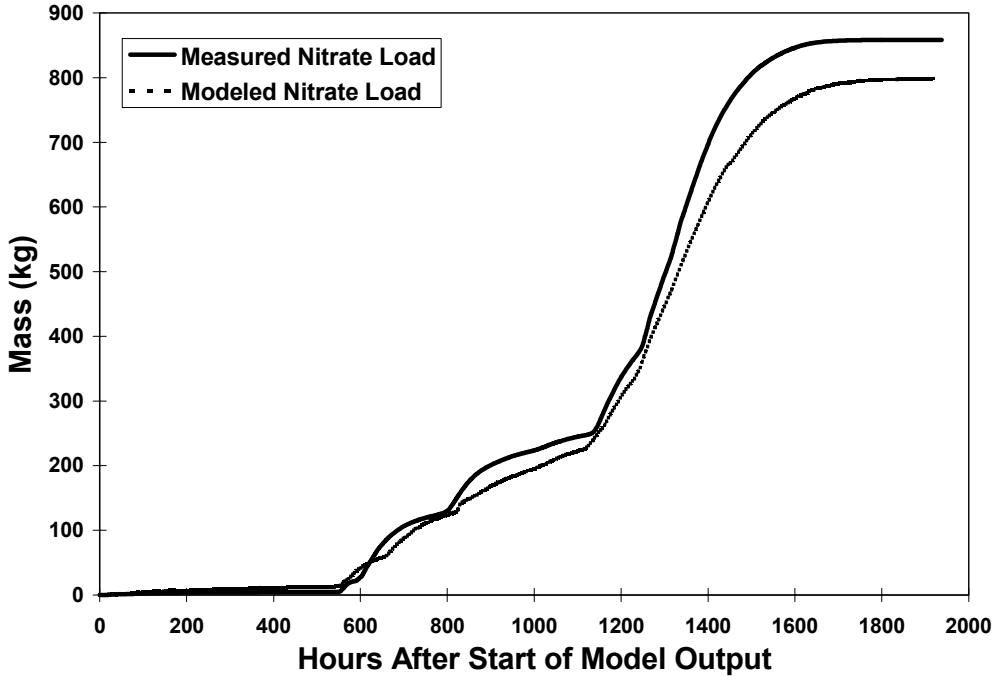

Figure 3.27. Modeled and measured nitrate loads for flow period 2002.

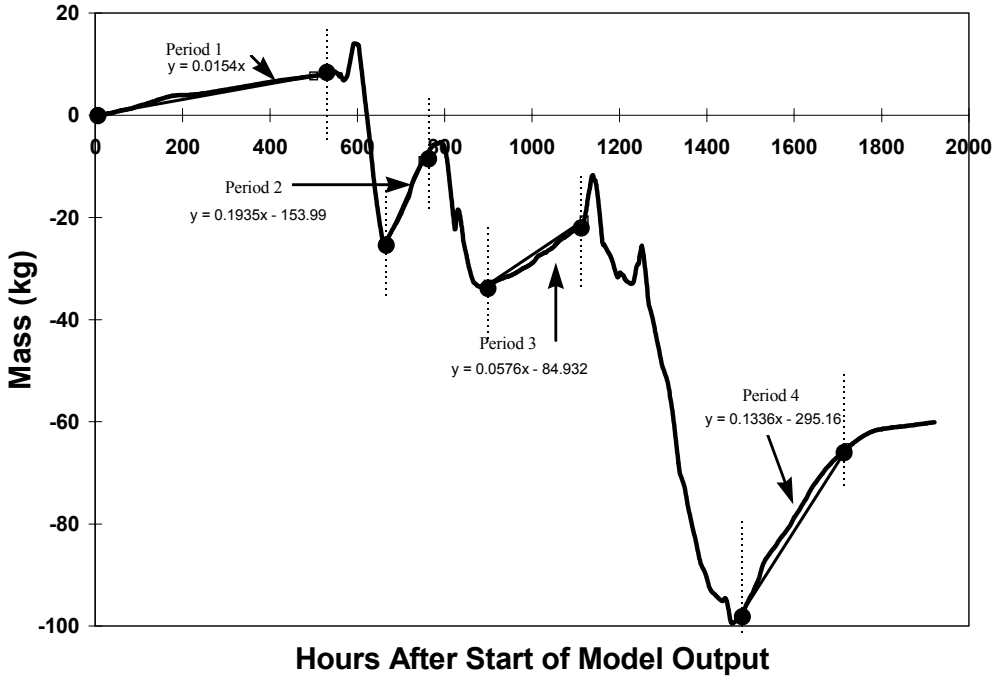

Figure 3.28. Mass difference between modeled and measured nitrate loads (modeled - measured) for flow period 2002.

Improvements to this method are the same as with the mass balance method: an increase in water quality sampling over time of all inflows and outflows to improve estimation of nitrate loads.

3.8 Comparison of Nitrate Depletion in the Field and Lab, Diffusion Calculation, and Modeling Methods

The average mass transfer coefficients for these four methods can be found in Table 3.15. The mass transfer coefficients calculated by the diffusion, field tanks, undisturbed cores of the lab, and modeling methods were compared (comparisons were made using 8^{o}C data as the field data, and modeling results had all been normalized to 8^{o}C). Comparison of the field to both the lab study and the modeling study is valid, as the lab study showed that circulation did not cause a significant difference between the mass transfer coefficients of the circulated and uncirculated treatments.

Table 3.15. Average mass transfer coefficients for each treatment for Methods 1, 2, 5, and 7.

Study	Treatment	Mass Transfer Coefficient (m/day)	
		Temperature	
		8^{o}C	21^{o}C
Method 1-Field	Uncirculated	0.016	0.064
Method 2-Lab	Uncirculated	0.004	0.049
	Circulated	0.006	0.044
	Circulated with Nitrification Inhibitor	0.012	0.068
Method 5-Diffusion	Diffusion-Calculated	0.003	0.004
Method 7-Modeling	Mass Balance	0.110	0.430

The average diffusion-calculated mass transfer coefficient was compared to the average field-calculated mass transfer coefficient and to the modeled mass transfer

coefficient. The difference between the diffusion-calculated and the field tank mass transfer coefficients was significant, as was the difference between the diffusion-calculated and modeled mass transfer coefficients. This indicates that the system is too complex to try to model with the simple diffusion calculations performed here.

The differences between the diffusion-calculated and lab study mass transfer coefficients were mixed. The difference between the uncirculated treatments and their corresponding diffusion-calculated mass transfer coefficients was statistically significant ($\propto = 0.05$). The difference between the circulated tanks with the nitrification inhibitor and their corresponding diffusion-calculated mass transfer coefficients was also statistically significant. However, the difference between the circulated tanks without the nitrification inhibitor and their corresponding diffusion-calculated mass transfer coefficients was not statistically significant. This is due to nitrification being ignored in the diffusion calculations. Again, this indicated the complexity of the system and the difficulty in trying to model it with a simple diffusion calculation.

The differences between lab study and field study mass transfer coefficients showed a stronger statistical difference between the field study and the uncirculated and circulated treatments ($P<0.0001$ for both comparisons) than between the field study and the circulated with nitrification inhibitor treatment ($P=0.0015$) of the lab study. The stronger statistical difference between the field study and the uncirculated and circulated treatments of the lab study can be explained by the lower pH of the field study (pH of 4.0 and 3.5 for the field runs vs. pH values greater than 5 in the lab studies). The lower pH acted as a nitrification inhibitor, resulting in only a minor-to-negligible amount of nitrification occurring in the field study. This resulted in higher mass transfer coefficients in the field.

The significant difference between the field study and the circulated with nitrification inhibitor treatment of the lab study is mostly due to the low values of the mass transfer coefficients in the cores of the lab study from the east and central locations (0.007 m/day and 0.006 m/day respectively) as compared to the western location (0.023 m/day). One would expect the mass transfer coefficients to be similar between the same location of the two studies or slightly lower for the field study due to the inhibitive effect on denitrification of the lower pHs seen in the field. This trend can be seen in the west location, where the lab study mass transfer coefficient (0.023 m/day) was higher than that of the field study (0.014 m/day). Both the east and the central location cores for all treatments of the lab study exhibited lower average mass transfer coefficients than the west cores at 8^{o}C (Table 3.8). This may be due to differences in forest cover in the surrounding fields for these locations. The east and central locations are flanked by young planted pine plantations, while the west location is flanked by an undisturbed natural hardwood stand (Figure 2.2). The effects of the differences in litter input on nitrification and denitrification may only become expressed when the system is isolated, as in the lab study. There is also a slight rise in the middle portion of the canal that acts as a dam during small flows during dry periods. This causes the western portion to remain wetter than the rest of the study canal. Differences in wetness and surrounding forest cover may lead to variability in denitrifier and nitrifier species present in the sediment at the three locations. These populations may have different tolerances for colder temperatures, resulting in lower nitrification and denitrification rates at the east and central locations in the lab study. This effect may not have been seen in the field, as the temperature slowly dropped over time, giving the populations time to acclimate, compared to the lab study, where the temperature was brought to 8^{o}C rapidly and then held constant.

The modeled mass transfer coefficient was significantly different from both of the nitrate depletion methods (P=0.0005). The difference in the mass transfer coefficients reflects the differences in the methods. The modeling method determined the mass transfer coefficient by computing the difference in the sum of the inputs and outputs, with the difference being assumed to be due to denitrification. This method introduces potential error with each input measured. The two nitrate depletion methods, on the other hand, directly measure the loss of nitrate from the water column, which has fewer potential errors.

3.9 Summary and Conclusions

The two nitrate depletion methods gave good representations of the mass transfer coefficient under differing conditions (moving or stagnant water, with or without nitrification inhibitors, at different temperatures) for surface waters (Table 3.15). They both resulted in direct measures of the nitrate removal rate and mass transfer coefficients.

The nitrate depletion in in-stream tanks method, conducted in situ, results in a closer estimate of the actual mass transfer coefficient (0.016 m/day at 8^{o}C and 0.064 m/day at 21^{o}C). Based on these mass transfer coefficients, the calculated overall nitrate removed during the two flow periods was 6.7 kg during the 2001 flow period and 19.8 kg during the 2002 flow period. The difference is due to the higher water column temperatures and nitrate concentrations during the 2002 flow period as compared to the 2001 flow period, making measurement in the field expose the processes of interest (nitrification and denitrification) to the environmental conditions found in the field, thus mimicking the natural system. In situ measurement is one of the easiest and cheapest methods employed to determine the mass transfer coefficient in this study. The chambers are inexpensive to construct and easily placed in the canal. Sampling and sample analysis are also simple and inexpensive.

The nitrate depletion in undisturbed cores method, a more controlled method than the previous method, allows for more information (such as the effects of temperature, depth, concentration, pH, etc.) to be gathered. The controlled environment also allowed for an accurate determination of potential mineralization and nitrification rates within the system. However, a lab-controlled environment does not mimic natural conditions and thus can cause changes in the processes of interest (nitrification and denitrification). The result may be over- or under-estimates of the overall mass transfer coefficient. Factors such as pH, dissolved oxygen content, dissolved organic carbon, and ammonium concentrations can easily vary between the field and the lab. In spite of this, an accurate representation of the mass transfer coefficient (0.012 m/day at 8^{o}C and 0.068 m/day at 21^{o}C) can be determined through a lab study if care is taken to replicate environmental conditions in the field as closely as possible. This method is simple, like the previous method, but is also less expensive. Where in the previous method one must travel to the study site to sample the chambers, this method was located near the lab, so samples could be taken without traveling to the field, thus making it more economical and convenient. Sampling and sample analysis are the same as in the previous method.

The background N^{15} and O^{18} method can be used to indicate the presence of denitrification in surface waters of both small and large watersheds. Samples are very easy and inexpensive to take using this method. This method has the disadvantages of being very labor-intensive, complicated, and expensive in terms of laboratory materials needed and hazardous waste produced during sample preparation and analysis. Another disadvantage is that it the method is not easily designed to allow for the calculation of a mass transfer coefficient from the data.

The N^{15} enrichment method can be used if the tanks are circulated. This method is simple and inexpensive to implement and sample (the same as the in situ method), as well as being able to easily calculate a mass transfer coefficient from the data. This method has some of the same major drawbacks as the background N^{15}, O^{18} method, in that it is very labor-intensive, complicated, and expensive in terms of laboratory materials needed and hazardous waste produced during sample preparation and analysis.

The nitrate diffusion calculation method as conducted during this study was initially fairly expensive in terms of having the sediment pore water samplers constructed, but it was very inexpensive to implement the method and sample and analyze the samples. This method, however, is not an accurate method for determining nitrate removal, due to the difficulty in accurately determining the nitrate gradient (dC/dz) in the sediment. The lack of an accurate way to account for nitrification also inhibits its use. This method underestimated the mass transfer coefficient at 21^{o}C as compared to measured rates from the two nitrate depletion methods (Table 3.15).

The mass balance method is not precise enough to try to determine the small difference denitrification will generate between the sum of the inputs and the sum of the outputs in a forested watershed. Each input and output must be measured using a sampling method that allows for accurate determination of the total mass or volume entering or leaving the system, resulting in a very expensive study. Each error in estimations of the inputs and outputs is additive, resulting in the possibility that the measuring errors are larger than the actual denitrification rate that is being determined. In this study, there was an overall gain in nitrate over the flow period during both seasons. With this method, one cannot determine

whether this is due to the addition of the measurement errors or some other factor not identified in the study.

The modeling method used in this study has the same drawbacks as the mass balance method, because the model uses the same data that were used in the mass balance method, although it is not limited to the single total mass calculated over the experiment. The breaking down of flow seasons into separate flow sections did allow for the estimation of an average mass transfer coefficient for the two flow periods (0.11 m/day at 8^{o}C and 0.43 m/day at 21^{o}C). These estimates, though, are higher than the two nitrate depletion method estimates of the mass transfer coefficient. The higher potential for introduced error associated with the modeling method as compared to the two nitrate depletion methods, with their fewer potential errors, makes the nitrate depletion methods a more accurate method for determining mass transfer coefficients in forested streams, where the effect of denitrification is very small in comparison to the total sum of the nitrate inflows and outflows.

Overall, the in situ field tank method and the undisturbed core method are the most accurate and inexpensive methods for determining mass transfer coefficients in flowing surface waters. The combination of the two will not only give a backup check of the mass transfer coefficients but will also help researchers understand how the different environmental factors are influencing them. The two N^{15}, O^{18} methods are too expensive, complicated, and labor-intensive to be used on a regular basis. The diffusion method, though not cost-prohibitive, is not accurate enough to be considered usable for determining mass transfer coefficients. The mass balance and modeling methods are too coarse to determine the small denitrification rates found in forested watershed streams and drainage networks, as well as being far too costly to implement in more than a very few locations.

References

Birgand, F. Quantification and Modeling of In-Stream Processes in Agricultural Canals in the Lower Coastal Plain. Dissertation, 469 pp, North Carolina State University, Raleigh, 2000.

Chang, C.C.Y., J. Langston, M. Riggs, D.H. Campbell, S.R. Silva, and C. Kendall. 1999. A method for nitrate collection for ?15N and ?18O analysis from waters with low nitrate concentrations. Can J. Fish Aquat. Sci. 56: 1856-1864.

Dawson, R.N. and K.L. Murphy. 1972. The temperature dependency of biological denitrification. Wat. Res. 6: 71-83.

Domenico, P.A. and F.W. Schwartz. 1990. Physical and Chemical Hydrogeology. 2nd Ed. John Wiley & Sons, Inc., New York.

DUFLOW (1992), A Micro-Computer Package for the Simulation of One-Dimensional Unsteady Flow and Water Quality in Open Channel Systems, Manual for DUFLOW version 2.00, ICIM, Rijswijk, Netherlands.

Farrell, R.E., P.J. Sandercock, D.J. Pennock, and C.V. Kessel. 1996. Landscape-scale variations in leaching nitrate: relationship to denitrification and natural nitrogen-15 abundance. Soil Sci. Soc. Am. J. 60: 1410-1415.

Helfferich, F. 1966. In: Marinsky, J.A., ed. Ion Exchange: A Series of Advances. Marcel Dekker, New York, pp 65-100.

Hillel, D. 1982. Introduction to Soil Physics. Academic Press, San Diego.

Kelly, C.A. J.W.M. Rudd, R.H. Hesslein, D.W. Schindler, P.J. Dillon, C.T. Driscoll, S.A. Gherini, and R.E. Hecky. 1987. Prediction of biological acid neutralization in acid-sensitive lakes. Biogeochem. 3: 129-140.

Kendall, C. and R. Aravena. 2000. Nitrate Isotopes in Groundwater Systems. In: Cook, P. and A.L. Herezeg, eds. Environmental Tracers in Subsurface Hydrology. Kluwer Academic Pub, pp 261-297.

Li, Y.H., and S. Gregory. 1974. Diffusion of ions in sea water and in deep sea sediments. Geochimica et Cosmochimica Acta. 38: 703-714.

Parkin, T.B., A.J. Sexstone, and J.M. Tiedje. 1985. Comparison of field denitrification rates determined by acetylene-based soil core and Nitrogen-15 Methods. Soil Sci. Soc. Am. J. 49: 94-99.

Standard Methods for the Examination of water and Waste Water. 17th ed. 1989. American Public Health Association, American Waterworks Association, and Water Pollution Control Federation.

Tisdale, S.L, W.L. Nelson, J.D. Beaton, and J.L. Havlin. 1993. Soil Fertility and Fertilizers. 5th ed. Macmillan Publishing Company, New York.

Waring, S.A., and J.W. Gilliam. 1983. The effect of acidity on nitrate reduction and denitrification in lower coastal plain soils. Soil Sci. Soc. Am. J. 47: 246-251.

Chapter 4

Development of Mathematical Relationship to Describe Nitrate Removal from Surface Waters

4.1 Mass Transfer Coefficient Concept

In the past, nitrate removal rates were determined by a mass balance method, the initial mass of nitrate present per unit area minus the final mass of nitrate per unit area over a given time period, and reported in units of mass/unit area/time (e.g., $mg/m^2/day$) at a specified nitrate concentration (e.g., Duff et al., 1984; Cooke and Cooper, et al., 1988; Seitzinger, 1994). This leads to the problem of misrepresenting the nitrate removal rate. The nitrate removal rate is determined by nitrate concentration as well as other factors (denitrifier population, temperature, pH, etc.). As the nitrate concentration decreases, nitrate removal slows due to the decreasing substrate (nitrate) for the denitrifiers, resulting in the typical decay curve representing nitrate removal in a closed system. Kelly et al. (1987) proposed a way to express this varying nitrate removal rate using what Kelly termed a mass transfer coefficient (ρ). The mass transfer coefficient represents the straight-line relationship of the nitrate removal rate to the water column nitrate concentration. The result is a very useful term that is constant over the entire range of water column nitrate concentrations, allowing for easy comparisons of denitrification between different studies. This proposal used a term called a mass transfer coefficient (ρ) that is determined by Equation 4.1.

$$\rho = RR/[C] \qquad \text{Equation 4.1}$$

where: ρ = mass transfer coefficient (m/day)
RR = measured nitrate removal rate ($mg/m^2/day$)
[C] = measured water column nitrate concentration (mg/m^3)

4.2 Development of a New Mass Transfer Coefficient Term

Kelly's approach works fairly well. The lack of a depth term, though, can cause this method to be somewhat study-specific. An alternative approach to determining Kelly's mass transfer coefficient proposed by Birgand (2000, personal communication) allows the depth of the water column to be incorporated into the equation, making it applicable to differing conditions. Birgands' method is based on a derivation using a mass balance approach (initial mass minus final mass equal to the removal) along with Kelly's mass transfer coefficient equation expanded from a removal rate to a mass removal. The initial mass is represented by Equation 4.2.

$$[C_o]*A*D = M_{NO3\text{-}N,0} \qquad \text{Equation 4.2}$$

where: $[C_o]$ = initial nitrate concentration (mg/m^3)
A = sediment surface area (m^2)
D = depth of the water column (m)
$M_{NO3\text{-}N,0}$ = initial mass of nitrate per unit area of sediment surface (mg/m^2)

The final mass is represented by Equation 4.3.

$$[C_1]*A*D = M_{NO3\text{-}N,t} \qquad \text{Equation 4.3}$$

where: $[C_1]$ = final nitrate concentration (mg/m^3)
A = sediment surface area (m^2)
D = depth of the water column (m)
$M_{NO3\text{-}N,t}$ = mass of nitrate per unit area of sediment surface at time t (mg/m^2)

The amount removed is equal to the initial mass minus the final mass, as represented by Equation 4.4.

$$R = M_{NO3\text{-}N,0} - M_{NO3\text{-}N,t} = ([C_o]-[C_1])*A*D \qquad \text{Equation 4.4}$$

where: R = mass of nitrate removed (mg)
$M_{NO3\text{-}N,0}$ = initial mass of nitrate per unit area of sediment surface (mg/m^2)
$M_{NO3\text{-}N,t}$ = mass of nitrate per unit area of sediment surface at time t (mg/m^2)
$[C_o]$ = initial nitrate concentration (mg/m^3)
$[C_1]$ = final nitrate concentration (mg/m^3)
A = sediment surface area (m^2)
D = depth of the water column (m)

The removal rate determined using Kelly's mass transfer coefficient is expanded to mass removed by the introduction of a time interval, Δt, and an area term, A. This mass removal is represented by Equation 4.5.

$$R = \rho_d*[C]*A*\Delta t \qquad \text{Equation 4.5}$$

where R = mass of nitrate removed (mg)
ρ_d = mass transfer coefficient for denitrification (m/day)
[C] = nitrate concentration at the beginning of the time interval (mg/m^3)
A = sediment surface area (m^2)
Δt = time interval (day)

The two equations (Equations 4.4 and 4.5) for the mass removed, R, can now be equated to each other as expressed in Equation 4.6.

$$R = ([C_o]-[C_1])*A*D = \rho_d*[C]*A*\Delta t \qquad \text{Equation 4.6}$$

By rearranging the terms and multiplying through by -1, Equation 4.7 is formed.

$$\frac{([C_1]-[C_0])}{\Delta t} = -\frac{\rho_d*[C]}{D} \qquad \text{Equation 4.7}$$

Taking the limit of Equation 4.7 as the time step becomes infinitely small, approaches zero,

$$\lim_{\Delta t \to 0} \frac{([C_1]-[C_0])}{\Delta t} = -\frac{\rho_d*[C]}{D}$$

where:

$$\lim_{\Delta t \to 0} \frac{([C_1]-[C_0])}{\Delta t} = \frac{dc}{dt}$$

the average change in concentration over the time interval resulting in differential equation represented by Equation 4.8.

$$\frac{dc}{dt} = -\frac{\rho_d * [C]}{D} \qquad \text{Equation 4.8}$$

By separating terms and integrating concentration and time over the intervals $[C_o]$to $[C_1]$ and o to t:

$$\int_{Co}^{C1} \frac{dc}{[C]} = \int_{0}^{t} -\frac{\rho_d * dt}{D}$$

Equation 4.8 becomes Equation 4.9.

$$\ln([C_1]) - \ln([C_o]) = \frac{-\rho_d * t}{D} \qquad \text{Equation 4.9}$$

Rearranging the terms, Equation 4.10 is developed.

$$\ln\left(\frac{[C_1]}{[C_o]}\right) = \frac{-\rho_d * t}{D} \qquad \text{Equation 4.10}$$

Equation 4.10 is important because it can be further developed in two ways, each resulting in a very valuable equation. By raising both sides of the equation to the exponential (e^x) and rearranging, the equation (which includes depth) to model denitrification in a system (Equation 4.11) is derived.

$$[C_1] = [C_o] * EXP(-\rho_d * t/D) \qquad \text{Equation 4.11}$$

When Equation 4.10 is rearranged to solve for the mass transfer coefficient, ρ_d, Equation 4.12 is derived. Equation 4.12 can be used to determine an accurate representation of the mass transfer coefficient using measured data over time.

$$\frac{\ln\left(\frac{[C_1]}{[C_o]}\right)}{(-t/D)} = \rho_d \qquad \text{Equation 4.12}$$

With a simple substitution,

$$k_d = (-\rho_d / D)$$

where k_d is the simple decay coefficient for denitrification (per day), Equation 4.11 can be related to the simple decay equation (Equation 4.13).

$$[C_1] = [C_o]*EXP(-k_d*t) \qquad \text{Equation 4.13}$$

The same steps can be followed to derive the equation to model nitrate in a system with both denitrification and nitrification occurring, Equation 4.14.

$$[C_1] = [C_o]*EXP(-\rho_{d+n}*t/D) \qquad \text{Equation 4.14}$$

where: ρ_{d+n} = mass transfer coefficient when both denitrification and nitrification occur (m/day)

As before, when Equation 4.14 is rearranged to solve for the mass transfer coefficient, ρ_{d+n}, Equation 4.15 is derived. Equation 4.15 can be used to determine an accurate representation of the mass transfer coefficient using measured data over time with both nitrification and denitrification occurring.

$$\frac{\ln\left(\frac{[C_1]}{[C_o]}\right)}{(-t/D)} = \rho_{d+n} \qquad \text{Equation 4.15}$$

A relationship between the two removal rates (when only denitrification is occurring and denitrification and nitrification are occurring together) can now be developed, using the previously derived equations (Equations 4.11 and 4.14).

$$[C_d] = [C_o]*EXP(-\rho_d*t/D) \qquad \text{Equation 4.11}$$

where: $[C_d]$ = the nitrate concentration after the time step with only denitrification occurring (mg/m^3)
ρ_d = mass transfer coefficient with only denitrification occurring (m/day)

$$[C_{d+n}] = [C_o]*EXP(-\rho_{d+n}*t/D) \qquad \text{Equation 4.14}$$

where: $[C_{d+n}]$ = the nitrate concentration after the time step with both denitrification and nitrification occurring (mg/m^3).
ρ_{d+n} = mass transfer coefficient with both denitrification and nitrification occurring (m/day)

Solving both equations for the initial concentration term:

$$[C_o] = \frac{[C_d]}{EXP(-\rho_d*t/D)}$$

$$[C_o] = \frac{[C_{d+n}]}{EXP(-\rho_{d+n}*t/D)}$$

the two equations can be set equal to each other, as shown in Equation 4.16.

$$[C_o] = \frac{[C_d]}{EXP(-\rho_d*t/D)} = \frac{[C_{d+n}]}{EXP(-\rho_{d+n}*t/D)} \qquad \text{Equation 4.16}$$

Again rearranging the terms:

$$\frac{[C_{d+n}]}{[C_d]} = \frac{EXP(-\rho_{d+N}*t/D)}{EXP(-\rho_d*t/D)}$$

and taking the natural log of both sides of the equation results in Equation 4.17.

$$\ln\left(\frac{[C_{d+n}]}{[C_d]}\right) = \ln\left(\frac{EXP(-\rho_{d+N}*t/D)}{EXP(-\rho_d*t/D)}\right) \qquad \text{Equation 4.17}$$

Separating the right hand side of the expression:

$$\ln\left(\frac{[C_{d+n}]}{[C_d]}\right) = \ln[EXP(-\rho_{d+N}*t/D)] - \ln[EXP(-\rho_d*t/D)]$$

and taking the natural log of the right hand side:

$$\ln\left(\frac{[C_{d+n}]}{[C_d]}\right) = (-\rho_{d+N}*t/D) - (-\rho_d*t/D)$$

results in Equation 4.18.

$$\ln\left(\frac{[C_{d+n}]}{[C_d]}\right) = \frac{(-\rho_{d+N} + \rho_d)*t}{D} \qquad \text{Equation 4.18}$$

Raising both sides of the expression to the exponential (e^x):

$$\left(\frac{[C_{d+n}]}{[C_d]}\right) = EXP[(-\rho_{d+N} + \rho_d)*t/D]$$

and rearranging results in an equation (Equation 4.19) relating the concentration of a system with only denitrification occurring to a system with both nitrification and denitrification occurring over the same time period.

$$[C_{d+n}] = [C_d] * EXP[(-\rho_{d+N} + \rho_d)*t/D] \qquad \text{Equation 4.19}$$

A new term, ρ_n, the mass transfer coefficient for nitrification, can be substituted for ($-\rho_{d+n} + \rho_d$), which gives rise to Equation 4.20. This new term describes the effect nitrification has on nitrate removal.

$$[C_{d+n}] = [C_d] * EXP[(\rho_n)*t/D] \qquad \text{Equation 4.20}$$

This equation can also be derived by relating the mass transfer coefficient for nitrification to the nitrate concentration in the water column in the same manner that the previous mass transfer coefficients (ρ_d and ρ_{d+n}) were derived, again starting with the basic equations as previously done. The mass at the initial concentration (Equation 4.2):

$$[C_o]*A*D = M_{NO3\text{-}N,o}$$

where: $[C_o]$ = initial nitrate concentration (mg/m^3)
A = sediment surface area (m^2)
D = depth of the water column (m)
$M_{NO3\text{-}N,o}$ = initial mass of nitrate per unit area of sediment surface (mg/m^2)

the mass at time t with only denitrification occurring (a variation of Equation 4.3):

$$[C_{d,t}]*A*D = M_{NO3\text{-}N,t}$$

where: $[C_{d,t}]$ = nitrate concentration at time t with only denitrification occurring (mg/m^3)
A = sediment surface area (m^2)
D = depth of the water column (m)
$M_{NO3\text{-}N,t}$ = mass of nitrate per unit area of sediment surface at time t (mg/m^2)

and the mass at time t with both denitrification and nitrification occurring (a second variation of Equation 4.3):

$$[C_{d+n,t}]*A*D = M_{NO3\text{-}N,t}$$

where: $[C_{d+n,t}]$ = nitrate concentration at time t with denitrification and nitrification occurring (mg/m^3)
A = sediment surface area (m^2)
D = depth of the water column (m)
$M_{NO3\text{-}N,t}$ = mass of nitrate per unit area of sediment surface at time t (mg/m^2)

Subtracting the differences in the mass of the nitrates at time t for this scenario (denitrification only occurring and denitrification and nitrification occurring) and multiplying the initial mass by the area and the depth gives the difference in the mass removed between the two scenarios (Equation 4.21).

$$dR = (([C_o] - [C_{d+n,t}]) - ([C_o] - [C_{d,t}])*A*D \qquad \text{Equation 4.21}$$

where: dR = the difference in the mass of nitrate removed at time t (mg)
$[C_o]$ = initial nitrate concentration
$[C_{d,t}]$ = nitrate concentration at time t with only denitrification occurring (mg/m^3)
$[C_{d+n,t}]$ = nitrate concentration at time t with both denitrification and nitrification occurring (mg/m^3)
A = sediment surface area (m^2)
D = depth of the water column (m)

By the same method, rewriting Equation 4.5, once for denitrification occurring and once for denitrification and nitrification occurring, results in the following equations:

$$R_d = \rho_d*[C]*A*\Delta t$$

where R_d = mass of nitrate removed with only denitrification occurring (mg)
ρ_d = mass transfer coefficient for denitrification (m/day)
[C] = nitrate concentration at the beginning of the time interval (mg/m^3)
A = sediment surface area (m^2)
Δt = time interval (day)

$$R_{d+n} = \rho_{d+n}*[C]*A*\Delta t$$

where R_{d+n} = mass of nitrate removed with both denitrification and nitrification occurring (mg)
ρ_{d+n} = mass transfer coefficient for denitrification (m/day)
[C] = nitrate concentration at the beginning of the time interval (mg/m^3)
A = sediment surface area (m^2)
Δt = time interval (day)

By subtracting the second equation from the first one, Equation 4.22, the difference in the amount of nitrate removed over the time period t, is developed.

$$dR = (\rho_{d+n} - \rho_d)*[C]*A*\Delta t \qquad \text{Equation 4.22}$$

where: dR = the difference in the mass of nitrate removed at time t (mg)
ρ_d = mass transfer coefficient for denitrification (m/day)
ρ_n = mass transfer coefficient for nitrification (m/day)
[C] = nitrate concentration at the beginning of the time interval (mg/m^3)
A = sediment surface area (m^2)
Δt = time interval (day)

Equating Equations 4.21 and 4.22, Equation 4.23 is developed.

$$dR = (([C_o] - [C_{d+n,t}]) - ([C_o] - [C_{d,t}]))*A*D = (\rho_{d+n} - \rho_d)*[C]*A*\Delta t \qquad \text{Equation 4.23}$$

Rearranging Equation 4.23:

$$\frac{([C_o] - [C_{d+n,t}]) - ([C_o] - [C_{d,t}])}{\Delta t} = \frac{(\rho_{d+n} - \rho_d)*[C]}{D}$$

taking the limit as time approaches zero:

$$\lim_{\Delta t \to 0} \frac{([C_{d+n,t}] - [C_o]) - ([C_{d,t}] - [C_o]))}{\Delta t} = -\frac{(\rho_{d+n} - \rho_d)*[C]}{D}$$

separating the limit operator:

$$\lim_{\Delta t \to 0} \frac{([C_{d+n,t}] - [C_o])}{\Delta t} - \lim_{\Delta t \to 0} \frac{([C_{d,t}] - [C_o])}{\Delta t} = -\frac{(\rho_{d+n} - \rho_d)*[C]}{D}$$

results in the differential equation, Equation 4.24.

$$\frac{d[C_{d+n,t}] - d[C_{d,t}]}{dt} = -\frac{(\rho_{d+n} - \rho_d)*[C]}{D} \qquad \text{Equation 4.24}$$

Next integrate over the desired interval:

$$\int_{Co}^{Cd+n,t} \frac{d[C_{d+n,t}]}{[C]} - \int_{Cd0}^{Cd,t} d[C_{d,t}] = \int_0^t -\frac{(\rho_{d+n} - \rho_d)*dt}{D}$$

resulting in:

$$(\ln([C_{d+n,t}]) - \ln([C_o])) - (\ln([C_{d,t}]) - \ln([C_o])) = -\frac{(\rho_{d+n} - \rho_d)*t}{D}$$

and consolidating terms results in Equation 4.25, an equation similar to Equation 4.10.

$$\ln\left(\frac{[C_{d+n,t}]}{[C_{d,t}]}\right) = -\frac{(\rho_{d+n} - \rho_d)*t}{D} \qquad \text{Equation 4.25}$$

Raising both sides of the equation to the exponential (e^x) results in Equation 4.26.

$$[C_{d+n,t}] = [C_{d,t}]*EXP(-\rho_{d+n} + \rho_d)*t/D) \qquad \text{Equation 4.26}$$

By making the substitution $\rho_n = (-\rho_{d+N} + \rho_d)$, the equation becomes identical to Equation 4.20.

$$[C_{d+n,t}] = [C_{d,t}]*EXP(\rho_n*t/D)$$

Rearranging Equation 4.20, one can again get an estimate for the mass transfer coefficient for effect of nitrification, ρ_n, as shown in Equation 4.27.

$$\frac{\ln\left(\frac{[C_{d+n,t}]}{[C_{d,t}]}\right)}{(-t/D)} = \rho_n \qquad \text{Equation 4.27}$$

The nitrate removal rate is affected by the temperature; as the temperature increases, the denitrification rate increases. This effect is accounted for using a relationship developed by Dawson and Murphy (1972). Their study showed an increase in microbial activity based on temperature increases that can be fitted with an empirical exponential curve (Figure 4.1) (Equation 4.28).

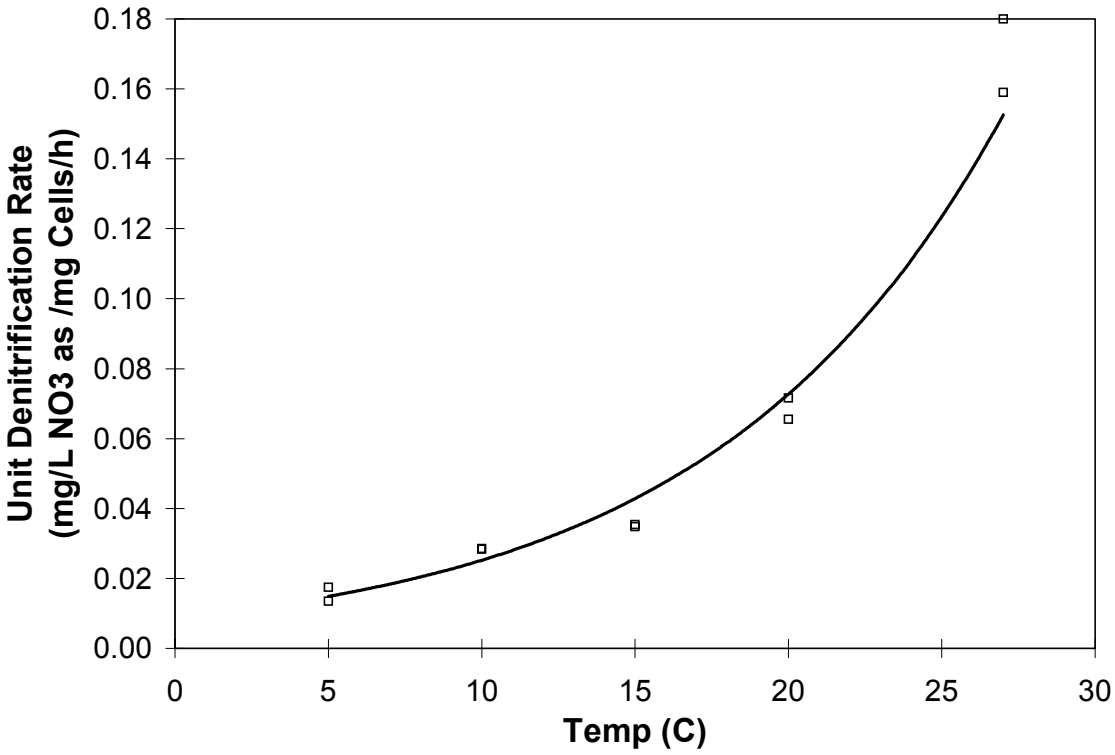

Figure 4.1. Relationship of temperature to denitrification rates using fixed denitrifying organism populations (from data presented by Dawson and Murphy, 1972).

$$D_r = 0.0087EXP(0.1059*T) \qquad \text{Equation 4.28}$$

where: D_r = denitrification rate (mg/L/h)
T = Temperature (^oC)

These data were developed using a fixed population of denitrifying microbes. The relationship of two nitrate removal rates determined using the exponential model based on the fixed population of Dawson and Murphy (1972) is approximately equal to the relationship of the two nitrate removal rates of another population at the same two temperatures (Equation 4.29).

$$D_{r2,T2,Model} / D_{r1,T1,Model} = D_{r2,T2,P2} / D_{r1,T1,P2} = C_{T1\text{-}T2} \quad \text{Equation 4.29}$$

where: $D_{r1,T1,Model}$ = denitrification rate at T1 of the modeled population (mg/L/h/mg cells)
$D_{r2,T2,Model}$ = denitrification rate at T2 of the modeled population (mg/L/h/mg cells)
$D_{r1,T1,P2}$ = denitrification rate at T1 of the population of interest (mg/L/h)
$D_{r2,T2,P2}$ = denitrification rate at T2 of the population of interest (mg/L/h)
$C_{T1\text{-}T2}$ = correction factor for the differences in temperature (unitless)

The denitrification rates (D_r) can be corrected for different temperatures by using Equation 4.30.

$$D_{rT2} = D_{rT1} * C_{T1\text{-}T2} \quad \text{Equation 4.30}$$

where: D_{rT1} = denitrification rate at temperature T1 ($mg/m^2/sec$)
$C_{T1\text{-}T2}$ = correction factor for the differences in temperature (unitless)
D_{rT2} = denitrification rate at temperature T2 ($mg/m^2/sec$).

The temperature correction factor $C_{T1\text{-}T2}$ between the two temperatures, 8^oC and 21^oC, used in this study was 3.961.

The mass transfer coefficient for when only denitrification is occurring (ρ_d) can be determined for different temperatures. The following formulation shows the development of this equation. Starting with the previous equation (Equation 4.30) (converting units on the denitrification rate from $mg/m^2/sec$ to $mg/m^2/day$) and solving for D_{rT1}:

$$D_{rT1} = D_{rT2} / C_{T1\text{-}T2}$$

where: D_{rT1} = denitrification rate at temperature T1 ($mg/m^2/day$)
$C_{T1\text{-}T2}$ = correction factor for the differences in temperature (unitless)
D_{rT2} = denitrification rate at temperature T2 ($mg/m^2/day$)

and Kelly's original equation for the mass transfer coefficient (Equation 4.31):

$$D_{rT1} = \rho_{dT1} * [C] \qquad \text{Equation 4.31}$$

where: D_{rT1} = denitrification rate at temperature T1 ($mg/m^2/day$)
ρ_{dT1} = mass transfer coefficient for denitrification at temperature T1 (m/day)
[C] = nitrate concentration (mg/m^3)

Combining Equation 4.30 and Equation 4.31 results in Equation 4.32.

$$D_{rT2} / C_{T1\text{-}T2} = \rho_{dT1} * [C] \qquad \text{Equation 4.32}$$

where: D_{rT2} = denitrification rate at temperature T2 ($mg/m^2/day$)
$C_{T1\text{-}T2}$ = correction factor for the differences in temperature (unitless)
ρ_{dT1} = mass transfer coefficient for denitrification at temperature T1 (m/day)
[C] = nitrate concentration (mg/m^3)

Rearranging Equation 4.32 results in Equation 4.33:

$$D_{rT2} = \rho_{dT1} * [C] * C_{T1\text{-}T2} \qquad \text{Equation 4.33}$$

The next step is to convert the denitrification rate (D_{rT2}) to a mass denitrified by multiplying both sides by a sediment surface area and a time interval.

$$A * \Delta t * D_{rT2} = \rho_{dT1} * [C] * C_{T1\text{-}T2} * A * \Delta t$$

where: A = sediment surface area (m^2)
Δt = time interval (day)

This results in Equation 4.34.

$$R_{T2} = \rho_{dT1} * [C] * C_{T1\text{-}T2} * A * \Delta t \qquad \text{Equation 4.34}$$

where: R_{T2} =is the mass of nitrate removed at temperature T2 (mg).

Once again a mass of nitrate removed can be related, as was done in Equation 4.4.

$$R = ([C_o]-[C_1])*A*D$$

where: R = mass of nitrate removed (mg)
$[C_o]$ = initial nitrate concentration (mg/m^3)
$[C_1]$ = final nitrate concentration (mg/m^3)
A = sediment surface area (m^2)
D = depth of the water column (m)

R in this case is equal to the nitrate mass removed under the temperature of interest (T2), as temperature is not represented in the equation. Thus, R is independent of temperature, resulting in Equation 4.4 becoming Equation 4.35.

$$R_{T2} = ([C_o]-[C_1]) * A * D \qquad \text{Equation 4.35}$$

where: R_{T2} = mass of nitrate removed at temperature T2 (mg)
$[C_o]$ = initial nitrate concentration (mg/m^3)
$[C_1]$ = final nitrate concentration (mg/m^3)
A = sediment surface area (m^2)
D = depth of the water column (m)

Equation 4.34 can now be equated to Equation 4.35.

$$([C_o]-[C_1]) * A * D = \rho_{dT1} * [c] * C_{T1-T2} * A * \Delta t$$

The areas cancel leaving:

$$([C_o]-[C_1]) * D = \rho_{dT1} * [c] * C_{T1-T2} * \Delta t$$

By rearranging the terms and multiplying through by -1:

$$\frac{([C_1]-[C_0])}{\Delta t} = -\frac{\rho_{dT1}*[C] * C_{T1-T2}}{D}$$

taking the limit as the time step becomes infinitely small, approaches zero:

$$\lim_{\Delta t \to 0} \frac{([C_1]-[C_0])}{\Delta t} = -\frac{\rho_{dT1}*[C] * C_{T1-T2}}{D}$$

where:

$$\lim_{\Delta t \to 0} \frac{([C_1]-[C_0])}{\Delta t} = \frac{dc}{dt}$$

the average change in concentration over the time interval resulting in differential equation (Equation 4.36):

$$\frac{d[C]}{dt} = -\frac{\rho_{dT1}*[C] * C_{T1-T2}}{D} \qquad \text{Equation 4.36}$$

separating terms and integrating concentration and time over the intervals $[C_o]$to $[C_1]$ and 0 to t:

$$\int_{Co}^{C1} \frac{dc}{[C]} = \int_{0}^{t} -\frac{\rho_{dT1}*dt* C_{T1-T2}}{D}$$

results in Equation 4.37:

$$\ln([C_1]) - \ln([C_o]) = \frac{-\rho_{dT1}*t* C_{T1-T2}}{D} \qquad \text{Equation 4.37}$$

rearranging the terms resulting in Equation 4.37a:

$$\ln\left(\frac{[C_1]}{[C_o]}\right) = \frac{-\rho_{dT1}*t* C_{T1-T2}}{D} \qquad \text{Equation 4.37a}$$

raising both sides of the equation to the exponential (e^x) and rearranging, the equation (Equation 4.38) to model denitrification in a system at a different temperature than the temperature at which data were collected is derived.

$$[C_1] = [C_o]*EXP(-\rho_{dT1}*t* C_{T1-T2}/D) \qquad \text{Equation 4.38}$$

From Equation 4.38, it can be deduced that the mass transfer coefficient (ρ) can easily be related to a change in temperature by Equation 4.39.

$$\rho_{dT2} = C_{T1-T2} * \rho_{dT1} \qquad \text{Equation 4.39}$$

where: ρ_{dT2} = mass transfer coefficient at a second temperature T2 (m/day)
C_{T1-T2} = correction factor for the change in temperature (unitless)
ρ_{dT1} = mass transfer coefficient at original temperature T1 (m/day).

This relationship is only valid for times when nitrification is not occurring. This is due to denitrification and nitrification being affected to differing degrees by changes in temperature. To overcome this restriction, Equation 4.39 can be rewritten as Equation 4.39a to incorporate the effect of temperature on nitrification by using the previously developed:

$$-\rho_{d+n} + \rho_d = \rho_n$$

which rearranged is:

$$\rho_{d+n} = \rho_d - \rho_n$$

Equation 4.39 can thus be rewritten as Equation 4.39a.

$$\rho_{d+nT2} = \rho_{dT1} * C_{d,T1-T2} - \rho_{nT1} * C_{n,T1-T2} \qquad \text{Equation 4.39a}$$

where: ρ_{d+nT2} = the mass transfer coefficient at the temperature of interest T2 when both nitrification and denitrification are occurring (m/day)
ρ_{dT1} = the mass transfer coefficient at the original temperature T1 (m/day)
$C_{d,T1-T2}$ = correction factor for the change in temperature for nitrification (unitless)
ρ_{nT1} = the mass transfer coefficient for the effect of nitrification at the original temperature (m/day)
$C_{n,T1-T2}$ = correction factor for the change in temperature for denitrification (unitless)

These two relationships are restricted to the same populations of denitrifiers and nitrifiers, usually meaning the same location and time, as denitrifier populations vary with time and location.

4.3 Conclusion

With the previously developed equations (Equations 4.12, 4.15, 4.27, and 4.39), one can determine the mass transfer coefficients for denitrification alone, as well as for nitrification and denitrification occurring together within a stream or drainage network regardless of the depth of the water column. Knowing these mass transfer coefficients allows

the effect of nitrification in the system on the mass transfer coefficient to be determined. These mass transfer coefficients can also be corrected for differing temperatures.

The most important use of these equations will be in modeling efforts. Of the equations derived, 4.15 and 4.40 are the most important to modeling efforts.

$$\frac{\ln\left(\frac{[C_1]}{[C_o]}\right)}{(-t/D)} = \rho_{d+n} \qquad \text{Equation 4.15}$$

$$[C_1] = [C_o]*EXP(-\rho_{d+nT1}*t*\ C_{T1-T2}/D) \qquad \text{Equation 4.40}$$

Equation 4.15 is used to determine a mass transfer coefficient (ρ_{d+n}) through experimentation using a method similar to the first two methods presented in this study (Section 3.1 Nitrate Depletion in In-Stream Tanks or Section 3.2 Nitrate Depletion in Undisturbed Cores). The mass transfer coefficient will have to be determined for each location where the model is used, as nitrifier and denitrifier populations vary from location to location. The correction factor for the change in temperature (C_{T1-T2}) can be determined using Equation 4.30:

$$D_{rT2} = D_{rT1} * C_{T1-T2} \qquad \text{Equation 4.30}$$

using measured data from two temperature determinations of the denitrification rate, or one could use the relationship derived by Dawson and Murphy (1972), shown in Equation 4.28:

$$D_r = 0.0087EXP(0.1059*T) \qquad \text{Equation 4.28}$$

along with Equation 4.29:

$$D_{r2,T2,Model} /D_{r1,T1,Model} = D_{r2,T2,P2} /D_{r1,T1,P2} = C_{T1-T2} \qquad \text{Equation 4.29}$$

to determine the correction factor for the change in temperature (C_{T1-T2}). Equation 4.40 is the same equation as Equation 4.38, with the exception that the mass transfer coefficient for only denitrification (ρ_d) is replaced with the mass transfer coefficient composed of the effects of

both denitrification and nitrification (ρ_{d+n}). This equation is preferable, as it requires the least amount of time and resources to determine, and it more accurately describes what is occurring in the system as far as nitrate loss using only one input parameter. It more accurately describes the nitrate loss because it does not try to separate nitrification and denitrification into two separate input parameters, which would make each process more difficult to determine due to the processes' effects on each other. Equation 4.40 can be inserted into a model and used to predict nitrate concentrations or loads from one time step to the next using inputs of initial or predicted nitrate concentrations, depth, time interval, and temperature. This method results in an accurate way to model nitrate concentrations in flowing surface water with few input parameters.

References

Cooke, J.G., and A.B. Cooper. 1988. Sources and sinks of nutrients in a New Zealand hill pasture catchment III. Nitrogen. Hydrol. Proc. 2: 135-149.

Dawson, R.N. and K.L. Murphy. 1972. The temperature dependency of biological denitrification. Wat. Res. 6: 71-83.

Duff, J.H., F.J. Triska, and R.S. Oremland. 1984. Denitrification associated with stream periphyton: chamber estimates from undisturbed communities. J. Environ. Qual. 13: 514-518.

Kelly, C.A., J.W.M. Rudd, R.H. Hesslein, D.W. Schindler, P.J. Dillon, C.T. Driscoll, S.A. Gherini, and R.E. Hecky. 1987. Prediction of biological acid neutrilization in acid-sensitive lakes. Biogeochem. 3: 129-140.

Seitzinger, S.P. 1994. Linkages between organic matter mineralization and denitrification in eight riparian wetlands. Biogeochem. 25: 19-39.

Chapter 5

Overall Summary and Conclusions

Through literature, the hydrologic and nutrient inputs and outputs and in-stream nutrient transformations of a typical forested stream were identified and their contributions to the canal quantified. Tables 5.1 and 5.2 compare the nitrogen and phosphorous species concentrations or content of each input, output, and transformation of the stream found in literature to that of their measured counterparts from this study.

Hydrologic inputs to the stream include: rainfall and/or throughfall, groundwater, surface runoff, and upstream or lateral branch inflows. Nutrients entered the stream through the hydrologic sources as well as autochthonous sources (in-stream production) and allochthonous sources (litterfall and lateral movement).

The hydrologic output to the stream is the outflow at the outlet. Nutrients were removed from the stream through outflow at the outlet as well as through emergent drift, denitrification, and human activities such as dredging.

The in-stream transformations involved in nitrogen and phosphorous transformations within the stream included physical processes (leaching and fragmentation), chemical processes (adsorption and chemical conversions), and biological processes (mineralization, immobilization, nitrification and denitrification).

Table 5.1. Range of nitrogen species concentrations[1] or contents of the inputs and outputs to a typical forested stream found in literature and measured during this study.

	Nitrogen Form							
Input/Output	**NH_4-N (Lit)[2]**	**NH_4-N (Meas)[3]**	**NO_3-N (Lit)[2]**	**NO_3-N (Meas)[3]**	**DON-N (Lit)[2]**	**DON-N (Meas)[3]**	**Total-N (Lit)[2]**	**Total-N (Meas)[3]**
Rainfall (mg/L)	0.02-2.01	0.35	0.22-1.46	0.22	0.11-0.86	0.86	0.20-1.43	1.43
Throughfall (mg/L)	0.04-12.74	0.39	0.02-2.38	0.63	0.03-0.44	2.31	0.09-2.68	3.33
Groundwater (mg/L)	0.00-0.91	0.28	0.01-15.54	1.48	0.04-0.50	1.35	0.17-1.13	3.11
Surface Runoff (mg/L)	0.18-2.59	-	0.02-0.59	-	0.52-1.95	-	0.72-5.13	-
Upstream Inflow (mg/L)	0.00-0.23	0.08	0.00-0.93	1.80	0.04-1.26	1.62	0.15-2.27	1.70
Litterfall (mg/g)	-	-	-	-	-	-	5.4-17.1	12.1
Lateral Movement (mg/g)	-	-	-	-	-	-	6.0	-
Outflow (mg/L)	0.00-0.23	0.08	0.00-0.93	1.80	0.04-1.26	1.62	0.15-2.27	1.70
Denitrification ($mg/m^2/day$)	-	-	7-490	382-409	-	-	-	-
Mineralization ($mg/m^2/day$)	-	-	-	-	-	29.6	-	-
Nitrification ($mg/m^2/day$)	-	0.00	-	-	-	-	-	-

[1] Concentrations are volume weighted concentrations.
[2] (Lit) denotes the range of values found in literature.
[3] (Meas) denotes measured values determined during this study.

Table 5.2. Range of phosphorous species concentrations[1] or contents of the inputs and outputs to a typical forested stream found in literature and measured during this study.

	Phosphorous Form			
Input/Output	**PO_4-P (Lit)[2]**	**PO_4-P (Meas)[3]**	**Total P (Lit)[2]**	**Total P (Meas)[3]**
Rainfall (mg/L)	0.00-0.03	0.03	0.00-0.08	0.08
Throughfall (mg/L)	0.00-0.01	0.24	0.00-0.11	0.35
Groundwater (mg/L)	0.00	0.01	0.00	0.01
Surface Runoff (mg/L)	1.03	-	0.47-1.03	-
Upstream Inflow (mg/L)	0.02	0.01	0.01-0.07	0.02
Litterfall (mg/g)	-	-	0.07-0.91	0.7
Lateral Movement (mg/g)	-	-	-	-
Outflow (mg/L)	0.02	0.01	0.01-0.07	0.02
Denitrification ($mg/m^2/day$)	-	-	-	-
Mineralization ($mg/m^2/day$)	-	-	-	-
Nitrification ($mg/m^2/day$)	-	-	-	-

[1] Concentrations are volume weighted concentrations.
[2] (Lit) denotes the range of values found in literature.
[3] (Meas) denotes measured values determined during this study.

Ammonium concentrations for all inputs and outputs for this study were within the normal range of values found in literature (Table 5.1), with the exception of a few elevated values (Belgium, England, and the Netherlands). The highest values — rainfall (2.01 mg/L), throughfall (12.74 mg/L), and groundwater (0.91 mg/L) — occur in locations that have very

high animal concentrations occurring upwind of the research locations. This results in highly elevated ammonium concentrations in rainfall and throughfall.

Nitrate concentrations for all inputs and outputs for this study are also within the normal range of values found in literature (Table 5.2), again with the exception of a few elevated values. The elevated value for rainfall (1.46 mg/L) is due to nitrification of the excess ammonium in the atmosphere near the areas of elevated ammonium discussed in the previous paragraph. The elevated nitrate in throughfall (2.38 mg/L) is less extreme than for ammonium because nitrification in the canopy, although occurring, is minimal. The dramatic elevation of nitrate concentrations in the groundwater (15.5 mg/L) in locations of high animal production is due to nitrification of elevated throughfall ammonium in the soil. The elevated stream nitrate concentrations in this study (1.80 mg/L) are due to the drought occurring during the two years (2001 and 2002) of the study. The drought causes prolonged dry periods, which results in large buildups of nitrate within the soil. When it eventually rains, these nitrate buildups are flushed from the soil.

This study had the highest dissolved organic nitrogen of all the studies presented in the literature review. This is most likely due to the organic soils present in the study area.

The phosphorous concentrations for all the inputs (with the exception of throughfall) and outputs for this study were similar to those found in literature (Table 5.2). These low values are common for forested watersheds. The elevated phosphorous throughfall values in this study are due to a combination of a lower-than-normal rainfall (resulting in a build-up on leaf surfaces of dust and other material containing the different forms of phosphorous) and a forest road running the length of the study canal on its north side (creating a source of dust containing the different phosphorous forms in close proximity to the study canal section).

These two factors will result in higher-than-normal phosphorous species concentrations in the throughfall inputs.

Due to the wide range of nutrient concentration values presented in literature for inputs to and outputs of forested streams, one must be careful to select information that closely matches the stream of interest. Using the wrong information would lead to erroneous results and conclusions.

The denitrification rates found in this study are in the higher range of those studies presented in the literature review. This is most likely due to the high average dissolved organic carbon concentrations (25.1 mg/L) and higher average nitrate concentrations (1.80 mg/L) found within the canal section of this study. One must be very cautious when using denitrification rates from literature, as most do not give temperature information or carbon concentrations along with denitrification rates, which could result in an over- or underestimation of denitrification within the system.

The results of this study and others show that denitrification is an important pathway for the removal of nitrates from surface waters in forested watersheds. During the two years of this study, 6.7 kg and 19.8 kg of nitrate were removed in 2001 and 2002 respectively from the 5700 m^2 sediment surface of the study canal section. This represents 3.1% of the 215 kg total nitrates that entered this canal section in 2001 and 2.6% of the 774 kg total nitrates that entered this canal section in 2002. These percentages do not seem high until one looks at the upstream inflow to the study canal section, which was 234 kg and 767 kg of nitrates during the 2001 and 2002 flow periods respectively. This means that during this study, denitrification removed not only the nitrate inputs to the canal (from rainfall, throughfall, groundwater, and nitrification) but also a portion of the nitrate inflow from upstream,

resulting in an overall decrease in the nitrate load from the beginning of the study canal section (S0) to the end of the study canal (S3). The denitrification rates and mass transfer coefficients for forested watersheds were found to be smaller than those of agriculturally dominated watersheds. This is due to the higher nitrate concentrations encountered in the agriculturally dominated watersheds as compared to the forested watersheds (see Birgand, 2000, for an extensive review and description of denitrification in agricultural streams).

A mathematical expression was developed (Equation 5.1) to make it possible to translate a depth-independent denitrification rate to different temperatures, making it possible to more accurately model denitrification.

$$[C_1] = [C_o]*EXP(-\rho_{d+nT1}*t*\ C_{T1-T2}/D) \qquad \text{Equation 5.1}$$

where: $[C_1]$ = nitrate concentration at time t occurring (mg/m^3)
$[C_o]$ = initial nitrate concentration (mg/m^3)
D = depth of the water column (m)
ρ_{d+nT1} = mass transfer coefficient for both denitrification and nitrification occurring at initial temperature (m/day)
t = time (day)
C_{T1-T2} = correction factor for the differences in temperature (unitless)

where C_{T1-T2} is determined using equation 5.2:

$$D_{T2} /D_{T1} = C_{T1-T2} \qquad \text{Equation 5.2}$$

where: D_{T1} = denitrification rate at T1 (mg/L/h)
D_{T2} = denitrification rate at T2 (mg/L/h)
C_{T1-T2} = correction factor for the differences in temperature (unitless)

and D_T is determined using Equation 5.3.

$$D_T = 0.0087EXP(0.1059*T) \qquad \text{Equation 5.3}$$

where: D_T = denitrification rate at temperature T(mg/L/h)
T = Temperature (^oC).

These three equations, along with one additional input parameter (the mass transfer coefficient) and one additional input data set (the sediment temperature over time), will enable models to more accurately represent the removal rates of nitrate from the system over time. The mass transfer coefficient can be easily determined using either the in-stream tank method or the undisturbed core study described in the denitrification section of this report. Depth over time does not have to be an additional input, as depth in the channel is a common output to most models. This method of determining denitrification rates is more accurate than previous methods, as the model can now determine different denitrification rates occurring at differing temperatures. At this point, it is best to use the mass transfer coefficient developed in this report, which results in a net effect of denitrification and nitrification (Equation 5.1). This is recommended because nitrification is still difficult to measure accurately. Also, it is much cheaper, easier, less resource-intensive, and more accurate to measure net denitrification than to measure each process individually.

Further studies are needed to improve the understanding of nutrient transformations within surface waters. The processes of nitrification and mineralization were only touched upon in this study. These processes need to be further investigated to find a method of determining how their participation in the transformations of nutrients affects the overall mass balance of the surface water system. Also in need of further investigation is the effect pH has on each of the transformation processes (mineralization, nitrification, and denitrification) and how its effect can be incorporated into the governing equations for each process.

References

Birgand, F. Quantification and Modeling of In-Stream Processes in Agricultural Canals of the Lower Coastal Plain. Dissertation, 469pp, North Carolina State University, Raleigh, 2000.

Appendices

Appendix A

Statistical Analysis Models for Denitrification Studies

The results of the methods used in the denitrification studies form first-order decay relationships. The use of Equation 4.12 allows for the determination of the mass transfer coefficients for each run. The mass transfer coefficients were then analyzed using the procGLM (General linear model of the SAS statistical software, SAS, 1999). This fits a linear model using least squares with indicator variables. The mass transfer coefficient was used rather than the slope of the raw data plotted as log[C] vs. time, which yields a straight line for an exponential decay curve, because of the depth differences in the study. The mass transfer coefficient removes depth difference as a variable, allowing for comparisons to be valid over the different depths. The mass transfer coefficients were log-transformed for the main effect analysis to give a normal distribution of the error. Interactions were also analyzed using the log transformation. This allows the determination of the interactions to be additive or non-additive by the mathematical property log(a*b) = log (a) + log(b), where (a*b) is the interaction of interest and (a) and (b) are the separated effects of the two factors. If the interaction is not significant on the log-transformed slopes then they are additive; if they are still significant, then they are not additive. Additive interactions can be ignored, while non-additive interactions indicate one factor enhancing the effect of another by its presence. Analyses were run on each method to determine the importance of the factors involved within each study as well as between the different methods to determine how well the methods agree with each other in determining the nitrate removal rate of the overall

study. The full data sets were subsampled to allow direct comparisons between the different factors.

Variables for Statistical Analysis

The following symbols are used in presenting the models for the statistical analysis of the data generated in the five methods. The symbol μ represents the average mass transfer coefficient. The symbols X^{L}_{i}, X^{C}, X^{In}, X^{I}_{i}, X^{T}, X^{IC}, X^{D} are dummy variables for:

X^{L}_{i} = location
X^{C} = circulation
X^{In} = nitrification inhibitor
X^{I}_{i} = treatment
X^{T} = temperature
X^{IC} = initial concentration
X^{D} = depth.

where: $X^{L}_{1} = \begin{cases} 1 \text{ if location 1} \\ 0 \text{ if location 2} \\ -1 \text{ if location 3} \end{cases}$

$X^{L}_{2} = \begin{cases} 0 \text{ if location 1} \\ 1 \text{ if location 2} \\ -1 \text{ if location 3} \end{cases}$

$X^{C} = \begin{cases} 1 \text{ if circulation = no} \\ -1 \text{ if circulation = yes} \end{cases}$

$X^{In} = \begin{cases} 1 \text{ if nitrification inhibitor = no} \\ -1 \text{ if nitrification inhibitor = yes} \end{cases}$

$X^{I}_{1} = \begin{cases} 1 \text{ if treatment 1} \\ 0 \text{ if treatment 2} \\ -1 \text{ if treatment 3} \end{cases}$

$X^{I}_{2} = \begin{cases} 0 \text{ if treatment 1} \\ 1 \text{ if treatment 2} \\ -1 \text{ if treatment 3} \end{cases}$

X^T = (1 -f temperature = 21°C
\ -1 if temperature = 8°C

X^C = (1 if initial concentration = 3
\ -1 if initial concentration = 6

X^D = (1 if depth = 20 cm
\ -1 if depth = 30 cm

The symbols α_i, ε, λ, β_i, τ_i η, δ represent the differences between the average mass transfer coefficient, μ, and the measured mass transfer coefficients. These representation are for the mass transfer coefficients relating to:

α_i = location
ε_j = circulation
λ_k = nitrification inhibitor
β_m = treatment
τ_n = temperature
η_p = initial concentration
δ_q = depth.

Nitrate Depletion in In-Stream Tanks

The design of nitrate depletion in the in-stream tanks method allows only for the main effect of location to be analyzed. The statistical model for determining the significance of the differences between the locations of the field tanks is shown in Equation A1.

Model: $E(t)=(\mu+\alpha_1 X^L{}_1+\alpha_2 X^L{}_2)t$ Equation A1

where: E(t) = the concentration at time t
u = the average mass transfer coefficient
α_1, α_2 represent the main effects of location on the mass transfer coefficient
t = time

The constraint of $\sum_i \alpha_i=0$. The hypothesis being tested is: H_o: $\alpha_i=0$ - no main effect of location on the mass transfer coefficient.

Nitrate Depletion in Undisturbed Cores

The design of nitrate depletion in undisturbed cores method allows for the main effects of location, circulation, nitrification inhibitor, treatment, temperature, initial concentration, and depth, along with their associated interactions, to be analyzed by subsampling the overall data set.

The variable depth was analyzed using the data subset created by holding temperature and initial concentration at 8°C and 6 mg/L respectively. The statistical model used for determining the statistical significance of this variable is shown in Equation A2.

$$\text{Model: } E(t)=(\mu+\alpha_1 X^L_1+\alpha_2 X^L_2+\beta_1 X^I_1+\beta_2 X^I_2+\delta X^D+(\alpha\beta)_{1,1}X^L_1X^I_1+ \quad \text{Equation A2}$$
$$+(\alpha\beta)_{1,2}X^L_1X^I_2+(\alpha\beta)_{2,1}X^L_2X^I_1+(\alpha\beta)_{2,2}X^L_2X^I_2+(\alpha\delta)_{1,1}X^L_1X^D+$$
$$+(\alpha\delta)_{2,1}X^L_2X^D+(\beta\delta)_{1,1}X^I_1X^D+(\beta\delta)_{2,1}X^I_2X^D+(\alpha\beta\delta)_{1,1,1}X^L_1X^I_1X^D+$$
$$+(\alpha\beta\delta)_{1,2,1}X^L_1X^I_2X^D+(\alpha\beta\delta)_{2,1,1}X^L_2X^I_1X^D+(\alpha\beta\delta)_{2,2,1}X^L_2X^I_2X^D)t$$

where: $E(t)$ = the concentration at time t
u = the average mass transfer coefficient
α_1, α_2, β_1, β_2, δ represent the main effects of location, treatment, and depth respectively on the mass transfer coefficient
$(\alpha\beta)_{1,1}$, $(\alpha\beta)_{1,2}$, $(\alpha\beta)_{2,1}$, $(\alpha\beta)_{2,2}$, $(\alpha\delta)_{1,1}$, $(\alpha\delta)_{2,1}$, $(\beta\delta)_{1,1}$, $(\beta\delta)_{2,1}$ represent the interactions of location*treatment, location*depth, and treatment*depth
$(\alpha\beta\delta)_{1,1,1}$, $(\alpha\beta\delta)_{1,2,1}$, $(\alpha\beta\delta)_{2,1,1}$, $(\alpha\beta\delta)_{2,2,1}$ represents the three way interactions of location*treatment*depth
t = time

The following constraints have been placed on the analysis: $\sum_i\alpha_i = 0$, $\sum_m\beta_m = 0$, $\sum_q\delta_q = 0$, $\sum_i(\alpha\beta)_{i,m} = 0$, $\sum_m(\beta\delta)_{m,q} = 0$, $\sum_i(\alpha\delta)_{i,q} = 0$, $\sum_m(\alpha\beta)_{i,m} = 0$, $\sum_q(\beta\delta)_{m,q} = 0$, $\sum_q(\alpha\delta)_{i,q} = 0$, $\sum_i(\alpha\beta\delta)_{i,m,q} = 0$, $\sum_m(\alpha\beta\delta)_{i,m,q} = 0$, $\sum_q(\alpha\beta\delta)_{i,m,q} = 0$.

The hypotheses being tested in this analysis are: H_o: $\delta_q=0$ - no main effect of depth, H_o: $(\alpha\beta)_{i,m}=0$ - no interaction between location and treatment, Ho: $(\beta\delta)_{m,q}=0$ - no interaction between treatment and depth, H_o: $(\alpha\delta)_{i,q}=0$ - no interaction between location and depth, and

H_o: $(\alpha\beta\delta)_{i,m,q}=0$ -no interactive effects between all three; location, treatment, and depth on the mass transfer coefficient.

The variable initial concentration was analyzed using the data subset created by holding temperature at 8°C. The statistical model used for determining the statistical significance of this variable is shown in Equation A3.

$$\text{Model: } E(t)=(\mu+\alpha_1X^L_1+\alpha_2X^L_2+\beta_1X^I_1+\beta_2X^I_2+\eta X^{IC}+(\alpha\beta)_{1,1}X^L_1X^I_1+ \quad \text{Equation A3}$$
$$+(\alpha\beta)_{1,2}X^L_1X^I_2+(\alpha\beta)_{2,1}X^L_2X^I_1+(\alpha\beta)_{2,2}X^L_2X^I_2+(\alpha\eta)_{1,1}X^L_1X^{IC}+$$
$$+(\alpha\eta)_{2,1}X^L_2X^{IC}+(\beta\eta)_{1,1}X^I_1X^{IC}+(\beta\eta)_{2,1}X^I_2X^{IC}+(\alpha\beta\eta)_{1,1,1}X^L_1X^I_1X^{IC}+$$
$$+(\alpha\beta\eta)_{1,2,1}X^L_1X^I_2X^{IC}+(\alpha\beta\eta)_{2,1,1}X^L_2X^I_1X^{IC}+(\alpha\beta\eta)_{2,2,1}X^L_2X^I_2X^{IC})t$$

where: E(t) = the concentration at time t
u = the average mass transfer coefficient
α_1, α_2, β_1, β_2, η represent the main effects of location, treatment, and initial concentration respectively on the mass transfer coefficient
$(\alpha\beta)_{1,1}$, $(\alpha\beta)_{1,2}$, $(\alpha\beta)_{2,1}$, $(\alpha\beta)_{2,2}$, $(\alpha\eta)_{1,1}$, $(\alpha\eta)_{2,1}$, $(\beta\eta)_{1,1}$, $(\beta\eta)_{2,1}$ represent the interactions of location*treatment, location*init. conc., and treatment*init. conc.
$(\alpha\beta\eta)_{1,1,1}$, $(\alpha\beta\eta)_{1,2,1}$, $(\alpha\beta\eta)_{2,1,1}$, $(\alpha\beta\eta)_{2,2,1}$ represents the three way interactions of location*treatment*init. conc.
t = time

The following constraints have been placed on the analysis: $\sum_i\alpha_i = 0$, $\sum_m\beta_m = 0$, $\sum_p\eta_p = 0$, $\sum_i(\alpha\beta)_{i,m} = 0$, $\sum_m(\beta\eta)_{m,p} = 0$, $\sum_i(\alpha\eta)_{i,p} = 0$, $\sum_m(\alpha\beta)_{i,m} = 0$, $\sum_p(\beta\eta)_{m,p} = 0$, $\sum_p(\alpha\eta)_{i,p} = 0$, $\sum_i(\alpha\beta\eta)_{ijm,p} = 0$, $\sum_m(\alpha\beta\eta)_{ijm,p} = 0$, $\sum_p(\alpha\beta\eta)_{ijm,p} = 0$.

The hypotheses being tested in this analysis are: H_o: $\eta_p=0$ - no main effect of the initial concentration, H_o: $(\alpha\beta)_{i,m}=0$ - no interaction between location and treatment, Ho: $(\beta\eta)_{m,p}=0$ - no interaction between treatment and initial concentration, H_o: $(\alpha\eta)_{i,p}=0$ - no interaction between location and initial concentration, and H_o: $(\alpha\beta\eta)_{i,m,p}=0$ -no interactive effects between all three; location, treatment, and initial concentration on the mass transfer coefficient.

The variables temperature, location, and treatment were analyzed using the full data set. The statistical model used for determining the statistical significance of these variables is shown in Equation A4.

$$\text{Model: } E(t)=(\mu+\alpha_1 X^L_1+\alpha_2 X^L_2+\beta_1 X^I_1+\beta_2 X^I_2+\tau X^T+(\alpha\beta)_{1,1}X^L_1 X^I_1+ \quad \text{Equation A4}$$
$$+(\alpha\beta)_{1,2}X^L_1 X^I_2+(\alpha\beta)_{2,1}X^L_2 X^I_1+(\alpha\beta)_{2,2}X^L_2 X^I_2+(\alpha\tau)_{1,1}X^L_1 X^T+$$
$$+(\alpha\tau)_{2,1}X^L_2 X^T+(\beta\tau)_{1,1}X^I_1 X^T+(\beta\tau)_{2,1}X^I_2 X^T+(\alpha\beta\tau)_{1,1,1}X^L_1 X^I_1 X^T+$$
$$+(\alpha\beta\tau)_{1,2,1}X^L_1 X^I_2 X^T+(\alpha\beta\tau)_{2,1,1}X^L_2 X^I_1 X^T+(\alpha\beta\tau)_{2,2,1}X^L_2 X^I_2 X^T)t$$

where: E(t) = the concentration at time t
u = the average mass transfer coefficient
α_1, α_2, β_1, β_2, τ represent the main effects of location, treatment, and temperature respectively on the mass transfer coefficient
$(\alpha\beta)_{1,1}$, $(\alpha\beta)_{1,2}$, $(\alpha\beta)_{2,1}$, $(\alpha\beta)_{2,2}$, $(\alpha\tau)_{1,1}$, $(\alpha\tau)_{2,1}$, $(\beta\tau)_{1,1}$, $(\beta\tau)_{2,1}$ represent the interactions of location*treatment, location*temperature, and treatment*temperature
$(\alpha\beta\tau)_{1,1,1}$, $(\alpha\beta\tau)_{1,2,1}$, $(\alpha\beta\tau)_{2,1,1}$, $(\alpha\beta\tau)_{2,2,1}$ represents the three way interactions of location*treatment*temperature
t = time

The following constraints have been placed on the analysis: $\sum_i\alpha_i = 0$, $\sum_m\beta_m = 0$, $\sum_n\tau_n = 0$, $\sum_i(\alpha\beta)_{i,m} = 0$, $\sum_m(\beta\tau)_{m,n} = 0$, $\sum_i(\alpha\tau)_{i,n} = 0$, $\sum_m(\alpha\beta)_{i,m} = 0$, $\sum_n(\beta\tau)_{m,n} = 0$, $\sum_n(\alpha\tau)_{i,n} = 0$, $\sum_i(\alpha\beta\tau)_{i,m,n} = 0$, $\sum_m(\alpha\beta\tau)_{i,m,n} = 0$, $\sum_n(\alpha\beta\tau)_{i,m,n} = 0$.

The hypotheses being tested in this analysis are: H_o: $\tau_n=0$ - no main effect of temperature, H_o: $\alpha_i=0$ - no main effect of location , H_o: $\beta_m=0$ - no main effect of treatment, H_o: $(\alpha\beta)_{i,m}=0$ - no interaction between location and treatment, Ho: $(\beta\tau)_{m,n}=0$ - no interaction between treatment and temperature, H_o: $(\alpha\tau)_{i,n}=0$ - no interaction between location and temperature, and H_o: $(\alpha\beta\tau)_{i,m,n}=0$ -no interactive effects between all three; location, treatment, and temperature on the mass transfer coefficient.

The variable nitrification inhibitor was analyzed using the data subset created by holding circulation as yes, tank being circulated. The statistical model used for determining the statistical significance of this variable is shown in Equation A5.

Model: $E(t)=(\mu+\alpha_1 X^L{}_1+\alpha_2 X^L{}_2+\lambda X^{In}+\tau X^T+(\alpha\lambda)_{1,1}X^L{}_1X^{In}+$ Equation A5
$+(\alpha\lambda)_{2,1}X^L{}_2X^{In}+(\alpha\tau)_{1,1}X^L{}_1X^T+$
$+(\alpha\tau)_{2,1}X^L{}_2X^T+(\lambda\tau)_{1,1}X^{In}X^T+(\alpha\lambda\tau)_{1,1,1}X^L{}_1X^{In}X^T+$
$+(\alpha\lambda\tau)_{2,1,1}X^L{}_2X^{In}X^T)t$

where: E(t) = the concentration at time t
u = the average mass transfer coefficient
α_1, α_2, λ_1, τ represent the main effects of location, nitrification inhibitor, and temperature respectively on the mass transfer coefficient
$(\alpha\lambda)_{1,1}$, $(\alpha\lambda)_{2,1}$, $(\alpha\tau)_{1,1}$, $(\alpha\tau)_{2,1}$, $(\lambda\tau)_{1,1}$ represent the interactions of location*nitrification inhibitor, location*temperature, and nitrification inhibitor*temperature
$(\alpha\lambda\tau)_{1,1,1}$, $(\alpha\lambda\tau)_{2,1,1}$ represents the three way interactions of location*nitrification inhibitor*temperature
t = time

The following constraints have been placed on the analysis: $\sum_i\alpha_i = 0$, $\sum_k\lambda_k = 0$, $\sum_n\tau_n = 0$, $\sum_i(\alpha\lambda)_{i,k} = 0$, $\sum_k(\lambda\tau)_{k,n} = 0$, $\sum_i(\alpha\tau)_{i,n} = 0$, $\sum_k(\alpha\lambda)_{i,k} = 0$, $\sum_n(\lambda\tau)_{k,n} = 0$, $\sum_n(\alpha\tau)_{i,n} = 0$, $\sum_i(\alpha\lambda\tau)_{i,k,n} = 0$, $\sum_k(\alpha\lambda\tau)_{i,k,n} = 0$, $\sum_n(\alpha\lambda\tau)_{i,k,n} = 0$.

The hypotheses being tested in this analysis are: H_o: $\lambda_k=0$ - no main effect of nitrification inhibitor, H_o: $(\alpha\lambda)_{i,k}=0$ - no interaction between location and nitrification inhibitor, Ho: $(\lambda\tau)_{k,n}=0$ - no interaction between nitrification inhibitor and temperature, H_o: $(\alpha\tau)_{i,n}=0$ - no interaction between location and temperature, and H_o: $(\alpha\lambda\tau)_{i,k,n}=0$ -no interactive effects between all three; location, nitrification inhibitor, and temperature on the mass transfer coefficient.

The variable circulation was analyzed using the data subset created when the nitrification inhibitor was not present. The statistical model used for determining the statistical significance of this variable is shown in Equation A6.

$$\text{Model: } E(t)=(\mu+\alpha_1 X^L{}_1+\alpha_2 X^L{}_2+\varepsilon X^C+\tau X^T+(\alpha\varepsilon)_{1,1}X^L{}_1X^C+ \quad \text{Equation A6}$$
$$+(\alpha\varepsilon)_{2,1}X^L{}_2X^C+(\alpha\tau)_{1,1}X^L{}_1X^T+$$
$$+(\alpha\tau)_{2,1}X^L{}_2X^T+(\varepsilon\tau)_{1,1}X^CX^T+(\alpha\varepsilon\tau)_{1,1,1}X^L{}_1X^CX^T+$$
$$+(\alpha\varepsilon\tau)_{2,1,1}X^L{}_2X^CX^T)t$$

where: E(t) = the concentration at time t
u = the average mass transfer coefficient
α_1, α_2, ε, τ represent the main effects of location, circulation, and temperature respectively on the mass transfer coefficient
$(\alpha\varepsilon)_{1,1}$, $(\alpha\varepsilon)_{2,1}$, $(\alpha\tau)_{1,1}$, $(\alpha\tau)_{2,1}$, $(\varepsilon\tau)_{1,1}$ represent the interactions of location*circulation, location*temperature, and circulation*temperature
$(\alpha\varepsilon\tau)_{1,1,1}$, $(\alpha\varepsilon\tau)_{2,1,1}$ represents the three way interactions of location*circulation*temperature
t = time

The following constraints have been placed on the analysis: $\sum_i\alpha_i = 0$, $\sum_j\varepsilon_j = 0$, $\sum_n\tau_n = 0$, $\sum_i(\alpha\varepsilon)_{i,j} = 0$, $\sum_j(\varepsilon\tau)_{j,n} = 0$, $\sum_i(\alpha\tau)_{i,n} = 0$, $\sum_j(\alpha\varepsilon)_{i,j} = 0$, $\sum_n(\varepsilon\tau)_{j,n} = 0$, $\sum_n(\alpha\tau)_{i,n} = 0$, $\sum_i(\alpha\varepsilon\tau)_{i,j,n} = 0$, $\sum_j(\alpha\varepsilon\tau)_{i,j,n} = 0$, $\sum_n(\alpha\varepsilon\tau)_{i,j,n} = 0$.

The hypotheses being tested in this analysis are: H_o: $\varepsilon_j=0$ - no main effect of circulation, H_o: $(\alpha\varepsilon)_{i,j}=0$ - no interaction between location and circulation, Ho: $(\varepsilon\tau)_{j,n}=0$ - no interaction between circulation and temperature, H_o: $(\alpha\tau)_{i,n}=0$ - no interaction between location and temperature, and H_o: $(\alpha\varepsilon\tau)_{i,j,n}=0$ -no interactive effects between all three; location, circulation, and temperature on the mass transfer coefficient.

In-Stream Background N^{15} and O^{18}

The in-stream background N^{15} and O^{18} method does not lend itself to statistical analysis.

N^{15} Enrichment

The N^{15} enrichment method was statistically analyzed in the same way the nitrate depletion in in-stream tanks method was to be analyzed for the significance of location.

Nitrate Diffusion Calculations

The nitrate diffusion method allows for the main effects of location and temperature but not their associated interaction on the diffusion-calculated mass transfer coefficient to be analyzed. Interactions cannot be analyzed, due to few degrees of freedom. The statistical model for determining the significance of the differences between the locations where the cores were taken on the mass transfer coefficient calculations is shown in Equation A7.

$$\text{Model: } E(t)=(\mu+\alpha_1 X^L{}_1+\alpha_2 X^L{}_2)t \qquad \text{Equation A7}$$

where: $E(t)$ = the concentration at time t
u = the average mass transfer coefficient
α_1, α_2 represent the main effects of location on the mass transfer coefficient
t = time

The following constraints have been placed on the analysis: $\sum_i \alpha_i = 0$.

The Hypothesis being tested is; H_o: $\alpha_i=0$ - no main effect of location on the diffusion calculated mass transfer coefficient.

The statistical model for determining the significance of the differences between the temperatures of the mass transfer coefficient calculations is shown in Equation A8.

Model: $E(t)=(\mu+\tau X^T)t$ Equation A8

where: E(t) = the concentration at time t
u = the average mass transfer coefficient
τ represent the main effects of temperature on the mass transfer coefficient
t = time

The following constraints have been placed on the analysis: $\sum_n \tau_n = 0$.

The Hypothesis being tested is; H_o: $\tau_i=0$ - no main effect of temperature on the diffusion calculated mass transfer coefficient.

Mass Balance

The mass balance method does not lend itself to statistical analysis.

Modeling

A simple standard deviation will be conducted on the modeling results, as there is no variation on location or depth and the temperature was averaged over long periods of time.

Statistics of Comparing Nitrate Depletion in the Field, Nitrate Depletion in the Lab, Diffusion Calculation, and Modeling Methods

The procGLM procedure will be used to compare the mass transfer coefficients determined in the field study and the three treatments of the lab study. The main effects of treatment and location, along with their associated interaction, were analyzed using field data normalized to 8^oC and lab data subset created when temperature was held at 8^oC. The statistical model for determining the significance of the differences between the locations and treatments on the mass transfer coefficient calculations is shown in Equation A9.

Model: $E(t)=(\mu+\alpha_1 X^L{}_1+\alpha_2 X^L{}_2+\beta_1 X^{IC}{}_1+\beta_2 X^{IC}{}_2+\beta_3 X^{IC}{}_2+$ Equation A9
$+\alpha_1\beta_1 X^L{}_1 X^{IC}{}_1+\alpha_1\beta_2 X^L{}_1 X^{IC}{}_2+\alpha_1\beta_3 X^L{}_1 X^{IC}{}_3+\alpha_2\beta_1 X^L{}_2 X^{IC}{}_1+$
$+\alpha_2\beta_2 X^L{}_2 X^{IC}{}_2+\alpha_2\beta_3 X^L{}_2 X^{IC}{}_3)t$

where: E(t) = the concentration at time t
u = the average mass transfer coefficient
α_1, α_2, β_1, β_2, β_3 represent the main effects of location and treatment on the mass transfer coefficient
$\alpha_1\beta_1$, $\alpha_1\beta_2$, $\alpha_1\beta_3$, $\alpha_2\beta_1$+, $\alpha_2\beta_2$, $\alpha_2\beta_3$ represent the interactions between location and treatment
t = time

The following constraints have been placed on the analysis: $\sum_m\beta_m = 0$, $\sum_i(\alpha\beta)_{i,m}=0$, $\sum_m(\alpha\beta)_{i,m}=0$.

The Hypotheses being tested are; H_o: $\alpha_I=0$ - no main effect of location on the mass transfer coefficient, H_o: $\beta_m=0$ - no main effect of treatment on the mass transfer coefficient. and H_o: $(\alpha\beta)_{i,m}=0$ no interaction between the treatment and location.

The same procedure will be used to compare the modeled mass transfer coefficient results to the results from the two nitrate depletion methods. The variation of the analysis is that only the treatment mass transfer coefficients will be compared (no location or temperature main effects or interations with treatment). The statistical model for determining the significance of the differences between the treatments on the mass transfer coefficient calculations is shown in Equation A10.

Model: $E(t)=(\mu+\beta_1 X^I{}_1+\beta_2 X^I{}_2+\beta_3 X^I{}_2)t$ Equation A10

where: E(t) = the concentration at time t
u = the average mass transfer coefficient
β_1, β_2, β_3 represent the main effects of treatment on the mass transfer coefficient
t = time

The following constraints have been placed on the analysis: $\sum_m\beta_m = 0$.

The Hypothesis being tested is, H_o: β_m=0 - no main effect of treatment on the mass transfer coefficient.

The procUNIVARIATE procedure was used to compare the diffusion study mass transfer coefficients to the field and lab mass transfer coefficients. This procedure treats the calculated diffusion mass transfer coefficients as a fixed known mean and as such compares the differences between this "fixed mean" and the measures data, the residuals, of the field or lab studies. The analysis results in paired t-tests. The t-test conducted between the diffusion study and the field study compares the average diffusion-calculated mass transfer coefficient to the average field-determined mass transfer coefficient. The lab study consisted of three t-tests: the three lab treatments compared to their associated diffusion-calculated mass transfer coefficients - ex. treatment one average (Tanks 1, 2, and 3) to the diffusion calculated average for Tanks 1, 2, and 3.

This same procedure will be used to compare the modeling methods results to the diffusion-calculated results. The only difference is that only the overall mass transfer coefficients will be compared (diffusion average calculated compared to the modeled average mass transfer coefficient).

Appendix B

Method of Normalizing Nitrate Removal Rates to a Similar Temperature for Statistical Comparisons

To normalize the data, the mass of nitrate removed at each measured concentration was calculated using the following method.

$$R = ([C_o]-[C_1])*A*D \qquad \text{Equation B.1}$$

where: R = mass of nitrate removed (mg)
$[C_o]$ = initial nitrate concentration (mg/m^3)
$[C_1]$ = final nitrate concentration (mg/m^3)
A = sediment surface area (m^2)
D = depth of the water column (m)

The mass of nitrate removed (R) was then corrected for temperature using Equation B.2.

$$D_{rT2} = D_{rT1} * C_{T1-T2} \qquad \text{Equation B.2}$$

where: D_{rT1} =denitrification rate at temperature T1 ($mg/m^2/sec$)
C_{T1-T2} = correction factor for the differences in temperature (unitless)
D_{rT2} = denitrification rate at temperature T2 ($mg/m^2/sec$).

The temperature-corrected mass removal was then used in Equation B.3 to determine the mass transfer coefficient (ρ) for each concentration.

$$\rho = RR/[C] \qquad \text{Equation B.3}$$

where: ρ = mass transfer coefficient (m/day)
RR = measured nitrate removal rate ($mg/m^2/day$)
[C] = measured water column nitrate concentration (mg/m^3)

This equation could be used because depths were normalized to 50 cm for all runs. The mass transfer coefficients were then averaged over concentrations for an average mass transfer coefficient (ρ). An average was used due to slight variations caused by the use of measured field data, which is affected by many environmental factors that can change over the period of time of a run.

Appendix C

Nitrate, Ammonium, and Phosphate Distribution in Sediment Pore Water and Water Column

Methods

A sediment pore water sampler developed by Hesslein (1976) and modified by Birgand (2000) was used to determine concentration gradients of nitrate, ammonium, and phosphate with respect to depth within the sediment and water column (Figure C.1). The sampler itself is composed of a Plexiglas block 10cm wide, 2.5 cm thick, and 37 cm long (Figure C.1) (Birgand, 2000). The first 32 cm has 0.5 cm slots located every 1 cm along its length, and the last 7 cm is tapered to allow for installation into the sediment with as little disturbance to the sediment as possible. The slots are covered on both sides to form an isolated chamber (approximately 5 ml in volume) with a permeable membrane (SPECTRA/POR® Membrane, MWCO: 6-8,000) that allowed diffusion of ions into the sampler chambers through osmosis. The sampler is assembled in a bath of distilled water prior to use. This allows the chambers to be filled with distilled water while assembling as well as excluding air bubbles from the sampling chambers. After assembly, the samplers are kept in a sealed container of distilled water to keep them from drying and accumulating dissolved oxygen from the atmosphere.

The sampler was constructed to be placed into the sediment with a small portion protruding into the water column along the surface of the sediment layer. Tanks 3, 6, 2, and 5 were used in the undisturbed core study in the lab so that both the circulated and uncirculated treatments were represented. Both the circulated and uncirculated tanks were sampled

simultaneously. The samplers were placed with the first 15 cm in the sediment (to the bottom of the tank) and the remaining 15 cm extending into the water column. Once installed, diffusion continues until concentrations inside the chambers are equal to those outside each chamber at their respective depth (Hesslein, 1976, determined this to take about a week), resulting in an representative ion concentration of the sediment pore water and the water column at the depth of each chamber. Samples were removed by use of a syringe utilizing a 1 mm (B-D 20g1 PrecisionGlide®) needle. The needle was inserted into a sample chamber through the membrane and the 5 mm sample was drawn out into the syringe and transferred to a vial, labeled, and placed in a cooler with ice. The syringe and needle were rinsed with distilled water between each chamber sampling. Samples were stored at 8^{o}C overnight and analyzed the following day (sample filtering is unnecessary as the membrane prevents particles of much smaller size than the filtering removes (0.45 μm) from entering the sample chamber).

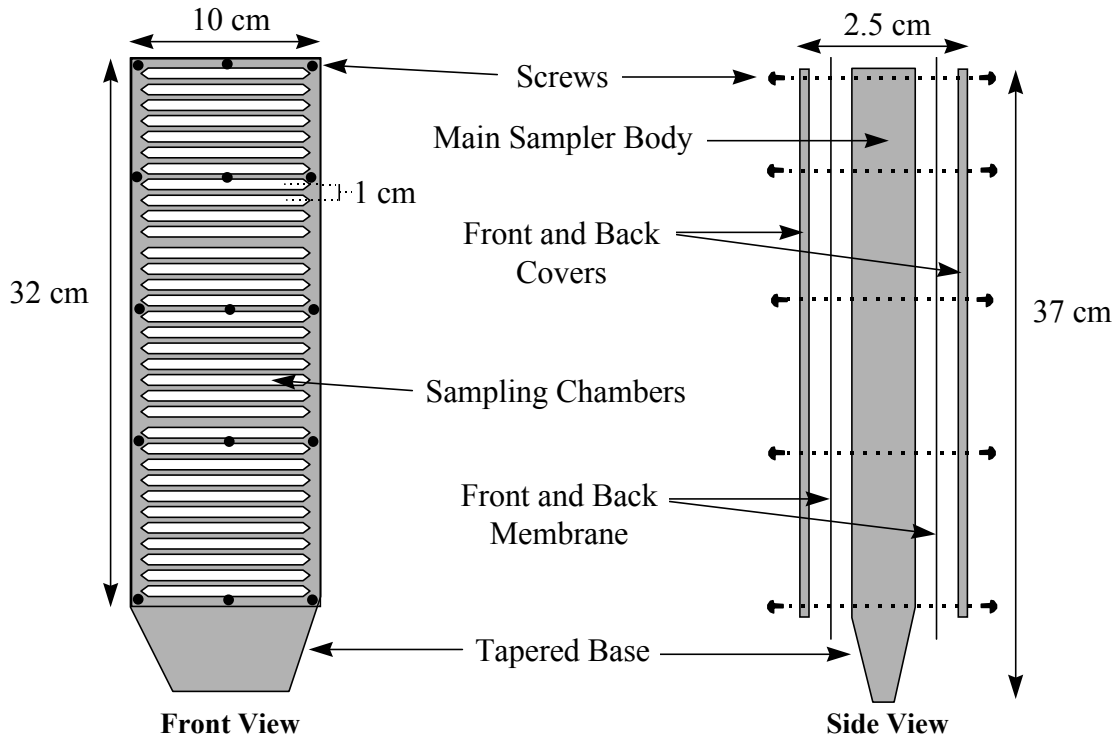

Figure C.1. Sediment pore water sampler.

Results and Discussion

Water column nitrate and ammonium concentration profiles can be found in Figure C.2. Conditions for each profile can be found in Table C.1. Phosphate concentrations were always below detection (<0.01 mg/L) throughout all profiles, thus they were not incorporated into the concentration profile plots of Figure C.2.

Table C.1. Water column parameters at times of pore water sampler use.

Tank[1]	Circulated	Water Column Concentration NO_3-N (mg/L)	Water Column Concentration NH_4-N (mg/L)	Temperature (^oC)	Dissolved Oxygen (mg/L)	pH[2]
3	No	3.53	1.0	21	3	5.25
6	Yes	4.35	0.24	21	9	5.31
2(a)[3]	No	5.18	1.41	8	6	-
5(a)[3]	Yes	4.41	0.68	8	10	-
2(b)[3]	No	3.38	1.50	8	8	-
5(b)[3]	Yes	2.57	1.10	8	10	-

[1]Tanks 3 and 6, 2(a) and 5(a), and 2(b) and 5(b) were run concurrently.
[2]pH values for tanks 2 and 5 are unavailable due to probe malfunction.
[3] a and b designations indicate different runs using same tanks.

Water column nitrate and ammonium concentrations remained constant with depth in the water column profile (0 cm is considered the surface of the litter layer; values greater than 0 cm are considered the water column) for all six of the concentration distributions measured regardless of temperature, circulation, and dissolved oxygen levels (Figure C.2) (Table C.1). This is expected in the circulated tanks (B, D, and F of Figure C.2), as the water columns of these tanks were continually mixed, making concentration gradient formation impossible to form in their water columns. The lack of a nitrate concentration gradient being formed in the uncirculated tanks (A, C, and E of Figure C.2) can be traced to two factors. First, concentration gradients are only formed where the majority of the denitrification occurs, in the deeper anaerobic portion of the sediments (reported by Tisdale et al, 1993). This is due to denitrification being inhibited in the water column by the presence of dissolved oxygen (Table C.1) as well as the minimal population of denitrifiers residing within the water column. Second, diffusion within a pure water medium (such as the water column) is faster than diffusion in sediments (Domenico and Schwartz, 1998). This means any nitrates

diffusing into the sediment will be replaced from further up in the water column more quickly than they move into the sediment, resulting in no gradients forming within the water column. Therefore, diffusion within the water column is sufficient to keep NO_3-N from stratifying within the water column.

The lack of an ammonium concentration gradient being formed in the water column of the uncirculated tanks (A, C, and E of Figure C.2) can also be traced to the same two factors — the lack of concentration gradient within the water column, and diffusion rates within the water column being higher than in the sediments. In the case of ammonium, gradients form due to nitrification, which primarily occurs in the aerobic upper portion of the sediment (all papers reviewed to this point only discuss nitrification occurring in the upper aerated portion of the sediment of aquatic systems, not in the water column). Nitrification may occur in the water column, but only to a negligible degree, as the nitrifying organisms reside primarily in the aerobic portion of the sediment. Ammonium diffusion, as discussed for nitrate, is faster within a pure water medium (such as the water column) than in sediments, resulting in a non-stratified water column.

Differences in the nitrate and ammonium profiles between the circulated tanks and uncirculated tanks start appearing just below the surface of the litter layer (a 5 cm layer overlaying the sediment).

In the circulated tanks, the concentrations of nitrate and ammonium remain constant, equal to that of the water column concentration throughout the litter layer as well as in the upper layer of the sediment to an average depth of 9 cm (depths are measured from the surface of the litter layer) (B, D, and F of Figure C.2). Below 9 cm, nitrate concentrations begin to decrease with depth in all three circulated tank profiles to 0 mg/L at an average

depth of 12 cm, while ammonium concentrations begin to increase with depth in the first circulated tank profiles (B of Figure C.2) and remain constant throughout the entire depth of the sediment in Tank profiles D and F of Figure C.2. In contrast, the uncirculated tanks all showed a decrease in nitrate concentration just below the surface of the litter layer (0 cm), reaching a concentration of 0 mg/L at an average depth of 10 cm, while all the ammonium concentration profiles remained constant with depth throughout the sediment, equal to that of the water column (A, C, and E of Figure C.2).

The constant nitrate and ammonium concentrations throughout the first 9 cm of depth in the circulated tanks is due to the circulated water within the water column also moving through the loose mat of leaves, twigs, branches, etc. of the litter layer and the large macropores of the upper sediment, which also includes decomposed leaves, twigs, branches, etc. This is consistent with Hynes' (1983) description of the hyporheic zone having advection as its primary method of transport. The introduction of dissolved oxygen into the upper portion of the sediment also inhibits denitrification driving the process deeper into the sediment. The introduction of dissolved oxygen to this zone also removes any oxygen limitations on nitrification.

The presence of dissolved oxygen in the litter layer and upper sediment, coupled with higher temperature of the circulated 21^{o}C run (B in Figure C.2), increase nitrification by 2.8-fold over that of mineralization (Figure D.2), resulting in a net removal of ammonium from the upper 9 cm of the sediment and litter level (reported by Tisdale et al, 1993). This removal rate is high enough to also decrease the high concentration of ammonium in the water column resulting from the study design, as described in Section 3.2 – Denitrification. The nitrates formed through nitrification are then circulated along with the pore water closer to

the denitrifying zone, where they diffuse into that zone and are denitrified at a rapid rate due to the near-optimal temperature.

At a depth of about 9 cm, the organic materials (leaves, twigs, etc.) become more decomposed, resulting in fewer macropores. This is the bottom range of advective transport and the beginning of diffusion transport. The reduced number of macropores decreases the potential diffusion rate of nitrate and dissolved oxygen below 9 cm. As the dissolved oxygen diffuses into this layer, it is utilized by nitrifiers and decomposers, which causes a decrease in dissolved oxygen concentration with depth (Kaushik et al, 1981). More anaerobic conditions lead to an increase in the denitrification rate with depth, resulting in the observed decrease in nitrate concentrations with depth. The decrease in dissolved oxygen with depth also causes a reduction in nitrification with depth, resulting in the observed increase in the ammonium concentration with depth in the concentration profile of the run shown in B of Figure C.2.

The changes in concentrations over the 3 cm change in depth create gradients (upward for ammonium and downward for both dissolved oxygen and nitrate) that drive the nitrification and denitrification processes. The thickness of this gradient layer is primarily determined by the ability of the compounds to diffuse. Increases in the number of macropores will broaden this zone and make it thicker, as observed in the uncirculated tank concentration profiles (A, C, and E of Figure C.2).

The nitrate reduction starting at the surface of the litter layer of the uncirculated tanks is due to the lack of advective transport in the litter layer and upper sediment. Nitrate and dissolved oxygen movement into the litter layer and sediment is now limited to diffusion. This causes dissolved oxygen levels to start to decrease just below the litter layer surface.

The presence of macropores as described previously allows the nitrate and dissolved oxygen to diffuse more quickly and more deeply than in a less porous medium (yet much more slowly than with advection), allowing nitrate and dissolved oxygen to reach almost as deep into the sediment in the uncirculated tanks as in the circulated tanks (though at lower concentrations). However, as depth increases, more of the diffusing dissolved oxygen is consumed by nitrifiers and decomposers (Kaushik et al, 1981), creating a concentration gradient of decreasing concentration with depth. Along this gradient, denitrification increases as conditions become more anaerobic with depth. The gradient is lower due to the wider range of this zone (from 0 cm to 10 cm for the uncirculated tanks vs. from 9 cm to 11 cm for the circulated tanks). The lack of nitrate below 11 cm is due to lower potential diffusion rates resulting from the reduced number of macropores present at lower depths.

The constant ammonium concentration profile exhibited by run A (Figure C.2) is most likely a combination of the effect of non-circulation, low dissolved oxygen levels, and high initial ammonium concentrations resulting from the study setup as described in Section 3.2 - Denitrification. In run A (Figure C.2), dissolved oxygen levels are low (approximately 3.0 mg/L) due to the lack of circulation and the warm temperature (21^{o}C) that defined this run. Warmer water not only has a lower ability to retain dissolved oxygen but also promotes microbial activity, which increases oxygen demand. These factors both act to reduce the dissolved oxygen content of the water column. The low oxygen concentration for this run decreases the potential for nitrification to occur, while having little effect on the mineralization rate. The equilibrium between the two results in a higher NH_4-N concentration than in circulated runs, which, coupled with the high initial NH_4-N concentration, created a homogeneous concentration profile throughout the water column

and the sediment at the beginning of the run. This homogeneous concentration profile never changed, due to the equilibrium between nitrification and mineralization. The two ammonium concentration profiles (D and F of Figure C.2) demonstrate a constant concentration pattern due to the lower temperature. The mineralization and nitrification rates are about equal at 8^{o}C (Figure D.2), causing an equilibrium between the two. From below 12 cm to the bottom of the tank, the sediment is entirely anaerobic, with only denitrification and mineralization occurring, resulting in the presence of only ammonium at that depth.

The two profiles (C and E of Figure C.2) also have homogeneous ammonium concentration profiles. This can be attributed to diffusion as the only transport mode and the decrease in temperature. Even though the water column dissolved oxygen level is higher for the two concentration profiles at 8^{o}C (6 mg/L and 8 mg/L respectively) than for the previous profile at 21^{o}C (3 mg/L), the amount entering the litter layer and sediment is still low due to diffusion being the main mode of transport. As described above, diffusion is a much slower mode of transport than advection, and it is dramatically reduced when it is occurring in a porous medium. This results in less dissolved oxygen entering the sediment, even though it can move deeper into the sediment due to the presence of macropores. Nitrification rates also decrease as temperatures decrease, as previously described. These two factors combined could result in an equilibrium between nitrification and mineralization, which would produce a higher NH_4-N concentration than in the circulated runs (Figure D.2).

Conclusions

The nitrate profiles presented here are representative of water column and sediment profiles found in other studies (e.g. Birgand, 2000; Elliott and Brooks, 1997). Nitrate within the water column remains constant due to advective and diffusive mixing. Within the

sediment, nitrate begins to decline at the surface of the litter layer in uncirculated systems as diffusion-supplied dissolved oxygen is utilized by nitrifiers and decomposers, while nitrate is utilized by denitrifiers. In circulated systems, nitrate and dissolved oxygen penetrate deeper into the sediment via advection, resulting in constant levels of nitrate and dissolved oxygen deeper in the sediments. Below the aerobic layer, anaerobic conditions obtain, resulting in total removal of nitrates.

Ammonium profiles developed here at 8^{o}C and at 21^{o}C in the uncirculated tanks could not be compared to other studies, as this study started with abnormally high ammonium concentrations in the water column (see Section 3.2 – Denitrification). The ammonium concentration profile at 21^{o}C when circulated was the similar to those developed in other studies (e.g. Birgand, 2000). Ammonium within the water column remained constant due to advective and diffusive mixing. Within the sediment, ammonium remained constant because mineralization and nitrate were at an equilibrium, due to low temperature in all of the 8^{o}C profiles and due to low dissolved oxygen levels in the uncirculated 21^{o}C profile. The ammonium concentrations rose with depth in the circulated 21^{o}C profile. The nitrification rate exceeded the mineralization rate by 2.8-fold within the upper 9 cm of sediment due to the high dissolved oxygen levels caused by advective mixing. Deeper in the sediment, nitrification became oxygen-limited, which reduced the nitrification rate with depth, resulting in higher ammonium levels with depth.

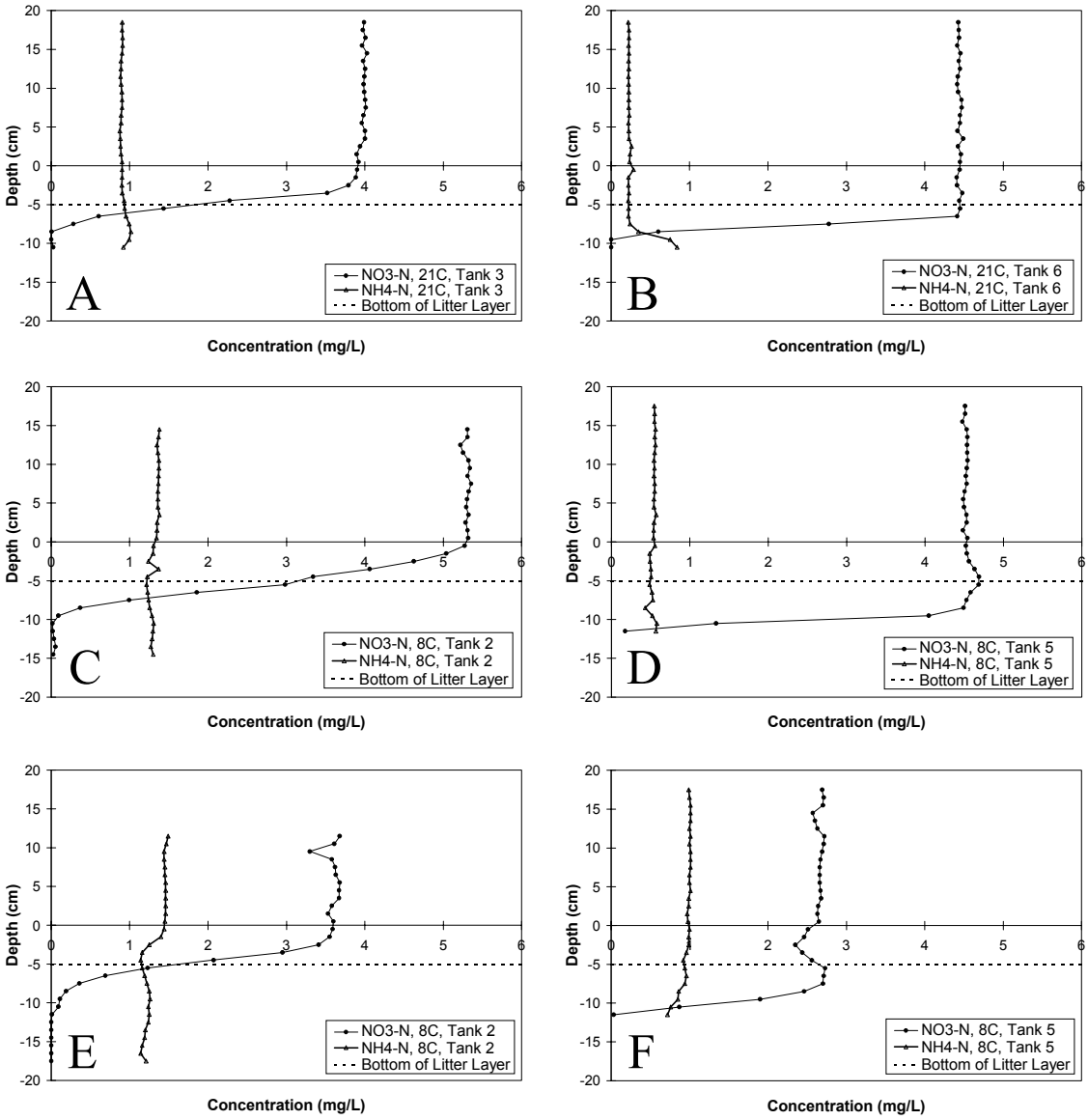

Figure C.2. Nitrate profiles in undisturbed core lab study for: (A) Tank 3, uncirculated, @ 21°C, (B) Tank 6, circulated, @ 21°C, (C) Tank 2, uncirculated, @ 8°C, (D) Tank 5, circulated, @ 8°C, (E) Tank 2, uncirculated, @ 8°C, and (F) Tank 5, circulated, @ 8°C (all without a nitrification inhibitor present).

References

Birgand, F. Quantification and Modeling of In-Stream Processes in Agricultural Canals of the Lower Coastal Plain. Dissertation. 469pp, North Carolina State University, Raleigh, 2000.

Domenico, P.A., and F.W. Schwartz. 1990. Physical and Chemical Hydrogeology. 2nd Ed. John Wiley & Sons., Inc., New York.

Elliott, A.H., and N.H. Brooks. 1997. Transfer of non-sorbing solutes to a streambed with bed forms: Laboratory experiments. Wat. Res. Res. 33(1): 137-151.

Hesslein, R.H. 1976. An in situ sampler for close interval pore water studies. Limnol. Oceanogr. 21: 912-914.

Hynes, H.N.B. 1983. Groundwater and stream ecology. Hydrobiologia. 100: 93-99.

Kaushik, N.K., J.B. Robinson, W.N. Stammers, and H.R. Whiteley. 1881. Aspects of Nitrogen Transport and Transformation in Headwater Streams. In: M.A. Lock and D.D. Williams, eds. Perspectives in Running Water Ecology. Plenum Press, New York, pp.113-139.

Tisdale, S.L., W.L. Nelson, J.D. Beaton, and J.L. Havlin. 1993. Soil Fertility and Fertilizers. 5th ed. MacMillan Pub. Co., New York.

Appendix D

Mineralization and Nitrification

Methods

Mineralization and nitrification were estimated using data from the previously described undisturbed core lab study. The ammonium concentrations of two of the tanks, one with a nitrification inhibitor (Tank 7) and one with no nitrification inhibitor (Tank 4), were compared over the five previously described denitrification study runs. Tanks 8 and 9 also contained nitrification inhibitor but were not used for this portion of the study, due to the low mass transfer coefficient values as described in Section 3.2 – Denitrification. The premise for this study is that any increase in ammonium within the water column over time in the tank with the nitrification inhibitor is due only to mineralization within the sediment. Stratification within the sediment is not expected, due to the results of the concentration profiles from Appendix C – Nitrate, Ammonium, and Phosphate Distribution in the Sediment Pore Water and Water Column. These results show that a constant ammonium concentration is expected within the entire profile when nitrification is minimized. The slope of ammonium concentration vs. time line (dC/dt_{Min}) would represent the mineralization rate under each temperature. Likewise, the slope of the ammonium concentration vs. time line (dC/dt_{Net}) for the tank with no nitrification inhibitor would represent the net ammonium change due to the interaction of mineralization and nitrification. The difference in these lines represents the amount of ammonium that has been nitrified (dC/dt_{Nit}) over the period.

Results and Discussion

The measured ammonium concentrations were converted to total ammonium loads

per square meter of sediment surface and plotted in Figure D.1 (A - D were conducted at 8°C, and E was conducted at 21°C). Individual rates of mineralization, nitrification, and net ammonium removal for each run can be found in Table D.1. Average mineralization and nitrification rates for both temperatures are shown in Figure D.2 (Average mineralization and nitrification rates for 8°C were determined by averaging the slopes for the runs.)

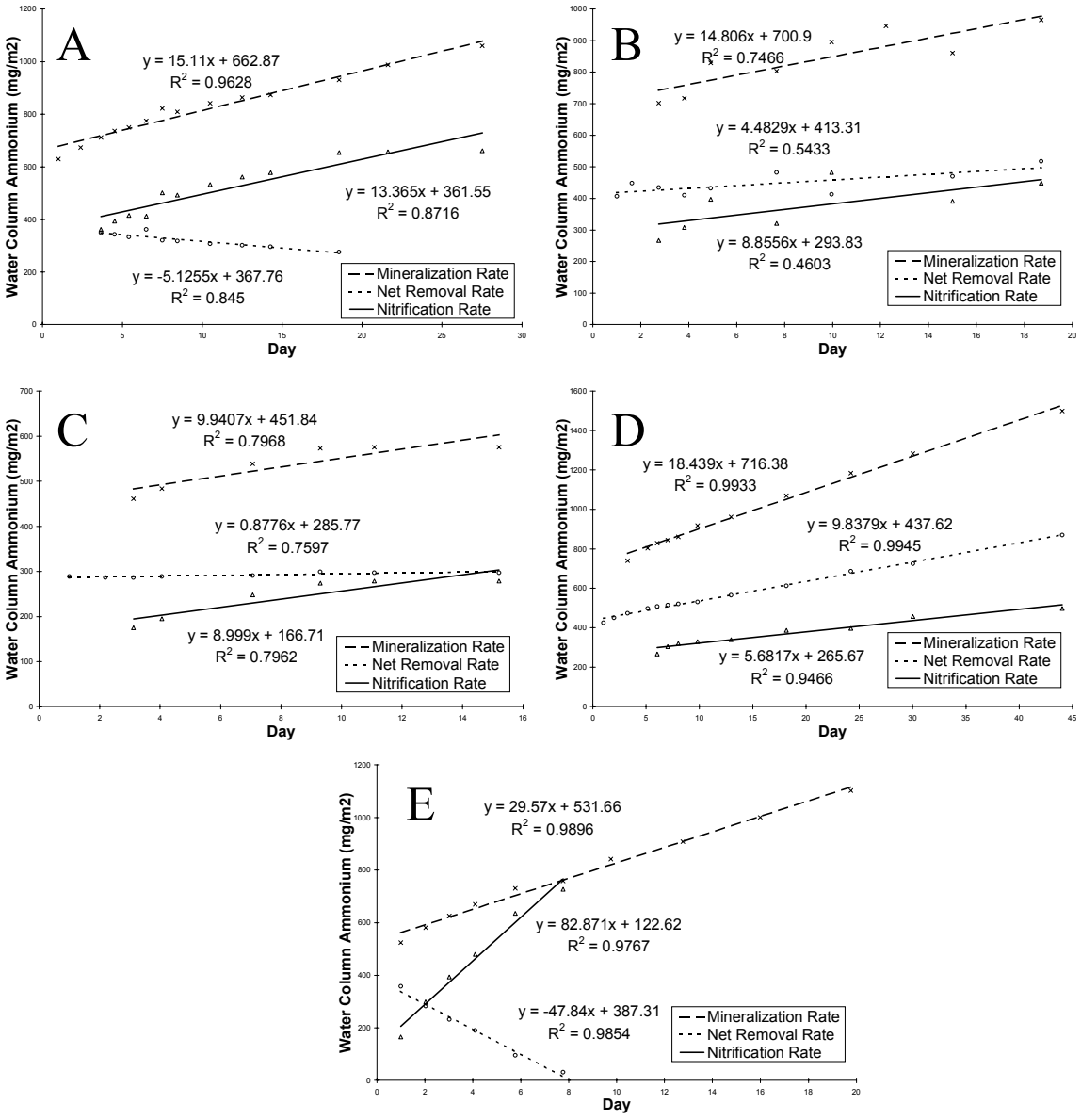

Figure D.1. Mineralization, nitrification, and ammonium removal rates for individual runs at 8°C (A-D) and 21°C (E). In Figure D.1 A to E: x = treatment with nitrification inhibitor present, o = treatment without nitrification inhibitor present, and ? = the difference between the two treatments.

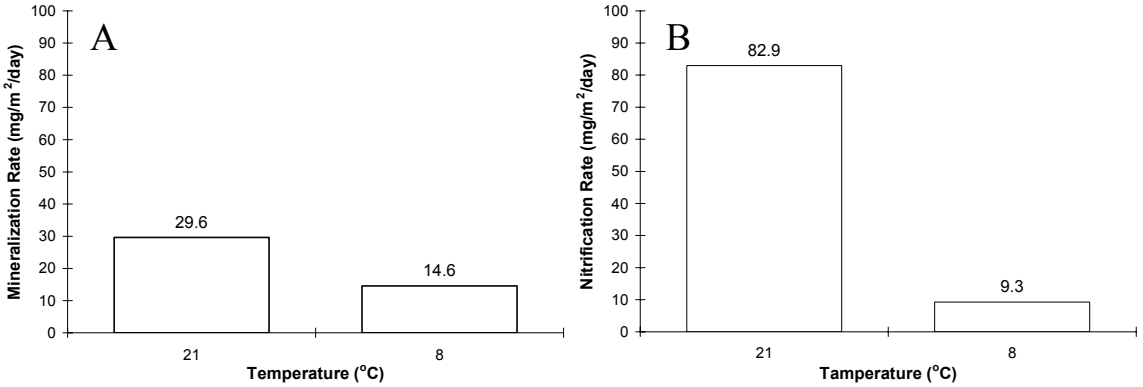

Figure D.2. Average rates of mineralization (A) and nitrification (B) at 8°C and 21°C.

The mineralization rate measured in Tank 7 for 21°C was 29.6 mg/m^2/d, while at 8°C it was 14.6 mg/m^2/d. The nitrification rate — the difference between the measured ammonium concentrations of Tanks 7 and 4 — for 21°C was 82.9 mg/m^2/d, and for 8°C it was 9.3 mg/m^2/d. The net removal rate, measured in Tank 4, for 21°C was -47.84 mg/m^2/d while at 8°C it was 2.5 mg/m^2/d.

Table D.1. Mineralization, nitrification, and net removal rates for ammonium at 21°C and 8°C.

Temperature (°C)	Mineralization Rate ($mg/m^2/day$)	Nitrification Rate ($mg/m^2/day$)	Ammonium Removal Rate ($mg/m^2/day$)
21°C	29.6[1] R^2=0.99	82.9 R^2=0.98	-47.8 R^2=0.99
8°C-1	15.1 R^2=0.96	13.4 R^2=0.87	-5.1 R^2=0.85
8°C-2	14.8 R^2=0.75	8.9 R^2=0.46	4.5 R^2=0.80
8°C-3	9.9 R^2=0.80	9.0 R^2=0.80	0.9 R^2=0.80
8°C-4	18.4 R^2=0.99	5.7 R^2=0.95	9.8 R^2=0.99
8°C-ave.	14.6	9.3	2.5

[1]Numbers are slopes of linear regressions of measured data. Positive slopes denote increases in ammonium concentration, and negative slopes denote decreases in ammonium concentration.

Mineralization

An increase in the mineralization rate as the temperature is increased from 8°C to 21°C is expected, as this is a biologically mediated process that is influenced by temperature. The increase in mineralization here (Q_{10}≈1.6) is less than expected based on the mineralization temperature coefficient reported by Tisdale et al. (1993), (Q_{10}=2), which indicates that as the temperature increases 10 degrees, the mineralization rate will double. This is due to the waterlogged status of sediment underlying surface waters. Though mineralization occurs throughout the sediment profile (in both the aerobic and anaerobic zones), it is slower in the anaerobic zone (see Section 1.4.3.1, Mineralization). This leads to a slower mineralization increase over the temperature change, resulting in the Q_{10}≈1.6 exhibited here. The C/N ratio of the organic material is not expected to contribute to the lower Q_{10} through immobilization, because the organic material that enters the system as litterfall has a C/N ratio of approximately 33%, which is in between what has been

determined to cause immobilization of nitrogen and mineralization (reported by Tisdale et al., 1993; Johnston, 1991). The ratio over time will become lower as carbon is used by decomposers and mineralizers, resulting in increased mineralization (Johnston, 1991; Lorenz et al., 2000).

Nitrification

Nitrification is expected to increase as temperature increases, because it also is mediated by biological processes. Low temperatures have a more limiting effect on nitrification than on mineralization (Van Scholl et al. (1997) found "considerable mineralization occurring at temperatures close to 0^oC"). In this study, the nitrification rate at 8^oC was approximately 9.3 $mg/m^2/d$, and it increased to 82.9 $mg/m^2/d$ as the temperature was raised to 21^oC. This is a 9.0-fold increase in the rate of nitrification for the temperature increase. This increase is similar to the average nitrification increase, 5.2-fold, that Malhi and McGill (1982) found in their study of three soils in Alberta. A possible reason why the sediment nitrification rate in this study exhibited a greater increase as the temperature was increased is the circulation of the surface water. This circulation brought high levels of dissolved oxygen (>10 mg/L) into the upper 9 cm of the sediment, resulting in no oxygen limitations, which allowed nitrification to occur at a rapid rate at the near-optimal temperature of 21^oC. In the soil described by Malhi and McGill (1982), oxygen diffuses into the soil from the surface. This means there is less oxygen available for nitrification, which creates an environment where oxygen may be a limiting factor, thus reducing nitrification below its optimal potential.

Conclusions

Mineralization and nitrification rates are very temperature-dependent, as they are both biologically driven processes. Nitrification was shown to be more temperature-dependent than mineralization. The mineralization rate from this study showed similar but lower increases (Q_{10}=1.6) in ammonium formation with an increase in temperature as reported by Tisdale et al. (1983) (Q_{10}=2). This lower increase is due to the differences in the submerged sediment of this study and aerated soil described by Tisdale et al. (1983). The nitrification rate in this study showed similar increases (9.0-fold) to that found in the study conducted by Malhi and McGill (1982) (5.2-fold). The higher rate of nitrification in this study compared to the Malhi and McGill (1982) study is probably due to advection vs. diffusion as transport mechanism, resulting in oxygen limitations within the soils of the latter study.

References

Johnston, C.A. 1991. Sediment and nutrient retention by freshwater wetlands: effects on surface water quality. CRC Crit. Rev. Environ. Control. 21: 491-565.

Lorenz, K., C.M Preston, S. Raspe, I.K. Morrison, and K.H. Fegrer. 2000. Litter decomposition and humus characteristics in Canadian and German Spruce ecosystems: information from tannin analysis and ^{13}C CPMAS NMR. Soil Bio. And Biochem. 32: 779-792.

Malhi, S.S. and W.B. McGill. 1982. Nitrification in three Alberta soils: effect of temperature, moisture and substrate concentration. Soil Biol. Biochem. 14: 393-399.

Tisdale, S.L., W.L. Nelson, J.D. Beaton, and J.L. Havlin. 1993. Soil Fertility and Fertilizers. 5th ed. MacMillan Publishing Company, New York.

Van Scholl, L., A.M. Van Dam, and P.A. Leffellaar. 1997. Mineralization of nitrogen from an incorporated catch crop at low temperatures: experiment and simulation. Plant and Soil. 188: 211-219.

Appendix E

Temperature

Methods

During the field studies, temperatures were taken at 0.5-hour intervals using a HOBO data logger at two locations, ¼ and ¾ the distance from the outlet to the start of the study canal length (Figure 2.2). Each location recorded temperatures at 5 cm above the canal's water surface, 5 cm below the canal's water surface, in the litter layer along the bottom of the canal, and 5 cm below the sediment surface (Figure E.1).

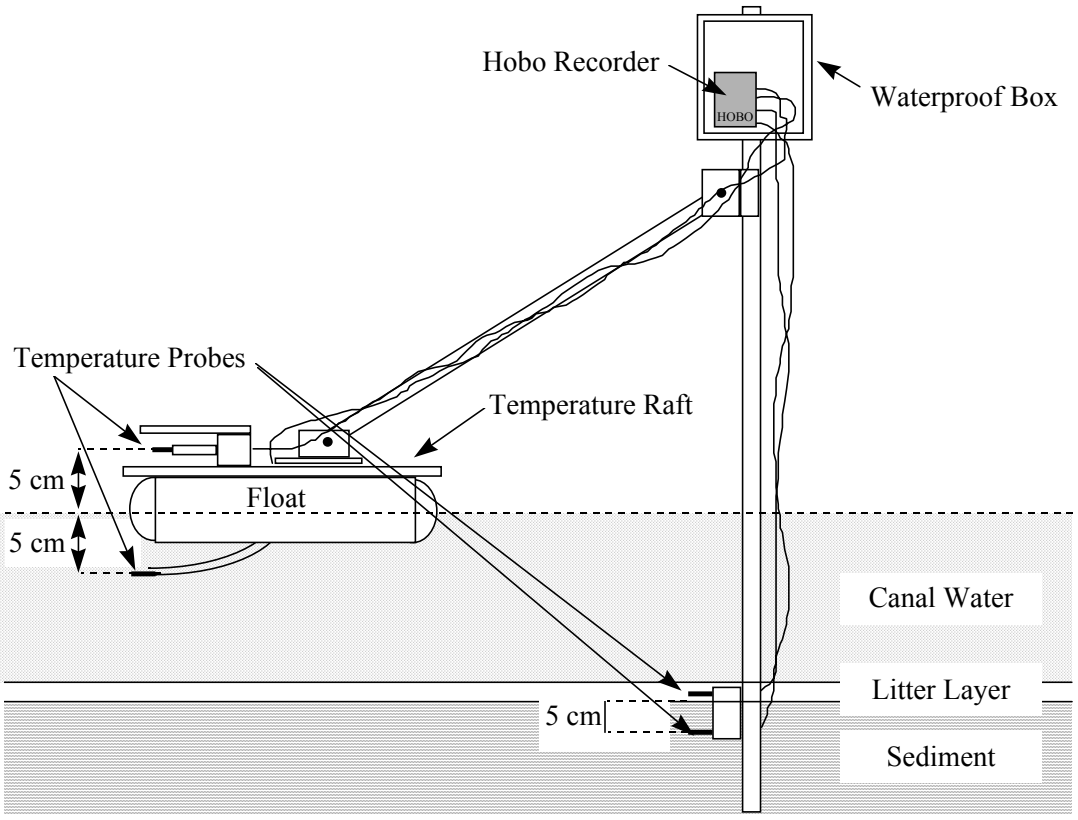

Figure E.1. Temperature probes in the field.

During the lab studies, temperatures were taken at 0.5 hour intervals using a HOBO data logger. Temperatures were taken at the midpoint in the water column and 5 cm below the sediment surface (Figure E.2).

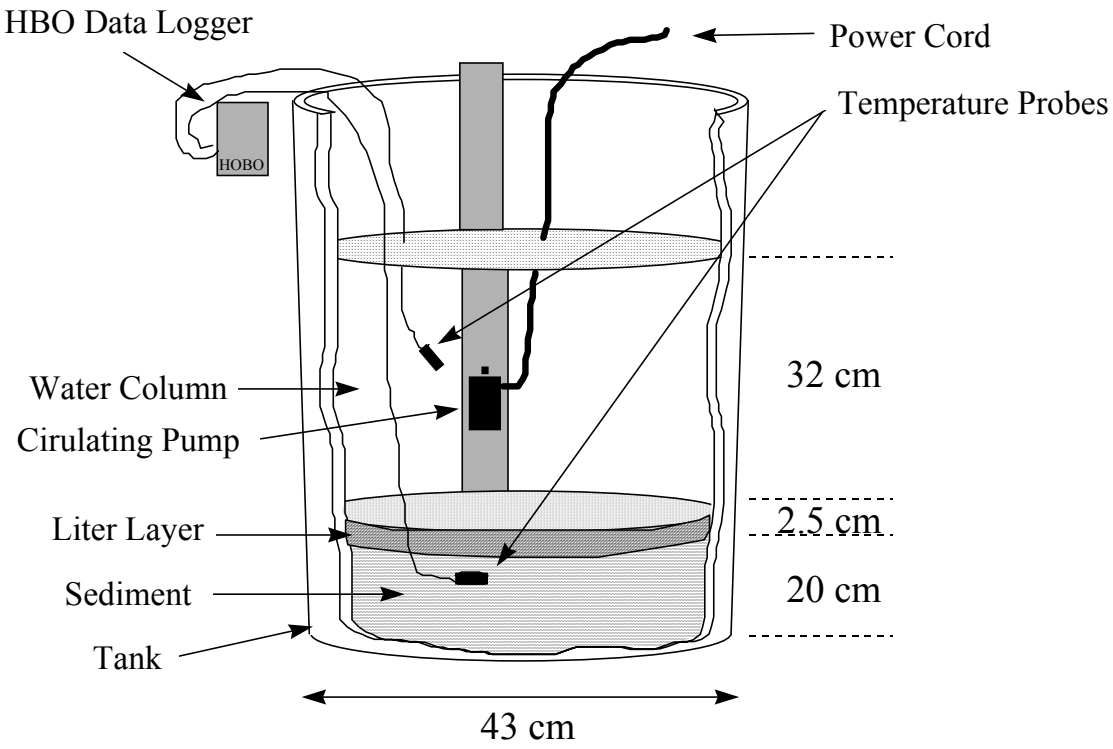

Figure E.2. Temperature probes in lab studies.

Results and Discussion

The temperature patterns of the field study are similar at both locations across the two years of the study (Figures 3.35-3.38). The water column and sediment temperatures alternated as to which were higher. When temperatures were on the rise, the water column was warmer than the sediment. When temperatures were on the decline, the sediment was

warmer than the water column. This is due to the transfer of heat energy in the system. As the air temperature cools below the water temperature, heat energy is lost from the water column to the air, resulting in a cooling of the water column. As the water column cools, heat energy will begin to be lost from the sediment and sediment pore water to the water column. In addition, the soil below the sediment at depth has a relatively constant temperature. This results in the sediment generally being warmer than the water column during the cooler months, with the opposite being true during the warmer months.

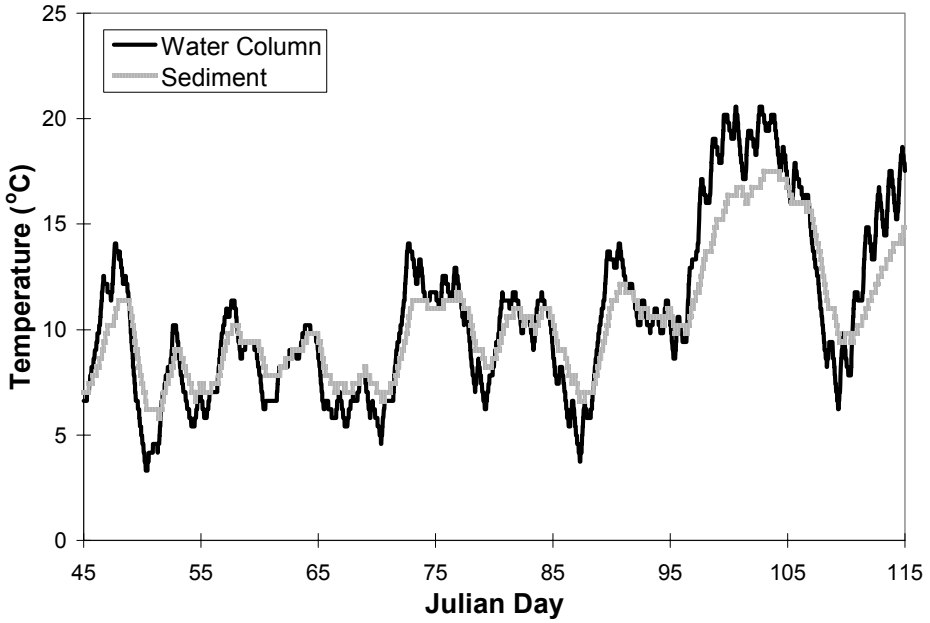

Figure E.3. Mid-depth water column and 5 cm depth sediment temperatures from the eastern location (T1) along the canal during the 2001 period of flow.

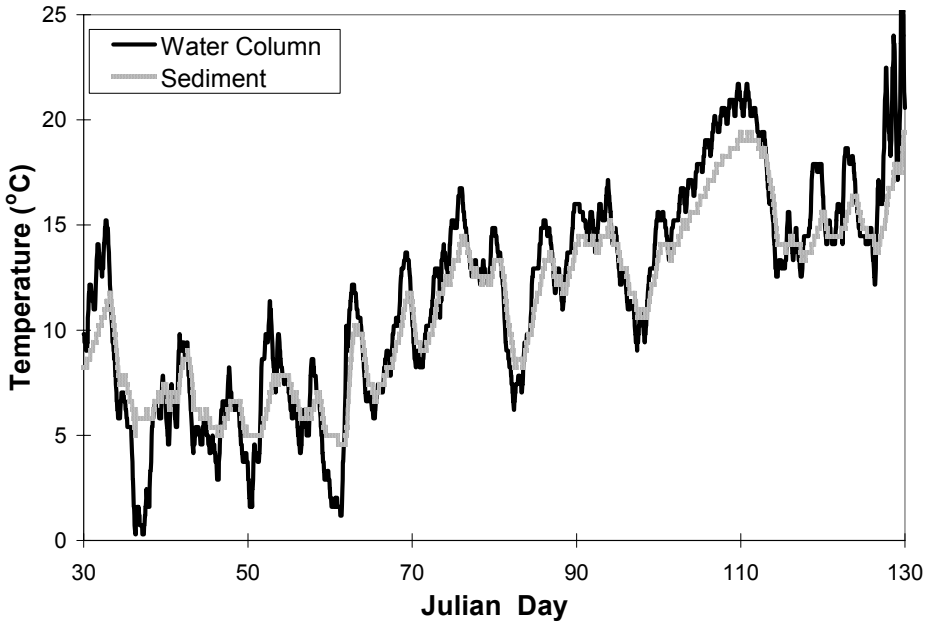

Figure E.4. Mid-depth water column and 5 cm depth sediment temperatures from the eastern location (T1) along the canal during the 2002 period of flow.

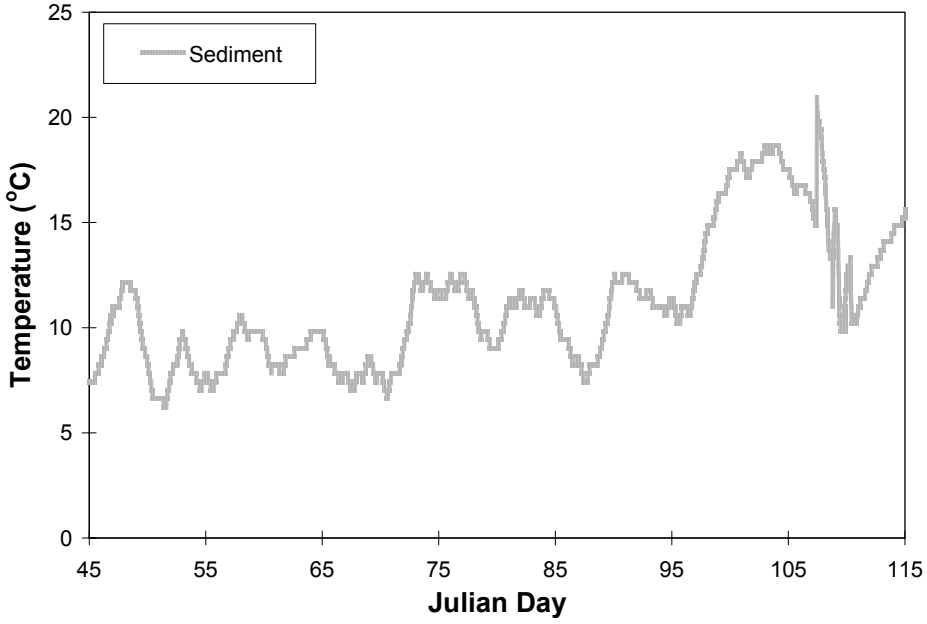

Figure E.5. Mid-depth water column and 5 cm depth sediment temperatures from the western location (T2) along the canal during the 2001 period of flow.

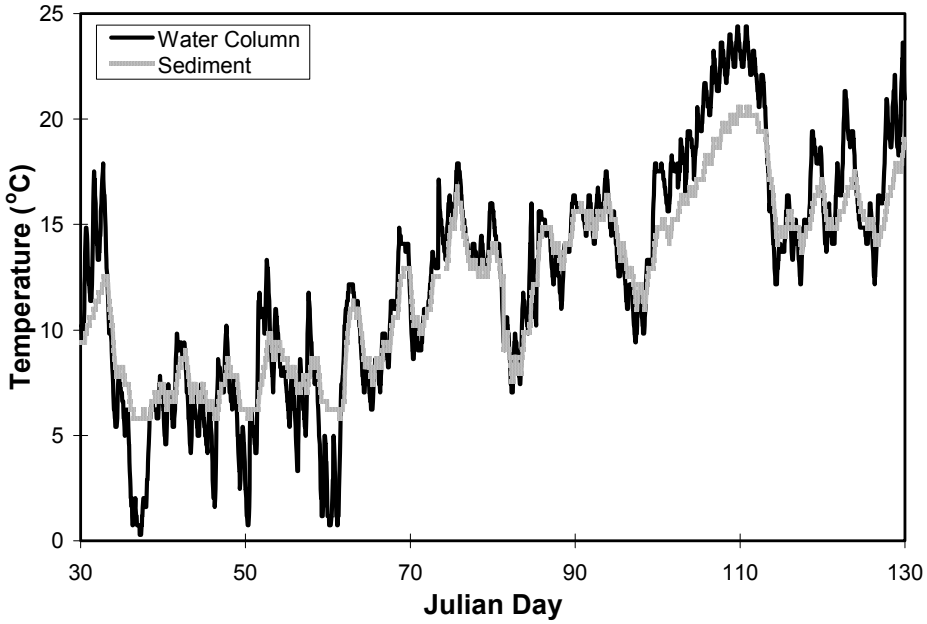

Figure E.6. Mid-depth water column and 5 cm depth sediment temperatures from the western location (T2) along the canal during the 2002 period of flow.

Figure E.7 shows temperatures for air, midpoint water column, midpoint litter layer, and 5 cm sediment depth for the 20-day span from days 100 to 120, in the springtime, during the 2002 flow period at the western location in the study canal. This figure shows the higher degree of temperature fluctuation typical of air temperatures due to the diurnal cycle. The midpoint water column temperatures follow the same pattern but show much less effect of diurnal temperature variation. The average temperatures for the air and water usually will track in a similar manner, the water warming when the air temperature is higher than the water temperature and cooling when the air temperature is cooler than the water temperature. This dampening is due to the slower heat transfer between different materials, water and air in this case, as compared to the convective mixing that occurs within the air or the water. In

this case, during the period between days 100 and 113, the average water temperature (20.5^{o}C) is slightly higher than the average air temperature (19.6^{o}C). The midpoint temperature of the litter layer and the 5 cm sediment depth average temperatures were similar (18.3^{o}C and 18.0^{o}C respectively) but lower than the air and water temperatures. This is due to the effect that the large mass of deeper saturated soil surrounding the canal has on the shallower sediment and litter layer of the hyporheic zone of the canal. This resulted in a decrease in temperature as one moves from the air above the canal through the water column and litter layer and into the sediment. After day 113, a sudden drop in the air temperature resulted in a reversal of this temperature profile. The sediment (16.0^{o}C average) is warmer than the litter layer (15.4^{o}C average), which is warmer than the water column (14.9^{o}C average), which is warmer than the air temperature (12.5^{o}C average) from day 113 to day 115.

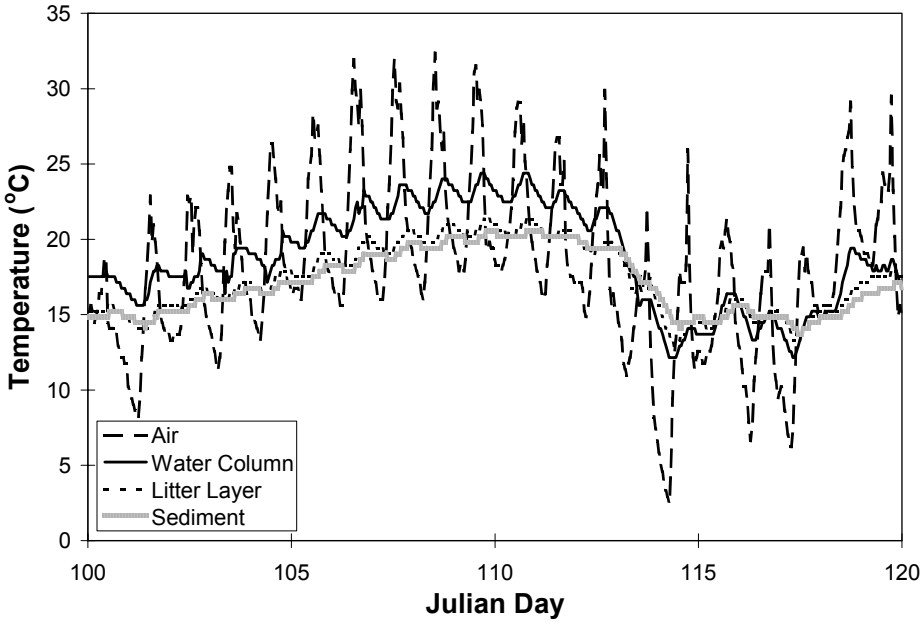

Figure E.7. Air, mid-depth water column, mid-litter layer, and 5 cm depth sediment temperatures from the western location (T2) along the canal between the Julian day 100 and 120 of the 2002 period of flow.

In the lab study, the average water column temperatures of run one, at 21°C, were all similar (21°C) with the exception of a slightly higher temperature (22°C) in the circulated tanks with no nitrification inhibitor (Figure E.8).

The water column temperatures of the second run, at 8°C, showed similar average temperatures between the air temperature and the uncirculated tanks (5.9°C), while the average temperatures of two circulated treatments were higher (7.2°C) (Figure E.9).

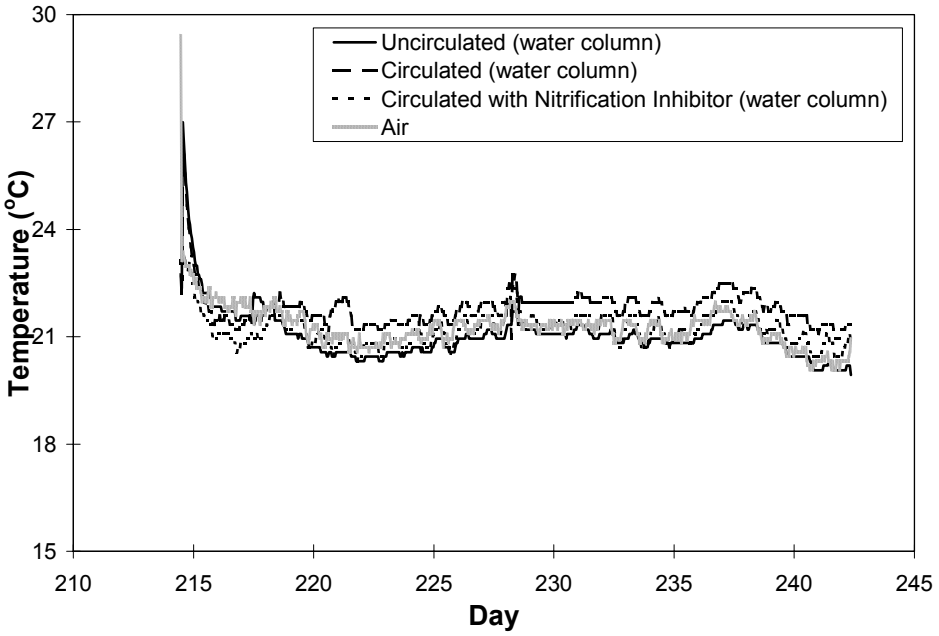

Figure E.8. Midpoint water column and air temperature patterns of lab tanks during run one at 21°C.

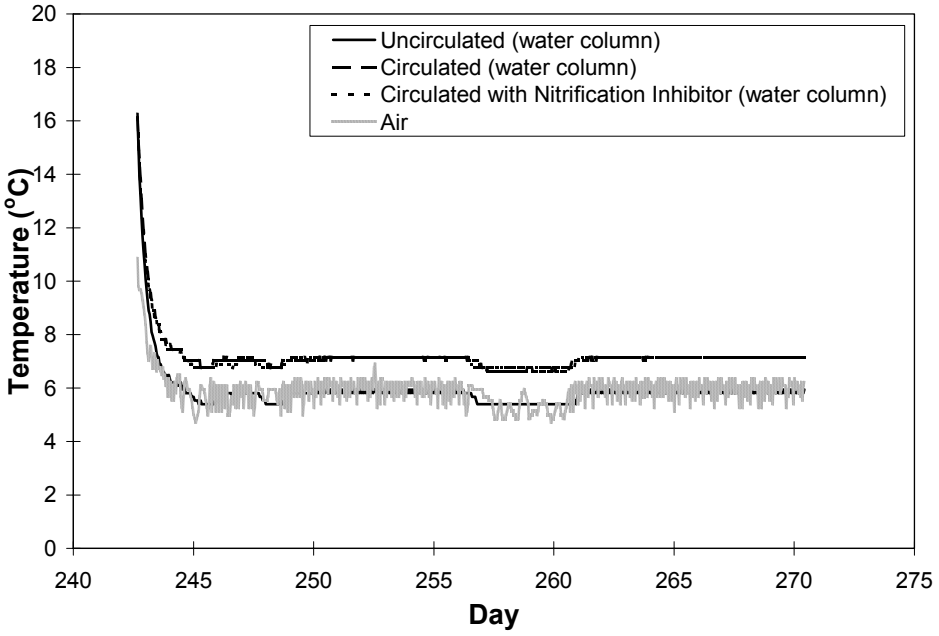

Figure E.9. Midpoint water column and air temperature patterns of lab tanks during run two at 8°C.

The water column temperatures of the third run, at 8°C, showed a similar difference in the average temperatures of circulated tanks, uncirculated tanks, and the air as the previous run (Figure E.10). The average temperatures of the water columns of the uncirculated tanks and the air were the same (6.0°C) while the circulated tanks with the nitrification inhibitor were higher (7.4°C). The temperatures recorded in the circulated tanks without the nitrification inhibitor were placed in the sediment for this run and resulted in an average sediment temperature (6.9°C) between the water column temperatures of the other two sets of tanks (circulated and uncirculated).

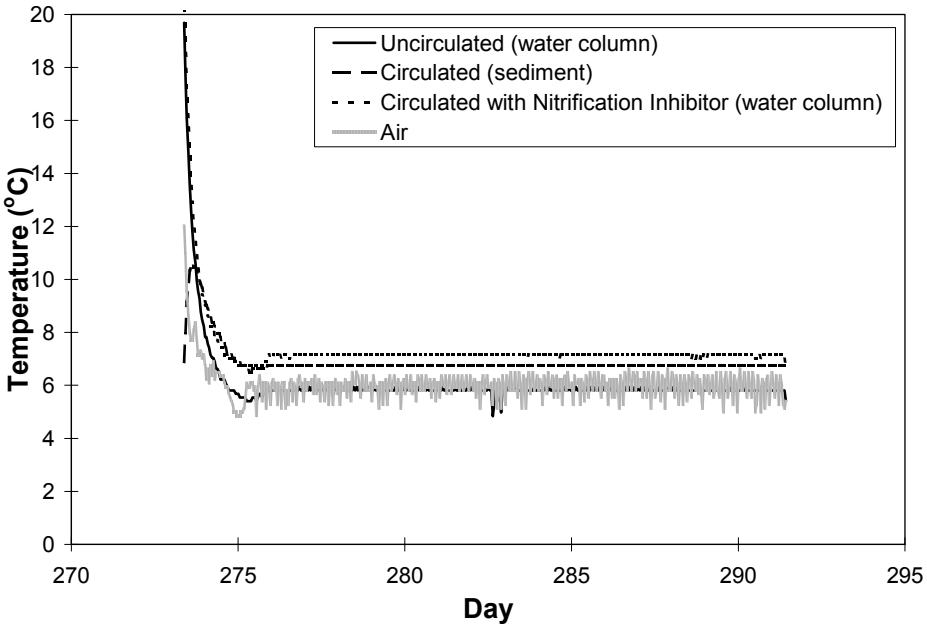

Figure E.10. Midpoint water column, 5 cm sediment depth, and air temperature patterns of lab tanks during run three at 8°C.

The water column temperatures of the fourth run, at 8°C, showed a similar difference in the average temperatures of circulated tanks, uncirculated tanks, and the air as the previous run (Figure E.11). The average temperatures of the water columns of the uncirculated tanks and the air were the same (5.8°C), while the circulated tanks with the nitrification inhibitor were higher (7.3°C). The temperatures recorded in the circulated tanks without the nitrification inhibitor were placed in the sediment for this run and resulted in an average sediment temperature (7.1°C) between the water column temperatures of the other two sets of tanks (circulated and uncirculated).

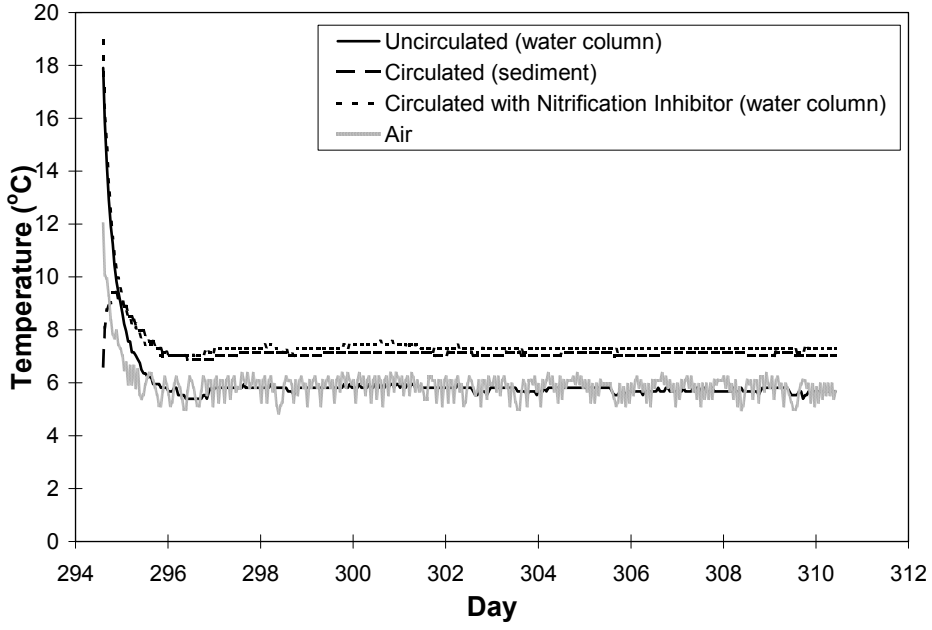

Figure E.11. Midpoint water column, 5 cm sediment depth, and air temperature patterns of lab tanks during run four at 8°C.

The water column temperatures of the fifth run, at 8°C, showed a similar difference in the average temperatures of circulated tanks, uncirculated tanks, and the air as the previous

run (Figure E.12). The average temperatures of the water columns of the uncirculated tanks and the air were the same (5.6°C), while the circulated tanks with the nitrification inhibitor were higher (7.0°C). The temperatures recorded in the circulated tanks without the nitrification inhibitor were placed in the sediment for this run and resulted in an average sediment temperature (6.7°C) between the water column temperatures of the other two sets of tanks (circulated and uncirculated).

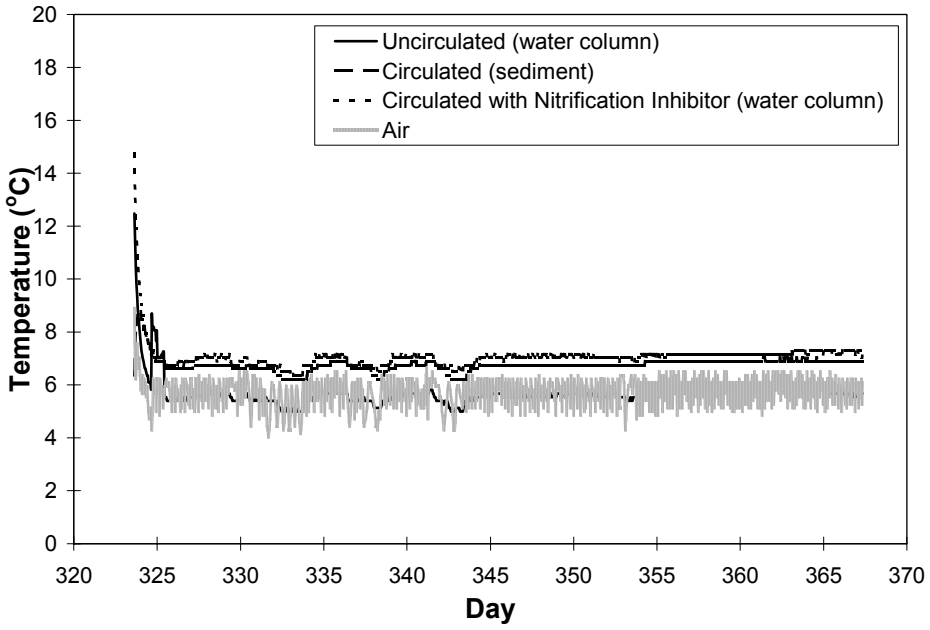

Figure E.12. Midpoint water column, 5 cm sediment depth, and air temperature patterns of lab tanks during run five at 8°C.

The reason for the differences in the average water column and air temperatures in the second run, at 8°C, is the presence of the circulating pumps. The two circulated treatments average water column temperatures were 1.3°C higher than the average air temperature and uncirculated treatment average water column temperature due to the heat

generated by the operation of the circulation pumps. The presence of the circulation pumps is also the reason for the differences between the average circulated and uncirculated treatments and air temperatures in the third, fourth, and fifth runs at 8^{o}C. The reason that the average sediment temperatures of the circulated treatments without the nitrification inhibitor were lower than the average water column temperatures of the circulated treatments with the nitrification inhibitors of the last three runs is due to the probes being placed in the sediment. The lab study did not allow for deep sediments, so there was a constant temperature surrounding the tanks, even at the bottom of the sediment cores. This resulted in both lateral and vertical heat loss from the sediment cores. Heat generated from the circulation pumps entered the sediment as the water was moved through the sediment via convection, resulting in the increase in the average sediment temperature. Some of this heat was lost laterally and downward as previously described, resulting in a lower temperature than in the water columns.

Conclusions

These temperature patterns show the importance of determining the temperature within the sediment when trying to predict mineralization, nitrification, and denitrification rates within the sediment. The difference in the air temperature or water column temperature from the sediment temperature could be significant (a difference of almost 2^{o}C measured in this study) depending on the season.

When doing lab studies, it is important to understand the experimental setup and how it may affect the results of the study. In this case, the addition of a circulation pump resulted in an average increase in the water column temperature of 1.3^{o}C. This can be easily corrected by adjusting the experimental temperature to offset this difference.

Appendix F

Dissolved Oxygen and pH

Methods

Dissolved oxygen and pH were measured at the midpoint in the water column in conjunction with sample removal from the inflow and discharge point samplers of the canal study section as well as sampling of field denitrification tanks. These parameters were also taken over two 24-hour periods on an hourly basis (3-13-2002 to 3-14-2002 and 4-10-2002 to 4-11-2002) to determine any fluctuations over the diurnal cycle. Readings were taken using a YSI Model 610D Multi-Parameter Water Quality monitor equipped with a dissolved oxygen and pH probe. These parameters were measured because they have a large impact on the in-stream processes that convert nutrients to different forms or remove them from the system.

Dissolved Oxygen

The dissolved oxygen concentration during the two years of data ranged from 5.4 mg/L to 8.8 mg/L (average 6.8 $\pm$ 0.6 mg/L) during the 2001 flow period and 3.6 mg/L to 8.1 mg/L (average 6.4 $\pm$ 0.3 mg/L) during the 2002 flow period. These values are high enough to discourage denitrification (2.0 mg/L to 6.0 mg/L, van Kessel, 1977; Rysgaard et al., 1994) and encourage nitrification in the water column and upper sediment. Figure F.1 shows the average water column dissolved oxygen content within the canal study section for both of the study years.

The water column dissolved oxygen concentration shows little variation (1.8 mg/L) over the 24-hour diurnal cycle (Figure F.2). The dissolved oxygen ranged from 7.6 mg/L during the daylight hours to 5.8 mg/L during the evening hours. This means the processes of

nitrification and denitrification will be affected similarly during both the daytime and nighttime periods.

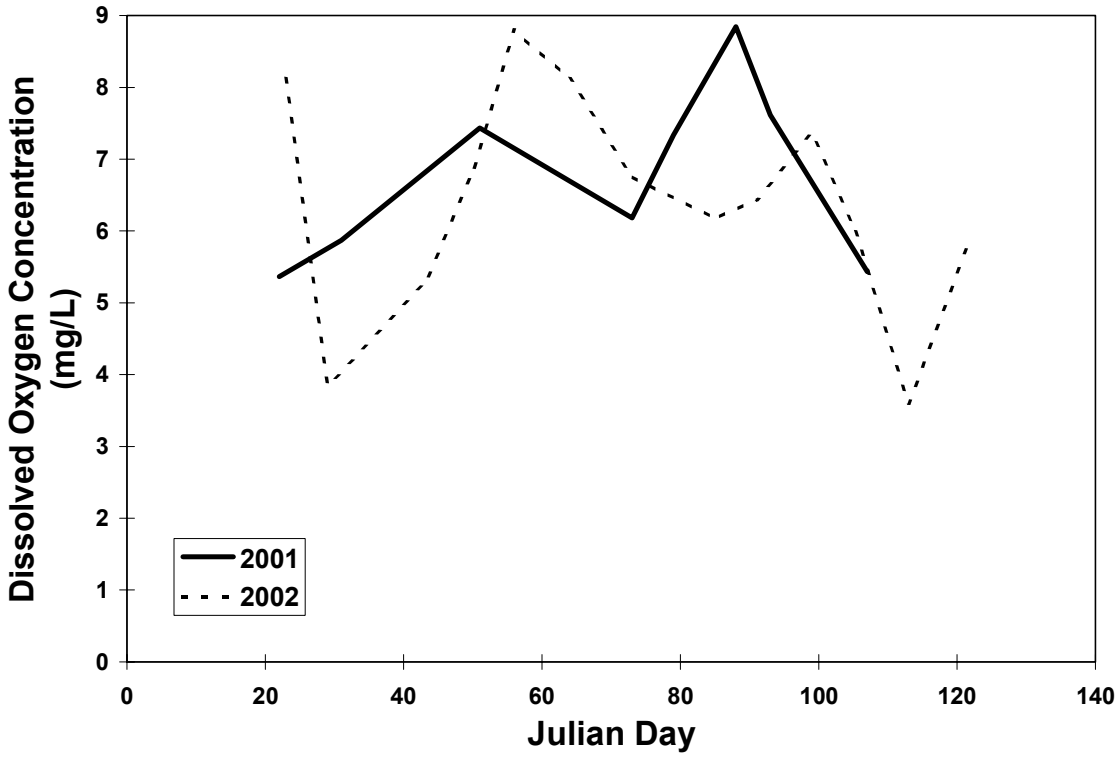

Figure F.1. Average dissolved oxygen concentration within the water column for flow periods 2001 and 2002.

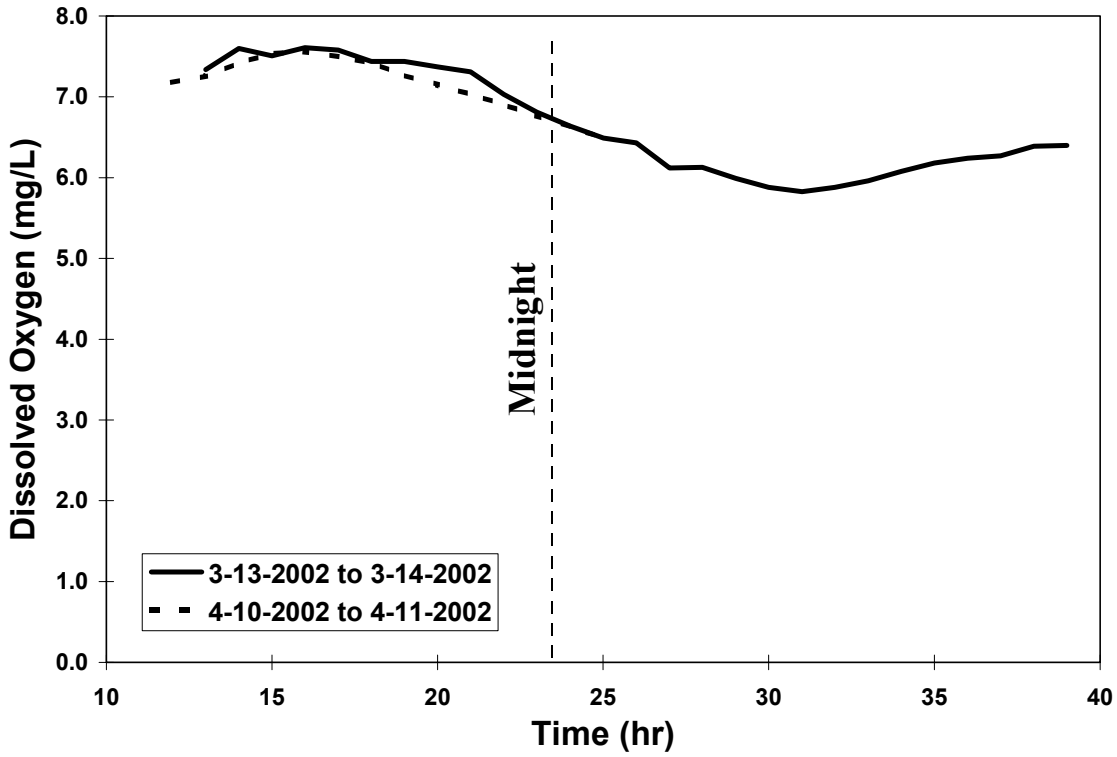

Figure F.2. Diurnal dissolved oxygen concentration pattern in the water column of the canal study section 3-13-2002 to 3-14-2002 and 4-10-2002 to 4-11-2002.

pH

The pH values during the two years of data ranged from 3.7 to 4.2 (average 4.1 $\pm$ 0.0) during the 2001 flow period and 3.5 to 6.3 (average 4.6 $\pm$ 0.0) during the 2002 flow period (Figure F.3). During the 2001 flow season, the pH remains relatively constant, with little variation. During the 2002 flow season, the pH averages 5.9 from the start of the flow season until around day 56 with little variation. After around day 56, the pH decreases to an average of 3.7, with little variation to the end of the flow season. The values during the 2001 flow season and the latter half of the 2002 flow season are low enough (<4.0 to 4.5, Tisdale et al., 1993) to inhibit nitrification within the water column and sediment. During the earlier portion of the 2002 flow season, the pH is high enough to allow nitrification to occur but has

a minimal impact, as the flow is minor until approximately day 62 (see Figure 2.22, Section 2.11, Mass Balance). The pH, on the other hand, had only a minor effect on the denitrification rate. Denitrification is little affected until pH reaches levels around 2.0 (Waring and Gilliam, 1983).

The water column pH shows almost no variation (0.1 on day 3-13-2002 and 0.0 on day 4-10-2002) over the 24-hour diurnal cycle (Figure F.4). The pH ranged from 4.7 during the daylight hours to 4.8 mg/L during the evening hours on day 3-13-2002, and remained constant at 4.4 over the entire period measured on day 4-10-2002. This means pH will affect the processes for nitrification and denitrification by the same amount during both the daytime and nighttime periods.

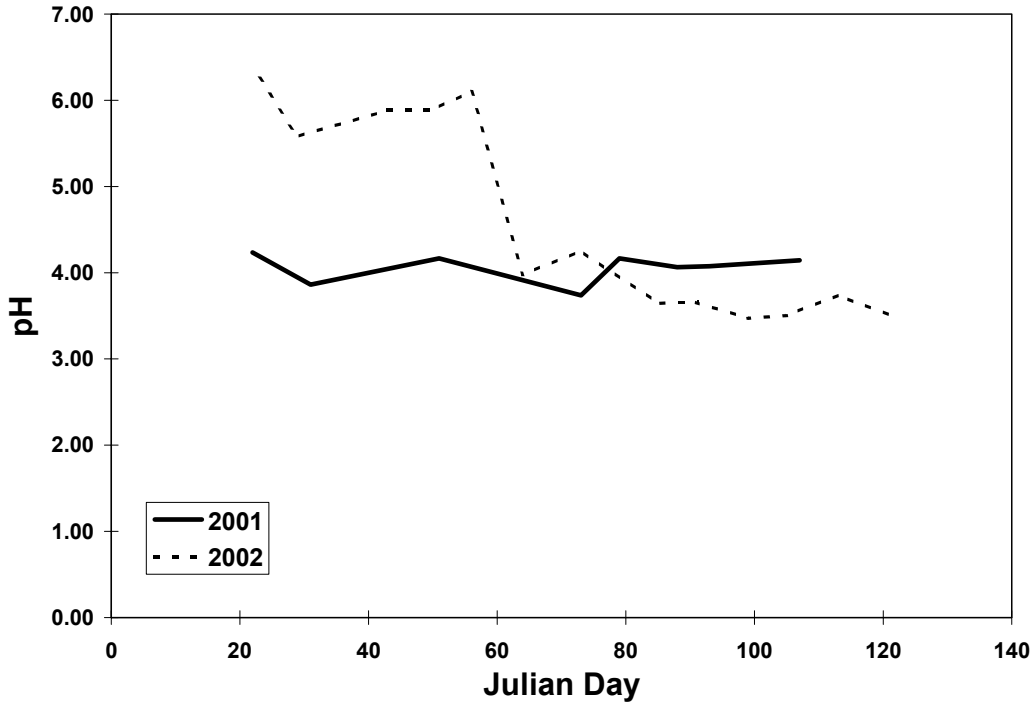

Figure F.3. Average pH within the water column for the flow periods 2001 and 2002.

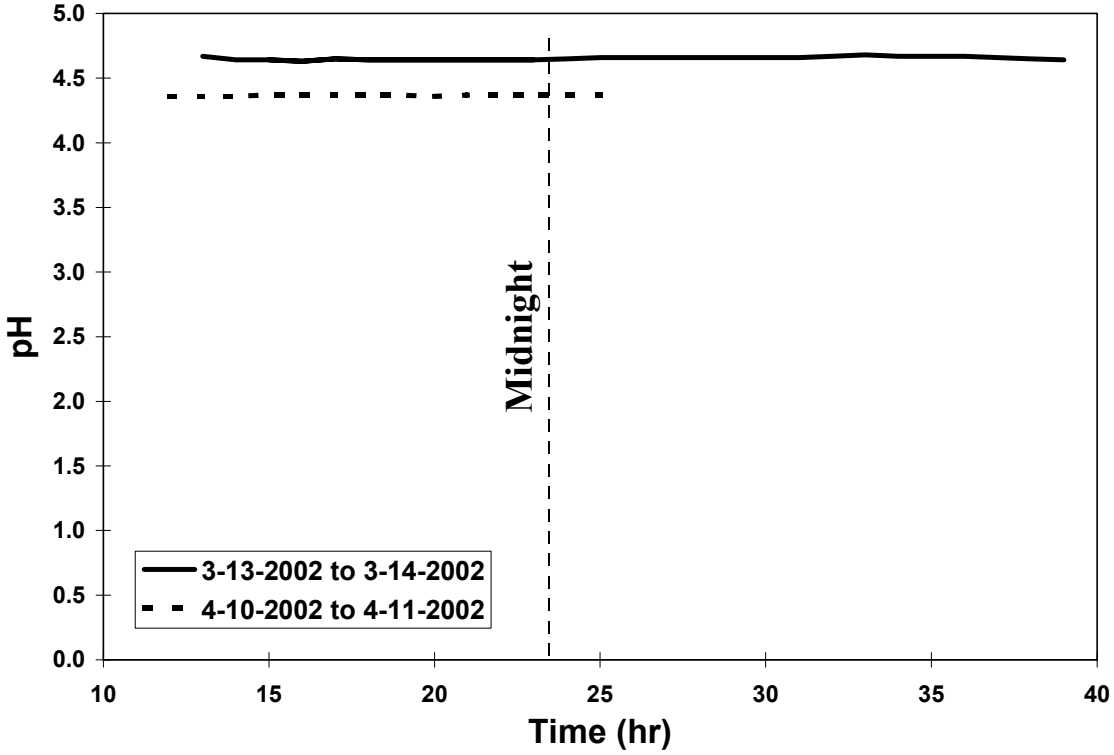

Figure F.4. Diurnal pH pattern in the water column of the canal study section 3-13-2002 to 3-14-2002 and 4-10-2002 to 4-11-2002.

Conclusions

The dissolved oxygen concentrations found during this study (5.6 mg/L to 8.1 mg/L over the two years of the study) are high enough to inhibit denitrification in the water column and upper sediments. Denitrification still occurs deeper in the sediments (10 cm and below; see Appendix C, Nitrate, Ammonium, and Phosphate Distribution in Sediment Pore Water and Water Column), but these dissolved oxygen levels favor nitrification in the water column and upper sediments.

The prevailing pH levels (3.5 to 4.2 over the two-year period, with the exception of a short period during very low flow in the beginning of the 2002 flow period when the pH

averaged 5.9) were low enough to inhibit nitrification within the water column and in the sediments. There is a possibility that there were some microsites in the upper sediments where the pH conditions could be more favorable for nitrification to occur on a small scale. However, the measured pH values are high enough that denitrification will not be significantly inhibited.

The pH values resulted in nitrification occurring within the canal study section at a reduced rate, while the dissolved oxygen levels caused denitrification deeper in the sediments (depths deeper than 10 cm).

References

Rysgaard, S., N. Rysgaard-Petersen, N.P. Sloth, K. Jensen, and L.P. Nielsen. 1994. Oxygen regulation of nitrification and denitrification in sediments. Limnol. Oceanogr. 39(7): 1643-1652.

Tisdale, S.L, W.L. Nelson, J.D. Beaton, and J.L. Havlin. 1993. Soil Fertility and Fertilizers. 5th ed. Macmillan Publishing Company, New York.

van Kessel, J.F. 1977. Factors affecting the denitrification rate in two water sediment systems. Water Res. 11: 259-267.

Waring, S.A., and J.W. Gilliam. 1983. The effect of acidity on nitrate reduction and denitrification in lower coastal plain soils. Soil Sci. Soc. Am. J. 47: 246-251.

Appendix G

Human Activities Resulting in Nitrogen and Phosphorous Removal

Methods

The amount of nitrogen, phosphorous, and carbon removed from the system through canal clean-out (removal of debris — sediment buildup, fallen trees, etc.) was determined by taking sediment samples from the study canal and analyzing them for their nitrogen, phosphorous, and carbon content. Three samples were taken at each of the three locations where the in-stream denitrification tanks were located (Figure 2.2). The triplicate samples were located with one set from the northern third of the canal, one set from the central third of the canal, and one set from the southern third of the canal at each location (Figure G.1). The samples were taken to a depth of 24 cm, the thickness of the organic layer in the canal. The samples were frozen until ground into a fine powder and subsampled for analysis.

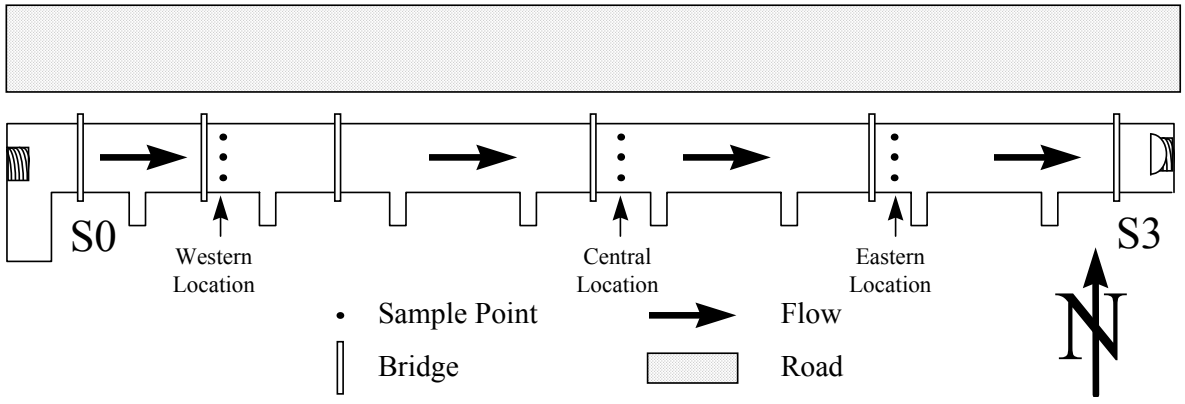

Figure G.1. Location and position of canal sediment samples.

The results of the sample analysis were expressed as percentage content of the nutrients tested. To convert this to a mass per volume, one simply need multiply the percentage content by the bulk density of the sediment for the mass of the nutrient of interest per volume of soil.

Statistical Analysis

A general linear model for the canal sediment nutrient removal is shown in Equation G.1.

$$\text{Model: } Y = \mu + \alpha_i + \varepsilon \qquad \text{Equation G.1}$$

where: Y = the mass of nitrogen removed through clean out per location
μ = the average mass of nitrogen per location
α_i represents the main effects of location on the mass of nitrogen (i = east, central, and west)
ε = error term.

The constraint of $\sum_i \alpha_i = 0$. The hypothesis being tested is: H_o: $\alpha_i = 0$ - no main effect of location (Steel and Torrie, 1980). The same statistical model and constraints were used for analyzing the phosphorous and carbon content of the sediments removed from the canal during clean-out operations from the three different locations. The same hypothesis was tested on each of the different sediment components. The same model, hypothesis, and constraints were used to analyze the results based on the position of the samples within the canal (northern third, central third, or southern third of the ditch) where Y = the mass of nutrient removed through clean-out per position, μ = the average mass of nutrient per position, α_i represents the main effects of position on the mass of nutrient (i = north, central, and south), and ε = error term. There were not enough data to include the interaction term for location and position. The data were transformed using a square root transformation to

stabilize the variance. The individual least squares means analysis was adjusted for multiple comparisons using Tukey for a more conservative comparison.

Results and Discussion

The statistical analysis showed no main effects for either location along the canal (Table G.1) or position within the canal (Table G.2). The small sampling did not allow for statistical analysis of the interaction between the two main effects.

Table G.1. Mass of nitrogen, phosphorous, and carbon per cubic meter of removed sediment per location.

Location	Nitrogen (kg/m^3)	Phosphorous (kg/m^3)	Carbon (kg/m^3)
East	3.2 A[1]	0.2 A	54.2 A
Central	2.0 A	0.1 A	37.6 A
West	1.3 A	0.1 A	24.9 A
Average	2.2	0.1	38.9
	R^2= 0.36, RMSE = 5.66	R^2= 0.31, RMSE = 1.64	R^2= 0.30, RMSE = 23.6

[1] Different letters indicate significant difference using the Least Squares Means adjusted for multiple comparisons using the Tukey adjustment at $\propto = 0.05$.

Table G.2. Mass of nitrogen, phosphorous, and carbon per cubic meter of removed sediment per position.

Location	Nitrogen (kg/m^3)	Phosphorous (kg/m^3)	Carbon (kg/m^3)
North	1.6 A[1]	0.1 A	27.6 A
Central	2.9 A	0.2 A	53.1 A
South	2.1 A	0.1 A	36.0 A
Average	2.2	0.1	38.9
	R^2= 0.22, RMSE = 6.24	R^2= 0.27, RMSE = 1.68	R^2= 0.26, RMSE = 24.2

[1] Different letters indicate significant difference using the Least Squares Means adjusted for multiple comparisons using the Tukey adjustment at $\propto = 0.05$.

The removal of material through canal clean-out (dredging) has several effects on the nutrient balances within the system. It creates a sudden additional large output of nutrients

from the system by physical removal. It also alters the previous equilibrium of nutrients within the canal. The main forms of nitrogen found in the sediments are organic and ammonium. With this removal, mineralization and nitrification within the upper layers all but cease due to the lack of substrate (organic nitrogen) for the microbes to utilize. Canal clean-out also removes the large source of carbon that provides the energy for all the in-stream processes (mineralization, nitrification, and denitrification) within the canal, resulting in a decrease in denitrification until additional carbon enters the system. The canal clean-out also creates a cleaner flow channel by removing obstructions such as earthen barriers, vegetation, fallen trees, and decomposing litter. This causes more water to be able to move through the canal with higher velocities and larger cross-sectional flow area, resulting in less residence time for the nutrients. This means less time for the in-stream processes to act on them for removal prior to reaching the outlet, resulting in higher nutrient loads at the outlet.

Based on the sediment pore water sampler results (Appendix C, Nitrate, Ammonium, and Phosphate Distribution in Sediment Pore Water and Water Column) and the lack of organic material below the hyporheic zone, it was determined that the bulk of the nitrogen, phosphorous, and carbon in the sediment are located in the hyporheic zone (Figure 1.2). By multiplying the average depth of the hyporheic zone by the canal bottom width and the length of the canal section cleaned, one can estimate the amount of nutrients removed. In the case of this study (depth of the hyporheic zone = 0.24 m, canal bottom width = 3 m, and the length of clean-out = 1900 m), the amount of nutrients removed due to a canal clean-out would approximately be 3010 kg of nitrogen, 137 kg of phosphorous, and 53,000 kg of carbon for the study section.

Conclusion

Canal maintenance, such as clean-out, results in not only a large output of nutrients through physical removal (2.2 kg/m^3 of nitrogen, 0.1 kg/m^3 of phosphorous, and 38.9 kg/m^3 of carbon) but also the potential for increases in nutrient loads at the outlet due to higher flow velocities reducing residence time within the drainage canals and the reduction of the energy source, carbon, required by denitrifiers to convert nitrate to nitrogen gas for removal from the system.

References

Steel, R.G.D., and J.H. Torrie. 1980. Principles and Procedures of Statistics: A Biomedical Approach. 2nd Ed. McGraw-Hill, Inc., New York.

Appendix H

Example of Diffusion-Generated Nitrate Decay Curve and Mass Transfer Coefficient

The diffusion-generated nitrate decay curve is based on the diffusion of nitrate into the sediments from the water column. Using the following equation (developed in Section 3.5, Nitrate Diffusion Calculations), the nitrate loss, or mass flux into the sediment, can be determined. The assumption is that all nitrate that diffuses into the sediment is denitrified.

$$J = -D_d` * dC/dz$$

where: J = mass flux ($mg/m^2/sec$)
$D_d`$ = effective diffusion coefficient (m^2/sec)
dC = the change in concentration (mg/m^3)
dz = the change in depth (m)

For this example, data from the field cores taken from the eastern location of the field tanks will be used at 8^oC. For this location, the average porosity was 0.91, which resulted in an effective diffusion coefficient ($D_d`$) of $5.57*10^{-6}$ cm^2/sec ($5.57*10^{-10}$ m^2/sec) (Table 3.11). The term dC/dz is determined using the empirical relationship developed in Figure 3.21:

$$dc/dz = 54.23*C$$

where: dC = the change in concentration (mg/m^3)
dz = the change in depth (m)
C = the water column nitrate concentration (mg/m^3).

Table H.1 shows the calculated decrease in nitrate mass and water column concentration over time for this example. This example used a one-square-meter sediment surface area, a depth of one meter, and a 4 mg/L (4000 mg/m^3) initial nitrate concentration.

Table H.1. Change in nitrate mass over time over one square meter of sediment surface with a one-meter water column depth using diffusion calculations.

Time (days)	Nitrate Mass Present (mg)	Mass Flux J ($mg/m^2/day$)	Water Column Concentration (mg/m^3)	dC/dz ($mg/m^3/m$)
0	4000	10.4	4000	216920
1	3990	10.4	3990	216354
2	3980	10.4	3980	215791
3	3970	10.4	3970	215229
5	3950	10.3	3950	214104
7	3930	10.3	3930	205133
9	3910	10.2	3910	211920
12	3880	10.1	3880	210261
15	3850	10.0	3850	208614
20	3800	9.9	3800	205890
25	3750	9.8	3750	203205
30	3700	9.7	3700	200548
35	3690		3690	

The mass transfer coefficient can be determined using the following equation developed in Chapter 4, Development of Mathematical Relationship to Describe Nitrate Removal from Surface Waters:

$$\frac{\ln\left(\frac{[C_1]}{[C_o]}\right)}{(-t/D)} = \rho_d$$

where: ρ_d = mass transfer coefficient for denitrification (m/day)
$[C_o]$ = initial nitrate concentration (mg/m^3)
$[C_1]$ = nitrate concentration at the end of the time interval (mg/m^3)
t = time interval (day)
D = water column depth (m)

$$\rho_d = \ln(3690\ mg/m^3 / 4000\ mg/m^3) / (-35\ day/1\ m)$$

$$\rho_d = 0.002 \text{ m/day}$$

The mass transfer coefficient determined in this example is in the range of those found in Table 3.12.